

POST-BUCKLING BEHAVIOUR OF METALLIC SKIN-STRINGER
ASSEMBLIES AND BUCKLING OF COMPOSITE FLAT PANELS

A THESIS SUBMITTED TO
THE GRADUATE SCHOOL OF NATURAL AND APPLIED SCIENCES
OF
MIDDLE EAST TECHNICAL UNIVERSITY

BY

ENES AYDIN

IN PARTIAL FULFILLMENT OF THE REQUIREMENTS
FOR
THE DEGREE OF MASTER OF SCIENCE
IN
AEROSPACE ENGINEERING

MARCH 2018

Approval of the thesis:

**POST-BUCKLING BEHAVIOUR OF METALLIC SKIN-STRINGER
ASSEMBLIES AND BUCKLING OF COMPOSITE FLAT PANELS**

Submitted by **ENES AYDIN** in partial fulfillment of the requirements for the degree of **Master of Science in The Department of Aerospace Engineering, Middle East Technical University** by,

Prof. Dr. Halil Kalıpçılar
Dean, Graduate School of **Natural and Applied Sciences**

Prof. Dr. Ozan Tekinalp
Head of Department, **Aerospace Engineering**

Prof. Dr. Altan Kayran
Supervisor, **Aerospace Engineering Department, METU**

Examining Committee Members:

Assoc. Prof. Dr. Demirkan Çöker
Aerospace Engineering Department, METU

Prof. Dr. Altan Kayran
Aerospace Engineering Department, METU

Assoc. Prof. Dr. Ercan Gürses
Aerospace Engineering Department, METU

Assoc. Prof. Dr. Melin Şahin
Aerospace Engineering Department,
METU

Asst. Prof. Dr. Barış Sabuncuoğlu
Mechanical Engineering, Hacettepe University

Date:

I hereby declare that all information in this document has been obtained and presented in accordance with academic rules and ethical conduct. I also declare that, as required by these rules and conduct, I have fully cited and referenced all material and results that are not original to this work.

Name, Last name: ENES AYDIN

Signature : _____

ABSTRACT

POST-BUCKLING BEHAVIOUR OF METALLIC SKIN-STRINGER ASSEMBLIES AND BUCKLING OF COMPOSITE FLAT PANELS

Aydın, Enes

M.S., Department of Aerospace Engineering

Supervisor: Prof. Dr. Altan Kayran

March 2018, 246 pages

Stiffened thin panels are very common and important structural elements in aerospace structures because of the weight and stiffness advantages they provide. The stiffener section is important to determine the support condition that the stiffener provides on the unloaded edges of the panel. In the first phase of the thesis study, the effect of the boundary conditions on the buckling coefficients of stiffened metal flat panels is investigated utilizing finite element and empirical approaches. Empirical approaches are limited for panels with classical boundary conditions. On contrary, finite element analysis is more accurate however costly. A database is prepared for the buckling coefficients of the selected skin-stringer combinations by finite element analysis to set up an artificial neural network and response surface for fast calculation of the buckling coefficients of stiffened panels. In the second phase of the study, a comparative study is presented on the post-buckling load redistribution in stiffened panels modeled with and without material nonlinearity. The effective widths of the panel are calculated right before the collapse of the panel using the load distributions determined by the finite element analyses of the panel models with and without material nonlinearity and comparisons are made with the effective width calculated by the classical effective

width formulation. In the final phase of the study, composite flat plate buckling is investigated utilizing finite element and analytical approach. A comparison study is done for composite buckling coefficients using various geometric properties of flat panels, boundary conditions, ply thicknesses and orientations. At the end, buckling charts for each ply orientation and boundary conditions are generated utilizing finite element analysis results.

Keywords: Metal Buckling, Stiffened Panels, Composite Buckling, Effective Width, Artificial Neural Network, Finite Element Analysis

ÖZ

KİRİŞLE GÜÇLENDİRİLMİŞ METAL YAPILARIN BURKULMA SONRASI DAVRANIŞI VE KOMPOZİT DÜZ PANELLERİN BURKULMASI

Aydın, Enes

Yüksek Lisans, Havacılık ve Uzay Mühendisliği Bölümü

Tez Yöneticisi: Prof. Dr. Altan Kayran

Mart 2018, 246 sayfa

Kirişle güçlendirilmiş ince paneller, sağladıkları ağırlık ve sağlamlık avantajlarından dolayı havacılık yapılarında çok yaygın ve önemli yapısal ögelerdir. Kirişin şekli, yük uygulanmayan kenarlarda bulunan kirişlerin sağladığı desteğin belirlenmesi için önemlidir. Tez çalışmasının ilk aşamasında, ampirik ve sonlu elemanlar yaklaşımı kullanılarak, sınır koşullarının kirişli metal panellerin burkulma katsayıları üzerindeki etkisi incelenmiştir. Ampirik yaklaşımlar, panellerin klasik sınır koşulları ile sınırlandırılmıştır. Aksine, sonlu elemanlar analizi daha doğru fakat zaman bakımından maliyetlidir. Sonlu elemanlar analizi ile kurulacak olan yapay sinir ağı ve yüzey tepki yöntemi kullanılarak, seçilen kabuk-kiriş kombinasyonlarının burkulma katsayılarını hızlı bir şekilde hesaplamak için bir veri tabanı hazırlanmıştır. Çalışmanın ikinci aşamasında, kirişli panellerde burkulma sonrası yükün yeniden dağılımı karşılaştırmalı bir çalışma sunulmuştur. Yapılan çalışma da yapı doğrusal ve doğrusal olmayan malzeme kullanılarak modellenmiştir. Panelin etkin genişliği, modelin sonlu elemanların analiziyle belirlenen yük dağıtımını kullanarak, malzemenin doğrusal olan ve olmayan yapının burkulmasından hemen önce hesaplanmıştır. Ek olarak sonlu

elemanların analizi ile hesaplanan etkin genişlik, klasik etkin genişlik formülüyle karşılaştırılmıştır. Çalışmanın son aşamasında, sonlu elemanlar yaklaşımı ve analitik yaklaşım kullanılarak kompozit düz plakaların burkulması incelenmiştir. Kompozit düz panellerin burkulma katsayıları çeşitli geometrik özellikleri, sınır koşulları, tabaka kalınlıkları ve dizilişi kullanılarak karşılaştırılmalı bir çalışma yapılmıştır. Çalışmanın sonunda, her tabaka dizilişi ve sınır koşulları için burkulma grafikleri, sonlu elemanlar analiz sonuçları kullanılarak üretilmiştir.

Anahtar Sözcükler: Metal Burkulma, Güçlendirilmiş Paneller, Kompozit Burkulma, Etkin genişlik, Yapay Sinir Ağı, Sonlu Elemanlar Analizi

To My Mother

ACKNOWLEDGMENTS

The author would like to express his sincere gratitude to his supervisor Prof. Dr. Altan Kayran for his advice, criticism, and excellent guidance throughout the study.

The author also thanks to Assoc. Prof. Dr. Ercan Gürses, Assoc. Prof. Dr. Demirkan Çöker, Assoc. Prof. Dr. Melin Şahin and Asst. Prof. Dr. Barış Sabuncuoğlu for their decent contributions to this study.

I would like to thank my family for their motivation and support.

I also wish to express my gratitude to my lover Özgün Memioğlu; for her understanding and continuous encouragement throughout my study and through the process of this research and writing.

There are many people who have significantly helped to this study so far; therefore, the author feels glad about the contribution of each one of them, whose names are not written here.

TABLE OF CONTENTS

ABSTRACT	v
ÖZ	vii
DEDICATION	ix
ACKNOWLEDGMENTS.....	x
TABLE OF CONTENTS	xi
LIST OF TABLES	xiv
LIST OF FIGURES	xvi
LIST OF ABBREVIATIONS	xxiii
CHAPTERS	
1. INTRODUCTION.....	1
1.1. Motivation of the Study	1
1.2. Scope of the Study	5
1.3. Content of the Study	6
1.4. Literature Survey	7
2. BUCKLING OF STIFFENED METALLIC FLAT PANELS	19
2.1. Buckling Analysis of Unstiffened Panels	20
2.2. Buckling Analysis of Stiffened Panels	29
2.2.1. Determination of buckling coefficients of skin-stringer assemblies by finite element analysis.....	29

2.2.2.	Setting up of Artificial Neural Network and Response Surface for fast determination of buckling coefficients.....	37
2.2.3.	Comparison of buckling coefficients of skin-stringer assemblies determined by FEA, Response Surface and Artificial Network	49
3.	POST BUCKLING LOAD DISTRIBUTION OF METAL STIFFENED PANELS.....	57
3.1.	Buckling Analysis of the Baseline Skin-Stringer Assembly	58
3.2.	Post-Buckling Analysis of Skin-Stringer Assembly using Linear and Non-linear Material Models	63
3.3.	Calculation of Effective Width by Finite Element Solution and Empirical Solution	68
3.4.	Effect of Stringer Section Types on the Post-Buckling Stage	75
3.4.1.	Skin-Stringer Assembly with J Section Stringer	76
3.4.2.	Skin-Stringer Assembly with Z Section Stringer	83
3.5.	Comparison of Load Carrying Capacity, Load Distribution and Effective Width of Skin-Stringer Assemblies with Three Different Stringer Types.....	100
4.	COMPOSITE PLATE BUCKLING	105
4.1.	Classical and First-Order Laminate Theories of Composite Plate.....	106
4.1.1.	Classical Laminated Plate Theory (CLPT).....	106
4.1.2.	First Order Shear Deformation Theory (FSDT).....	110
4.2.	Analysis of Specially Orthotropic Plates under Uniaxial Compressive Load using CLPT and FSDT	114
4.2.1.	CLPT	115
4.2.2.	FSDT	119
4.3.	Finite Element Model of Composite Plates	125

4.4. Comparison of Buckling Coefficient Curves obtained by CLPT, FSDT and FEA	134
5. CONCLUSION AND FUTURE WORK.....	145
REFERENCES.....	151
APPENDICES	
A. PROCEDURE OF LINEAR BUCKLING ANALYSIS	157
B. MATERIAL PROPERTIES ALUMINUM 2024 T3 CLAD SHEET.....	159
C. LOCAL BUCKLING STRINGERS IN SKIN-STIFFENER ASSEMBLIES	163
D. ELASTIC COEFFICIENT AND COMPLIANCE MATRICES AND GOVERNING EQUILIBRIUM EQUATIONS OF COMPOSITE PLATES	165
D.1 Elastic Coefficient and Compliance Matrices of Composite Plates	165
D.2 Governing Equations of Composite Plates	168
E. MATERIAL PROPERTIES HEXPLY 8552 AS4	173
F. SCRIPTS	175
F.1 Linear Metal Single Panel Buckling Python Scripts	175
F.2 Linear Metal Stiffened Panel Buckling Python Scripts	181
F.3 ANN Matlab Script.....	193
F.4 Metal Stiffened Panel Post-Buckling Python Scripts	196
F.5 Composite Single Panel Buckling Python Scripts.....	226

LIST OF TABLES

TABLES

Table 2.1: Definition of the constraints for the simply supported panel.....	21
Table 2.2: Definition of the constraints for the clamped panel.....	21
Table 2.3: Material Properties of Aluminum 2024-T3 Clad Sheet.....	22
Table 2.4: Input parameters of the skin panels used in script.....	22
Table 2.5: Critical buckling stress results for various element sizes.....	26
Table 2.6: Input parameters of the skin-stringer assembly used in the finite element model.....	33
Table 2.7: FEA input parameters for additional analyses for skin-stringer assemblies with 'J' type stringer.....	49
Table 2.8: Buckling coefficients of skin-stringer assemblies with J type stringers / FEA results/ RS results / ANN results.....	50
Table 2.9: FEA input parameters for additional analyses for skin-stringer assemblies with 'Z' type stringer.....	51
Table 2.10: Buckling coefficients of skin-stringer assemblies with Z type stringers / FEA results/ RS results / ANN results.....	52
Table 2.11: FEA input parameters for additional analyses for skin-stringer assemblies with 'T' type stringer.....	53
Table 2.12: Buckling coefficients of skin-stringer assemblies with T type stringers / FEA results/ RS results / ANN results.....	54
Table 3.1: Input parameters of the unstiffened skin panel used to verify stiffened panel edge condition.....	59

Table 3.2: Parameters of the skin-stringer assembly used in the finite element model with I section stringer	62
Table 3.3: Comparison of the effective widths (I-section stringer)	75
Table 3.4: Parameters of the skin-stringer assembly used in the finite element model with J section stringer.....	77
Table 3.5: Comparison of the effective widths (J-section stringer).....	83
Table 3.6: Parameters of the skin-stringer assembly used in the finite element model with Z section stringer.....	84
Table 3.7: Comparison of the effective widths (Z-section stringer)	92
Table 3.8: Parameters of the skin-stringer assembly used in the finite element model with Z_2 section stringer	93
Table 3.9: Comparison of the effective widths (Z_2 -section stringer).....	100
Table 3.10: Comparison of the effective widths with Three Different Stringer Types	102
Table 4.1: Material properties of HexPly 8552 AS4 composite plate	126
Table 4.2: Input parameters of the example composite plates used in comparison .	129
Table 4.3: Thin and thick composite plates thickness and stiffness properties	130
Table 4.4: Buckling load parameters of composite plates used in comparison	130
Table B.1: True stress-strain data of Aluminum 2024 T3 clad sheet [36] [39]	160
Table B.2 Continued	161
Table D.1: Typical shear correction coefficient [49]	167

LIST OF FIGURES

FIGURES

Figure 1.1: Thin fuselage stiffened panel.....	2
Figure 1.2: Load distribution in the skin-stringer assembly before and after buckling [1]	4
Figure 1.3: Top view of compressive loaded skin-stringer assembly	12
Figure 1.4: Load distribution before the panel buckling [1]	12
Figure 1.5: Load distribution after the panel buckling [1]	12
Figure 2.1: Definition of different geometrical parameters of the flat panels and the coordinate system.....	20
Figure 2.2: Compressive load demonstration for the single panel case	23
Figure 2.3: Shear load demonstration for the single panel case.....	23
Figure 2.4: View of sample single panel model with all edges simply supported under compressive loading	24
Figure 2.5: The critical buckling stress with respect to element number of flat panel	25
Figure 2.6: Comparison of compressive buckling charts for flat rectangular panels with simply supported loaded and unloaded edges	27
Figure 2.7: Comparison of compressive buckling charts for flat rectangular panels with clamped loaded and unloaded edges	27
Figure 2.8: Comparison of shear buckling charts for flat rectangular panels with simple supported loaded and unloaded edges	28
Figure 2.9: Comparison of shear buckling charts for flat rectangular panels with clamped loaded and unloaded edges	28

Figure 2.10: Isometric view of skin-stringer assembly analyzed.....	30
Figure 2.11: Constraint configuration of the skin-stringer assembly.....	30
Figure 2.12: Cross section view of skin-stringer assembly analyzed	31
Figure 2.13: Isometric view of skin-stringer assembly with mesh	31
Figure 2.14: Fastener pattern configuration on the stringer	32
Figure 2.15: Stringer section types used in skin-stringer assemblies	35
Figure 2.16: Configuration of artificial neural network.....	38
Figure 2.17: Performance plot of the ANN for skin-J type stringer assembly	40
Figure 2.18: Performance plot of the ANN for skin-Z type stringer assembly.....	41
Figure 2.19: Performance plot of the ANN for skin-T type stringer assembly.....	42
Figure 2.20: Overall, training, validation and testing regression plots of the ANN for skin-J type stringer assembly	43
Figure 2.21: Overall, training, validation and testing regression plots of the ANN for skin-Z type stringer assembly	44
Figure 2.22: Overall, training, validation and testing regression plots of the ANN for skin-T type stringer assembly	45
Figure 2.23: Number of validation fails, mu and gradient with respect to number of training iterations of ANN for skin-J type stringer assembly	46
Figure 2.24: Number of validation fails, mu and gradient with respect to number of training iterations of ANN for skin-Z type stringer assembly	47
Figure 2.25: Number of validation fails, mu and gradient with respect to number of training iterations of ANN for skin-T type stringer assembly	48
Figure 3.1: Baseline skin-stringer assembly	60
Figure 3.2: Constraints applied to the baseline skin-stringer assembly	61
Figure 3.3: Edge descriptions of the skin-stringer assembly	64
Figure 3.4: Load displacement curve of the skin-stringer assembly with linear material model (I section stringer)	65
Figure 3.5: Load displacement curve of the skin-stringer assembly with nonlinear material model (I section stringer)	66

Figure 3.6: FE view of skin-stringer assembly with nonlinear material model (I section stringer) at local buckling starting point	66
Figure 3.7: FE view of skin-stringer assembly with nonlinear material model (I section stringer) at collapse point	67
Figure 3.8: Comparison of load displacement curves of models with linear and nonlinear material properties (I section stringer section).....	67
Figure 3.9 Top view of skin-stringer assembly under compressive loading.....	68
Figure 3.10: Actual load distribution in the post-buckled stage [1].....	69
Figure 3.11: Equivalent load distribution using the concept of effective width [1]... ..	69
Figure 3.12: Load distribution in the skin-stringer assembly with the linear material model just before the skin buckling (I section stringer).....	70
Figure 3.13: Load distribution in the skin-stringer assembly with the linear material model at the collapse displacement (1.736 mm) of the nonlinear material model case (I section stringer)	71
Figure 3.14: Closed view of load distribution in the skin-stringer assembly with the linear material model at the collapse displacement (1.736 mm) of the nonlinear material model case (I section stringer)	71
Figure 3.15: Load distribution in the skin-stringer assembly with the nonlinear material property just before the skin buckling (I section stringer)	72
Figure 3.16: Load distribution in the skin-stringer assembly with nonlinear material property at the collapse displacement of 1.736 mm (I section stringer)	73
Figure 3.17: Comparison of the load distribution in the skin-stringer assemblies with linear and nonlinear material properties (I section stringer)	73
Figure 3.18: Stringer section types used in this study	76
Figure 3.19: Load displacement curve of the skin-stringer assembly with linear material model (J section stringer)	78
Figure 3.20: Load displacement curve of the skin-stringer assembly with nonlinear material model (J section stringer)	79
Figure 3.21: Load distribution in the skin-stringer assembly with the linear material model just before the skin buckling (J section stringer).....	79

Figure 3.22: Load distribution in the skin-stringer assembly with the linear material model the collapse displacement (1.726 mm) of the nonlinear material model case (J section stringer).....	80
Figure 3.23: Load distribution in the skin-stringer assembly with the nonlinear material model just before the skin buckling (J section stringer)	81
Figure 3.24: Load distribution in the skin-stringer assembly with the nonlinear material model at the collapse displacement of 1.726 mm (J section stringer)	81
Figure 3.25: Comparison of the load distribution of skin-stringer assemblies with linear and nonlinear material properties (J-section stringer).....	82
Figure 3.26: Single and double fastener configurations with Z section stringer	83
Figure 3.27: Load-displacement curve of the skin-stringer assembly with linear material model (Z section stringer)	85
Figure 3.28: Buckled shape of mid panel before and after views of second drop point	86
Figure 3.29: Load displacement curve of the skin-stringer assembly with nonlinear material model (Z section stringer)	87
Figure 3.30: Comparison of load displacement curves of models with linear and nonlinear material properties (Z section stringer).....	87
Figure 3.31: Load distribution in the skin-stringer assembly with the linear material model just before the skin buckling (Z-section stringer)	88
Figure 3.32: Load distribution in the panel with the linear material model at the compressive collapse displacement of 0.823 mm (Z- section stringer).....	89
Figure 3.33: Load distribution of the model with nonlinear material property just before the skin buckling (Z-section stringer).....	89
Figure 3.34: Load distribution of the model with nonlinear material property at the compressive displacement of 0.823 mm (Z stringer section type).....	90
Figure 3.35: Comparison of load distribution of models with linear and nonlinear material properties (Z-section stringer).....	91
Figure 3.36: Load-displacement curve of the skin-stringer assembly with linear material model (Z ₂ section stringer).....	94

Figure 3.37: Load displacement curve of the skin-stringer assembly with nonlinear material model (Z_2 section stringer).....	95
Figure 3.38: Comparison of load displacement curves of models with linear and nonlinear material properties (Z_2 section stringer).....	96
Figure 3.39: Load distribution in the skin-stringer assembly with the linear material model just before the skin buckling (Z_2 -section stringer)	96
Figure 3.40: Load distribution in the panel with the linear material model at the compressive collapse displacement of 1.637 mm (Z_2 -section stringer).....	97
Figure 3.41: Load distribution of the model with nonlinear material property just before the skin buckling (Z_2 -section stringer).....	97
Figure 3.42: Load distribution of the model with nonlinear material property at the compressive displacement of 1.637 mm (Z_2 stringer section type)	98
Figure 3.43: Comparison of load distribution of models with linear and nonlinear material properties (Z_2 -section stringer)	99
Figure 3.44: Comparison of load carrying capacity of skin-stringer assemblies with I, J, Z and Z_2 section stringers (Nonlinear material properties)	101
Figure 3.45: Comparison of load distribution of skin-stringer assemblies with I, J, Z and Z_2 section stringers (Nonlinear material properties)	101
Figure 4.1: Undeformed and deformed geometries of an edge of a plate under the Kirchhoff assumptions [41].....	107
Figure 4.2: Undeformed and deformed geometries of an edge of a plate under the assumptions of the first-order plate theory [43]......	111
Figure 4.3: Plate with uniaxial compression load [41].....	115
Figure 4.4: Definition of different geometrical parameters of the composite panels and the coordinate system	125
Figure 4.5: Compressive buckling coefficients for composite plates with simply supported loaded and unloaded edges (Ply orientation: $0^\circ/0^\circ S$).....	131
Figure 4.6: Compressive buckling coefficients for composite plates with simply supported loaded and unloaded edges (Ply orientation: $0^\circ/90^\circ S$).....	131

Figure 4.7: Compressive buckling coefficients for composite plates with simply supported loaded and unloaded edges (Ply orientation: $45^\circ/0^\circ/-45^\circ/90^\circ S$).....	132
Figure 4.8: Compressive buckling coefficients for composite plates with clamped loaded and unloaded edges (Ply orientation: $0^\circ/0^\circ S$)	132
Figure 4.9: Compressive buckling coefficients for composite plates with clamped loaded and unloaded edges (Ply orientation: $0^\circ/90^\circ S$)	133
Figure 4.10: Compressive buckling coefficients for composite plates with clamped loaded and unloaded edges (Ply orientation: $45^\circ/0^\circ/-45^\circ/90^\circ S$).....	133
Figure 4.11: Compare of compressive buckling coefficients with all edges simply supported (Ply orientation: $0^\circ/0^\circ S$, thickness of plate=1.04 mm)	134
Figure 4.12: Compare of compressive buckling coefficients with all edges simply supported (Ply orientation: $0^\circ/0^\circ S$, thickness of plate=2.08 mm)	135
Figure 4.13: Compare of compressive buckling coefficients with all edges simply supported (Ply orientation: $0^\circ/90^\circ S$, thickness of plate=1.04 mm)	135
Figure 4.14: Compare of compressive buckling coefficients with all edges simply supported (Ply orientation: $0^\circ/90^\circ S$, thickness of plate=2.08 mm)	136
Figure 4.15: Compare of compressive buckling coefficients with all edges simply supported (Ply orientation: $45^\circ/0^\circ/-45^\circ/90^\circ S$, thickness of plate=2.08 mm)	136
Figure 4.16: Compare of compressive buckling coefficients with all edges simply supported (Ply orientation: $45^\circ/0^\circ/-45^\circ/90^\circ S$, thickness of plate=4.16 mm)	137
Figure 4.17: Compare of compressive buckling coefficients with all edges clamped (Ply orientation: $0^\circ/0^\circ S$, thickness of plate=1.04 mm)	137
Figure 4.18: Compare of compressive buckling coefficients with all edges clamped (Ply orientation: $0^\circ/0^\circ S$, thickness of plate=2.08 mm)	138
Figure 4.19: Compare of compressive buckling coefficients with all edges clamped (Ply orientation: $0^\circ/90^\circ S$, thickness of plate=1.04 mm)	138
Figure 4.20: Compare of compressive buckling coefficients with all edges clamped (Ply orientation: $0^\circ/90^\circ S$, thickness of plate=2.08 mm)	139
Figure 4.21: Compare of compressive buckling coefficients with all edges clamped (Ply orientation: $45^\circ/0^\circ/-45^\circ/90^\circ S$, thickness of plate=2.08 mm)	139

Figure 4.22: Compare of compressive buckling coefficients with all edges clamped (Ply orientation: $45^\circ/0^\circ/-45^\circ/90^\circ S$, thickness of plate=4.16 mm)	140
Figure 4.23: Compare of compressive buckling coefficients with all edges simply supported at the same plate thickness (2.08 mm).....	140
Figure 4.24: Compare of compressive buckling coefficients with all edges clamped at the same plate thickness (2.08 mm)	141
Figure 4.25: Example view of first buckled mode shape of plate with all edges simply supported (Ply orientation: $0^\circ/0^\circ S$, thickness of plate=2.08 mm).....	142
Figure 4.26: Example view of first buckled mode shape of plate with all edges simply supported (Ply orientation: $0^\circ/90^\circ S$, thickness of plate=2.08 mm)	143
Figure 4.27: Example view of first buckled mode shape of plate with all edges simply supported (Ply orientation: $45^\circ/0^\circ/-45^\circ/90^\circ S$, thickness of plate=2.08 mm).....	143
Figure B.1: Material properties of aluminum 2024 T3 clad sheet [36].....	159
Figure B.2: True stress-strain graph of Aluminum 2024 T3 clad sheet [36] [39]....	160
Figure C.1: Buckling factors for several edge conditions [1]	164
Figure D.1: Cross section view of a laminate	167
Figure D.2: A differential element with in-plane force resultants [42].....	168
Figure D.3: A differential element with moment resultants, shear force resultants and applied transverse forces [42]	169
Figure D.4: Force projection of in-plane normal and shear forces in the z direction [50]	170
Figure E.1: Material properties of HexPly 8552 AS4 at dry and room temperature [51]	173

LIST OF ABBREVIATIONS

ANN	Artificial neural network
A_{eff}	Area under the load distribution curve of skin
CLPT	Classical laminated plate theory
E	Elastic modulus
E_c	Compressive elastic modulus
F_{crip}	Stringer crippling allowable stress
F_{cy}	Yield compressive allowable stress
F_{lb}	Stringer local buckling allowable stress
F_{max}	Skin maximum stress in the post-buckling stage
F_{str}	Stringer Stress
F_{tu}	Tensile ultimate allowable stress
FE	Finite element
FEA	Finite element analysis
FEM	Finite element model
FSDT	First order shear deformation theory
k	Buckling coefficient
k_{eff}	Effective width constant
l_{lf}	Lower flange width of stringer
l_x	Skin length in the x direction
l_y	Skin length in the y direction
mm	Millimeter
MPa	Megapascal
n_c	Ramberg-Osgood factor of plasticity in compression
N	Newton

N_{app}	Compressive shell edge load
NACA	National advisory committee for aeronautics
NASA	National aeronautics and space administration
RS	Response surface
t	Skin thickness
u_{FE}	Applied displacement
u_{cr}	Critical displacement
ν	Poisson ratio
w_{eff}	Effective width of skin
σ_{cr}	Critical buckling stress
λ_{FE}	First eigenvalue obtained from finite element analysis

CHAPTER 1

INTRODUCTION

1.1. Motivation of the Study

Stiffened thin panels are very common and vital structural elements in aerospace structures because of the weight and stiffness advantages that they provide. Stiffened panels, as shown in Figure 1.1, are built by thin walled panels supported by stiffeners. Up to 1980s, stiffened panels are only made from Aluminum material. The reason is the construction of aluminum based structure is feasible by verified design methods, validated analysis tools with an enormous measure of test outputs. In addition, aluminum based structures' strength properties and failure scenarios are studied since the end of the eighteenth century. However, in recent decades, advanced materials like fibrous carbon composites have attracted great interest for use in aerospace industry owing to their favorable properties, such as high specific strength and stiffness. For the last thirty years, through the onset of composite materials, many studies have been performed to replace the conventional aluminum based shell structure with composite materials.

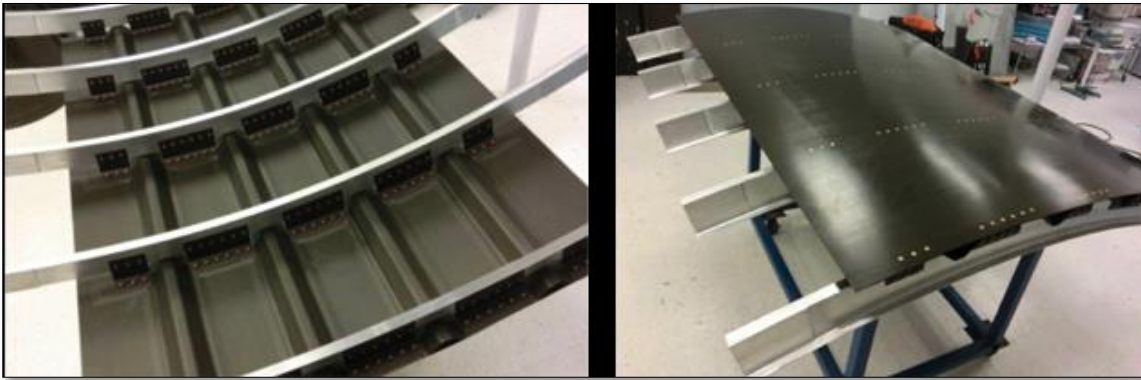


Figure 1.1: Thin fuselage stiffened panel

However, independent of the material strength, stiffened panel configurations in the aviation industry tends to buckle because of the thin panels. The main reason of panel buckling is the compressive stresses in the stiffened thin panels. Due to the compressive stresses, thin panels may buckle long before the limit load of the panel. Therefore, local buckling is usually allowed in the design of the aerospace structures. Once the critical buckling load is reached, the panel is incapable of supporting any further load, and stiffeners carry the additional loads which the buckled panel cannot resist. Hence in the aerospace industry, stiffeners are designed to support panels when panel buckling is encountered. Therefore, determination of buckling load of panels and the post-buckling behaviour of skin-stringer assemblies have become important topics to design an aircraft vehicle.

The stiffener section is also important to determine the support condition that the stiffener provides on the unloaded edges of the panel. Even though, a lot of similar studies about linear metal buckling have been performed in aircraft industry, this research is done because of the lack of the investigation about the stringer section effect on the linear metal buckling. In the literature, analytical solutions obtained using classical boundary conditions allowed for the preparation of buckling coefficient charts with various loading conditions. However, in reality, neither simply supported nor clamped conditions are sufficient to describe the behavior of the true edge condition of stiffened panels, because the actual stiffener provides a condition which is in between these two. Therefore, buckling coefficient graphs provided in the

literature are not sufficient to use effectively in aerospace structures which predominantly have stiffened thin walled panels. To have an optimum skin-stringer assembly design, the structure must be modelled with the correct boundary conditions.

Post buckling behaviour of skin-stringer assemblies is also very crucial in aerospace structures since local buckling of panels may be allowed in some design practices. As mentioned before, once the critical buckling load is reached, the skin of a stiffened panel loses its load carrying capacity and stiffeners carry the additional loads which the buckled skin cannot carry. Besides the stiffeners, the effective section of the skin panel also carries small proportion of the load applied, but depending on the skin-stringer assembly the load carried by the skin varies. Load carrying capacity of a stiffened panel is significantly affected by the design of the skin-stringer assembly. Until the local buckling of the skin, both middle portion of skin and skin part at the stringer location have the same stress level. After the local buckling of the skin panel, which is referred to as the post-buckling stage, stress distribution over the skin panel is nonlinear. Because of the buckled skin, that is no longer effective to carry the additional compressive load, the additional load is redistributed to the adjacent stiffer structural members which are stringers and frames in semi-monocoque structures. Figure 1.2 shows the actual load distribution over the panel before, after buckling and equivalent load distribution over the panel after buckling. In the classical approach, in order to handle the non-uniform load over the skin panel after buckling, equivalent width concept has been used commonly. Equivalent width pertains to the part of the skin that is assumed to carry the uniform load. However, in this method, effect of material nonlinearity is not taken into consideration. Same as the linear buckling method, classical boundary condition assumption is made in the literature in conjunction with the effective width method. However, in reality, classical boundary conditions are not sufficient to describe the behavior of the true edge condition of stiffened panels, because the actual stiffener provides a condition which is in between these two. Therefore, effective width formulation provided in the literature is not sufficient to use effectively in aerospace structures. To measure the true load capacity of the skin-stringer assembly design, the structure must be modelled with the correct boundary conditions in the post-buckling stage.

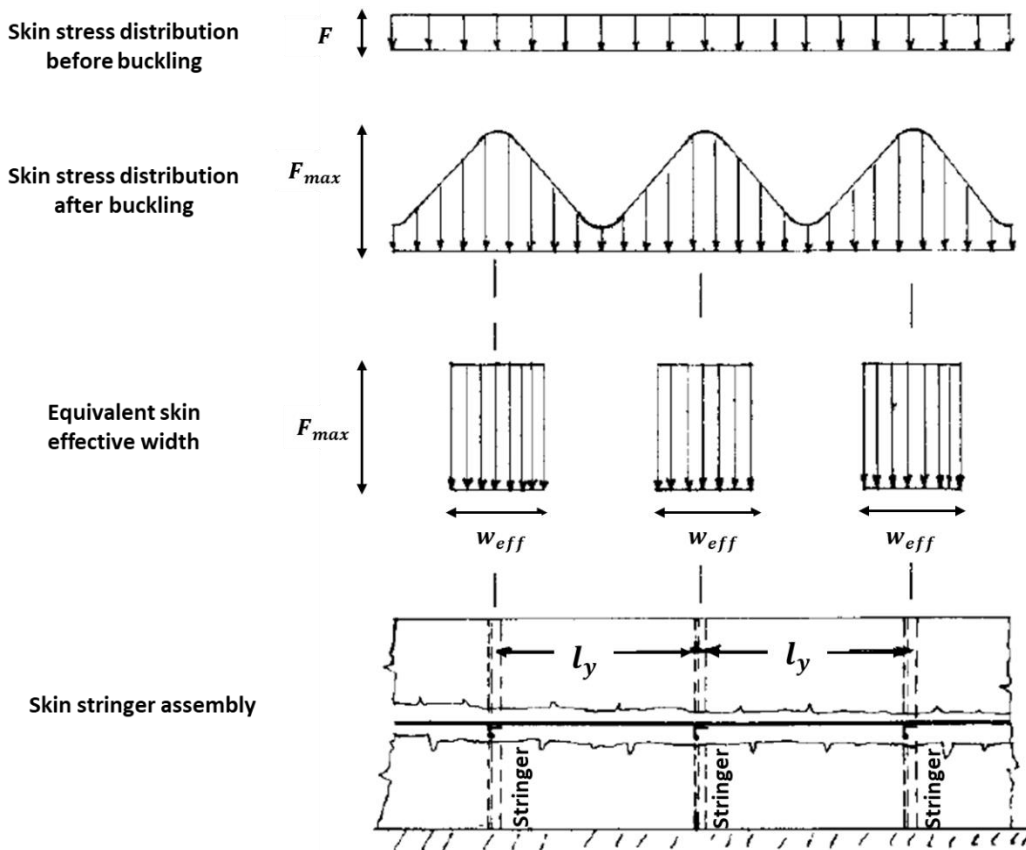


Figure 1.2: Load distribution in the skin-stringer assembly before and after buckling [1]

Furthermore, for composite panels, buckling charts are required to for faster evaluation of buckling response of composite panels. To save the time in the aviation industry, parametric studies has to be done for specific configurations which are commonly used in this industry.

1.2. Scope of the Study

In this study, the two parts of this research focuses on the buckling and post-buckling behaviour of the unstiffened and stiffened panels applied to uniaxial compressive loadings. In the first part of the research, a database is prepared for the buckling coefficients of the selected skin-stringer combinations. Then, the differences between the buckling coefficients of the real skin-stringer geometries and the analytically determined buckling coefficients which rely on classical boundary conditions are identified. Created database is processed with the ANN and RS methods to reach the result quickly compare to finite element analysis. In the second part of the research, load distribution of the skin-stringer assembly in the post-buckling stage is investigated. Stringer section effect on the load distribution and load capacity of the skin-stringer assembly is the main objective of the second part of the thesis study. In the third part of the thesis, buckling coefficient charts for unstiffened composite panels are obtained. To restrict the panel edges, classical boundary conditions are used in the modelling of the unstiffened panel. In this part, each chart has a specific laminate orientation. These charts are obtained with 3 different methods. These methods are the classical laminate plate theory (CLPT), first order shear deformation theory (FSDT) and finite element analysis. Analytical methods' results are compared with the finite element results in this part.

1.3. Content of the Study

- In Chapter 2, brief information about buckling formulation and buckling procedure in finite element analysis are given. Buckling phenomenon for unstiffened panels is explained and the buckling coefficient graphs are described. Determination of buckling coefficients of unstiffened panels with classical boundary conditions by finite element analysis is described. After the verification of unstiffened panel boundary conditions with analytical solution, stiffened panel modelling is explained. Using this modelling technique, 2000 analysis are done for each stringer section type. At the end of the chapter, artificial neural network and response surface for fast determination of buckling coefficients are constructed.
- In Chapter 3, firstly, brief information about post-buckling stage is given. In addition, determination of the baseline skin-stringer assembly is explained. Then, post-buckling analysis of skin-stringer assemblies using linear and nonlinear material models is studied. Methodology of effective width calculation by the finite element solution and empirical solution is presented. At the end of the chapter, results for different stringer section types are presented.
- In the Chapter 4, firstly, brief information and formulation about the classical laminated plate theory (CLPT) and the first order shear deformation theory (FSDT) is given. Buckling analysis of specially orthotropic plates under the compressive load using CLPT and FSDT is explained. Finite element model of the composite plates is described. Using the finite element model results, buckling coefficient charts are obtained for each ply orientation and thickness of composite plates. Finally, buckling results obtained by the CLPT and FSDT theories are presented and comparisons are made with finite element results.
- In the Chapter 5, the results are discussed. In addition, summary and the future work of the study are given in this part.

1.4. Literature Survey

Stiffened thin panel configuration is considered to be very efficient way to carry the loads in aerospace structures because of the weight and stiffness advantages they provide. Accurate analysis of buckling and post-buckling behaviour of skin-stringer assemblies used in aerospace structures is very crucial, because local buckling is permitted in some designs practices of aerospace structures.

In the first and second phases of the thesis study, buckling and post buckling behaviour of the stiffened thin panel with metallic material properties are investigated. In the literature, there are many studies about buckling and post buckling phenomena. A few of them are mentioned in this sub-chapter.

In theory, buckling refers to the loss of stability of a component and it is commonly independent from the material strength. In practically, due to compressive stresses in the stiffened thin panel, thin panel may be buckled long before the limit load of the panel. Therefore, local panel buckling is usually allowed in the design of the aerospace structures.

Study about the plate buckling started in the early of the 19th century. Claude-Louis Navier derived the stability equation for a rectangular thin plate. This derivation is based on Gustav Robert Kirchhoff assumptions in 1822 [2]. In 1891, the critical buckling stress equation for a rectangular thin plate with simply supported edge condition under uniaxial compression load is formulated by Bryan [2]. In his study, energy method is used to determine the critical load. One of the known detailed study about the buckling is written in the NACA Handbook of Structural Stability document [3]. This handbook presents a rather comprehensive review and compilation of theories and experimental data relating to the buckling phenomena. The various factors governing the buckling of flat plates are reviewed and results are summarized in comprehensive series of charts and tables in this handbook. In 1925, Timoshenko [4] also solved the same problem using another method. He assumed the plate to be buckled into several sinusoidal half waves in the direction of compression. He also explored the buckling of uniformly compressed rectangular plates that are simply

supported along the edges perpendicular to the direction of applied load and other two edges subjected to various end conditions. Results have been reported in standard texts [4, 5, 6].

In the aerospace industry, stiffeners are designed to support panels when panel buckling is encountered. The stiffener section is important to determine the support condition that the stiffener provides on the unloaded edges of the panel. In the literature, analytical solutions obtained using classical boundary conditions allowed for the preparation of buckling coefficient charts with various loading conditions [1]. These charts also show the change in buckled shape as the boundary conditions are altered on the unloaded edges from free to fully restraint condition. Classical boundary conditions are commonly known as free, simply supported and clamped. In reality, neither simply supported nor clamped conditions are sufficient to describe the behavior of the true edge condition of stiffened panels, because the actual stiffener provides a condition which is in between these two.

In airframe structural design data book [6], various wing design loads are given as shears, bending moments and torsion which results from air pressures and inertia loadings. In addition to these types of loads, buckling coefficients are given for each boundary conditions and geometric panel description.

In the study of the Paul et al. [2], a standard transport aircraft wing is considered and buckling analysis is carried out. The initial design is found to buckle. So, several design modifications were made to make the design safe against buckling. In this study, FE analysis and theoretical study are performed to get realistic results in the wing buckling analysis. Yu [7] has studied the buckling behavior of rectangular plates subjected to intermediate and end loads. He considered both elastic buckling and plastic buckling behavior of plates. Plate considered is simply supported along two opposite edges that are parallel to the direction of applied loads. The two edges may take any other combination of clamped, simply supported and free edge boundary conditions. Study also investigates the effect of various plate aspect ratios, intermediate load positions, boundary conditions on buckling factors [7]. In the study of the Muameleci [8], linear and nonlinear buckling analyses of plates with and without

cut-out using finite element method are investigated. Various classical boundary conditions and loading conditions are used to model the shear web beam structures. The main point of this study is to investigate the buckling behaviour of plates but also the capabilities of the MSC Nastran and ABAQUS finite element tools for performing linear and nonlinear buckling analyses. Riks [9] has applied finite strip method for the calculation of the buckling load of stiffened panels in wing box structures. This article describes the implementation of the finite strip method. The finite strip method extends the scope of the analysis of the determination of the post buckling stiffness of the panels. Finite strip model (one dimensional) is the simplification of finite element model (two dimensional). Some of the computer implementations of the finite strip method are BUCLASP [10] and VIPASA [11]. In the study of Riks, the method used for the analysis of the finite strip model is PANBUCK which has the ability to analyze the initial post buckling behavior too.

In the literature, there have been many studies on the post-buckling behaviour of skin-stringer assemblies. The paper of Murphy [12] reports on the development of a modeling approach to increase the accuracy of the global model, accounting variations in stiffness due to nonlinear structure behavior. In the study of Lync and Sterling [13], a finite element methodology has been presented for the compressive post-buckling. In this study, test data are compared to results of four different finite element modelling approaches for the skin-stringer assembly. Moreover, in the study of Weimin et al. [14], experimental and analytical study results of post buckling simulation of an integral aluminum fuselage stiffened panel have been presented. In this study, load is applied as axial compression load and the panel is a curved panel. Rhodes [15] examined some of the research on the elastic and plastic post-buckling behaviour of plates and plate like structures. In this study, post buckling behaviour of individual thin plates is governed by non-linear differential equations set up by Von Karman. In the study of the Eirik Byklum et al. [16], a computational model for the analysis of global buckling and post-buckling of stiffened panels has been derived. The model was developed as part of a tool for buckling phenomenon of stiffened panels. It is formulated using large deflection plate theory and energy principles. Deflections are assumed in the form of trigonometric function series. In addition, the principle of

stationary potential energy is used for deriving the equilibrium equations. For the loading case, lateral pressure is accounted for by taking the deflection as a combination of a clamped and a simply supported deflection mode. The global buckling model is based on Marguerre's nonlinear plate theory, by deriving a set of anisotropic stiffness coefficients to account for the plate stiffening. Local buckling is treated in a separate local model developed. The anisotropic stiffness coefficients used in the global model are derived from the local analysis. Together, the two models provide a tool for buckling phenomena of stiffened panels. Any combination of biaxial in-plane compression or tension, shear, and lateral pressure are analyzed in this study. The procedure is semi-analytical in the sense that all energy formulations are derived analytically, while a numerical method is used for solving the resulting set of equations, and for incrementing the solution. The load deflection curves produced by the proposed model are compared with results from nonlinear FEM. In the study of the Kopecki et al. [17], the results of experiments and numerical analyses of thin-walled shells used as components of aircraft structures are presented. In this study, integral ribs are used to stiffen the structure. A comparative analysis has been carried out between the suggested design solution and the reference structure. In the experimental part of the study, an optical scanner with digital image correlation has been used. Nonlinear numerical analyses have been carried out with the use of software based on the finite element method. The suggested method for verifying the results of non-linear numerical analysis by applying the principle of equivalent solutions seems to be effective, and the obtained results are sufficiently credible. This constituted the foundation for carrying out an initial comparative analysis of the physical properties of the load-bearing structures in question. In the light of this analysis, the solution based on the use of integral ribs seems to be very promising from the point of view of its application in load-bearing aircraft structures.

The study of the Graciano et al. [18] is aimed at studying the influence of initial geometric imperfections on the post-buckling behavior of longitudinally stiffened plate girder webs subjected to patch loading. A sensitivity analysis is conducted herein using two approaches (deterministic and probabilistic) in order to investigate the effect of imperfection shape and amplitude on both, the post-buckling response and ultimate

strength of plate girders under patch loading. According to the results from the deterministic approach, the amplitude of the imperfections in most cases leads to a reduction in patch loading resistance. This sensitivity analysis is performed by means of nonlinear finite element analysis. At first, the initial shape imperfections are modeled using the buckling mode shapes resulting from an eigenvalue buckling analysis. Afterwards, the amplitude of the buckling shapes for the various modes is varied, and then introduced in the nonlinear analysis. The results also showed a more complex interaction between the imperfection shapes and the computed resistances. Nevertheless, the shape of the initial imperfection that results in the lowest strength for a girder differs for each size of imperfection and stiffener location. It is also important to point out that initial imperfection for patch loaded girder webs can be modeled using a shape resembling either the first eigen mode or a sinus-wave.

Load carrying capacity of a stiffened panel is vital topic and significantly affected by the design of the skin-stringer assembly. Until the local buckling of the skin, both skin and stringers have the same stress level. After the local buckling of the skin panel, which is referred to as the post-buckling stage, stress distribution over the stiffened panel is nonlinear. Because of the buckled skin, that is no longer effective to carry the additional compressive load, the additional load is redistributed to the adjacent stiffer structural members which are the stringers and frames in semi-monocoque structures. Figure 1.3 shows the top view of skin-stringer assembly under compressive loading. Figure 1.4 and Figure 1.5 show the load distribution over the panel before and after buckling, respectively. As shown in Figure 1.5, the section of skin panels, at the stiffener attachment lines, do not buckle. This means that the stiffener and skin still have the same strain level at the attachment line. However, at the mid-panel, skin panel can no longer carry the additional load after the panel buckling [19]. In the classical approach, in order to handle the non-uniform load over the skin panel after buckling, equivalent width concept has been used commonly [1]. Equivalent width pertains to the part of the skin that is assumed to carry uniform load. In the classical approach, effective width concept has been widely used in the post-buckling analysis of skin-stringer assemblies [1, 6].

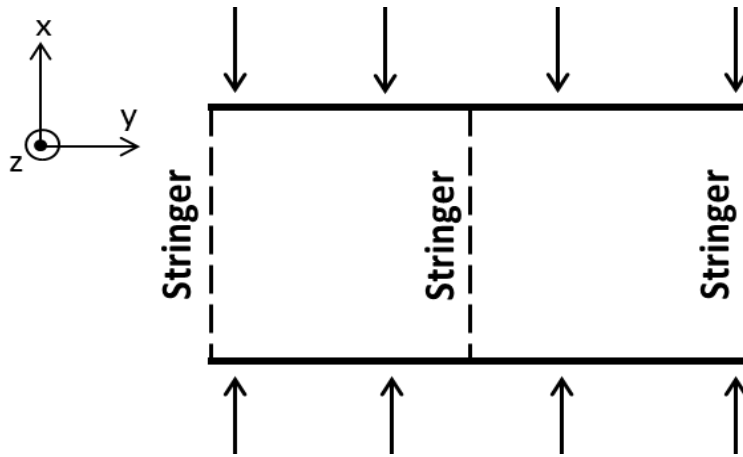


Figure 1.3: Top view of compressive loaded skin-stringer assembly

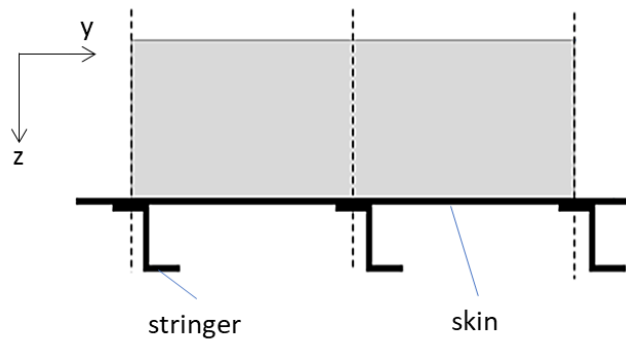


Figure 1.4: Load distribution before the panel buckling [1]

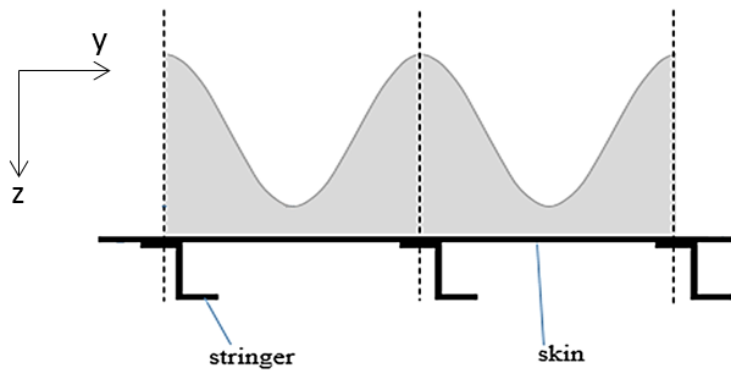


Figure 1.5: Load distribution after the panel buckling [1]

Mert [19] has offered a methodology to calculate the effective width of skin panels and internal loads through the iterative application of the linear static finite element analysis. In the study of the Bedair [20], the effective width concept has been

investigated since it is widely used in engineering practice for the computation of ultimate strength of slender members. The paper of Osama [20] presents analytical closed form expressions for the computation of effective width of thin plates under non-homogeneous in-plane loading. The longitudinal edges are assumed to be straight and free to translate in the plane of the plate. In this study, it is considered that the proposed expressions are very useful for limit state design of slender I-sections of beam columns or channel sections under this general type of loading. The unloaded edges were assumed to be straight and free to translate in the plane of the plate. The compatibility differential equation is first solved analytically to obtain a closed form solution for the stress function. The equilibrium differential equation is then solved approximately using the Galerkin method. Based on the characteristics of the post-buckling stress field, analytical expressions for the effective width were proposed. The sensitivity and mechanics of the effective width to the stress gradient parameter was shown. The resulting analytical expressions have simple forms, suitable for hand-calculation and avoid the cost and effort that any numerical non-linear analysis may require. In the study of the Dannemann [21], the author presents a complementary criterion for effective width which is based on tests performed on thin trapezoidal sheets, when flanges buckle in the elastic range. This method compares well with the observed behavior and ultimate strength of test specimens. The author's suggestion is that for inelastic buckling the AISI and correlated design codes are valid but when sheets are very slender and they buckle elastically, a modified effective width criterion has to be applied. This proposed method not only shows excellent correlation with tests, but also facilitates a rational agreement between stiffened and unstiffened flange behavior when plates are very thin, fulfilling physical requirements not accomplished by the classical effective width method. In addition, this method allows the calculation of the post buckling strength of flanges and webs by using physically measurable values instead of empirical parameters. The effective width concept is a classical resource for representing local buckling effects on stiffened flat flanges. There has been a great deal of testing and investigations on this matter. The most important contribution to the adoption of this method was proposed in Winter [22] included by AISI in their Specification of Light Gage Structural Members of 1946. As known, the

effective width concept is based on Von Karman's proposition of 1932 where the uneven stress distribution of buckled flanges was replaced by evenly stressed fictitious strips along the corners of the flanges. This structural artifice has shown excellent results in design practice of metal structures. A great number of tests in different countries confirm the accuracy of this method mainly in plates buckling in the inelastic range, but from time to time some discrepancies have been detected and published for flanges buckling elastically.

Finite element modelling and analysis of the actual skin-stringer assembly takes very long time in the design optimization process. One of the efficient method to optimize the structure is the artificial neural network (ANN). In the literature, there are a few studies about the prediction of the failure modes using ANN.

A study of optimization of a compression member conducted by Sheidaii and Bahraminejad [23] is an example of the use of ANN in optimization. In the study, load-displacement relation of different types of columns was obtained using analytical methods. The results were utilized to form a data set to train an ANN. Similar to the study of Sheidaii et al., ANN is used to predict bolt reaction force and average equivalent flange stress without using finite element model in the study of Yildirim [24]. In this study, a bolted flange design tool is created by using ANN. As the general sense, a data set was created with finite element model parameters and corresponding analysis results. The data set was used in training, validating and testing of ANN. At the end, the ANN results were compared with FEA and analytical methods. Comparison results are sufficient to use the ANN tool in the further design of bolted flanges. Another optimization study which is written by Gomes et al. [25] was conducted on anisotropic laminated composites. In this study a genetic algorithm and two ANNs were used to optimize the design of a laminated composite. It was stated that the use of these methods leads to accurate enough solutions and decrease the time required for the design process. Gajewski et al. [26] studied the use of the ANN for the optimization of a thin-walled structure. FEA results of the structure were used to train the ANN. This study is another example that the ANN is an appropriate tool in design and analysis of airframe structures.

Buckling and collapse loads of panels have also been studied to create analysis tools based on ANN. Sadovský and Soares [27] obtained post-buckling strength of a thin rectangular plate by creating an ANN as a function of initial imperfections. The created ANN was found to be able to provide reasonable collapse load results. The post-buckling optimization by using ANN was utilized for stiffened panels in a study of Lanzi and Giavotto [28]. The study used different optimization methods including ANN to optimize composite stiffened panels subjected to axial compression. The results were verified by tests and it was seen that accurate results can be obtained for both the buckling load and the collapse load. Mallela and Upadhyay [29] also used the ANN to calculate the buckling load. The study was focused on buckling load prediction of composite stiffened panels working under shear loads. FEA results for different composite structures were collected in a database to train an ANN tool. An efficient tool that can be used in optimization was created in the study. In the study of Cankur [30], an ANN based structural analysis tool to predict the buckling and collapse loads of the stiffened panels is created. The ANN is trained by using a database created with the input parameters and the FEA results of 1440 metallic skin-stringer assemblies subjected to uniaxial compression. The first buckling load and the collapse load are extracted from the nonlinear FEA results of the assembly. Using the results of the same analysis for the buckling and the collapse load, the time required for the generation of the training database is significantly reduced. Also, the first buckling load is obtained with an enhanced accuracy by using nonlinear analysis instead of linear buckling analysis.

In the final phase of the thesis study, buckling behaviour of the unstiffened thin composite panels is studied. In the last three decades, there have been many studies performed on composite buckling. Same as the metallic part, some of the studies about the composite buckling in the literature are presented in this sub-chapter.

In the study of the Yang [31], CLPT and FSDT analysis methods are investigated for composite plate buckling. These methods are developed for plates subjected to uniaxial compression loading and both simply supported and clamped edge plates have been studied. Analysis methods for plates subjected to biaxial compression loading, in-

plane shear loading and combined loading, with simply supported edges have been studied. To validate the analysis methods, FE analyses is performed using ANSYS. The methods based on FSDT give a better estimation than CLPT. According to Qiao, these methods are suitable for thin and moderately thick plates. Furthermore, in this study, the considered methods are limited to linear case. In the study of the Masood et al. [32], a composite skin-stringer panel was designed for compression testing under axial compression loads beyond initial skin buckling. The panel was fabricated using Carbon/Epoxy prepreg through autoclave moulding process. A finite element model was developed to predict the buckling and post-buckling response of the panel. Digital Image Correlation captured the onset of skin buckling and deformations/mode shapes in the post-buckled regime. Experimental observations were then correlated with numerical simulations. In the post buckled regime, severe bending and twisting of the skin and stringers were observed, resulting in complete loss of global axial stiffness of the panel. It is investigated that stress at the post buckled regime in the panel could lead to delamination, debonding or fiber failures. Local skin buckling is also confirmed through strain measurements using a number of strain gages bonded on the panel skin. In the study of the Abramovich and Weller [33], an extensive test series on circular cylindrical laminated composite stringer-stiffened panels subjected to axial compression, shear loading. The test program was an essential part of an ongoing effort undertaken aiming at the design of low cost, low weight airborne structures that was initiated. Test results on curved composite panels stiffened by J-stringers were presented and discussed. Test results were compared with predictions obtained by an in-house developed code and the commercial FE code ABAQUS. Accompanying supporting calculations were presented as well; they were performed with a fast calculation tool developed and based on the effective width method modified to handle laminated circular cylindrical stringer-stiffened composite panels. In the study of Möcker et al. [34], it is shown how the finite element code ABAQUS can be used for an accurate and reliable prediction of the post-buckling behaviour. When performing finite element simulations, a large amount of time is often needed to build up the finite element model, in particular if the model consists of several parts with complex geometries. For this reason, the preprocessing tool ABAQUS/CAE provides an

interface which allows the user to automate repetitive tasks. The main focus of this paper is on discussing several modelling techniques that are used to enable a realistic idealization of the physical problem and on presenting simulation results for an exemplary structure. Based on this example, the influence of modelling details like mesh density and geometric imperfections on the prediction of the failure load is discussed.

CHAPTER 2

BUCKLING OF STIFFENED METALLIC FLAT PANELS

Buckling load highly depends on the boundary condition, loading type, material property and geometric properties of the panel. In the literature, calculation of the buckling load is limited with the classical boundary conditions [1, 6]. However, in realistic cases, boundary conditions of the panel are provided by stiffeners on the loaded and unloaded edge of the panel. To get realistic value of the buckling load, finite element analyses (FEA) of the stiffened panel is necessary, but finite element analysis is time consuming considering the preparation time required for the analysis model and the analysis time required. ABAQUS is chosen in the finite element modelling of the structures. ABAQUS is the commercial finite element software which is commonly used in the aerospace industry. In this study, ABAQUS up to date version 6.14 is used in the finite element modelling. To find the buckling load in this study, ABAQUS “buckling” step for the linear buckling analysis is utilized. In FEA, the procedure of obtaining buckling eigenvalue is described in Appendix A.

In this chapter, it is aimed to prepare databases for the buckling coefficients of selected metallic skin-stringer assemblies by means of parametric modeling approach via the script language followed by automated finite element analysis. With this approach, databases of buckling coefficients for skin-stringer assemblies can to be generated similar to the available buckling coefficient charts for the panels which have classical

boundary conditions along the edges. Skin-stringer assemblies are established for T, Z and J type stringers. For each skin-stringer type, a database is created. Using these databases, the buckling load and the compression buckling coefficient of the skin-stringer assembly can be obtained much faster than modeling and analyzing the skin-stringer assembly by the finite element method. Thus, skin-stringer optimizations can be performed very quickly. To construct the databases, numerous skin-stringer assemblies are modeled with different sizes and types in ABAQUS 6.14. Database is created by writing a script in Python 2.7 which is then used in ABAQUS to generate the parametric models of the skin-stringer assemblies followed by automated finite element analysis controlled by the Python script.

2.1. Buckling Analysis of Unstiffened Panels

In the first phase of the study performed in this chapter, buckling coefficients of flat panels with classical boundary conditions are determined by finite element analysis and comparisons are made with the analytical solutions of the buckling coefficients provided in the literature. This study is performed to gain confidence in the finite element analysis results. The geometry and the coordinate of the flat panel are presented in Figure 2.1. For a panel which is simply supported at 4 edges, boundary conditions at the edges are given in Table 2.1 [8].

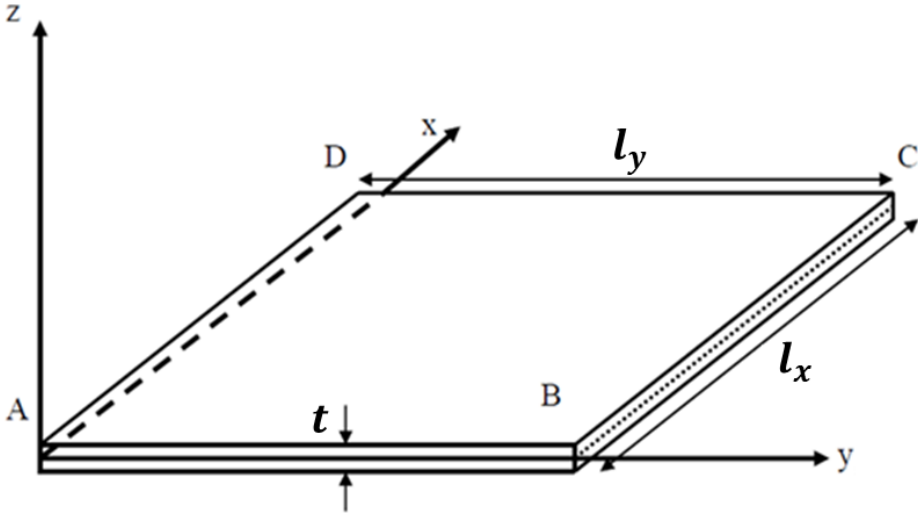


Figure 2.1: Definition of different geometrical parameters of the flat panels and the coordinate system

In Table 2.1, U1, U2 and U3 represent the translational degrees of freedom of the nodes around the x, y and z axes, respectively. Similarly in Table 2.2, R1, R2 and R3 represent the rotational degrees of freedom of nodes around the x, y and z axes, respectively.

Table 2.1: Definition of the constraints for the simply supported panel

Locations	U1	U2	U3	R1	R2	R3
Edge A to B			X			
Edge B to C			X			
Edge C to D			X			
Edge D to A			X			
Point A	X	X	X			
Point B						
Point C		X				
Point D						

Table 2.2 presents the boundary conditions for a panel which is clamped at four edges.

Table 2.2: Definition of the constraints for the clamped panel

Locations	U1	U2	U3	R1	R2	R3
Edge A to B			X		X	
Edge B to C			X	X		
Edge C to D			X		X	
Edge D to A			X	X		
Point A	X	X	X			
Point B						
Point C		X				
Point D						

For flat panels with different boundary conditions, a script is written in Python to model numerous panels with different sizes subject to different loading conditions such as compression or shear loading. Lowest eigenvalues obtained in the buckling analysis are used to calculate the buckling coefficients. In this script, Aluminum 2024 T3 Clad sheet material is used. Material properties are seen in the Table 2.3 [36]. F_{cy} is the yield compressive allowable stress of panel. F_{tu} is the tensile ultimate allowable

stress. E is the elastic modulus of the panel material and E_c is the compression elastic modulus of the panel material. In addition, ν is the poisson ratio and n_c is the Ramberg-Osgood factor of plasticity in compression. Panel dimensions used in the script is shown in the Table 2.4. Step size of plate length x is chosen as 5 mm.

Table 2.3: Material Properties of Aluminum 2024-T3 Clad Sheet

F_{cy}, MPa	269	F_{tw}, MPa	441
E, MPa	72395	E_c, MPa	73774
ν	0.33	n_c	15

Table 2.4: Input parameters of the skin panels used in script

Skin panel material	Aluminum 2024 T3 Clad Sheet
Skin panel thickness (mm)	2.0
Skin panel length x (mm)	100:5:500
Skin panel length y (mm)	100

Critical buckling stress calculation formula is given by Equation (2.1) [1],

$$\sigma_{cr} = \frac{\pi^2 * k * E_c}{12(1 - \nu^2)} \left(\frac{t}{l_y} \right)^2 \quad (2.1)$$

where t is the thickness of the panel, E_c is the compression elastic modulus of the panel material and factor k is the buckling coefficient which depends on the boundary conditions, geometric characteristic (l_x/l_y ratio) and the loading condition (compression or shear). Compressive and shear buckling coefficient curves are given in Bruhn [1].

In the finite element analyses, according to Figure 2.1, loading is applied in the x direction along edges AB and DC and the unloaded edges of the panel are AD and BC. The critical buckling stress is calculated using the lowest eigenvalue obtained in the buckling analysis performed in ABAQUS as shown in Equation (2.2),

$$\sigma_{cr} = \frac{N_{app}}{t} * \lambda_{FE} \quad (2.2)$$

where N_{app} is the compressive or shear shell edge load which is given as 1 N/mm as seen in Figure 2.2 and Figure 2.3, respectively. In addition, λ_{FE} is the first eigenvalue obtained from finite element analysis.

For the normal load case, load is applied as compression load on both sides of the panel, as shown in Figure 2.2. For the shear load case, load is applied parallel to the edges as shear on the all edges of the panel, as shown in Figure 2.3.

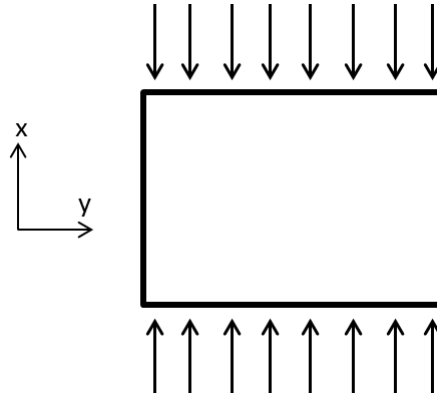


Figure 2.2: Compressive load demonstration for the single panel case

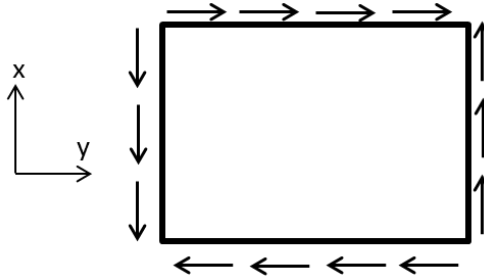


Figure 2.3: Shear load demonstration for the single panel case

By substituting Equation (2.1) into Equation (2.2), compression buckling coefficient is calculated as,

$$k = \frac{N_{app}}{t} * \lambda_{FE} * \frac{12(1 - \nu^2)}{\pi^2 * E_c} * \left(\frac{l_y}{t}\right)^2 \quad (2.3)$$

To construct the finite element model, ABAQUS, is used in the analyses of unstiffened panel models [35]. As in all commercial FEA programs, the modelling process starts with creating the geometry, then with meshing is performed and material properties are assigned to the unstiffened panel. The modelling process finishes by defining load and boundary conditions. Scope of the study is limited to flat thin panels under unidirectional compression and shear loads which are applied separately. Loads are given as edge unit load and boundary conditions are used as described in Table 2.1 and Table 2.2. Thin panel is modelled as a shell structure in the FE model as seen in Figure 2.4. In the meshing part, S4R elements (4-node element with one integration point), with hourglass control and membrane strain is chosen. This type element is recommended by ABAQUS in modelling of shell structures [35]. For the unstiffened panel models, “Buckle” step of ABAQUS [35] is used to obtain the lowest buckling eigenvalue. Subspace solver is chosen in order to avoid divergence problem. In the Subspace solver, there are 3 input parameters can be defined by users in the ABAQUS. These are the number of intended eigenvalues, vectors used per iteration and maximum number of iteration. In this study, three eigenvalues, ten vectors used per iteration and 3000 maximum number of iterations are chosen to avoid divergence. These values are recommended by the ABAQUS manuel for the buckling analysis [35].

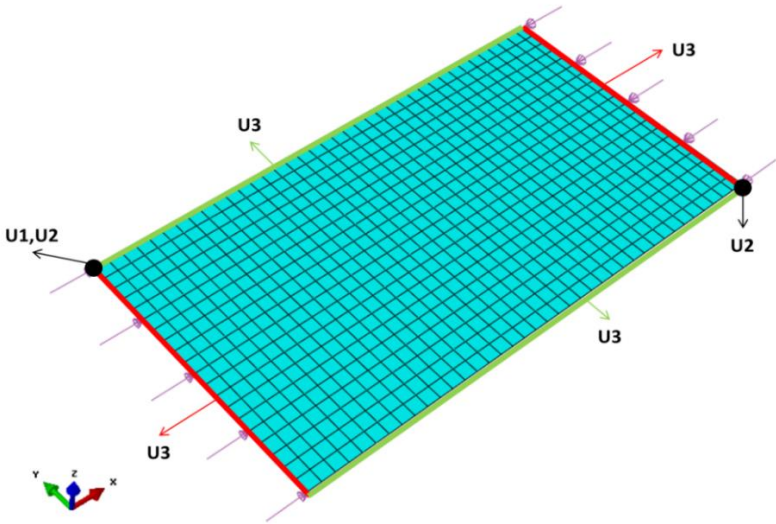


Figure 2.4: View of sample single panel model with all edges simply supported under compressive loading

Before the verification of finite element model's boundary conditions, element sizes used in the rest of study is determined by the mesh convergence study. To get fast and accurate result, nine different mesh sizes is chosen (course mesh, fine mesh and regular mesh). In the convergence study, example panel dimensions are chosen as 100 mm length x and 200 mm length y. Thickness of panel is decided as 1 mm. Material of the panel is also decided as Aluminum 2024 T3 Clad sheet [36]. Detailed material properties can be seen in Appendix B, Figure B.1. Boundary condition of the panel is chosen as simply supported boundary condition defined in Table 2.1 and load is given as unit shell edge load in the x direction along the edges AB and DC shown in Figure 2.1. Figure 2.5 shows the critical buckling stress with respect to element number used in the finite element mesh in the panel. In addition, element sizes used in this convergence study and the corresponding critical buckling stress results are given in Table 2.5. As seen in Table 2.5, as the element size is decreased, the critical buckling stress converges to approximately 27.1 MPa. After the element size become 5 mm and less, critical buckling stress does not significantly change. Hence, to minimize the computation time and not to lose accuracy, element size is taken as 5 mm.

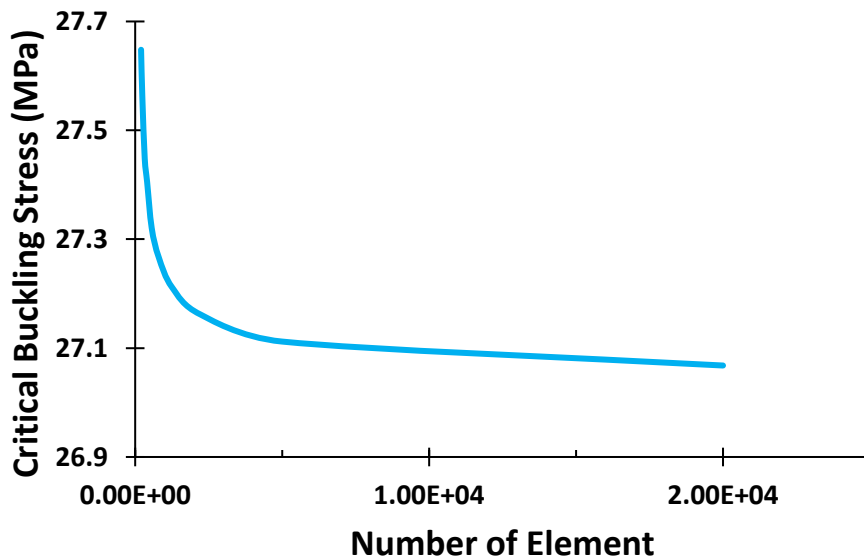


Figure 2.5: The critical buckling stress with respect to element number of flat panel

Table 2.5: Critical buckling stress results for various element sizes

Element Size (mm)	Number of Elements	Critical Buckling Stress (MPa)
1	20000	27.068
2	5000	27.112
3	2211	27.162
4	1250	27.212
5	800	27.267
6	561	27.321
7	406	27.405
8	325	27.448
9	242	27.563
10	200	27.648

After the convergence study, to compare the finite element analysis results for the compression buckling coefficient with those provided by Bruhn [1], figures of buckling coefficients given by Bruhn are digitized to compare with the FEA results. Interval of the panel length x is chosen as the 100 mm to 500 mm with 5 mm step size. In addition, panel length y is chosen as constant 100 mm and the panel thickness is decided as constant 2 mm.

Comparison of buckling coefficient versus plate aspect ratio curves are given in Figure 2.6-Figure 2.9, for different loading and boundary conditions.

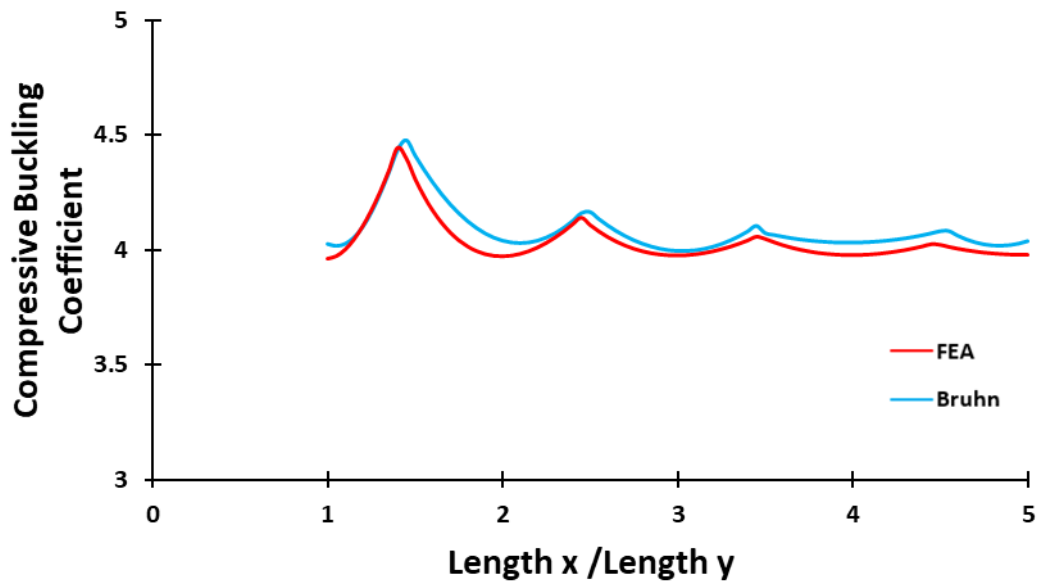


Figure 2.6: Comparison of compressive buckling charts for flat rectangular panels with simply supported loaded and unloaded edges

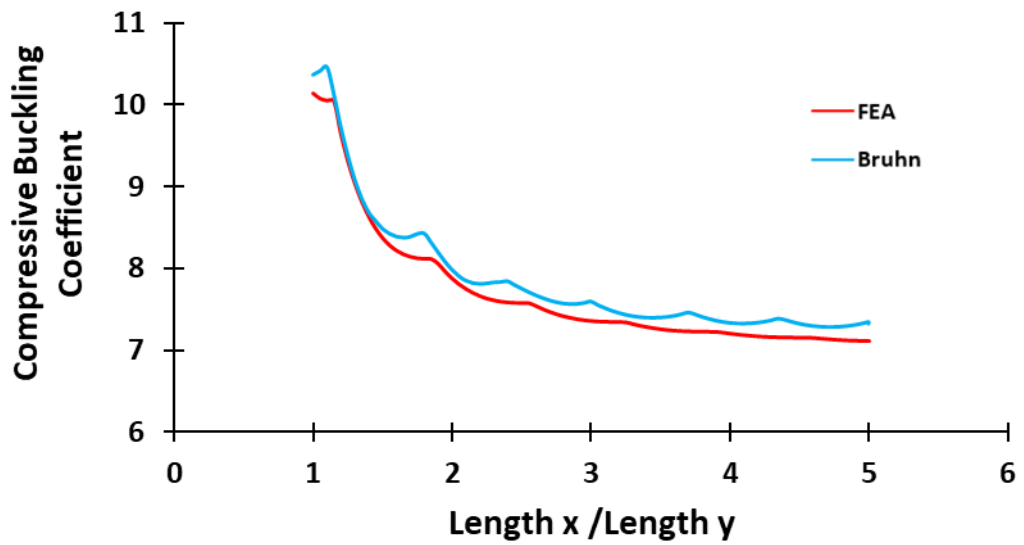


Figure 2.7: Comparison of compressive buckling charts for flat rectangular panels with clamped loaded and unloaded edges

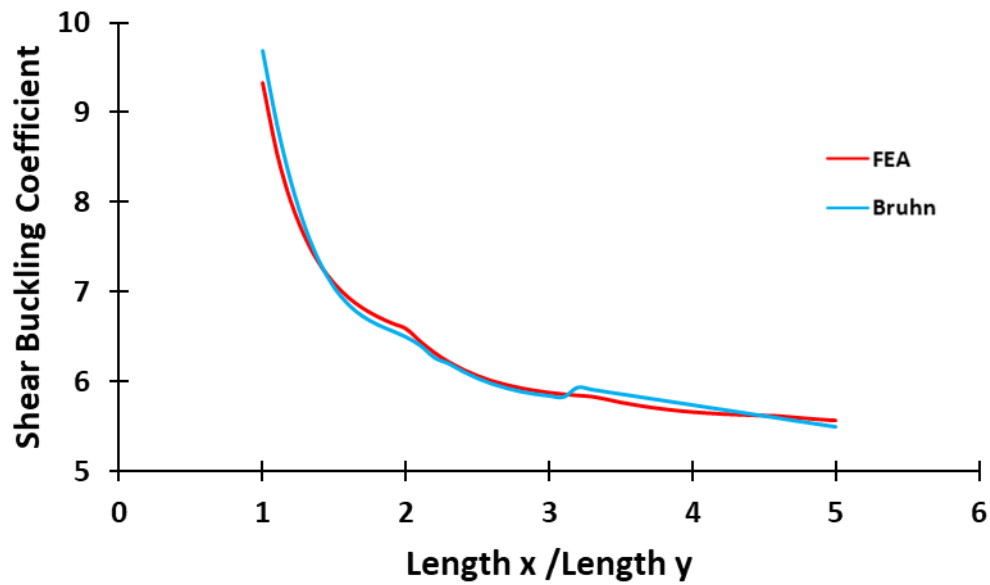


Figure 2.8: Comparison of shear buckling charts for flat rectangular panels with simple supported loaded and unloaded edges

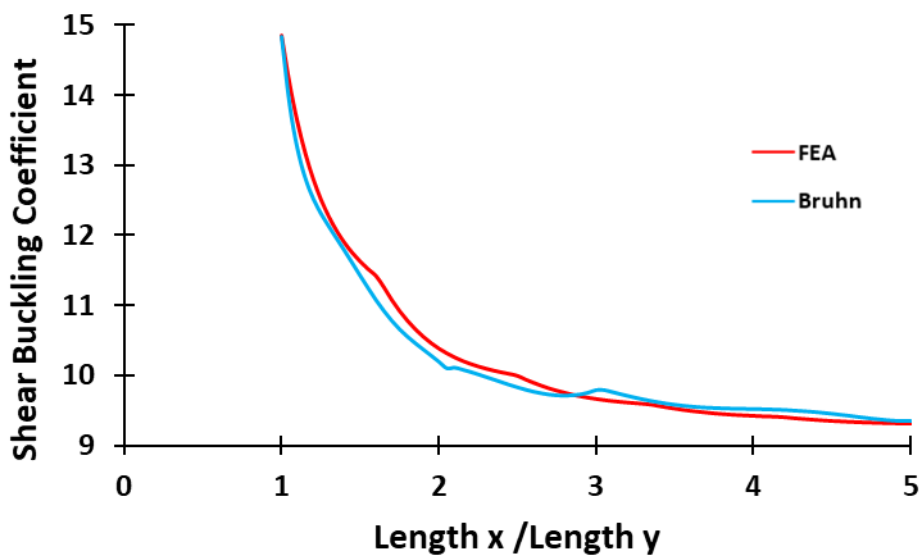


Figure 2.9: Comparison of shear buckling charts for flat rectangular panels with clamped loaded and unloaded edges

It should be noted that average of the differences between the buckling coefficients obtained by the finite element analysis and analytically determined buckling coefficients provided by Bruhn are around %1-2 in Figure 2.6-Figure 2.9. It is also noted that differences are mainly due to digitizing the plots given by Bruhn [1].

2.2. Buckling Analysis of Stiffened Panels

2.2.1. Determination of buckling coefficients of skin-stringer assemblies by finite element analysis

Following the verification of the boundary conditions of a single panel by the finite element analysis, stiffened panel modelling is performed using the verified boundary conditions along the loaded edges of the panel. However, for the stiffened panels, restraint along the unloaded edges is provided by the stiffeners on the panel. The boundary condition of the loaded edges of skin-stringer assembly is considered as clamped edge condition.

The first skin-stringer assembly considered consists of three flat skin panels and two stringers with I cross section. Skin-stringer assembly and the skin panel numbering are demonstrated in Figure 2.10. In addition, cross section view of skin-stringer assembly is seen in Figure 2.12. Compression load is applied on the three skin panels from one of the edges along the y-axis as 1 N/mm edge load in the -x direction. Figure 2.11 demonstrates the restraints applied to the loaded and the opposite edges of the panel. The degrees of freedom restrained along the loaded edge are U3 and R2. Along the other edge of the three skin panels, degrees of freedom U1, U3 and R2 are restrained. In addition, the middle edge of panel 2 is not allowed move in the y direction to avoid rigid body motion of the assembly, as shown in Figure 2.11. Moreover, unloaded side edges of the panels 1 and 3 are restrained in z-translation (U3 degree of freedom) and x-rotation (R1 degree of freedom).

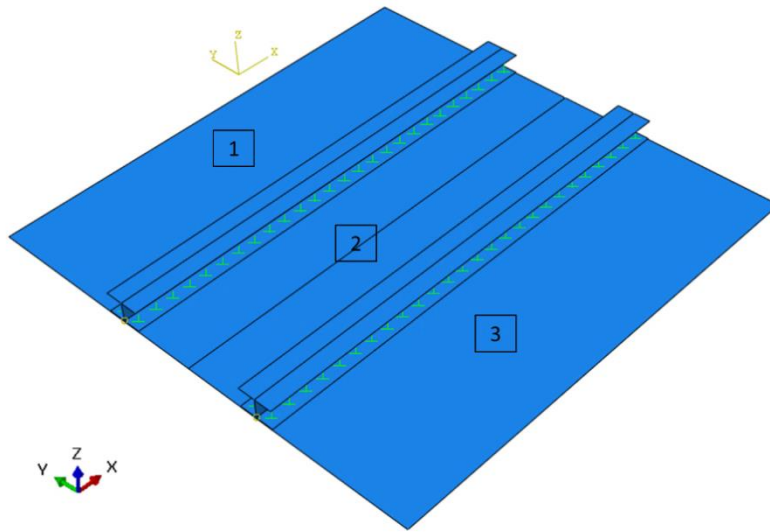


Figure 2.10: Isometric view of skin-stringer assembly analyzed

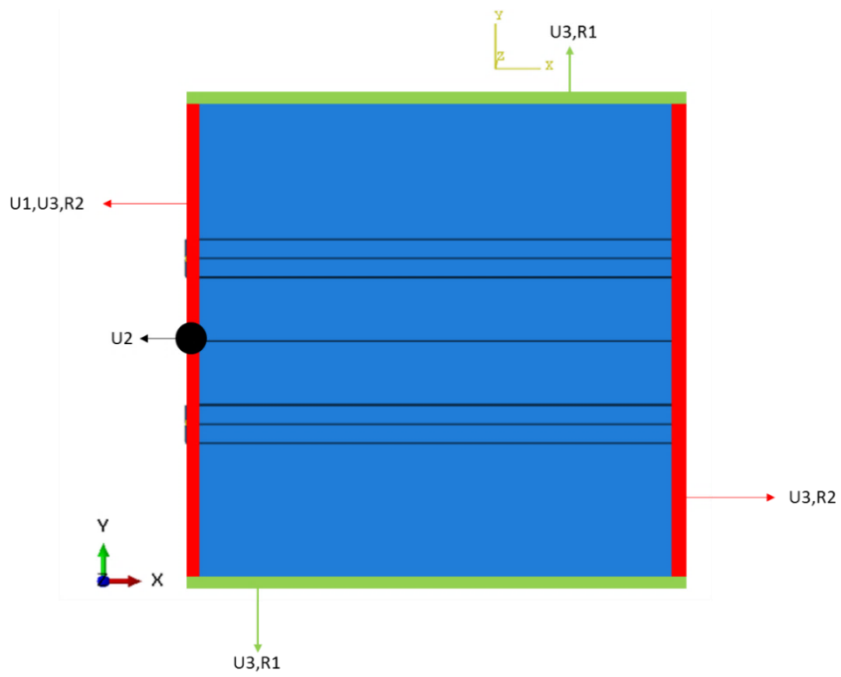


Figure 2.11: Constraint configuration of the skin-stringer assembly

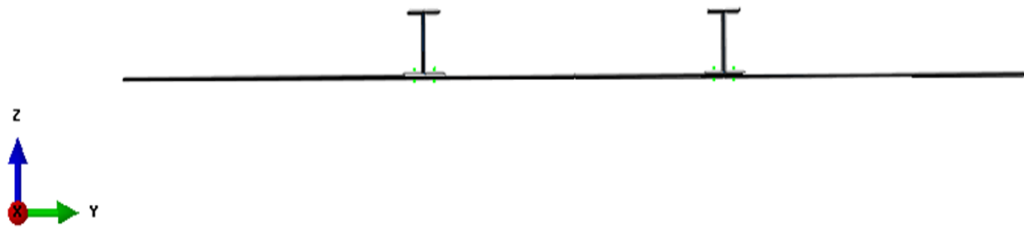


Figure 2.12: Cross section view of skin-stringer assembly analyzed

In the finite element model of the skin-stringer assembly, all stringers and skin panels are modelled as 2D shell elements with Aluminum 2024 T3 sheet material properties as shown in Figure 2.13 same as the unstiffened panel model. Element type used is shell element, S4R type which is a 4-node element with one integration point. Material properties of Aluminum 2024 T3 sheet is given in Table 2.3 [36]. Stringers element size is chosen as 2 mm and skin element size is chosen as 5 mm same as the unstiffened panel model. Stringer mesh density is chosen higher than skin mesh density because the dimension of stringer cross section is smaller than skin dimensions. Stringers are connected to the skins by 3.2 mm diameter fasteners in double row arrangement. Fastener spacing is taken as 5 times the fastener diameter and fastener edge distance is the 2 times the fastener diameter plus 1 mm as shown in Figure 2.14. These figures are commonly used in the aerospace industry.

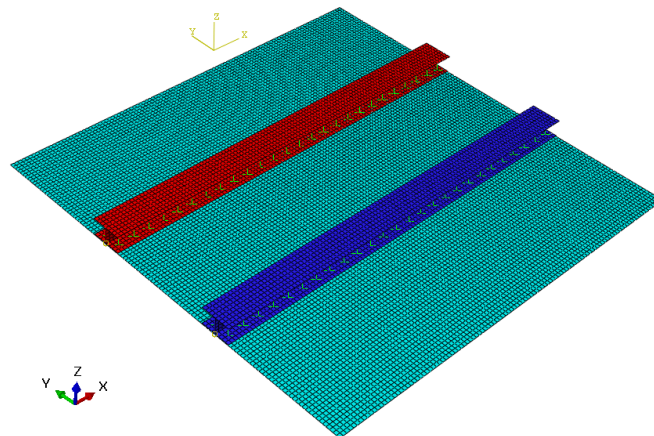


Figure 2.13: Isometric view of skin-stringer assembly with mesh

Since it is too costly to model each fastener using its real geometry with a 3D model, fastener idealization is made. For this purpose, mesh-independent fastener is considered as a convenient method to define a point-to-point connection between two or more surfaces such as in a fastener connection. Thus, in the finite element model of the skin-stringer assembly, fasteners are modelled with the mesh-independent fastener module in ABAQUS [35].

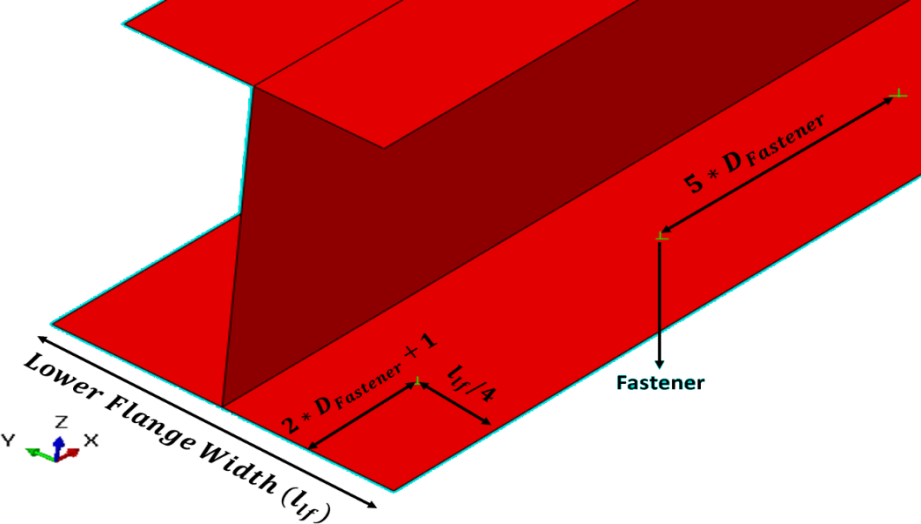


Figure 2.14: Fastener pattern configuration on the stringer

For the skin-stringer assembly, “Buckle” step of ABAQUS is used to obtain the lowest buckling eigenvalue [35]. Lowest eigenvalue obtained by finite element analysis is used in Equation (2.3) to calculate the compression buckling coefficient pertaining to the local buckling of the skin supported by the side stiffeners.

A case study is performed for a panel with the loaded edges which are considered as clamped edge conditions and the unloaded edges closely simulating the clamped edge conditions with the help of stringer stiffness. Compression buckling coefficients calculated by the finite element solution are compared with the analytically determined compression buckling coefficient for panel 2 (mid panel) in the skin-stringer assembly as shown in Figure 2.10. Input parameters of this example assembly are shown in Table 2.6. The parameters given in Table 2.6 are decided iteratively such that with these parameters the unloaded edges simulate the clamped condition closely. The skin-

stringer model is solved by using “Buckle” step of ABAQUS for the lowest buckling eigenvalue as described previously [35].

Table 2.6: Input parameters of the skin-stringer assembly used in the finite element model

Skin panel material	Aluminum 2024 T3 Clad Sheet
Skin panel thickness (mm)	0.813
Skin panel length x (mm)	450.0
Skin panel length y (mm)	150.0
Stringer material	Aluminum 2024 T3 Clad Sheet
Stringer thickness (mm)	1.016
Stringer height (mm)	14.0
Stringer upper flange width (mm)	9.0
Stringer lower flange width (mm)	11.5

N_{app} is compressive shell edge load applied on the three skin panels from one of the edges along the y-axis which is given as 1 N/mm in the -x direction. For the skin-stringer assembly specified in Table 2.6, the lowest eigenvalue is obtained as,

$$\lambda_{FE} = 12.006 \quad (2.4)$$

Using this eigenvalue, the corresponding compressive stress and the compressive buckling coefficient are calculated as,

$$\sigma_{cr} = 14.768 \text{ N/mm}^2 \quad (2.5)$$

$$k = 7.383 \quad (2.6)$$

If the skin panel 2 in Figure 2.10 is modeled with the same input parameters but classical clamped edge condition is assigned to the unloaded edges, for the panel aspect ratio of 3, compressive buckling coefficient is obtained as:

$$k = 7.382$$

(2.7)

In this example, it is seen that for the skin-stringer assembly defined in Table 2.6, the unloaded edge of panel 2 closely simulates the clamped edge condition. However, depending on the stringer type and how the stringer is connected to the skin, buckling coefficients obtained from the finite element analysis may or may not agree with the buckling coefficients obtained from pure analytical study utilizing the classical boundary conditions.

According to the model description made, a script is written Python 2.7 in order to create an ABAQUS finite element model, run the model and collect the lowest eigenvalue from the analysis results. The purpose of this process is the preparing databases for the buckling coefficients of selected metallic skin-stringer assemblies by means of parametric modelling approach via the script language. With this approach, databases of buckling coefficients for skin-stringer assemblies can to be generated similar to the available buckling coefficient charts for the panels which have classical boundary conditions along the edges.

In this chapter, most commonly used stringer sections Z, J and T are investigated. Stringer section types' geometric descriptions are shown in Figure 2.15. As seen in Figure 2.15, T and J stringer section types use the double row joint configuration at the connection of skin and the lower flange of the stringer. In contrast, in the Z type stringer section, the single row joint configuration is used the finite element models. The scripts are written for each skin-stringer assembly and the following parameters are specified;

- Skin panel thickness
- Skin panel length y
- Stringer thickness
- Stinger height

- Stringer lower flange length
- Stringer upper flange length (In stringer section type T, there is no upper flange)

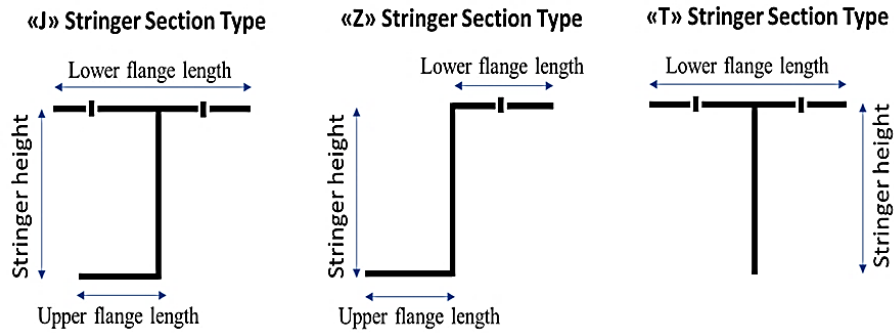


Figure 2.15: Stringer section types used in skin-stringer assemblies

To minimize the time and sources, some of the parameters of the skin-stringer assemblies are fixed to certain values as,

- Skin panel length $x = 450$ mm
- Fastener diameter = 3.2 mm
- Material: Aluminum 2024 T3 Clad Sheet

Discrete values of the design parameters of the skin-stringer assemblies are specified in a range. Upper and lower limits of the design parameters are decided based on the commonly used values in the industry.

For the skin-stringer assemblies with Z and J type stringers, the following parameters are specified between the upper and lower limits, and in total 2160 finite element analyses are performed to form a database for the buckling coefficients.

- Skin panel thickness = [0.813, 1.016, 1.27] mm
- Skin panel length $y = [150.0, 225.0, 300.0, 375.0, 450.0]$ mm

- Stringer thickness = [0.813, 1.016, 1.27] mm
- Stinger height = [10.0, 17.0, 24.0, 30.0] mm
- Stringer lower flange length = [10.0, 14.0, 18.0, 22.0] mm
- Stringer upper flange length = [10.0, 14.0, 18.0] mm

For the skin-stringer assembly with the T section stringer, the following parameters are specified between the upper and lower limits, and in total 2100 finite element analyses are performed to form a database for the buckling coefficients.

- Skin panel thickness = [0.813, 1.016, 1.10, 1.27] mm
- Skin panel length y = [150.0, 225.0, 300.0, 375.0, 450.0] mm
- Stringer thickness = [0.813, 1.016, 1.10, 1.27] mm
- Stinger height = [10.0, 15.0, 20.0, 25.0, 30.0] mm
- Stringer lower flange length = [10.0, 13.0, 16.0, 19.0, 22.0] mm

To minimize the number of finite element analysis, for each parameter minimum number of discrete values are selected within the upper-lower limits of each parameter. Skin length y has a remarkable effect on the buckling phenomena. Hence, for the skin length y, more number of discrete analysis points is used in the finite element analyses. However, for Z and J stringer section types, inner flange length is restricted to three values in order to minimize the number of analyses.

2.2.2. Setting up of Artificial Neural Network and Response Surface for fast determination of buckling coefficients

For fast determination of the buckling coefficients of skin-stringer assemblies with different stringer types, in this chapter, artificial neural network and response surface are set up utilizing the finite element analysis results for the buckling coefficients. The output parameter, buckling coefficient, obtained from finite element analyses and input parameters of the skin-stringer assemblies are collected in an Excel file for the generation of the ANN and the RS for fast and accurate determination of buckling coefficients without resorting to finite element analysis. For the generation of the response surface, inputs and outputs are processed in MATLAB RSTOOL [37]. Response surface model is chosen as “Full Quadratic”. Full quadratic response surface consists of constant term, the linear terms, the interaction terms and the squared terms.

As the second fast and accurate analysis tool, an artificial neural network is chosen. Artificial neural networks (ANNs) are computational modeling tools to model linear and nonlinear complex systems with most traditional statistical approaches. ANNs have characteristic advantages such as being suitable for nonlinear problems and ANNs have parallel working ability. Furthermore, ANNs can process imprecise and fuzzy information. Thus, they can provide accurate solutions for uncertain data. These capabilities deliver important benefits of excellent data fitting, adaptability and modeling of unlearned data [38].

ANN consists of multiple numbers of individual artificial neurons. These individual artificial neurons are grouped to create a layer in an artificial neural network. Neurons of each layer are connected to the neurons of the next layer. The ANN is composed of three layers which are input layer, hidden layer and output layer. The number of neurons in the input and the output layers are determined by the number of the input and the output parameters. Each neuron is associated with one input or output parameter. Thus, computational ability of an ANN is determined by the number and the content of hidden layers [37, 38]. Number of neurons in hidden layers is determined by trial and error to adjust the ANN with desired capabilities. Example of an artificial neural network configuration is shown in Figure 2.16. In this configuration, three

neurons input layer that is used to take three input parameters to the system, one neuron output layer that returns an output as result of the computation process, and two neurons for hidden layers.

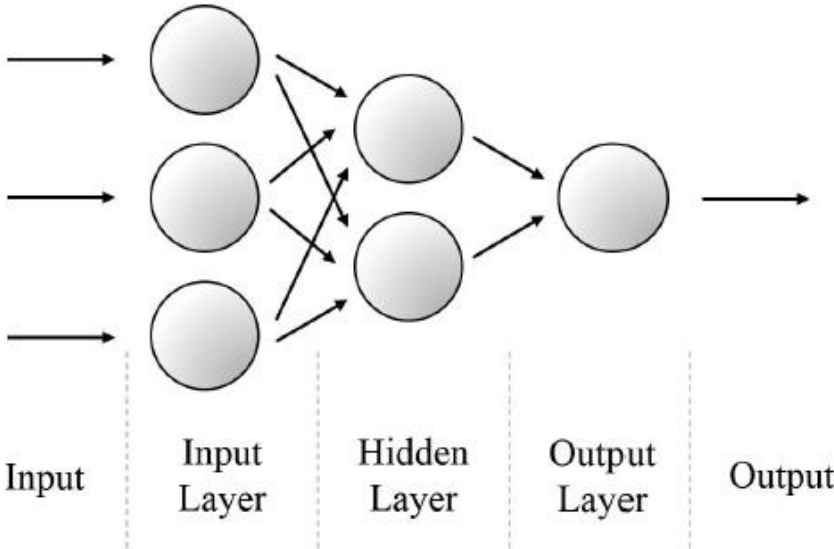


Figure 2.16: Configuration of artificial neural network

In this study, an artificial neural network is established for each skin-stringer assembly by using the input parameters and the output parameter which is the buckling coefficient. Buckling coefficients are in the range of 6-8 for the skin-stringer assemblies with J, Z and T type stringers. Inputs and output of numerous analyses are processed in MATLAB NNTOOL to create an artificial neural network (ANN) [24, 37, 38]. In the ANN, total layer number is chosen as 2, one for output layer and the other one for hidden layer. Number of neuron number in the ANN is decided by trial and error method for each type of stringer section. Levenberg-Marquardt backpropagation is chosen for training method of ANN. One of the termination criteria of neural network training process are decided as maximum “mu” which is known as the momentum term to slow the speed of the descent so that the search value does not fly back and forth across the minimum without stopping sufficiently near it. Another termination criterion is the minimum performance gradient which is gradient of the square of the error function with respect to the unknown weights and biases. As the

third and fourth termination criteria, maximum number of iteration, which is the number of iterations without any improvement and the epoch limit which is defined as the limit of the iteration number are used. In this study, these criteria are chosen as $1e10$ for maximum “mu”, $1e-7$ for minimum performance gradient, 500 for maximum number of iteration without any improvement and 1500 for epoch limit. For each type of stringer section, different ANN parameters are chosen to obtain accurate results. These parameters are neuron number, percentage of data sets used in the training set, percentage of data sets used in the validation set and percentage of data sets used in the test set. According to these parameters, performance of network is measured based on the mean squared error calculated using difference of ANN and FEA results.

The best network performance is obtained for the skin-stringer assembly with J type stringer section for the following set of parameters:

- 1 Neuron number
- % 70 of the data set used in the training of the ANN
- % 15 of the data set used in the validation of the ANN
- % 15 of the data set used in the test of the ANN

Using these parameters in ANN, for the skin-stringer assemblies with J type stringer section, mean square error is calculated as $5.12 * 10^{-4}$ as seen in Figure 2.17.

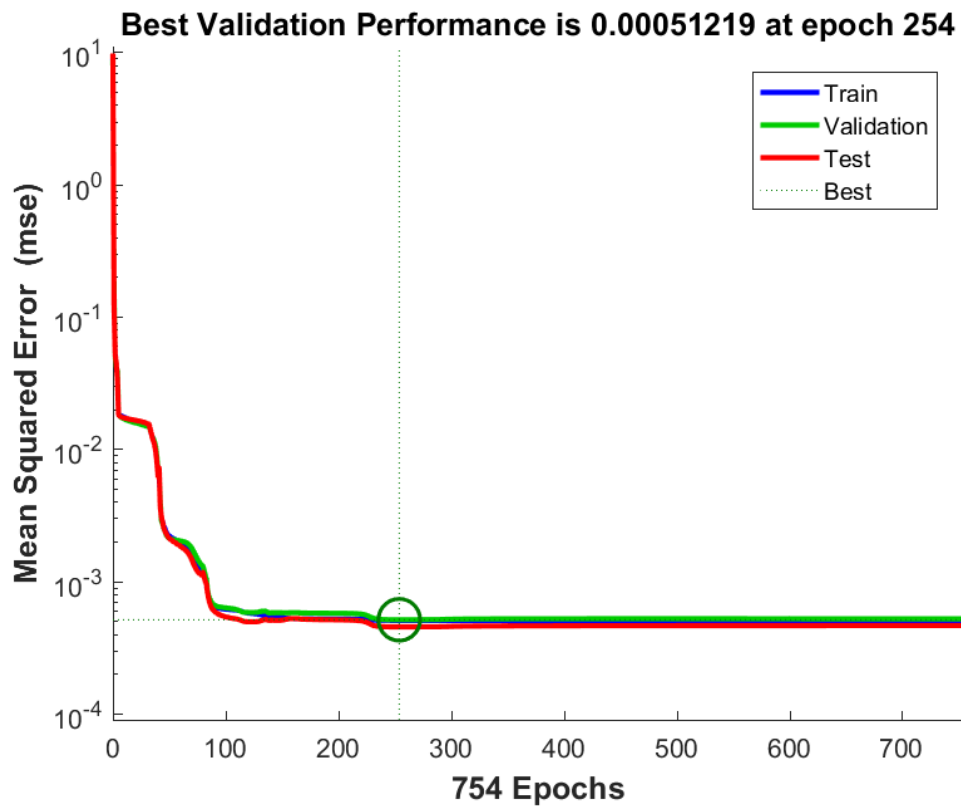


Figure 2.17: Performance plot of the ANN for skin-J type stringer assembly

The best network performance is obtained for Z type stringer section for the following set of parameters:

- 10 Neuron number
- % 70 of the data set used in the training of the ANN
- % 15 of the data set used in the validation of the ANN
- % 15 of the data set used in the test of the ANN

Using these parameters in ANN, for the skin-stringer assemblies with Z type stringer section, mean square error is calculated as $4.92 * 10^{-4}$ as seen in Figure 2.18.

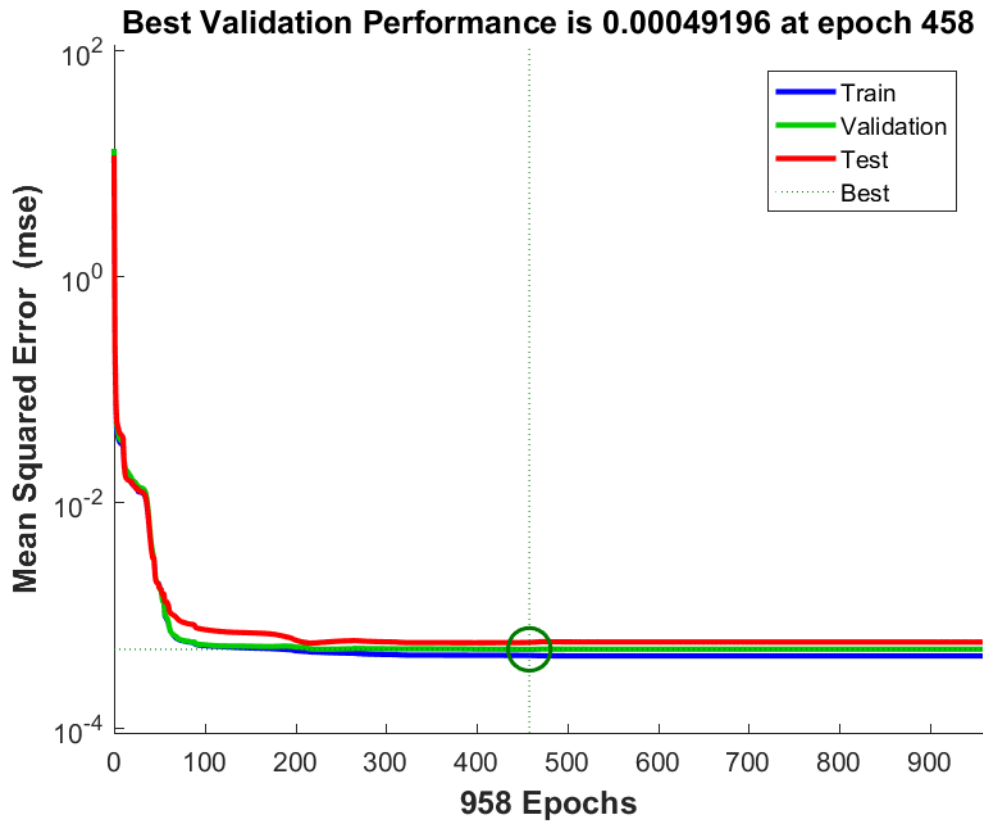


Figure 2.18: Performance plot of the ANN for skin-Z type stringer assembly

The best network performance is obtained for T type stringer section for the following set of parameters:

- 10 Neuron number
- % 75 of data set used in the training of the ANN
- % 15 of data set used in the validation of the ANN
- % 10 of data set used in the test of the ANN

Using these parameters in the ANN, for skin-stringer assemblies with T type stringer section, mean square error is calculated as $5.64 * 10^{-4}$ as seen in Figure 2.19.

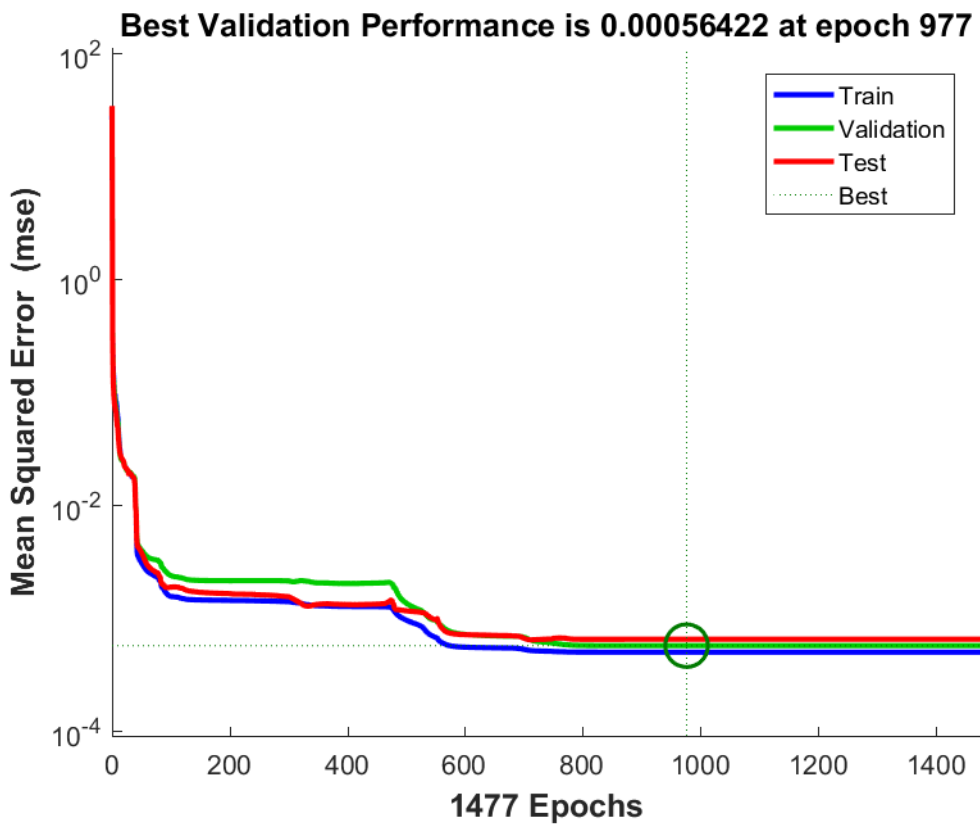


Figure 2.19: Performance plot of the ANN for skin-T type stringer assembly

ANN performance can also be shown with the regression lines given in Figure 2.20, Figure 2.21 and Figure 2.22 for the J, Z and T type of stringers, respectively. In the plots, vertical axis shows the ANN outputs which are obtained by using input database and the horizontal axis shows the FEA results that are used in training of the ANN. The dashed lines in the figures represent the perfect fit and the colorful lines are the fits that are created by training process. It is seen that colorful lines are very close to the dashed lines in each figures.

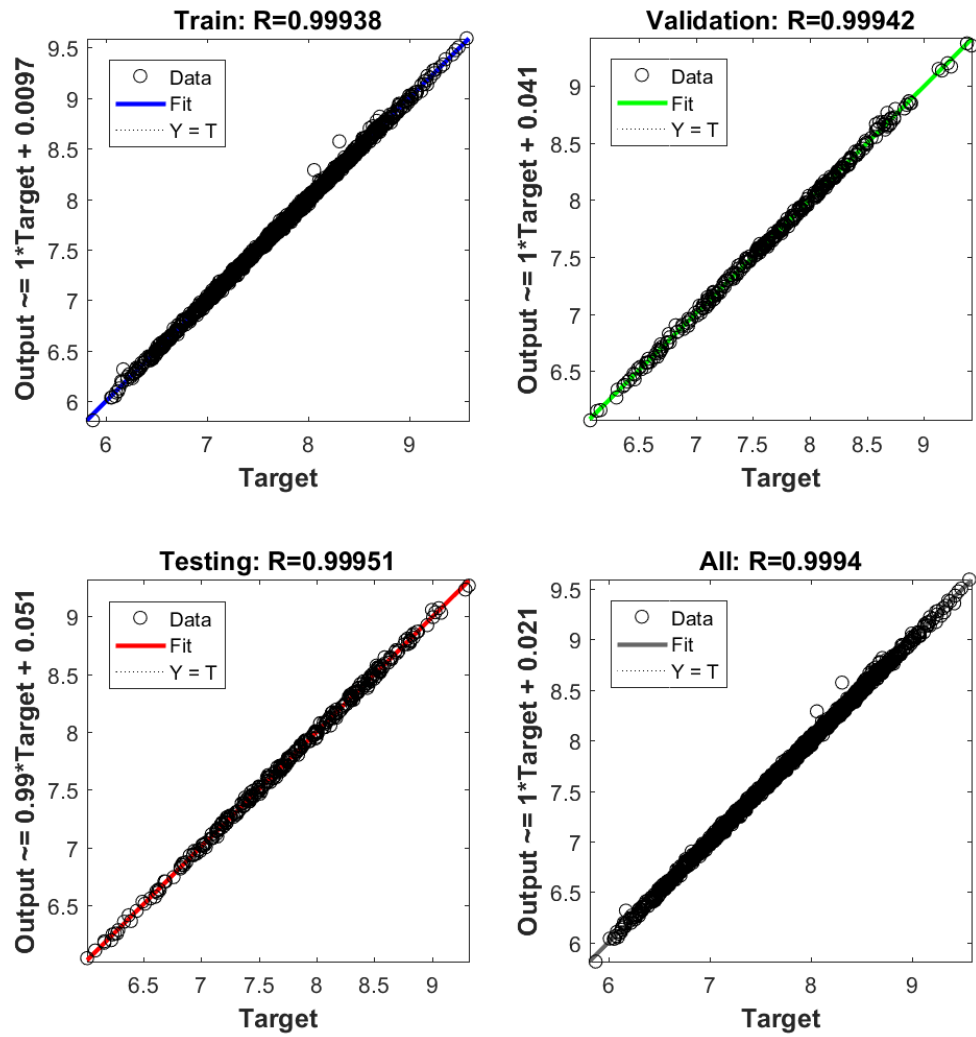


Figure 2.20: Overall, training, validation and testing regression plots of the ANN for skin-J type stringer assembly

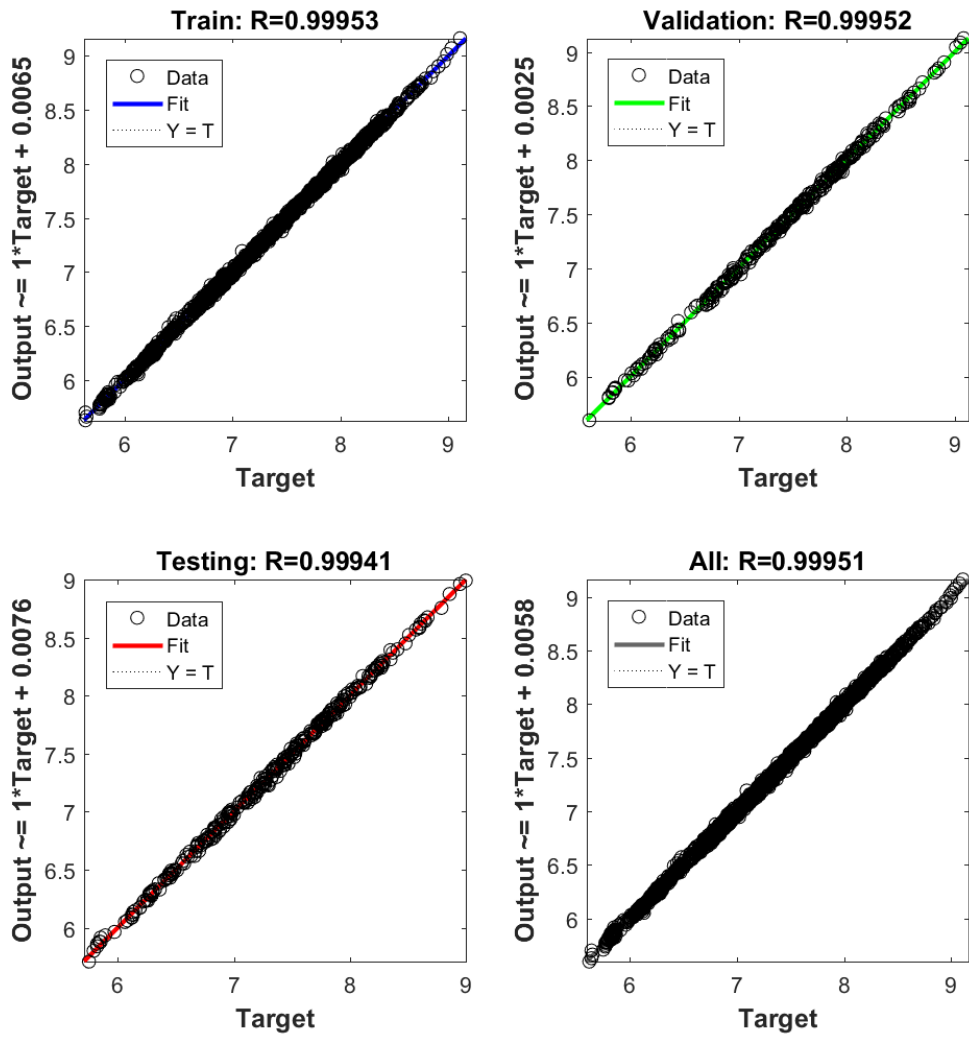


Figure 2.21: Overall, training, validation and testing regression plots of the ANN for skin-Z type stringer assembly

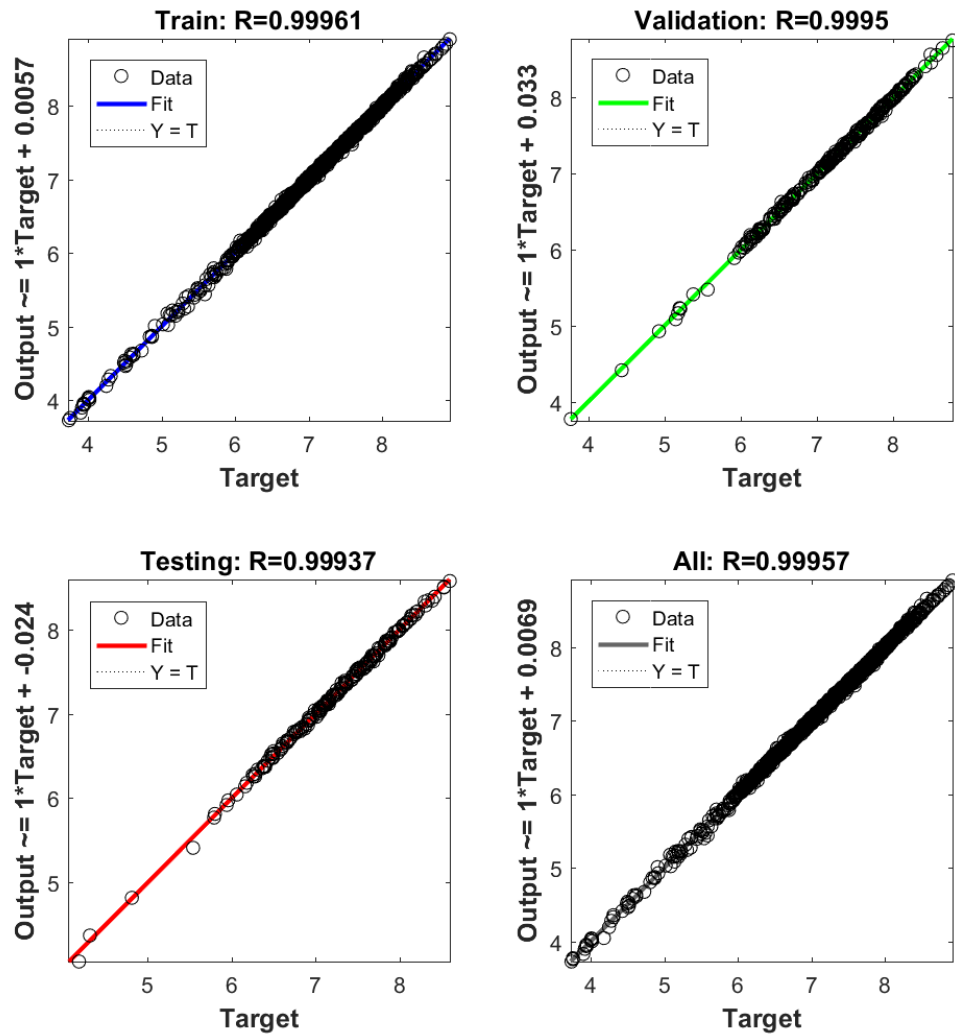


Figure 2.22: Overall, training, validation and testing regression plots of the ANN for skin-T type stringer assembly

In addition, Figure 2.23, Figure 2.24 and Figure 2.25 show the cause for termination of the training for the skin-stringer assemblies with J, Z and T type of stringers, respectively. It is seen that the ANN performance for the skin-stringer assemblies with J type of stringer does not increase after 254 iteration as shown in Figure 2.23. Thus, the validation fails 500th times at the iteration 754. As seen in the Figure 2.23, gradient of ANN for the skin-stringer assemblies with J type of stringer is obtained as 2.436e-5 which is higher than minimum gradient value. In addition, “mu” value of this ANN is obtained as 1e-7 which is lower than maximum “mu” value at the iteration 754. For

skin-stringer assembly with Z type of stringer, the ANN performance does not increase after 458 iteration as seen in Figure 2.24. Moreover, for skin-stringer assembly with T type of stringer, the ANN performance does not increase after 977 iteration as seen in Figure 2.25.

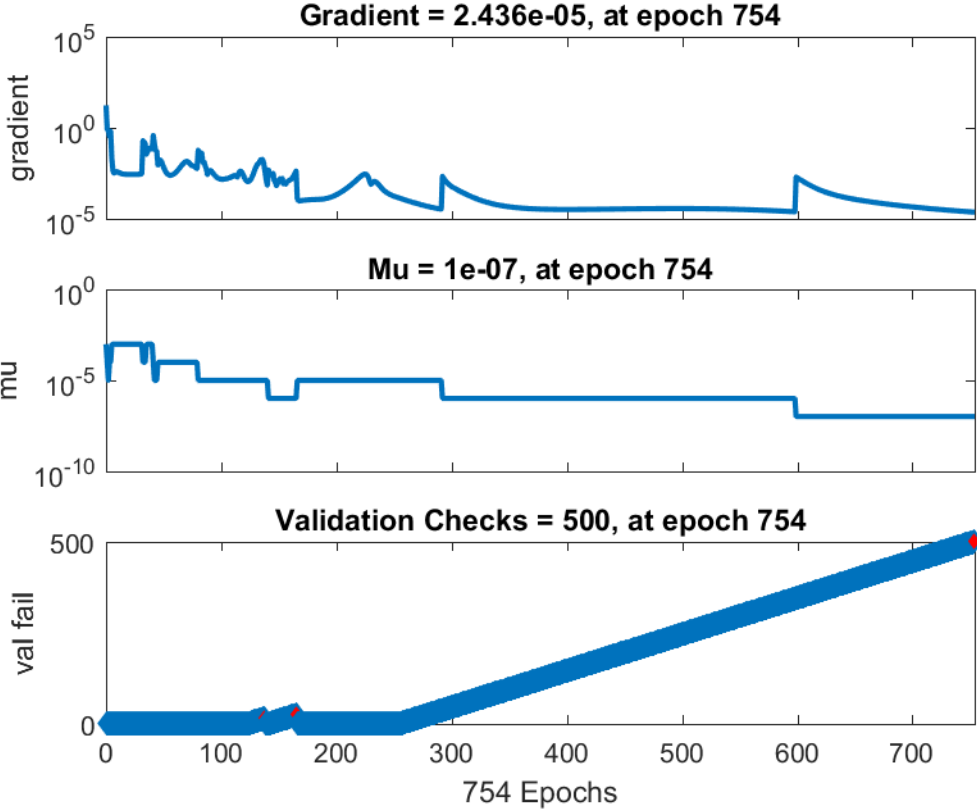


Figure 2.23: Number of validation fails, mu and gradient with respect to number of training iterations of ANN for skin-J type stringer assembly

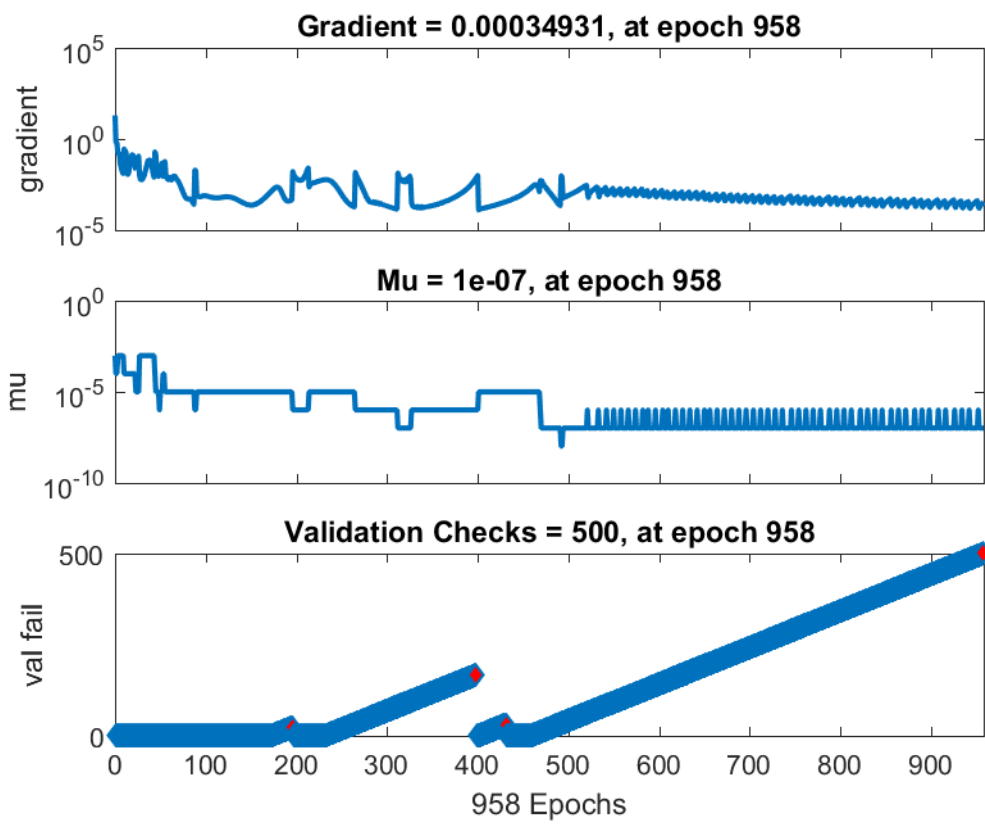


Figure 2.24: Number of validation fails, mu and gradient with respect to number of training iterations of ANN for skin-Z type stringer assembly

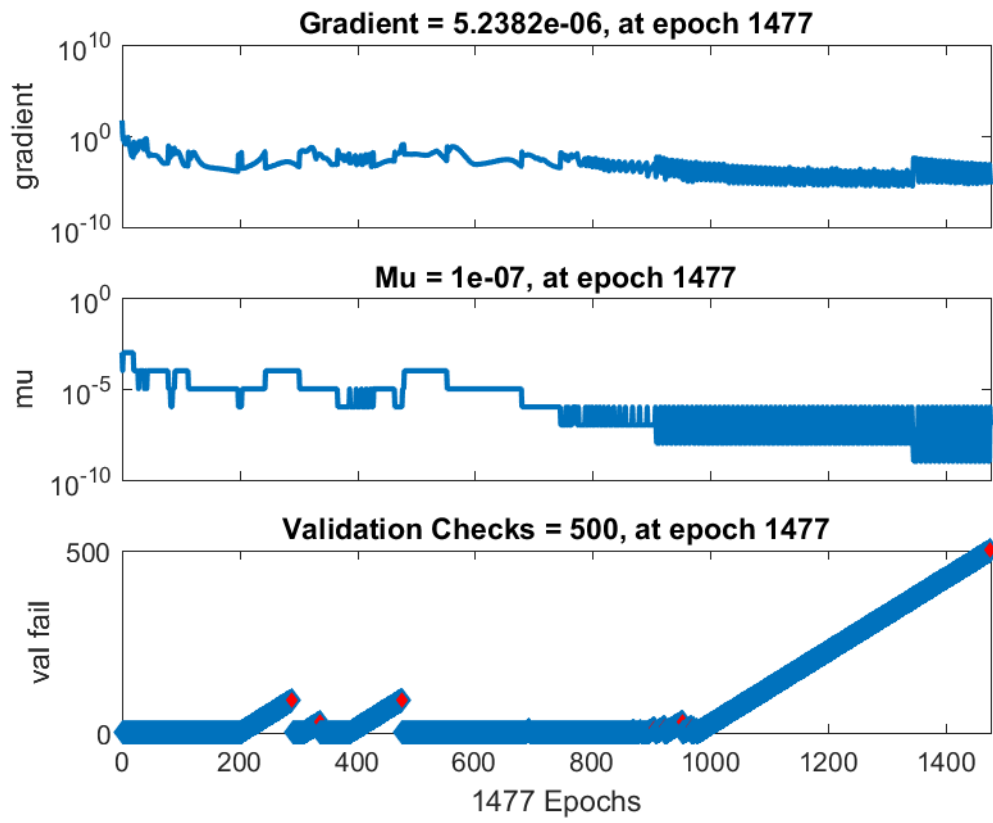


Figure 2.25: Number of validation fails, mu and gradient with respect to number of training iterations of ANN for skin-T type stringer assembly

2.2.3. Comparison of buckling coefficients of skin-stringer assemblies determined by FEA, Response Surface and Artificial Network

2.2.3.1. BUCKLING COEFFICIENTS OF SKIN-STRINGER ASSEMBLIES WITH J TYPE STRINGERS

Table 2.7 shows the input parameters of 10 additional analyses for the determination of buckling coefficients of skin-stringer assemblies. Parameters given in Table 2.7 are selected in between the parameters used in the finite element analyses used for the setup of the finite element database. Table 2.8 gives the finite element analysis (FEA), response surface (RS) and the artificial neural network (ANN) results.

Table 2.7: FEA input parameters for additional analyses for skin-stringer assemblies with ‘J’ type stringer

FEA	1	2	3	4	5	6	7	8	9	10
Skin panel thickness (mm)	1.05	0.85	1.2	1.2	1.15	1.05	1	0.9	1.1	1.15
Skin panel length x (mm)	450	450	450	450	450	450	450	450	450	450
Skin panel length y (mm)	350	200	325	320	400	275	200	175	235	325
Stringer thickness (mm)	1.1	1	1.2	1.25	1.2	1.07	1.03	1	1.15	1.2
Stringer height (mm)	18	13	28	25.5	17.5	16	19	18	22	23
Stringer upper flange width (mm)	15	12	17	16	15.5	11	13.5	10.5	15.5	16.5
Stringer lower flange width (mm)	16.5	15	17.5	17	15.5	12.5	14.75	11	15.75	17.75

Table 2.8: Buckling coefficients of skin-stringer assemblies with J type stringers / FEA results/ RS results / ANN results

#	FEA Results	RS Results	% Absolute Difference (RS)	ANN Results	% Absolute Difference (ANN)
1	7.83	7.963	1.69	7.842	0.15
2	7.59	7.628	0.51	7.559	0.41
3	8.08	7.958	1.50	8.049	0.39
4	8.07	7.959	1.37	8.058	0.15
5	7.9	8.118	2.76	7.901	0.02
6	7.27	7.330	0.83	7.394	1.70
7	7.47	7.489	0.25	7.444	0.34
8	7.26	7.320	0.82	7.326	0.91
9	7.52	7.675	2.06	7.517	0.04
10	7.88	7.994	1.45	8.068	2.38

For the skin-stringer assembly with J type stringer, Table 2.8 shows that the established ANN performs better than the RS. For the randomly selected 10 set of design parameters, root mean square (RMS) error with respect to the finite element results is 0.0760 for the ANN and 0.1176 for the RS.

2.2.3.2. BUCKLING COEFFICIENTS OF SKIN-STRINGER ASSEMBLIES WITH Z TYPE STRINGERS

Table 2.9 shows the input parameters of 10 additional analyses for the determination of buckling coefficients of skin-stringer assemblies. Parameters given in Table 2.9 are selected in between the parameters used in the finite element used for the setup of the finite element database. Table 2.10 gives the finite element analysis (FEA), response surface (RS) and the artificial neural network (ANN) results.

Table 2.9: FEA input parameters for additional analyses for skin-stringer assemblies with ‘Z’ type stringer

FEA	1	2	3	4	5	6	7	8	9	10
Skin panel thickness (mm)	1.05	0.85	1.2	1.2	1.15	1.05	1	0.9	1.1	1.15
Skin panel length x (mm)	450	450	450	450	450	450	450	450	450	450
Skin panel length y (mm)	350	200	325	320	400	275	200	175	235	325
Stringer thickness (mm)	1.1	1	1.2	1.25	1.2	1.07	1.03	1	1.15	1.2
Stringer height (mm)	18	13	28	25.5	17.5	16	19	18	22	23
Stringer upper flange width (mm)	15	12	17	16	15.5	11	13.5	10.5	15.5	16.5
Stringer lower flange width (mm)	16.5	15	17.5	17	15.5	12.5	14.75	11	15.75	17.75

Table 2.10: Buckling coefficients of skin-stringer assemblies with Z type stringers / FEA results/ RS results / ANN results

#	FEA Results	RS Results	% Absolute Difference (RS)	ANN Results	% Absolute Difference (ANN)
1	7.46	7.601	1.88	7.475	0.20
2	7.01	7.096	1.23	7.014	0.06
3	7.63	7.547	1.09	7.593	0.49
4	7.64	7.552	1.15	7.612	0.37
5	7.61	7.812	2.66	7.593	0.22
6	6.98	7.019	0.55	7.108	1.83
7	6.92	6.958	0.55	6.888	0.46
8	6.83	6.918	1.29	6.932	1.50
9	6.97	7.174	2.93	6.919	0.74
10	7.46	7.575	1.54	7.600	1.88

For the skin-stringer assembly with Z type stringer, Table 2.10 shows that the established ANN performs better than the RS. For the randomly selected 10 set of design parameters, root mean square (RMS) error with respect to the finite element results is 0.0726 for the ANN and 0.1219 for the RS.

2.2.3.3. BUCKLING COEFFICIENTS OF SKIN-STRINGER ASSEMBLIES WITH T TYPE STRINGERS

Table 2.11 shows the input parameters of 10 additional analyses for the determination of buckling coefficients of skin-stringer assemblies. Parameters given in Table 2.11 are selected in between the parameters used in the finite element analyses used for the setup of the finite element database. Table 2.12 gives the finite element analysis (FEA), response surface (RS) and the artificial neural network (ANN) results.

Table 2.11: FEA input parameters for additional analyses for skin-stringer assemblies with 'T' type stringer

FEA	1	2	3	4	5	6	7	8	9	10
Skin panel thickness (mm)	1.05	0.85	1.2	1.2	1.15	1.05	1	0.9	1.1	1.15
Skin panel length x (mm)	450	450	450	450	450	450	450	450	450	450
Skin panel length y (mm)	350	200	325	320	400	275	200	175	235	325
Stringer thickness (mm)	1.1	1	1.2	1.25	1.2	1.07	1.03	1	1.15	1.2
Stringer height (mm)	18	13	28	25.5	17.5	16	19	18	22	23
Stringer lower flange width (mm)	16.5	15	17.5	17	15.5	12.5	14.75	11	15.75	17.75

Table 2.12: Buckling coefficients of skin-stringer assemblies with T type stringers / FEA results/ RS results / ANN results

#	FEA Results	RS Results	% Absolute Difference (RS)	ANN Results	% Absolute Difference (ANN)
1	7.39	7.591	2.73	7.300	1.22
2	6.91	6.932	0.32	6.878	0.46
3	7.46	7.575	1.55	7.475	0.20
4	7.49	7.604	1.52	7.500	0.13
5	7.55	7.805	3.37	7.619	0.91
6	6.9	6.863	0.53	7.020	1.74
7	6.71	6.893	2.73	6.697	0.19
8	6.56	6.758	3.02	6.569	0.14
9	6.82	7.164	5.04	6.824	0.06
10	7.36	7.614	3.45	7.337	0.32

For the skin-stringer assembly with T type stringer, Table 2.12 shows that the established ANN performs better than the RS. For the randomly selected 10 set of design parameters, root mean square (RMS) error with respect to the finite element results is 0.0542 for the ANN and 0.1972 for the RS.

2.2.3.4. DISCUSSION OF RESULTS OBTAINED BY FEA, ANN AND RS FOR J, Z AND T TYPE OF STRINGER

In these additional 10 analyses, it is seen that for the skin-stringer assemblies defined in Table 2.7, Table 2.9 and Table 2.11 for 'J', 'Z' and 'T' type of stringer sections, absolute difference between RS results and FEA results is not greater than 5%. RS gives fast convergence but this method does not give accurate results as the ANN. Absolute difference between the ANN results and FEA results is not greater than 2.5%. However, ANN also has a problem with convergence. If the neuron number is increased too much, for instance over 10 for the buckling problem, over fitting occurs. It should be noted that when over fitting occurs, error of the training set is driven to a very small value, but for the new data in between the data points used to generate the database, the error is large. Moreover, to get an accurate ANN result, many data sets are required. For the determination of the buckling coefficients, at least 2000 data sets are required to obtain reasonable results which are close to the finite element results with acceptable difference. Nevertheless, the established ANN can be used very effectively to determine the buckling coefficients of skin-stringer assemblies with common J, Z and T type stiffeners. If desired ANN can be utilized to construct buckling coefficients charts similar to the buckling coefficient charts available for panel buckling with classical boundary conditions.

CHAPTER 3

POST BUCKLING LOAD DISTRIBUTION OF METAL STIFFENED PANELS

In this chapter, post buckling load distribution and the effect of material nonlinearity on the load redistribution in the post-buckled stage is investigated using linear and nonlinear material models with different stringer types of skin-stringer assemblies by ABAQUS finite element analysis. For this purpose, in the first part of the study, a baseline stiffened panel is generated for further investigation of the material nonlinearity on the post-buckling behavior and on the effective width of the stiffened panel. To make a direct comparison with the classical approach for the determination of the effective width of the skin panel, a stiffener section which provides classical clamped edge condition is designed such that the compression buckling coefficient determined by the finite element analysis agreed closely with the analytically determined buckling coefficient of the clamped edge panel.

In the second part of the chapter, post-buckling analysis of the stiffened panel is performed utilizing linear and nonlinear material models with three different stringer types (I, J and Z) in the finite element analysis and the effect of material plasticity on the post-buckling behavior of the panel is studied. The effective width of the panel is calculated before the collapse load of the panel using the load distributions obtained by finite element analysis with linear and nonlinear material models and comparisons

are with the effective width calculated using the classical effective width formulation. At the end of the chapter, finite element model analysis results are obtained for combination of each stringer types and material models. Its means that totally 6 finite element model is created and effective width results are compared to each other.

3.1. Buckling Analysis of the Baseline Skin-Stringer Assembly

Baseline stiffened panel is designed in an iterative fashion to decide on the dimensions of the side stiffeners such that side stiffeners provided nearly clamped edge condition. For this purpose, compressive buckling coefficient of the stiffened flat panel is calculated by the finite element analysis until a close agreement is reached with the determined compressive buckling coefficient by the finite element analysis of clamped edge unstiffened panel.

Before the decision of the proper stiffener cross-section, buckling analysis of the flat panel with the classical clamped edge conditions is performed and the compression buckling coefficient is also obtained via finite element analysis before the addition of the side stiffeners. As previously defined in Figure 2.1, the geometry and the coordinate system of the panel is used in the construction of the unstiffened panel. Boundary condition of the unstiffened panel is defined as all edges clamped defined in Table 2.2.

However, in this case, load is applied from the DC edge along the y-axis of the single panel as 2.0 mm displacement in the “-x” direction (compression) and the reaction edge of the panel is taken as AB edge. Thus, in this case, in addition to boundary conditions defined in Table 2.2, AB edge is also restricted in translational degree of freedom in the x direction. Although, this additional boundary condition has no effect on the buckling coefficient result, it is necessary to fix the edge AB in order to be able to read reaction forces from the nodes along the edge AB in post-buckling analyses presented in this chapter.

After the determination of the boundary condition and the input displacement, input parameters of the unstiffened skin panel studied are decided as given in Table 3.1. The

unstiffened panel model without any side stiffeners is solved by using “Buckle” step of ABAQUS in linear buckling analysis for the lowest buckling eigenvalue [35].

Table 3.1: Input parameters of the unstiffened skin panel used to verify stiffened panel edge condition

Skin panel material	Aluminum 2024 T3 Sheet
Skin panel thickness (mm)	0.813
Skin panel length x (mm)	450
Skin panel length y (mm)	150

For the unstiffened panel model described in Table 3.1, lowest eigenvalue is obtained as,

$$\lambda_{FE} = 0.0450 \quad (3.1)$$

Using this eigenvalue, the corresponding compressive stress and the compressive buckling coefficient are calculated as,

$$u_{cr} = u_{FE} * \lambda_{FE} = 0.090 \text{ mm} \quad (3.2)$$

$$\sigma_{cr} = \frac{u_{cr}}{l_x} E_c = 14.77 \text{ MPa} \quad (3.3)$$

$$k = \sigma_{cr} \frac{12(1 - \nu^2)}{\pi^2 E_c} \left(\frac{l_y}{t} \right)^2 = 7.38 \quad (3.4)$$

After calculation of the buckling coefficient of the unstiffened panel with all edges clamped boundary conditions by the finite element analysis, stiffened panel modeling is performed using the clamped boundary conditions along the loaded edges of the panel. For the stiffened panels, side stiffeners provide constraint along the unloaded edges of the panel. To generate the clamped edge condition along the unloaded edges of the stiffened panel, an iterative procedure is used to decide on the dimensions of the stiffener. To study the post-buckling behavior of the stiffened panel, the considered skin-stringer assembly consists of three flat skin panels and two stringers with I cross section. Mesh-independent fasteners available in ABAQUS are used in the skin-

stringer connection [35]. Skin-stringer assembly and the skin panel numbering are demonstrated in Figure 3.1. For the skin-stringer assembly, a compression load is applied in the -x direction as prescribed displacement on one of the edges along the y-direction.

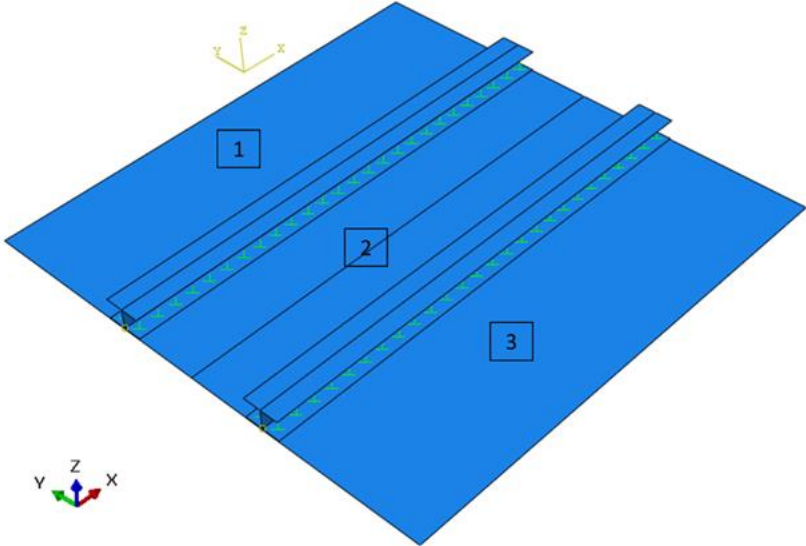


Figure 3.1: Baseline skin-stringer assembly

Figure 3.2 shows the restraints applied to the loaded and the opposite edges of the skin-stringer assembly. To simulate the clamped edge condition, the degrees of freedom restrained along the loaded edges are U3 (z-direction displacement) and R2 (rotation about the y-axis). Along the opposite edge of the loading edge of the skin-stringer assembly, degrees of freedom U1, U3 and R2 are restrained. In addition, the mid-point of panel 2 is not allowed move in the y-direction to avoid rigid body motion of the assembly, as shown in Figure 3.2. Moreover, unloaded side edges of the panels 1 and 3 are restrained in z-translation (U3 degree of freedom) and x-rotation (R1 degree of freedom).

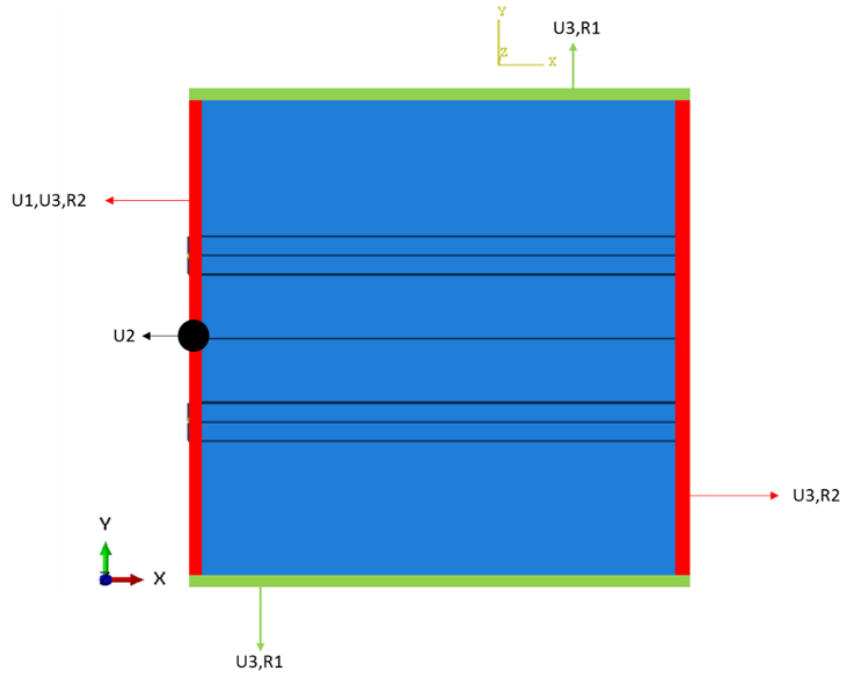


Figure 3.2: Constraints applied to the baseline skin-stringer assembly

In the finite element model of the baseline skin-stringer assembly, all stringers and skin panels are modeled as 2D shell elements with Aluminum 2024 T3 sheet material properties [36]. Same fastener configurations and modelling technics written in chapter 2.2 are used in the finite element model of baseline skin-stringer assembly. Fastener configurations used in baseline skin-stringer assembly is shown in Figure 2.14.

For the skin-stringer assembly, “Buckle” step of ABAQUS is used in linear buckling analysis to obtain the lowest buckling eigenvalue [35]. The lowest buckling eigenvalue is used in Equation (3.4) to calculate the compression buckling coefficient pertaining to the local buckling of the skin supported by the side stiffeners. By comparing the compression buckling coefficient calculated by the finite element solution with the determined compression buckling coefficient by finite element model of unstiffened panel defined in Table 3.1, clamped edge condition provided by the side stiffeners is verified.

Stringer dimensions are changed until the compression buckling coefficient obtained by the finite element analysis agreed closely with the finite element result of 7.38 given

by Equation (3.1). For this purpose, parametric modeling of the skin-stringer assembly is performed via the script language followed by automated finite element analysis by ABAQUS [35]. I type of stringer dimensions which simulate the clamped edge boundary condition closely are given in Table 3.2 together with the overall dimensions of the skin-stringer assembly.

For the buckling analysis, a compression load is applied on one of the edges of the skin-stringer assembly with the I type of stringer section along the y-axis as 2.0 mm prescribed displacement in the “-x” direction. For the skin-stringer assembly described in Table 3.2, lowest eigenvalue is obtained as,

$$\lambda_{FE} = 0.0450 \quad (3.5)$$

Table 3.2: Parameters of the skin-stringer assembly used in the finite element model with I section stringer

Skin panel material	Aluminum 2024 T3 Sheet
Skin panel thickness (mm)	0.813
Skin panel length x (mm)	450
Single skin panel length y (mm)	150
Stringer material	Aluminum 2024 T3 Sheet
Stringer thickness (mm)	1.016
Stringer height (mm)	25
Stringer upper flange width (mm)	15
Stringer lower flange width (mm)	20

Using this eigenvalue, the corresponding compressive stress and the compressive buckling coefficient of skin-stringer assembly with I stringer section type are calculated as,

$$u_{cr} = u_{FE} * \lambda_{FE} = 0.090 \text{ mm} \quad (3.6)$$

$$\sigma_{cr} = \frac{u_{cr}}{l_x} E_c = 14.77 \text{ MPa} \quad (3.7)$$

$$k = \sigma_{cr} \frac{12(1 - \nu^2)}{\pi^2 E_c} \left(\frac{l_y}{t} \right)^2 = 7.38 \quad (3.8)$$

Comparing the results given by Equation (3.4) and Equation (3.8), it is concluded that the properties of the I section stringer given in Table 3.2 provides the clamped edge condition along the unloaded edges of the skin-stringer assembly.

3.2. Post-Buckling Analysis of Skin-Stringer Assembly using Linear and Non-linear Material Models

Following the verification of the compression buckling coefficient of the stiffened panel with finite element model, the post-buckling behavior of the skin-stringer assembly is investigated with two different models; with linear and nonlinear material models. In both models, “Non-linear Geometric Static Analysis” step of ABAQUS is used to observe the post-buckling behavior of the stiffened panel [35]. For both models, load carrying capacity of the assembly and the effective width of the skin panel are calculated using the finite element results. Moreover, effective width calculation is also done utilizing the empirical relation following Bruhn [1].

For the analysis of the post-buckling load distribution, nodal forces in the x-direction of the restrained edge of the skin panel are summed up to calculate load capacity of assembly. Additionally, one of the nodes in the loaded edge is used to trace the displacement of skin-stringer assembly. Restrained and loaded edges are shown in Figure 3.3 with red and green lines, respectively.

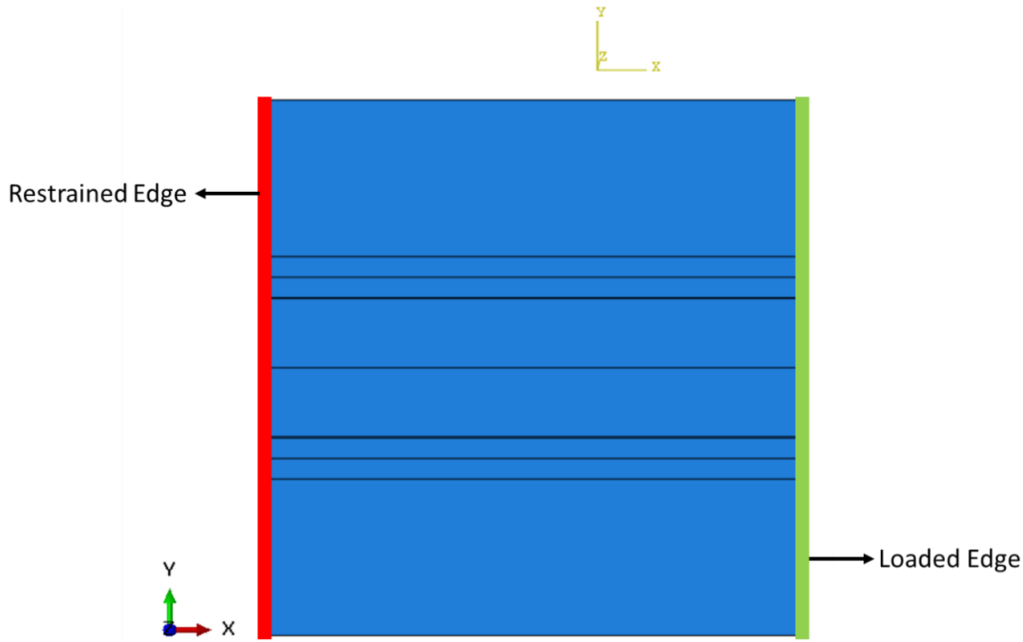


Figure 3.3: Edge descriptions of the skin-stringer assembly

To investigate the post-buckling behavior of the skin-stringer assembly, geometrically nonlinear analysis of the skin-stringer assembly with I section stringer is conducted by the “Non-linear Static Analysis” step of ABAQUS [35]. As in the previous analyses, a compression load is applied on one of the edges of the skin-stringer assembly along the y-axis as 2.0 mm prescribed displacement in the “-x” direction. Material and geometric description of the previous assembly which is used for verification of the clamped edge condition in chapter 3.1, is used for the both material models created in this chapter. In addition to the linear material model, nonlinear stress-strain data given in Appendix B is used in the ABAQUS material description. Defining material plasticity in ABAQUS is presented in the research report by Rasmussen [39]. Material properties of the aluminum 2024-T3 sheet are given in Figure B.1 [36]. For aluminum 2024-T3, stress-strain curve including the plastic region is given in Figure B.2. For the nonlinear material model, the stress-strain data given in Table B.1 is used in the post-buckling analysis.

Firstly, using the linear material model for the skin-stringer assembly, load-displacement curve is obtained by ABAQUS analysis as shown in Figure 3.4.

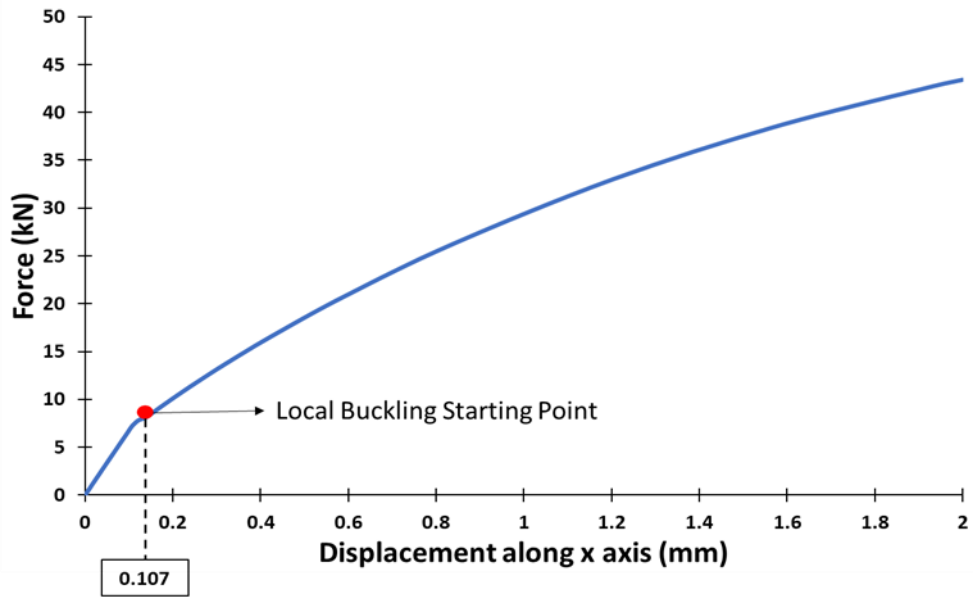


Figure 3.4: Load displacement curve of the skin-stringer assembly with linear material model (I section stringer)

As shown in Figure 3.4, the first break in the load-displacement curve represents the initiation of the local buckling. Local buckling starts when the applied displacement is 0.107 mm. This result is different than the critical displacement determined in linear buckling analysis ($u_{cr} = 0.090 \text{ mm}$). The reason of this difference is attributed to including the geometric non-linearity in the post-buckling model. Beyond the initiation of the local buckling, post-buckling stage of the skin-stringer assembly starts. It should be noted that because of the geometric non-linearity, load displacement curve is nonlinear beyond the initiation of the local buckling of the skin. However, the collapse of the skin-stringer assembly is not seen in Figure 3.4 because of the use of linear material properties.

Secondly, Figure 3.5 shows the load-displacement curve obtained by using the nonlinear material model in the finite element analysis. As shown in Figure 3.5, local buckling of the skin starts at a displacement of 0.104 mm and this value is almost same as the local buckling displacement (0.107 mm) of the skin-stringer assembly with the linear material model. Beyond the initiation of the local skin buckling, load-displacement curve again becomes nonlinear and when the displacement reaches 1.736 mm collapse of the skin-stringer assembly occurs.

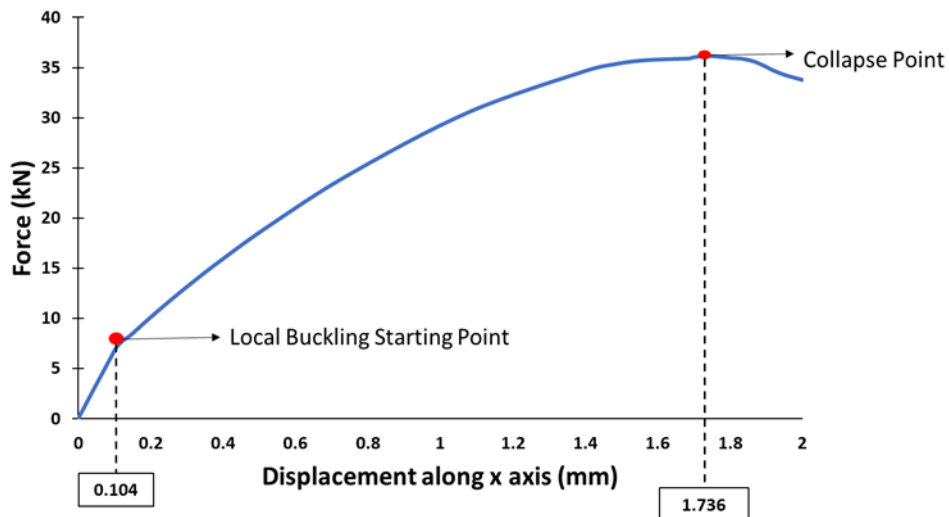


Figure 3.5: Load displacement curve of the skin-stringer assembly with nonlinear material model (I section stringer)

Figure 3.6 and Figure 3.7 show the finite element view of skin-stringer assembly with nonlinear material model at the local buckling starting point and collapse point, respectively.

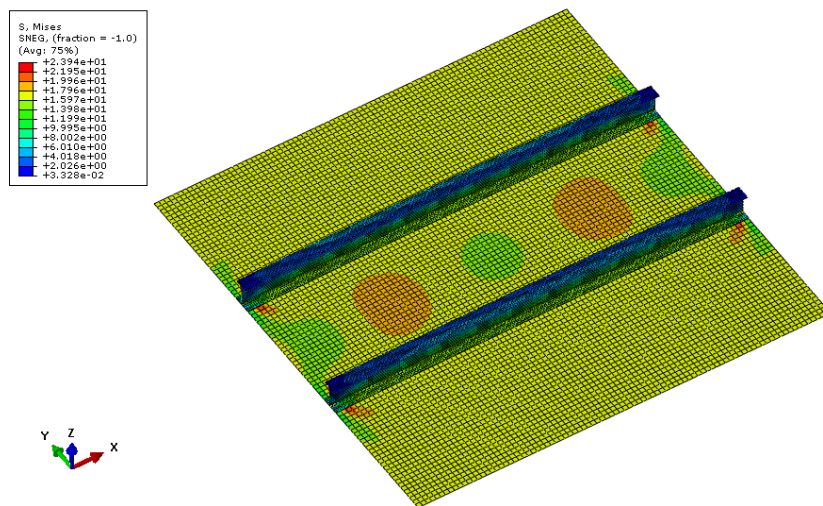


Figure 3.6: FE view of skin-stringer assembly with nonlinear material model (I section stringer) at local buckling starting point

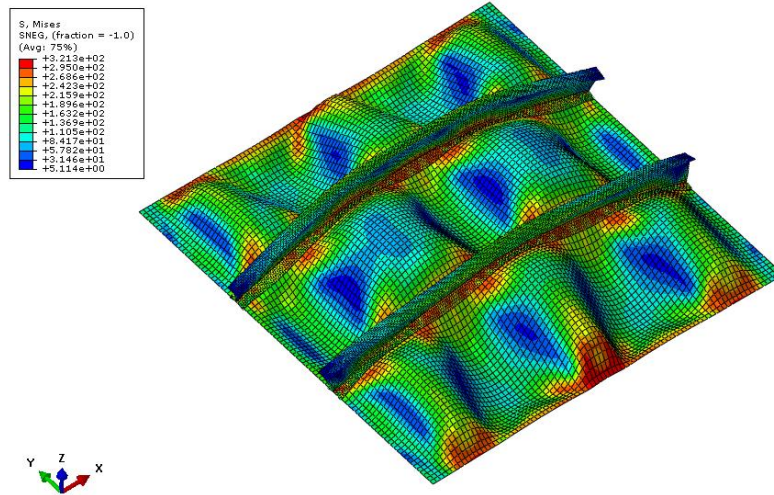


Figure 3.7: FE view of skin-stringer assembly with nonlinear material model (I section stringer) at collapse point

Figure 3.8 compares the load displacement curves obtained by the linear and nonlinear material models. The effect of material nonlinearity on the post-buckling behavior of the skin-stringer assembly is clearly seen in Figure 3.8. After the local buckling of the skin, when the applied displacement reaches 1 mm or so, material nonlinearity effect becomes dominant. It should be noted that the collapse of the assembly with the nonlinear material model is merely due to the nonlinear material property since no damage model exists in the finite element models.

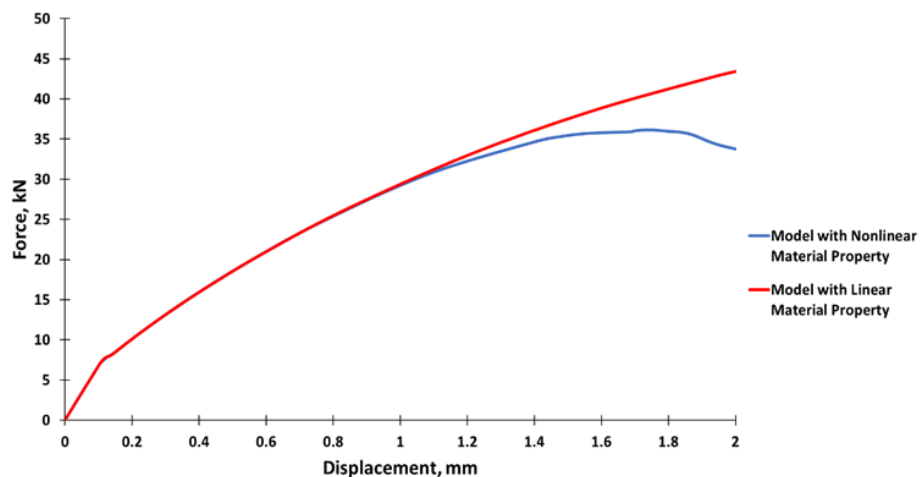


Figure 3.8: Comparison of load displacement curves of models with linear and nonlinear material properties (I section stringer section)

3.3. Calculation of Effective Width by Finite Element Solution and Empirical Solution

To calculate the effective width of the skin panel using the finite element results, for each node on the restrained edge of the skin panel, forces in the x-direction are obtained separately to see how the load is distributed along the y-direction. Effective width at the location of the restrained edge of the skin panel as seen in Figure 3.9 is then calculated with the idealization of the actual nonlinear load distribution in the post-buckled stage. Using the x-direction nodal forces, load distribution is pictured, as shown in Figure 3.10. This idealization is made by equating the area under the nonlinear load distribution to the idealized rectangular load distribution, as shown in Figure 3.11. To find the effective width of the buckled panel, the area under the nonlinear load distribution curve is divided by the peak load [1], as shown in Equation (3.9).

$$w_{eff} = \frac{A_{eff}}{F_{max}} \tag{3.9}$$

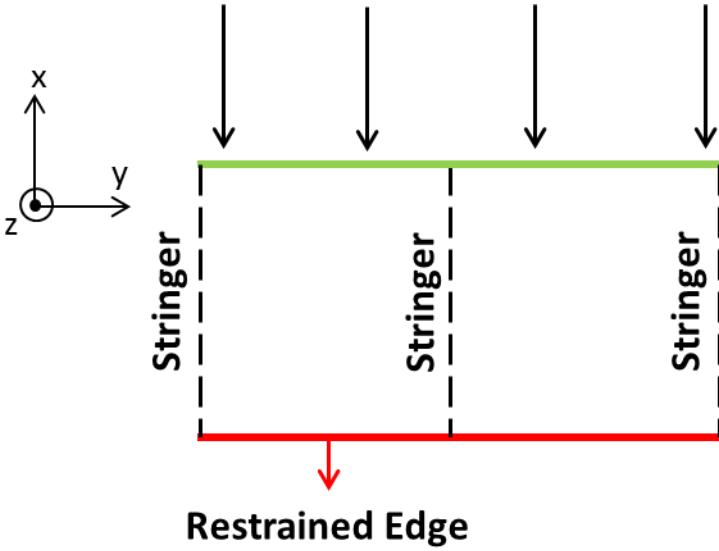


Figure 3.9 Top view of skin-stringer assembly under compressive loading

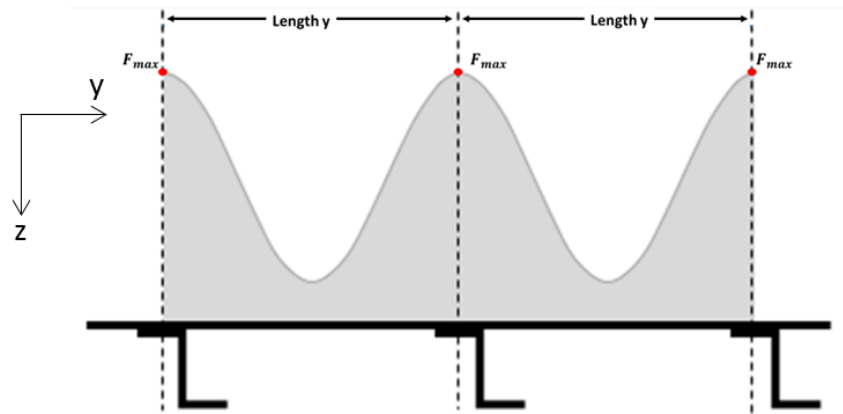


Figure 3.10: Actual load distribution in the post-buckled stage [1]

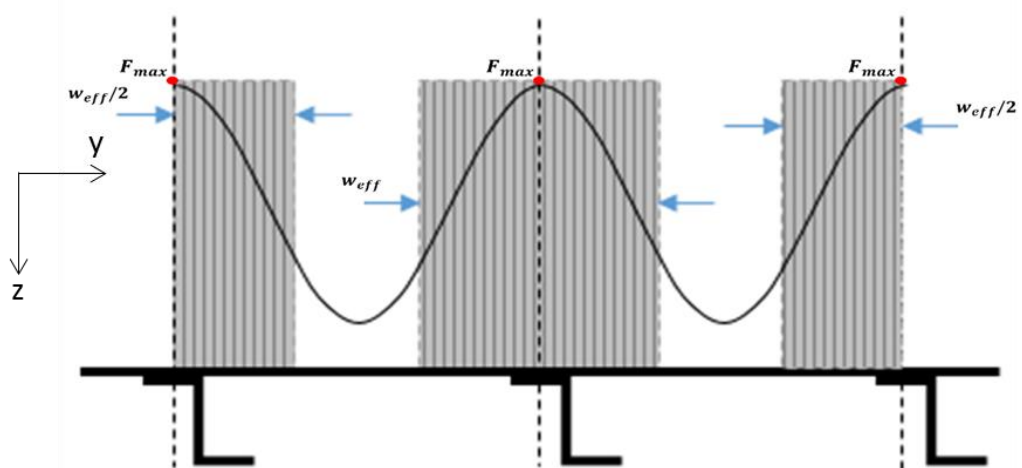


Figure 3.11: Equivalent load distribution using the concept of effective width [1]

Same as previous sub-chapter, the first finite element model of the skin-stringer assembly is constructed using the linear material properties of the aluminum 2024-T3 sheet in the finite element, and load distribution in the post-buckled stage and the effective width are calculated accordingly. The second finite element model of the skin-stringer assembly is constructed with nonlinear material properties of the aluminum 2024-T3 sheet and material plasticity is accounted for. Again, for the skin-stringer assembly with the nonlinear material model, load distribution in the post-buckled stage and the effective width are calculated and comparisons are made with the results obtained with the linear material model. Finally, effective widths calculated

by both models are compared with the effective width calculated by the classical effective width formulation provided by Bruhn [1].

In order to calculate the effective widths, load distributions along the y-axis at the restrained edge of the skin-stringer assembly with I stringer cross section are extracted from the finite element analysis results of the skin-stringer assemblies with linear and the nonlinear material models. In Figure 3.12, load distribution of the skin-stringer assembly with the linear material property is presented just before the local buckling of the skin panel. It is seen that skin carries the same load on each element of the restrained edge along the y-axis before the local skin buckling, as expected. The two peaks correspond to the location of the fasteners in the finite element model.

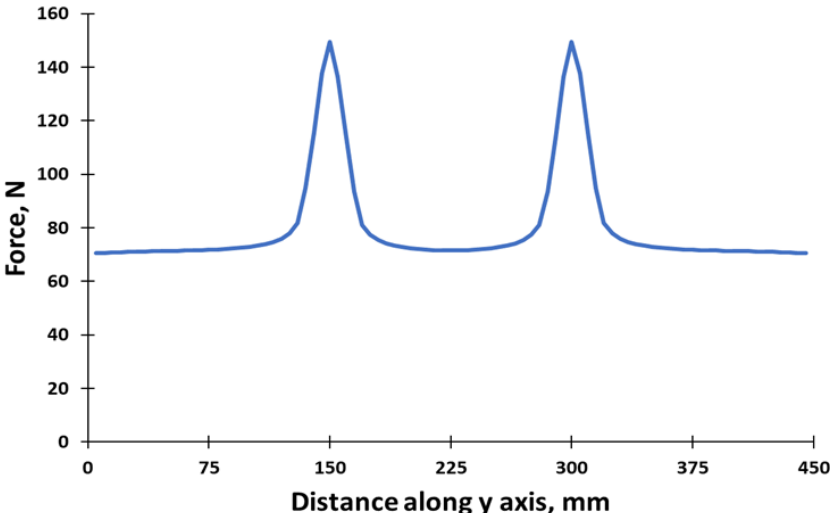


Figure 3.12: Load distribution in the skin-stringer assembly with the linear material model just before the skin buckling (I section stringer)

In Figure 3.13, load distribution is presented for the skin-stringer assembly with linear material model at the compressive displacement of 1.736 mm, which is the collapse displacement obtained by the nonlinear material model. In addition, Figure 3.13 shows the location of stringers and edges which are restrained by classical boundary conditions. First and last skin panels are located between the restrained edge and the stringer. Second skin panel is located between two stringers. In this study, load distribution is calculated at the only second skin panel location. In the post-buckled

stage, as expected, load distribution after the local buckling of the skin is highly different from the load distribution given in Figure 3.12. Skin sections at the stringer locations carry more loads compared to the skin part at the middle of skin sections. Figure 3.13 also shows the idealized load distribution with red dash line, known as the effective width. For the skin-stringer assembly with the linear material model, effective width is calculated as 49.20 mm using actual load distribution area scanned by the green lines seen in Figure 3.14.

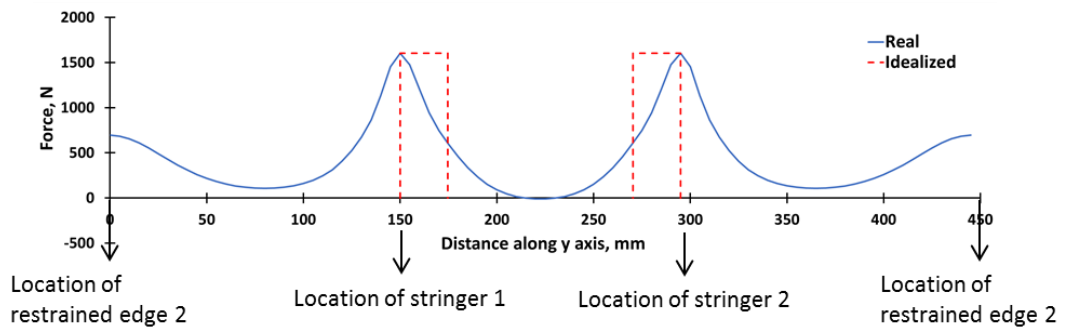


Figure 3.13: Load distribution in the skin-stringer assembly with the linear material model at the collapse displacement (1.736 mm) of the nonlinear material model case (I section stringer)

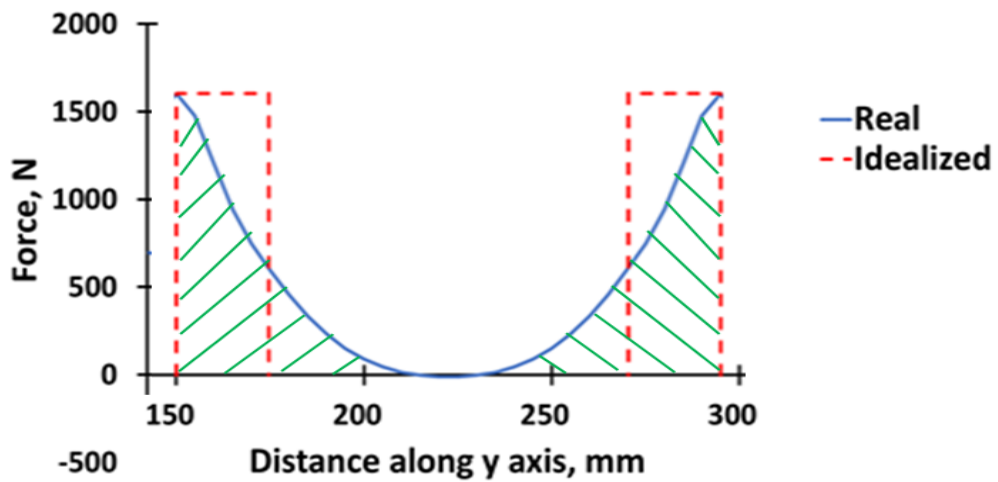


Figure 3.14: Closed view of load distribution in the skin-stringer assembly with the linear material model at the collapse displacement (1.736 mm) of the nonlinear material model case (I section stringer)

In Figure 3.15, load distribution is presented for the model with the nonlinear material property just before the local buckling of the skin panel. Before the local buckling of the skin, load distribution given in Figure 3.15 is exactly same as the load distribution (Figure 3.12) obtained using the linear material model, as expected.

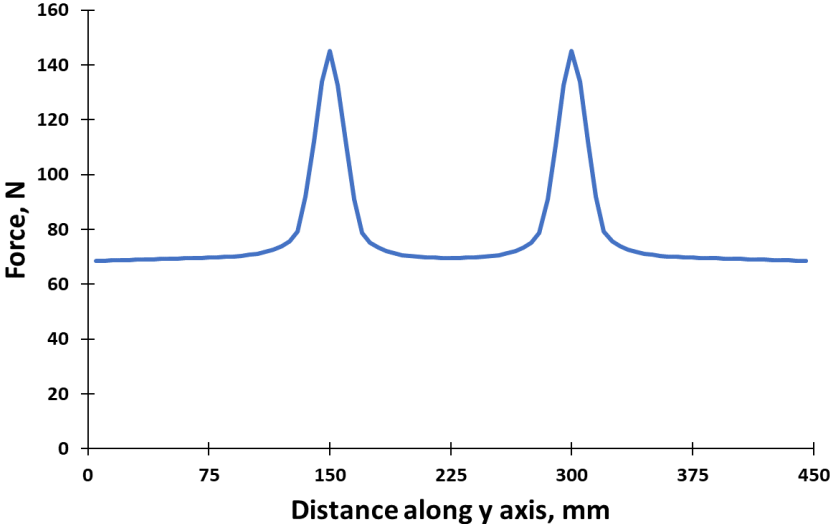


Figure 3.15: Load distribution in the skin-stringer assembly with the nonlinear material property just before the skin buckling (I section stringer)

In Figure 3.16, load distribution is presented for the model with the nonlinear material property at the collapse displacement of 1.736 mm. As expected, load distribution in the post-buckled stage is highly different from the load distribution in the pre-buckled configuration. For the skin-stringer assembly with the nonlinear material model, effective width is calculated as 60.67 mm. It should be noted that since the peak load for the skin-stringer assembly with the nonlinear material model is lower than the peak load for the assembly with the linear material model, effective width is higher.

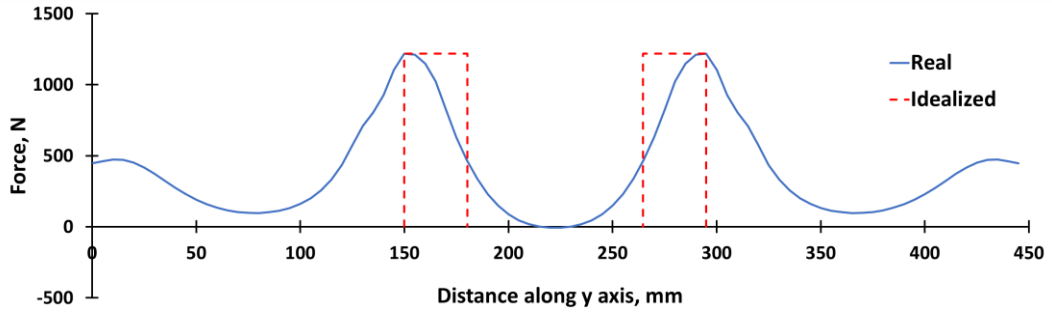


Figure 3.16: Load distribution in the skin-stringer assembly with nonlinear material property at the collapse displacement of 1.736 mm (I section stringer)

Figure 3.17 shows the load distribution obtained by the linear and nonlinear material models in the finite element analysis in the same plot. It is seen that the main effect of including material nonlinearity is on the peak load level which drops significantly for the skin-stringer assembly with the nonlinear material model. Moreover, equivalent width calculated based on finite element analysis using nonlinear material model is higher than the equivalent width calculated using linear material model. For the skin-I section stringer assembly, ratio of the equivalent widths calculated using the linear and the nonlinear material models is 0.81.

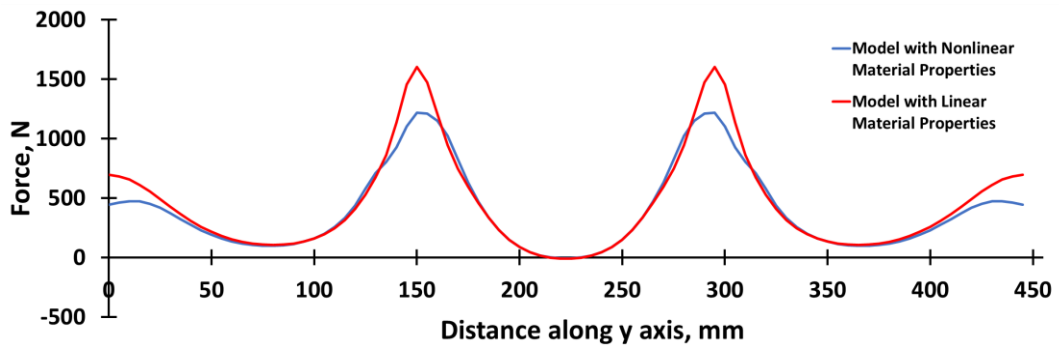


Figure 3.17: Comparison of the load distribution in the skin-stringer assemblies with linear and nonlinear material properties (I section stringer)

In this study, effective width is also calculated using the empirical relation given by Bruhn [1], Equation (3.10). In Equation (3.10), stringer stress (F_{str}) is taken as the minimum of the stringer local buckling stress (F_{lb}), stringer crippling failure stress (F_{crip}) and the material yield stress of the stringer (F_{cy}). For the skin-stringer

assembly, local buckling stress F_{lb} is calculated as 280.98 MPa [1], and the crippling stress of the stringer is calculated as 282.61 MPa [40]. Calculation methodology of local buckling stress of the stringer is given Appendix C. For Aluminum 2024 T3, material yield stress is 269 MPa [36]. Therefore, stringer stress (F_{str}) is taken as the minimum of the three as 269 MPa. Moreover, half of the lower flange width (l_{lf}) is added to the effective width formula because of the double row fastener configuration for the I-section stringer. For the clamped edge condition, effective width constant k_{eff} is specified as 2.52 in Bruhn [1]. Thus, for the skin-stringer assembly effective width is calculated as 43.61 mm.

In addition, effective width is also calculated using the stringer stress in the lower flange obtained from finite element analysis at the collapse point and the empirical relation given by Bruhn [1], Equation (3.10). In the model with the linear material property, absolute maximum stringer stress (F_{str}) is obtained as 263.9 MPa (Equation (3.12)). Thus, for the skin-stringer assembly effective width is calculated as 43.93 mm. Moreover, in the model with nonlinear material property, absolute maximum stringer stress (F_{str}) is obtained as 248.6 MPa (Equation (3.13)). Thus, for the skin-stringer assembly effective width is calculated as 44.96 mm.

$$w_{eff} = k_{eff} * t_{sk} * \sqrt{E/F_{str}} + 0.5 * l_{lf} \quad (3.10)$$

$$(F_{str})_{Bruhn} = \min(F_{crip}, F_{lb}, F_{cy}) = 269 \text{ MPa} \quad (3.11)$$

$$(F_{str})_{Linear-Fem} = 263.9 \text{ MPa} \quad (3.12)$$

$$(F_{str})_{Nonlinear-Fem} = 248.6 \text{ MPa} \quad (3.13)$$

Table 3.3 compares the effective widths calculated by the finite element analysis utilizing linear and nonlinear material models with the effective width calculated by the classical empirical approach and the effective width calculated by a combination of the classical approach and the stringer stress determined by the finite element analysis at the collapse point determined by the finite element analysis using linear and nonlinear material property. It is seen that the effective width calculated by the classical method is close to the effective width calculated by the finite element analysis

performed utilizing the linear material model. When the nonlinear material model is used in the finite element analysis, a higher effective width is calculated. The classical approach gives smallest effective width compared to finite element analysis results. It is also noticed that effective widths calculated by using the stringer stresses determined at the collapse point by the finite element analysis with the linear and the nonlinear material models are strikingly close to the effective width calculated by the classical empirical relation given by Bruhn [1].

Table 3.3: Comparison of the effective widths (I-section stringer)

	Finite element (Linear material model)	Finite element (Nonlinear material model)	Equation (3.10)	Equation (3.10) with Stringer Stress from FE Analysis (Linear material model)	Equation (3.10) with Stringer Stress from FE Analysis (Nonlinear material model)
Effective width (mm)	49.20	60.67	43.61	43.93	44.96

3.4. Effect of Stringer Section Types on the Post-Buckling Stage

To see the effect of different section stringers on the buckling load, collapse load and the effective width, the stringer dimensions of the I stringer are used for the skin-stringer assemblies with J and Z type stringers. Geometric descriptions of the stringers with different sections are shown in Figure 3.18. As seen in Figure 3.18, I and J section stringers use double row joints at the connection of skin and the lower flange of the stringer. On the other hand, in the Z section stringer, double and single row joint configurations are used in the finite element model. Figure 3.18 shows the single row joint configuration of Z section stringer.

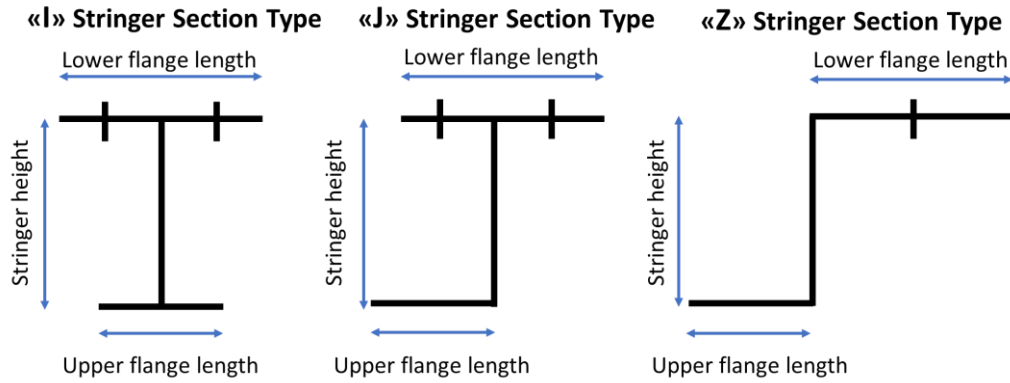


Figure 3.18: Stringer section types used in this study

Same procedure for the skin-stringer assembly with the I stringer section is also applied to the skin-stringer assemblies with the J and Z type of stringer sections. To make direct comparisons between the different stringer types, the dimensions of the I section stringer, which provides clamped edge condition, are directly used for the J and Z section stringers. Dimensions of the J and Z section stringers are given in Table 3.5 and Table 3.6 together with the overall dimensions of the skin-stringer assembly, respectively.

3.4.1. Skin-Stringer Assembly with J Section Stringer

Same as the skin-I section stringer assembly, first linear buckling analysis has been performed. In this analysis, a compression load is applied on one of the edges of the skin-stringer assembly with the J type of stringer section along the y-axis as 2.0 mm prescribed displacement in the “-x” direction. For the skin-stringer assembly with the J type of stringer section described in Table 3.4 lowest eigenvalue is obtained as,

$$\lambda_{FE} = 0.0451 \quad (3.14)$$

Using this eigenvalue, the compressive buckling coefficient of skin-stringer assembly with the J stringer section type is calculated as,

$$k = \sigma_{cr} \frac{12(1 - \nu^2)}{\pi^2 E_c} \left(\frac{l_y}{t} \right)^2 = 7.40 \quad (3.15)$$

Table 3.4: Parameters of the skin-stringer assembly used in the finite element model with J section stringer

Skin panel material	Aluminum 2024 T3 Sheet
Skin panel thickness (mm)	0.813
Skin panel length x (mm)	450
Single skin panel length y (mm)	150
Stringer material	Aluminum 2024 T3 Sheet
Stringer thickness (mm)	1.016
Stringer height (mm)	25
Stringer upper flange width (mm)	15
Stringer lower flange width (mm)	20

Based on the compression buckling coefficients determined from the linear buckling analysis of the skin-stringer assemblies with J stringer section, it is confirmed that the restraints provided by the J section stringers are appropriate to simulate the classical clamped edge condition as the I section stringer case. The reason of this similarity, both stringer types uses same double row fastener configuration as seen in Figure 3.18. The upper flange connection has a small effect on the buckling behaviour of the skin-stringer assembly. Hence, buckling coefficients of these two skin-stringer assembly are close to each other.

After the calculation of the buckling coefficient of skin-J stringer section assembly, geometrically nonlinear static analysis has been conducted for the skin-stringer assembly with J type stringer. For the skin-stringer assembly with the linear material model, load-displacement curve that is obtained by ABAQUS analysis is shown in Figure 3.19.

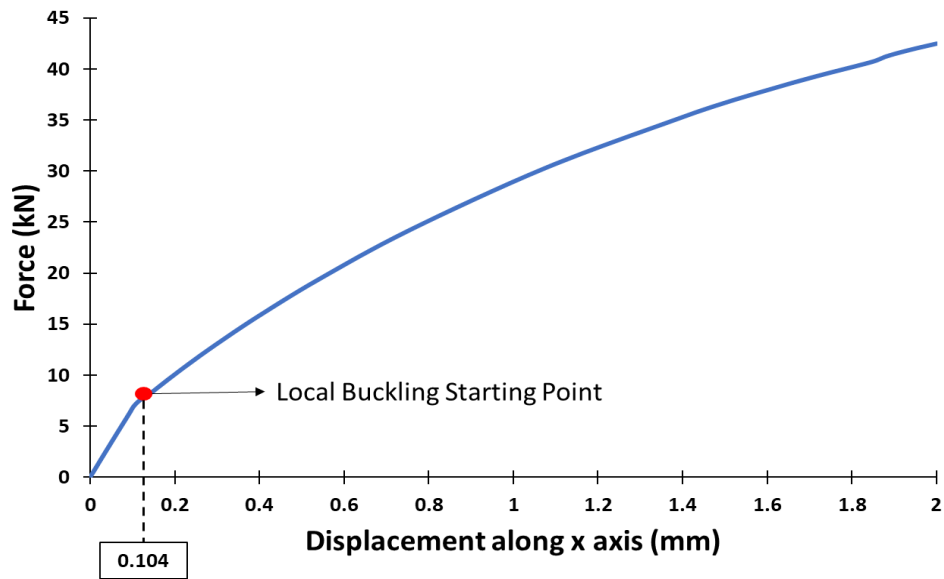


Figure 3.19: Load displacement curve of the skin-stringer assembly with linear material model (J section stringer)

As shown in Figure 3.19, load displacement curve for the skin-stringer assembly with the J type stringer is similar to the I section stringer case. For the skin-stringer assembly with the J section stringer, local buckling displacement is same as the skin-stringer assembly with the I section stringer.

Figure 3.20 shows the load-displacement curve obtained by using the nonlinear material model in the finite element analysis. As shown in Figure 3.20, local buckling of the skin starts at the same displacement of 0.104 mm which is same as the local buckling displacement of the skin-stringer assembly with the linear material model. Beyond the initiation of the local skin buckling, load-displacement curve again becomes nonlinear and when the displacement reaches 1.726 mm collapse of the skin-stringer assembly occurs. For the skin-stringer assembly with the J section stringer, collapse load is reached at a slightly lower displacement than the skin-stringer assembly with the I section stringer.

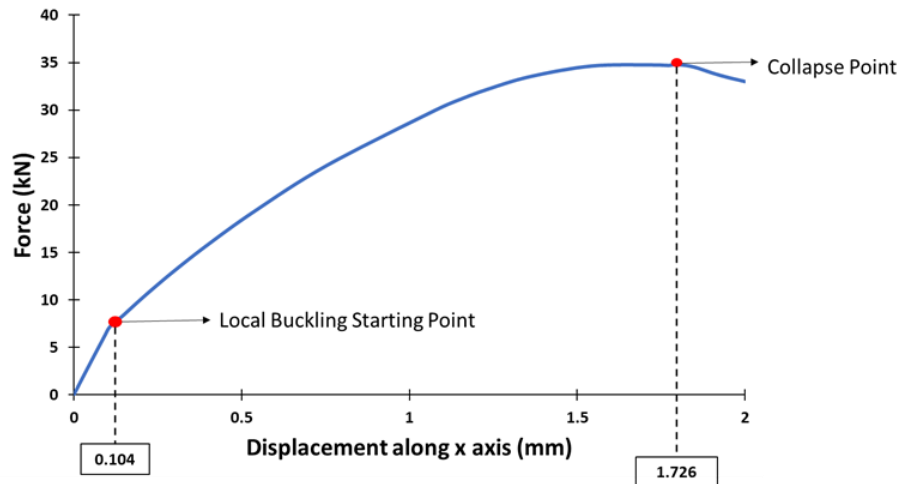


Figure 3.20: Load displacement curve of the skin-stringer assembly with nonlinear material model (J section stringer)

For the skin-stringer assembly with the J section stringer, Figure 3.21 shows the load distribution in the skin-J stringer assembly with the linear material model just before the local buckling of the skin panel. Comparing Figure 3.12 with Figure 3.21, one can see that the load distributions in the skin-stringer assemblies with I and J section stringer are almost the same.

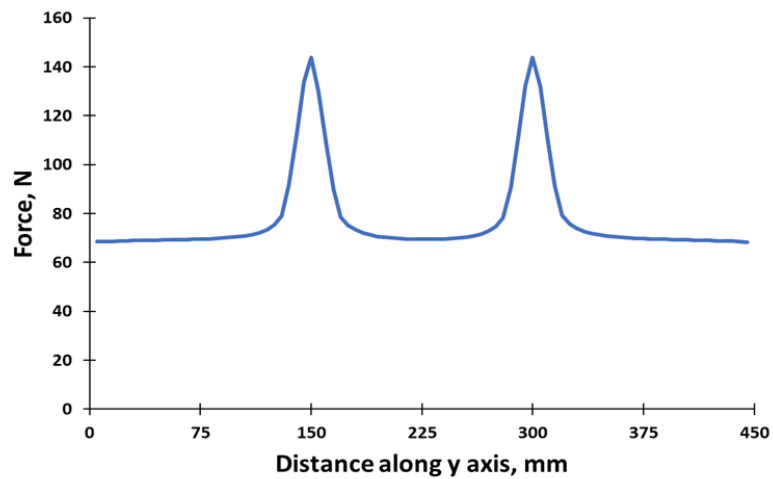


Figure 3.21: Load distribution in the skin-stringer assembly with the linear material model just before the skin buckling (J section stringer)

In Figure 3.22, load distribution is presented for skin-stringer assembly model with J section stringer with the linear material model at the compressive displacement of

1.726 mm which is the collapse displacement obtained by the nonlinear material model. Figure 3.22 also shows that idealized load distribution with red dash line, known as the effective width. For the skin-stringer assembly with the linear material model and J section stringer, effective width is calculated as 47.59 mm using area under the actual load distribution given by the blue line. It should be noted that for the J stringer case, skin-stringer assembly is not symmetric with respect to the center of the middle panel, therefore load distribution in the assembly is also not symmetric with respect to the center of the middle panel.

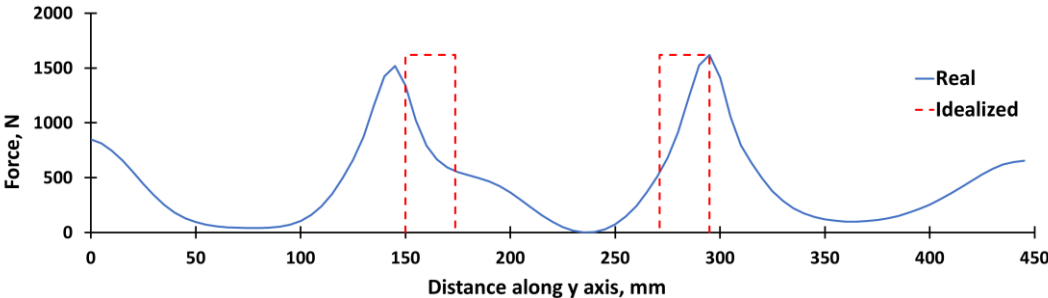


Figure 3.22: Load distribution in the skin-stringer assembly with the linear material model the collapse displacement (1.726 mm) of the nonlinear material model case (J section stringer)

In Figure 3.23, load distribution is presented for the skin-J section stringer assembly with the nonlinear material model just before the local buckling of the skin panel. It is again noted that before the local buckling of the skin, load distribution given in Figure 3.23 is almost same as the load distribution (Figure 3.21) obtained using the linear material model, as expected.

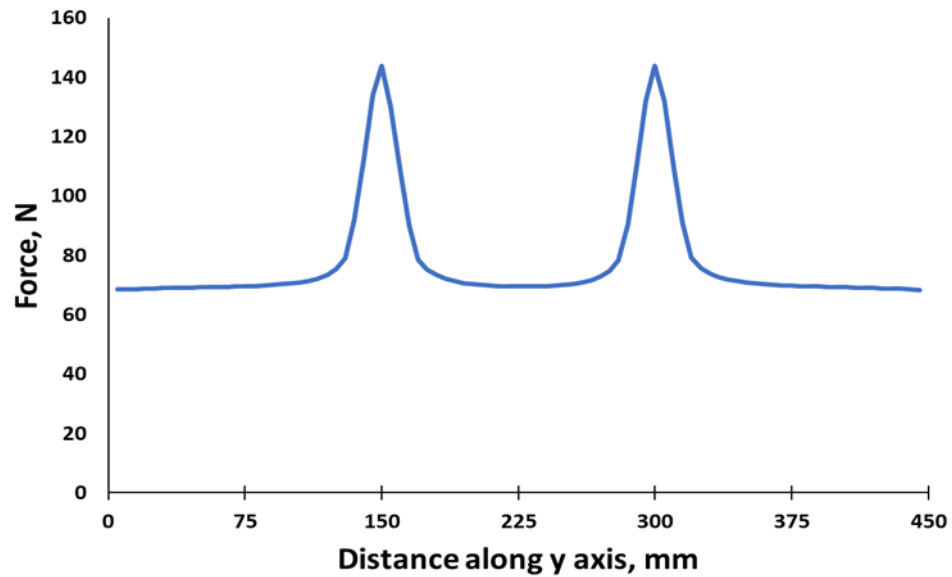


Figure 3.23: Load distribution in the skin-stringer assembly with the nonlinear material model just before the skin buckling (J section stringer)

In Figure 3.24, load distribution is presented for the skin-J section stringer assembly with the nonlinear material model at the collapse displacement of 1.726 mm. For the skin-stringer assembly with the nonlinear material model, effective width is calculated as 57.48 mm.

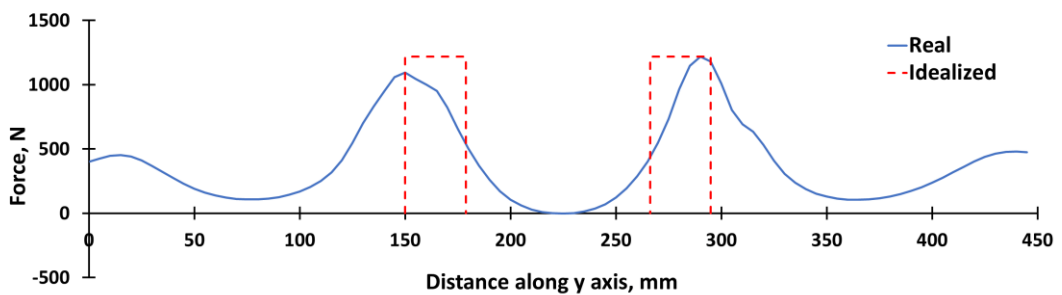


Figure 3.24: Load distribution in the skin-stringer assembly with the nonlinear material model at the collapse displacement of 1.726 mm (J section stringer)

Figure 3.25 compares the load distributions in the skin-J section stringer assemblies obtained by the linear and nonlinear material models in the finite element analysis in the same plot. It is seen that as in the I-section stringer case, the main effect of including material nonlinearity is on the peak load level which drops significantly for

the skin-stringer assembly with the nonlinear material model. Moreover, equivalent width calculated based on finite element analysis using nonlinear material model again is higher than the equivalent width calculated using linear material model. For the skin J-section stringer assembly, ratio of the equivalent widths calculated using the linear and nonlinear material models is 0.83. It is also noted that skin J-section stringer assembly has lower equivalent width than the skin-I section stringer assembly.

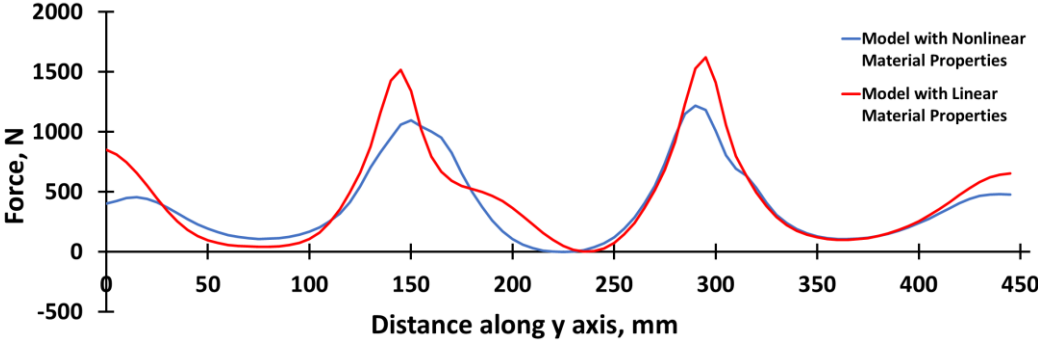


Figure 3.25: Comparison of the load distribution of skin-stringer assemblies with linear and nonlinear material properties (J-section stringer)

Following the same analysis procedure applied for the skin I-section stringer assembly, effective widths for the skin J-section stringer assembly are calculated by the classical empirical approach of Bruhn [1] and also utilizing the combination of the classical approach and the stringer stress determined by the finite element analysis. For the skin J-section stringer assembly, local buckling stress (F_{lb}) is calculated as 233.65 MPa [1], and crippling stress of the stringer is calculated as 248.66 MPa [40]. For Aluminum 2024 T3, material yield stress is 269 MPa [36]. Therefore, stringer stress (F_{str}) is taken as the minimum of the three as 233.65 MPa. Thus, for the skin J-section stringer assembly, effective width is calculated as 46.06 mm from Equation (3.10). Table 3.5 compares the effective widths calculated by different approaches. Again, for the skin J-section stringer assembly, equivalent widths calculated by the linear finite element analysis and by the classical empirical approach of Bruhn agree considerably well. Similar to the I-section stringer case, equivalent width calculated by the finite element analysis with the nonlinear material property is the highest for the skin J-section stringer assembly.

Table 3.5: Comparison of the effective widths (J-section stringer)

	Finite element (Linear material model)	Finite element (Nonlinear material model)	Equation (3.10)	Equation (3.10) with Stringer Stress from FE Analysis (Linear material model)	Equation (3.10) with Stringer Stress from FE Analysis (Nonlinear material model)
Effective width (mm)	47.59	57.48	46.06	44.11	45.48

3.4.2. Skin-Stringer Assembly with Z Section Stringer

In this chapter, to see the effect of fastener configuration on the buckling load, collapse load and the effective width, two skin-stringer assemblies with single row fastener Z section stringer and with double row fastener Z section stringer are modelled with ABAQUS as seen in Figure 3.26. After that point, Z section stringer with double row fastener configuration is defined as Z_2 .

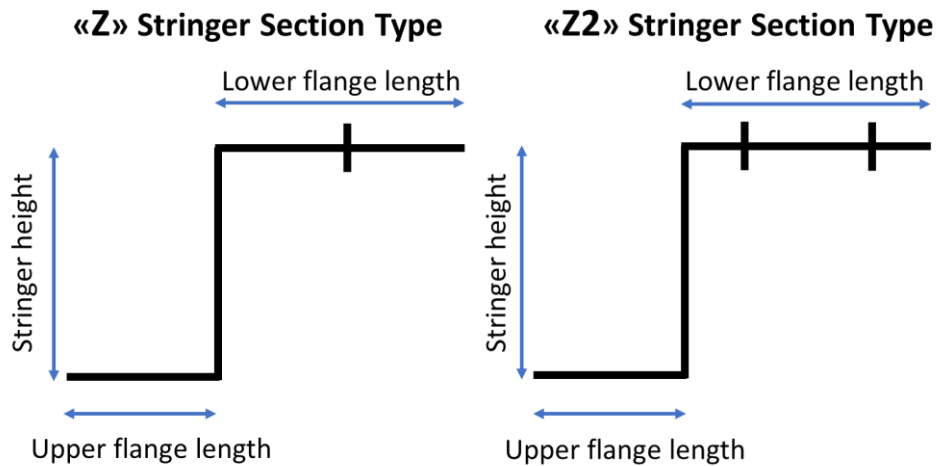


Figure 3.26: Single and double fastener configurations with Z section stringer

3.4.2.1. SINGLE ROW FASTENER CONFIGURATION

Skin-stringer assembly with Z section stringer which has a single row fastener configuration is obtained using same geometric and material properties of skin-stringer assembly as the I stringer section as mentioned before. Firstly, linear buckling analysis is performed for the skin-stringer assembly. For the buckling analysis of the skin-stringer assembly with Z section stringer, a compression load is applied on one of the edges of the skin-stringer assembly with the Z type of stringer section along the y-axis as 2.0 mm prescribed displacement in the “-x” direction. For the skin-stringer assembly with the Z type of stringer section described in Table 3.6, lowest eigenvalue is obtained as,

$$\lambda_{FE} = 0.0408 \quad (3.16)$$

Using this eigenvalue, the corresponding compressive buckling coefficient of skin-stringer assembly with Z stringer section type are calculated as,

$$k = \sigma_{cr} \frac{12(1 - \nu^2)}{\pi^2 E_c} \left(\frac{l_y}{t} \right)^2 = 6.69 \quad (3.17)$$

Table 3.6: Parameters of the skin-stringer assembly used in the finite element model with Z section stringer

Skin panel material	Aluminum 2024 T3 Sheet
Skin panel thickness (mm)	0.813
Skin panel length x (mm)	450
Single skin panel length y (mm)	150
Stringer material	Aluminum 2024 T3 Sheet
Stringer thickness (mm)	1.016
Stringer height (mm)	25
Stringer upper flange width (mm)	15
Stringer lower flange width (mm)	20

Buckling coefficient calculated shows that Z stringer section is not sufficient to provide the clamped edge condition as the I and J stringer sections. The main reason for this is the rivet configurations of the skin-stringer assemblies. In the models with I and J types of stringer sections, double fastener configuration is used to connect the skin to the lower flange of the stringer. On the contrary, in the model with the Z type of stringer section, single fastener configuration is used to connect the skin to lower flange of the stringer. However, in this study the main geometric properties of the Z section stringer are kept same as the I section stringer and no attempt has been made to provide the clamped edge condition as the I and J section stringer types.

For the skin-stringer assembly with the Z section stringer and the linear material model, load-displacement curve that is obtained by ABAQUS analysis by incorporating geometric nonlinearity is given in Figure 3.27.

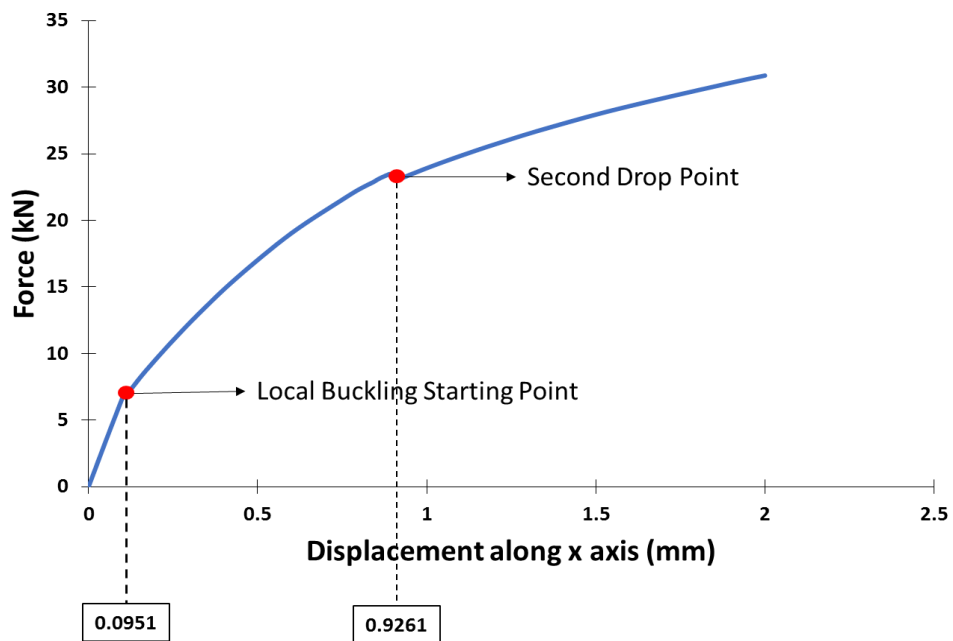


Figure 3.27: Load-displacement curve of the skin-stringer assembly with linear material model (Z section stringer)

As shown in Figure 3.27, the first break in the load-displacement curve represents the initiation of the local buckling. Local buckling starts when the applied displacement is 0.0951 mm. Beyond the initiation of the local buckling, post-buckling stage of the

skin-stringer assembly starts. In Figure 3.27, there is a second load drop followed by again an increase in the load. As seen in Figure 3.28, this second drop occurs due to the sudden increase in the wavelength of the buckled mid panel which is non-existent in the skin-stringer assemblies with I and J section stringers. The reason of this increase is the distance between free edge of lower flange and fastener location of Z type of stringer is twice of distance in the skin-stringer assemblies with double row fasteners. This difference makes the strength of Z type stringer is lower than the strength of stringer with double row fasteners. It is deemed that in the skin-stringer assemblies with I and J section stringers, there are two fastener connections in the lower flange-skin connection which does not allow the sudden jump in the buckled wavelength of the middle panel as is the case for the assembly with Z section stringer. For the skin-stringer assembly with the Z section stringer, local buckling displacement is slightly lower than the corresponding displacement for the skin-stringer assemblies with I and J section stringers. This is an expected behaviour since the single row joint configuration of the Z section stringer cannot provide the clamped edge condition as the I section and J section stringers.

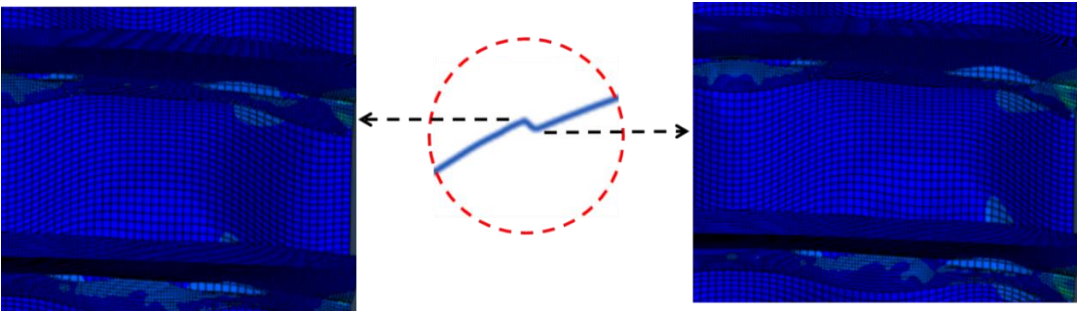


Figure 3.28: Buckled shape of mid panel before and after views of second drop point

Figure 3.29 shows the load-displacement curve obtained by using the nonlinear material model in the finite element analysis. As shown in Figure 3.29, local buckling of the skin starts at a displacement of 0.0997 mm which is very close to the local buckling displacement of the skin-stringer assembly with the linear material model. Beyond the initiation of the local skin buckling, load-displacement curve again becomes nonlinear and when the displacement reaches 0.823 mm, collapse of the skin-stringer assembly occurs. Collapse load for this case occurs at a displacement of 0.823

mm which is significantly again lower than the collapse loads of the skin-stringer assemblies with I and J section stringers.

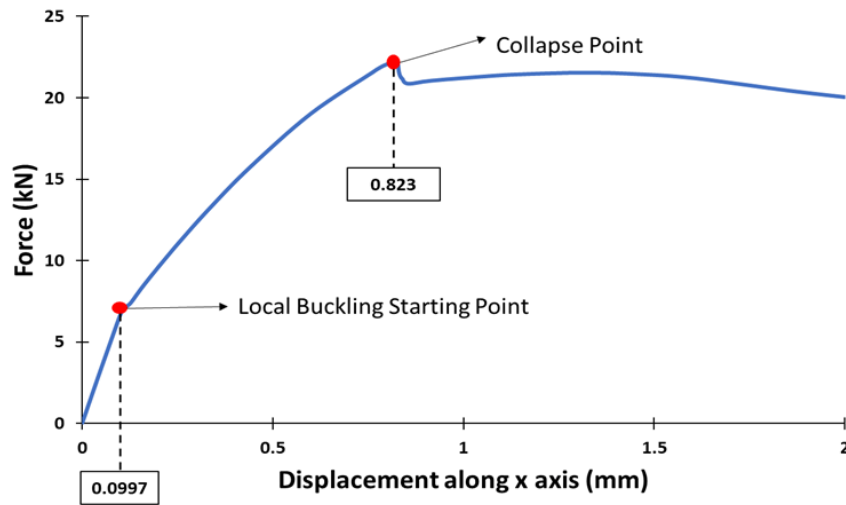


Figure 3.29: Load displacement curve of the skin-stringer assembly with nonlinear material model (Z section stringer)

The effect of material nonlinearity on the post-buckling behavior of the skin-stringer assembly is clearly seen in Figure 3.30. As shown in Figure 3.30, after the local buckling of the skin, when the applied displacement reaches 0.8 mm or so, material nonlinearity effect becomes dominant.

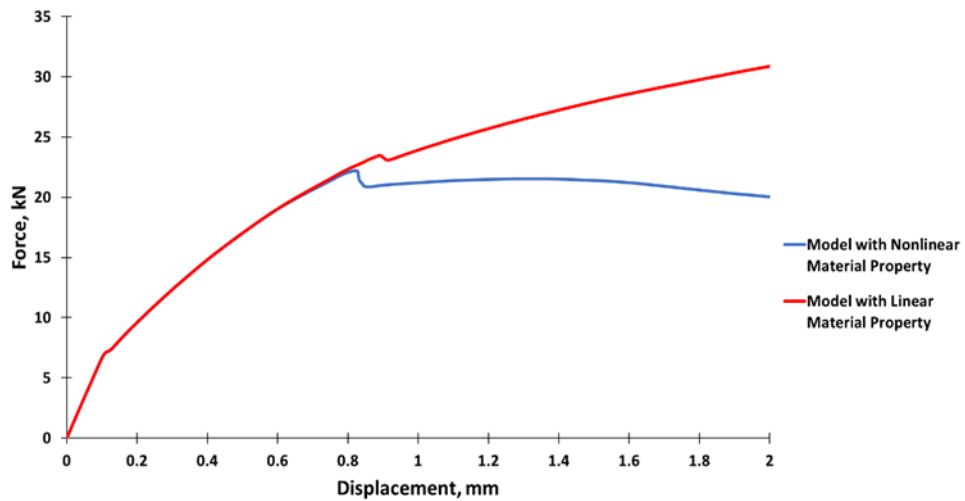


Figure 3.30: Comparison of load displacement curves of models with linear and nonlinear material properties (Z section stringer)

For the skin-stringer assembly with the Z-section stringer, Figure 3.31 shows the load distribution with the linear material model just before the local buckling of the skin panel. It is noticed that the load distribution in the skin Z-section stringer assembly is slightly lower than the load distribution in the skin-stringer assemblies with I or J section stringers.

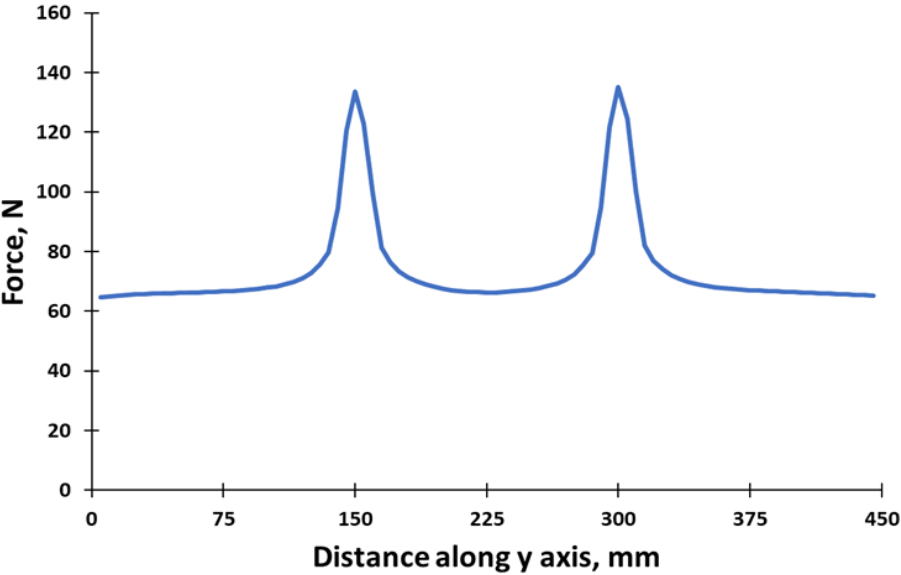


Figure 3.31: Load distribution in the skin-stringer assembly with the linear material model just before the skin buckling (Z-section stringer)

In Figure 3.32, load distribution is presented for skin-stringer assembly model with Z-section stringer with the linear material model at the compressive displacement of 0.823 mm which is the collapse displacement obtained by the nonlinear material model. Figure 3.32 also shows that idealized load distribution with red dash line, known as the effective width. For the skin-stringer assembly with the linear material model and Z section stringer, effective width is calculated as 54.01 mm using area under the actual load distribution given by the blue line.

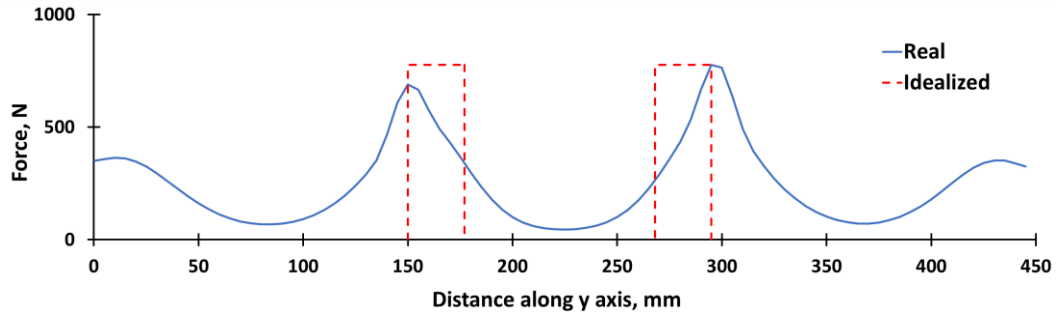


Figure 3.32: Load distribution in the panel with the linear material model at the compressive collapse displacement of 0.823 mm (Z-section stringer)

In Figure 3.33, load distribution is presented for the model with the nonlinear material property just before the local buckling of the skin panel. Before the local buckling of the skin, load distribution given in Figure 3.33 is almost same as the load distribution (Figure 3.31) obtained using the linear material model, as expected.

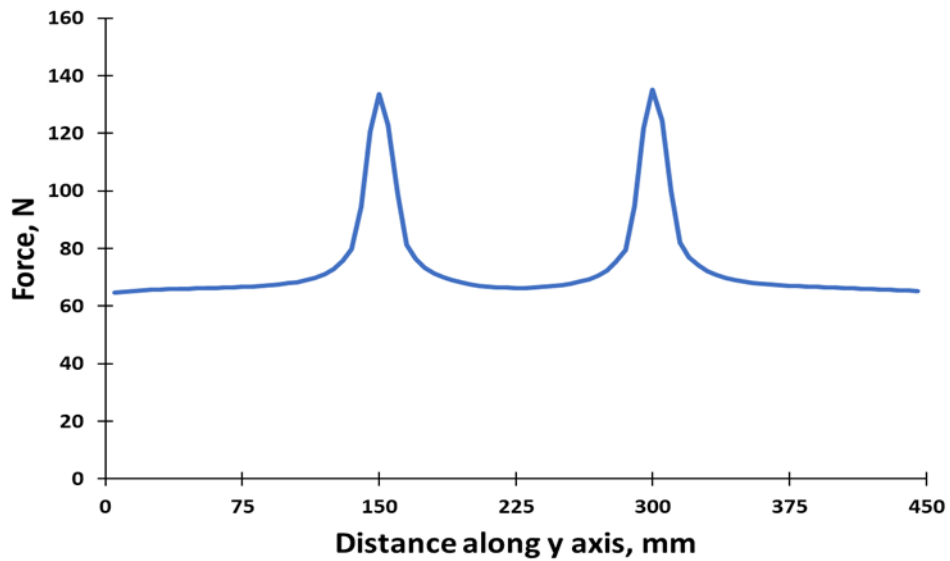


Figure 3.33: Load distribution of the model with nonlinear material property just before the skin buckling (Z-section stringer)

In Figure 3.34, load distribution is presented for the model with the nonlinear material property at the compressive collapse displacement of 0.823 mm. As expected, load distribution in the post-buckled stage is highly different from the load distribution in the pre-buckled configuration. For the skin-stringer assembly with the nonlinear material model, effective width is calculated as 58.61 mm. It is again noted that since

the peak load for the skin-stringer assembly with the nonlinear material model is lower than the peak load for the assembly with the linear material model, effective width is higher. Similar to the skin J-section stringer assembly, load distribution is not symmetric since the Z section destroys the symmetry of the skin-stringer assembly with respect to the center of the middle panel.

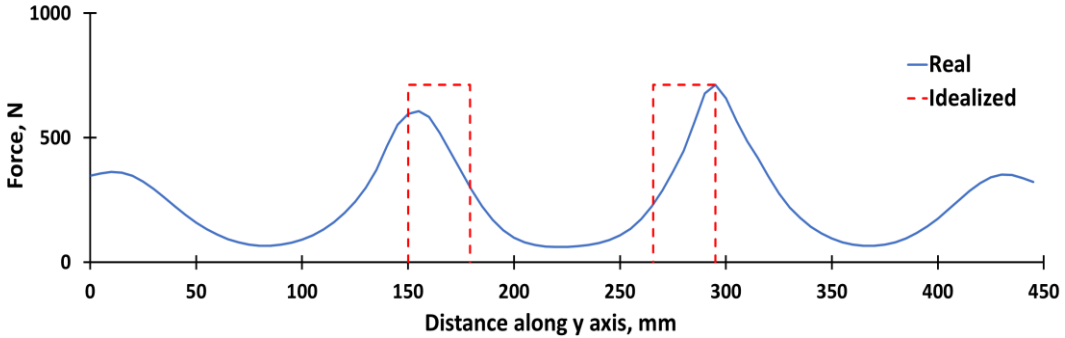


Figure 3.34: Load distribution of the model with nonlinear material property at the compressive displacement of 0.823 mm (Z stringer section type)

Figure 3.35 compares the load distributions in the skin Z-section stringer assemblies obtained by the linear and nonlinear material models in the finite element analysis in the same plot. It is seen that as in the I and J section stringer cases, the main effect of including material nonlinearity is on the peak load level which drops for the skin-stringer assembly with the nonlinear material model. Moreover, equivalent width calculated based on finite element analysis using nonlinear material model is again higher than the equivalent width calculated using linear material model. For the skin Z-section stringer assembly, ratio of the equivalent widths calculated using the linear and nonlinear material models is 0.92.

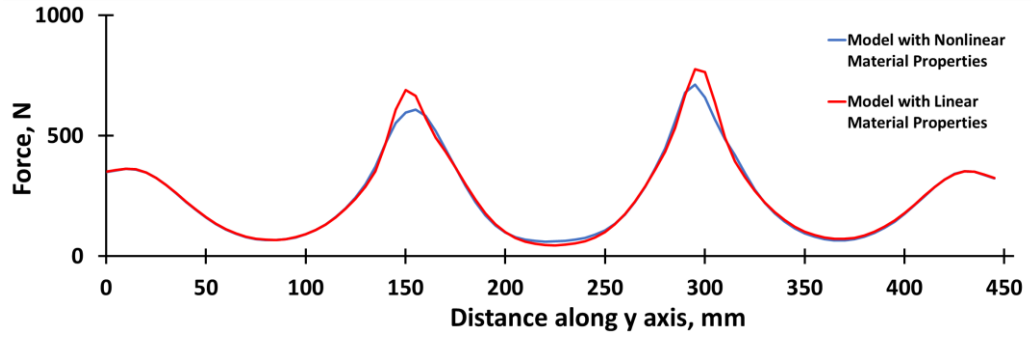


Figure 3.35: Comparison of load distribution of models with linear and nonlinear material properties (Z-section stringer)

Following the same analysis procedure applied for J and I section stringer-skin assemblies, effective widths for the skin-Z section stringer assembly are also calculated by the classical empirical approach of Bruhn [1] and also utilizing the combination of the classical approach and the stringer stress determined by the finite element analysis. For the skin Z-section stringer assembly, local buckling stress (F_{lb}) is calculated as 138.25 MPa [1] and crippling stress of the stringer is calculated as 208.86 MPa [40]. For Aluminum 2024 T3, material yield stress is 269 MPa [36]. Therefore, stringer stress (F_{str}) is taken as the minimum of the three as 138.25 MPa. It should be noted that for the Z-section stringer, because of the single row fastener arrangement half of the lower flange length is not added to the effective width. Thus, for the skin Z-section stringer assembly effective width is calculated as 46.88 mm. Table 3.7 compares the effective widths calculated by different approaches. It is seen that the classical approach gives smallest effective width compared to the finite element based analysis results.

Table 3.7: Comparison of the effective widths (Z-section stringer)

	Finite element (Linear material model)	Finite element (Nonlinear material model)	Equation (3.10)	Equation (3.10) with Stringer Stress from FE Analysis (Linear material model)	Equation (3.10) with Stringer Stress from FE Analysis (Nonlinear material model)
Effective width (mm)	54.01	58.61	46.88	58.22	61.62

3.4.2.2. DOUBLE ROW FASTENER CONFIGURATION

Skin-stringer assembly with Z_2 section stringer which has double row fastener configuration is obtained using same geometric and material properties of skin-stringer assembly as the I stringer section as mentioned before. Firstly, linear buckling analysis is performed for the skin-stringer assembly similar to previous chapter. For the buckling analysis of the skin-stringer assembly with Z_2 section stringer, a compression load is applied on one of the edges of the skin-stringer assembly with the Z_2 type of stringer section along the y-axis as 2.0 mm prescribed displacement in the “-x” direction. For the skin-stringer assembly with the Z_2 type of stringer section described in Table 3.8, lowest eigenvalue is obtained as,

$$\lambda_{FE} = 0.0442 \quad (3.18)$$

Using this eigenvalue, the corresponding compressive buckling coefficient of skin-stringer assembly with Z_2 stringer section type are calculated as,

$$k = \sigma_{cr} \frac{12(1 - \nu^2)}{\pi^2 E_c} \left(\frac{l_y}{t} \right)^2 = 7.239 \quad (3.19)$$

Table 3.8: Parameters of the skin-stringer assembly used in the finite element model with Z_2 section stringer

Skin panel material	Aluminum 2024 T3 Sheet
Skin panel thickness (mm)	0.813
Skin panel length x (mm)	450
Single skin panel length y (mm)	150
Stringer material	Aluminum 2024 T3 Sheet
Stringer thickness (mm)	1.016
Stringer height (mm)	25
Stringer upper flange width (mm)	15
Stringer lower flange width (mm)	20

Based on the compression buckling coefficients determined from the linear buckling analysis of the skin-stringer assemblies with Z_2 stringer section, it is confirmed that the restraints provided by the Z_2 section stringers is slightly different than the classical clamped edge condition as the I section stringer case. The main reason of this similarity, both stringer types uses same double row fastener configuration and dimensions as seen in Table 3.6. However, the stringer web location has an effect on the buckling behaviour of the skin-stringer assembly. In the skin-stringer assemblies with I or J stringers, the mid web is supported by the flanges on both sides of the web, whereas in the skin-stringer assembly with Z type stinger, the mid web is supported only on one side by the flange. Even though double fasteners are used in the Z section stringer, the support that it provides is not as strong as the support that I or J section stringer provides. Hence, buckling coefficients of these two skin-stringer assembly are slightly different than each other.

After the calculation of the buckling coefficient of skin- Z_2 stringer section assembly, geometrically nonlinear static analysis has been conducted for the skin-stringer assembly with Z_2 type stringer. For the skin-stringer assembly with the linear material

model, load-displacement curve that is obtained by ABAQUS analysis is shown in Figure 3.36.

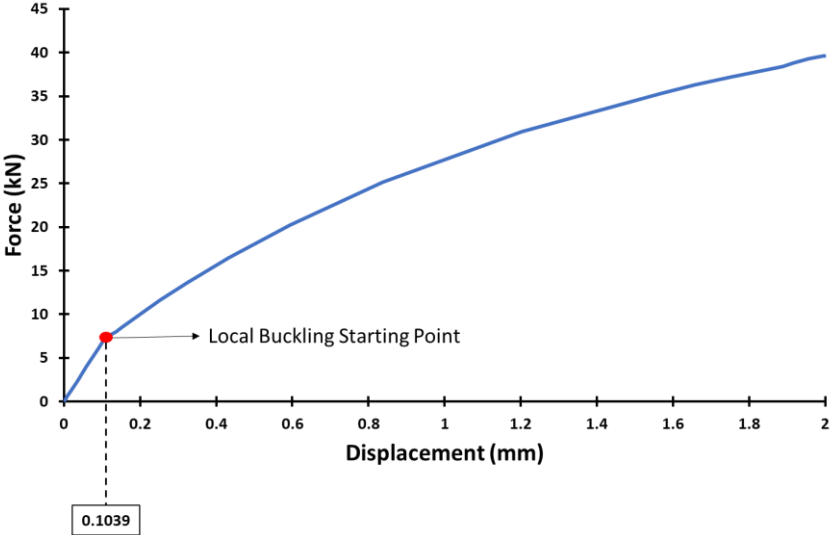


Figure 3.36: Load-displacement curve of the skin-stringer assembly with linear material model (Z_2 section stringer)

As shown in Figure 3.36, the first break in the load-displacement curve represents the initiation of the local buckling. Local buckling starts when the applied displacement is 0.1039 mm. Beyond the initiation of the local buckling, post-buckling stage of the skin-stringer assembly starts. In Figure 3.36, there is no second load drop followed by again an increase in the load as in the Z type of stringer with single row configuration. It is assumed that in the skin-stringer assemblies with I, J and Z_2 section stringers, there are two fastener connections in the lower flange-skin connection which does not allow the sudden jump in the buckled wavelength of the middle panel as is the case for the assembly with Z section stringer. For the skin-stringer assembly with the Z_2 section stringer, local buckling displacement is equal to the corresponding displacement for the skin-stringer assemblies with I and J section stringers.

Figure 3.37 shows the load-displacement curve obtained by using the nonlinear material model in the finite element analysis. As shown in Figure 3.37, local buckling of the skin starts at a displacement of 0.1087 mm which is very close to the local buckling displacement of the skin-stringer assembly with the linear material model.

Beyond the initiation of the local skin buckling, load-displacement curve again becomes nonlinear and when the displacement reaches 1.637 mm, collapse of the skin-stringer assembly occurs. Collapse load for this case occurs at a displacement of 1.637 mm which is slightly lower than the collapse loads of the skin-stringer assemblies with I and J section stringers.

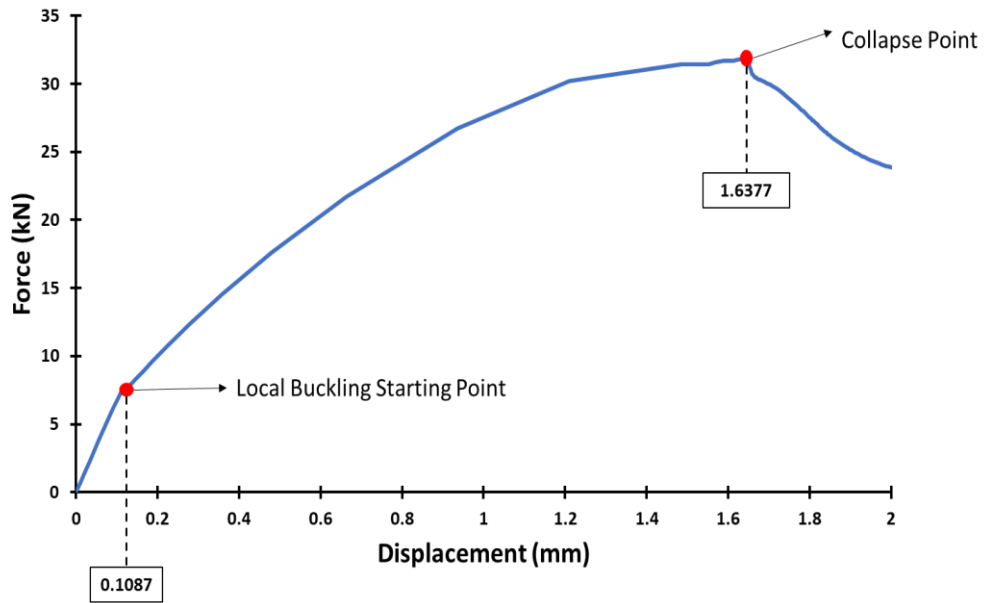


Figure 3.37: Load displacement curve of the skin-stringer assembly with nonlinear material model (Z_2 section stringer)

The effect of material nonlinearity on the post-buckling behavior of the skin-stringer assembly is clearly seen in Figure 3.38. As shown in Figure 3.38, after the local buckling of the skin, when the applied displacement reaches 1.637 mm or so, material nonlinearity effect becomes dominant.

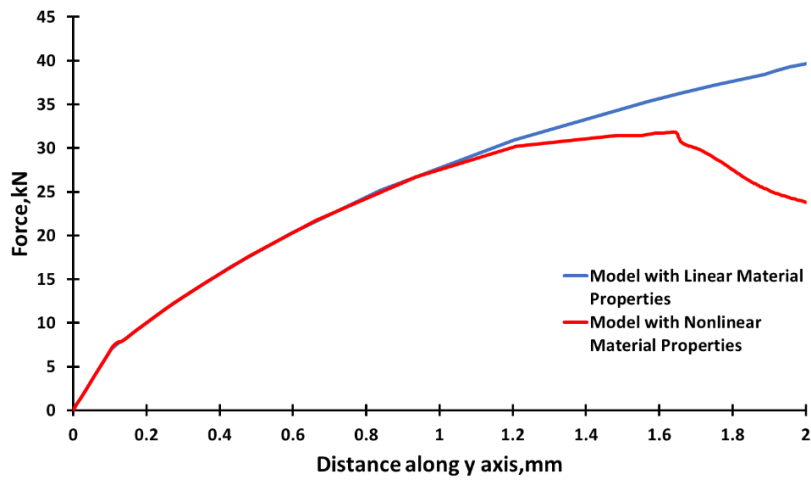


Figure 3.38: Comparison of load displacement curves of models with linear and nonlinear material properties (Z_2 section stringer)

For the skin-stringer assembly with the Z_2 -section stringer, Figure 3.39 shows the load distribution with the linear material model just before the local buckling of the skin panel. It is noticed that the load distribution in the skin Z_2 -section stringer assembly is same as the load distribution in the skin-stringer assemblies with I or J section stringers.

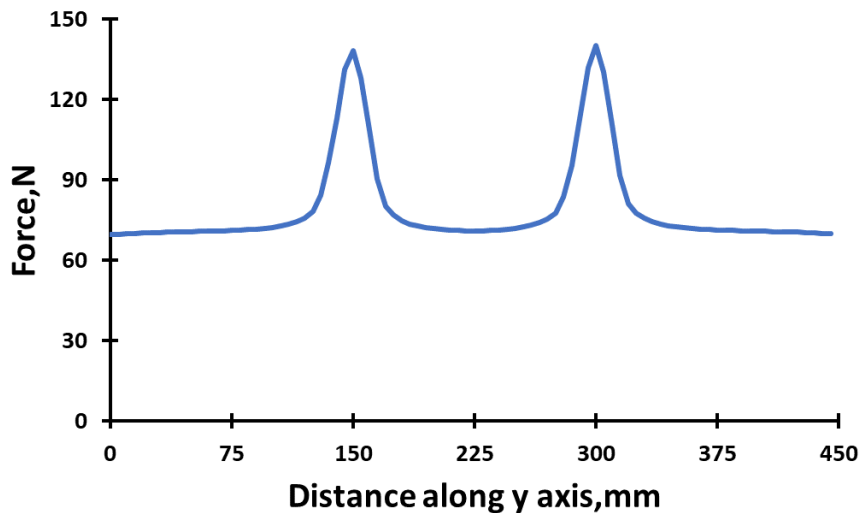


Figure 3.39: Load distribution in the skin-stringer assembly with the linear material model just before the skin buckling (Z_2 -section stringer)

In Figure 3.40, load distribution is presented for skin-stringer assembly model with Z_2 -section stringer with the linear material model at the compressive displacement of 1.637 mm which is the collapse displacement obtained by the nonlinear material model. Figure 3.40 also shows that idealized load distribution with red dash line, known as the effective width. For the skin-stringer assembly with the linear material model and Z_2 section stringer, effective width is calculated as 54.28 mm using area under the actual load distribution given by the blue line.

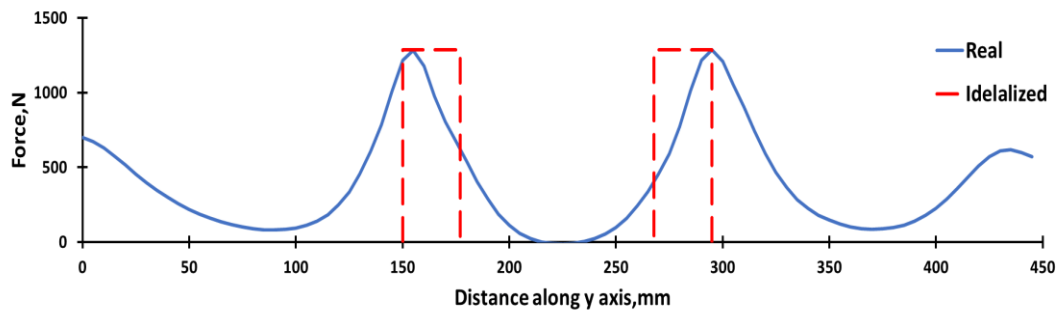


Figure 3.40: Load distribution in the panel with the linear material model at the compressive collapse displacement of 1.637 mm (Z_2 -section stringer)

In Figure 3.41, load distribution is presented for the model with the nonlinear material property just before the local buckling of the skin panel. Before the local buckling of the skin, load distribution given in Figure 3.41 is almost same as the load distribution (Figure 3.39) obtained using the linear material model, as expected.

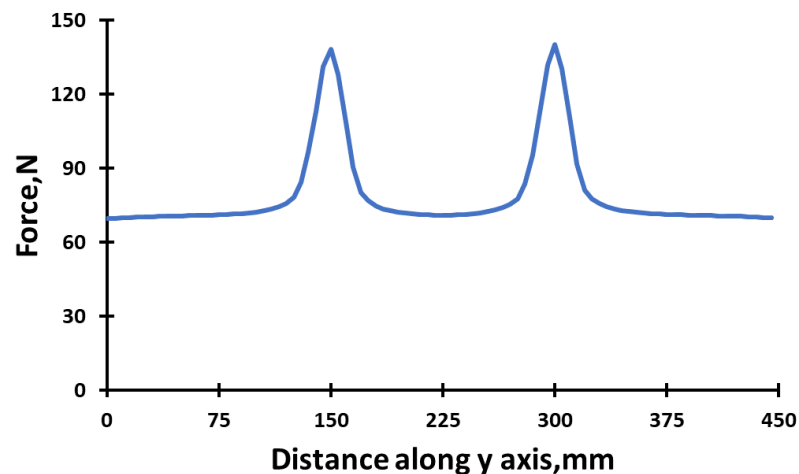


Figure 3.41: Load distribution of the model with nonlinear material property just before the skin buckling (Z_2 -section stringer)

In Figure 3.42, load distribution is presented for the model with the nonlinear material property at the compressive collapse displacement of 1.637 mm. As expected, load distribution in the post-buckled stage is highly different from the load distribution in the pre-buckled configuration. For the skin-stringer assembly with the nonlinear material model, effective width is calculated as 54.18 mm. According to this result, effective width calculated by nonlinear material model is almost equal to effective width calculated by linear material model. It is again noted that since the peak load for the skin-stringer assembly with the nonlinear material model is lower than the peak load for the assembly with the linear material model, effective width is expected as higher. However, area under the first stringer location is significantly lower than area under the second stringer location. These two differences between linear and nonlinear material models is balanced each other. In addition, similar to the skin J-section stringer assembly, load distribution is not symmetric since the Z_2 section destroys the symmetry of the skin-stringer assembly with respect to the center of the middle panel.

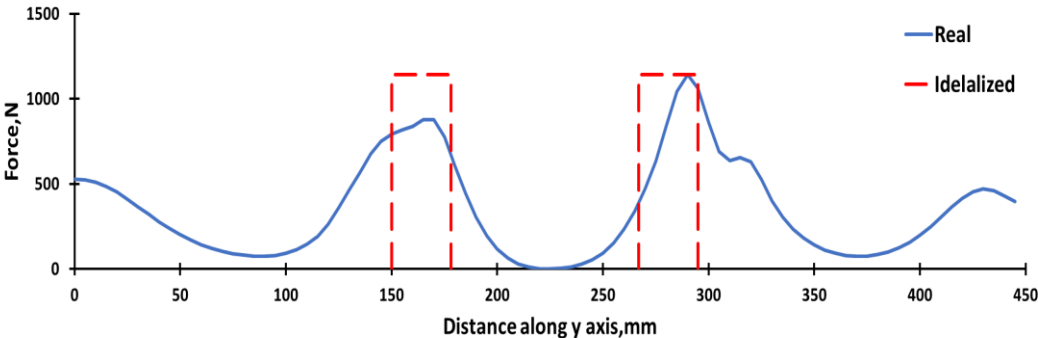


Figure 3.42: Load distribution of the model with nonlinear material property at the compressive displacement of 1.637 mm (Z_2 stringer section type)

Figure 3.43 compares the load distributions in the skin Z_2 -section stringer assemblies obtained by the linear and nonlinear material models in the finite element analysis in the same plot. It is seen that as in the I and J section stringer cases, the main effect of including material nonlinearity is on the peak load level which drops for the skin-stringer assembly with the nonlinear material model. Moreover, equivalent width calculated based on finite element analysis using nonlinear material model is almost equal to the equivalent width calculated using linear material model. For the skin Z_2 -

section stringer assembly, ratio of the equivalent widths calculated using the linear and nonlinear material models is 1.002.

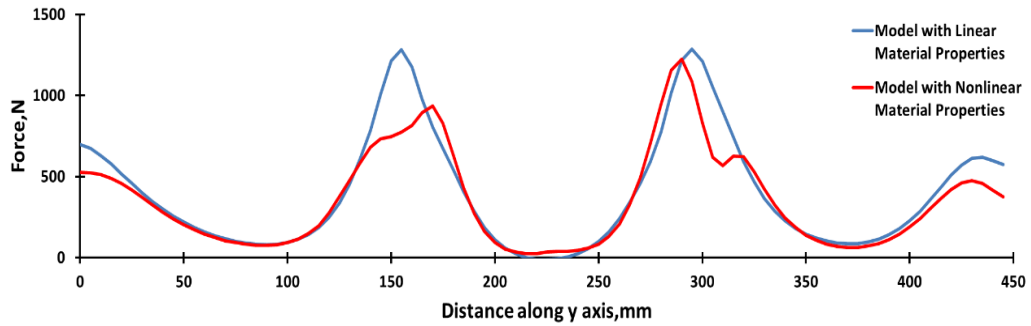


Figure 3.43: Comparison of load distribution of models with linear and nonlinear material properties (Z_2 -section stringer)

Following the same analysis procedure applied for I, J and Z section stringer-skin assemblies, effective widths for the skin- Z_2 section stringer assembly are also calculated by the classical empirical approach of Bruhn [1] and also utilizing the combination of the classical approach and the stringer stress determined by the finite element analysis. For the skin Z_2 -section stringer assembly, local buckling stress (F_{lb}) is calculated as 138.25 MPa [1] and crippling stress of the stringer is calculated as 208.86 MPa [40]. For Aluminum 2024 T3, material yield stress is 269 MPa [36]. Therefore, stringer stress (F_{str}) is taken as the minimum of the three as 138.25 MPa. It should be noted that for the Z_2 -section stringer, because of the double row fastener arrangement half of the lower flange length is added to the effective width. Thus, for the skin Z_2 -section stringer assembly effective width is calculated as 56.88 mm. Table 3.9 compares the effective widths calculated by different approaches. It is seen that the classical approach gives almost same effective width compared to the finite element based analysis results.

Table 3.9: Comparison of the effective widths (Z_2 -section stringer)

	Finite element (Linear material model)	Finite element (Nonlinear material model)	Equation (3.10)	Equation (3.10) with Stringer Stress from FE Analysis (Linear material model)	Equation (3.10) with Stringer Stress from FE Analysis (Nonlinear material model)
Effective width (mm)	54.28	54.18	56.88	50.97	57.02

3.5. Comparison of Load Carrying Capacity, Load Distribution and Effective Width of Skin-Stringer Assemblies with Three Different Stringer Types

Load carrying capacities of the skin-stringer assemblies determined by the finite element analysis employing nonlinear material model for the three different stringer types are compared Figure 3.44. It is seen that all skin stringer assemblies behave same in the linear range before the local buckling of the skin panel occurs. However, after the local buckling of the skin panels, post-buckling behavior of the skin-stringer assemblies differ from each other. Load carrying capacity of the skin-stringer assembly with I, J and Z_2 type of stringer sections are almost equal to each other. Skin-stringer assembly with the I section stringer has slightly higher collapse load than the assembly with J and Z_2 section stringer. However, skin Z-section stringer assembly has considerably lower collapse load than the skin-stringer assemblies with I, J and Z_2 section stringers. The reason of this difference is deemed to be due to the fastener row configuration. In the I, J and Z_2 types of stringers, double row fastener configuration is used, on the contrary, in the Z type of stringer, single row fastener configuration is used.

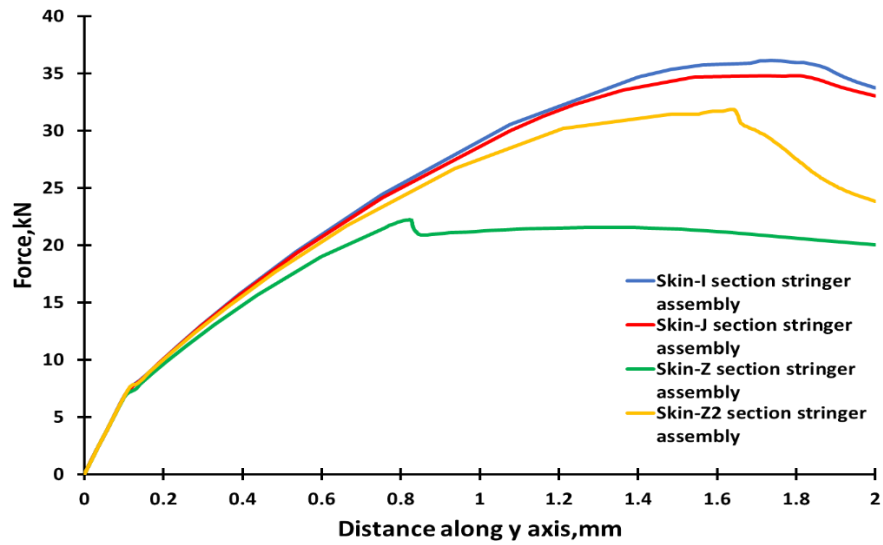


Figure 3.44: Comparison of load carrying capacity of skin-stringer assemblies with I, J, Z and Z_2 section stringers (Nonlinear material properties)

Secondly, load distributions determined at the point of collapse by the finite element analysis of skin-stringer assemblies with nonlinear material properties are compared in Figure 3.45. Figure 3.45 clearly shows that the peak load in the skin Z-section assembly is significantly lower than the skin-stringer assemblies with double row fasteners.

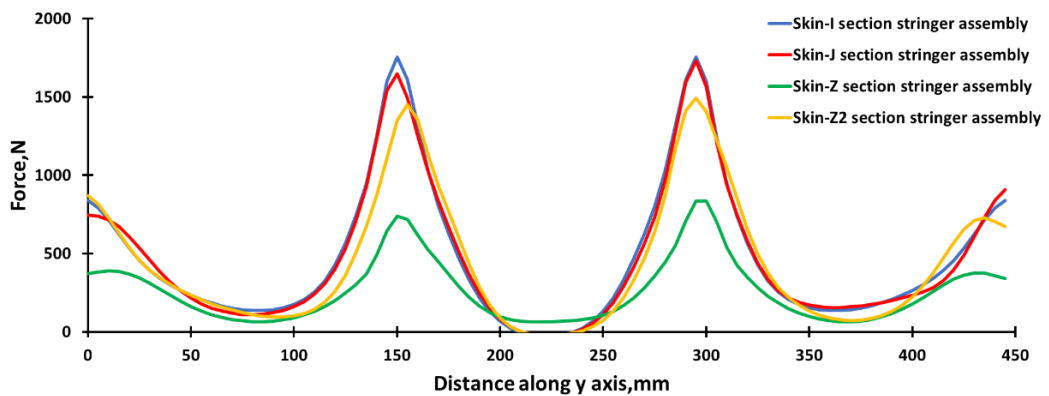


Figure 3.45: Comparison of load distribution of skin-stringer assemblies with I, J, Z and Z_2 section stringers (Nonlinear material properties)

Finally, effective widths of the skin-stringer assemblies determined by the finite element analysis employing five different calculation methods for the three different stringer types are compared in Table 3.10.

Table 3.10: Comparison of the effective widths with Three Different Stringer Types

Effective width (mm)	Finite element (Linear material model)	Finite element (Nonlinear material model)	Equation (3.10)	Equation (3.10) with Stringer Stress from FE Analysis (Linear material model)	Equation (3.10) with Stringer Stress from FE Analysis (Nonlinear material model)
I Stringer Section	49.20	60.67	43.61	43.93	44.96
J Stringer Section	47.59	57.48	46.06	44.11	45.48
Z Stringer Section	54.01	58.61	46.88	58.22	61.62
Z₂ Stringer Section	54.28	54.18	56.88	50.97	57.02

Based on the comparison of the effective widths calculated by different methods which are presented in Table 3.10, the following conclusions can be drawn:

- Effective widths calculated by the finite element based analysis by employing nonlinear material property are higher than the effective widths calculated by employing linear material property. Since the peak loads drop when nonlinear material property is used in the finite element analysis, the increase in the effective width is reasonable.

- If the effective widths calculated by the finite element analysis employing finite element analysis with nonlinear material properties are taken as reference, for the skin stringer assemblies studied, classical effective width formula underestimates the effective widths by 28 % for the skin I-section stringer assembly, and by 20 % for the skin J and Z section stringer assemblies. However, classical effective width formula result almost equals to the finite element analysis effective width result for the skin Z_2 -section stringer assembly.
- In general, classical empirical approach of Bruhn gives the smallest effective width except skin-stringer assembly with Z_2 type stringer.
- Effective widths calculated by the finite element based analysis by employing linear material property agree better with the effective widths calculated by the classical empirical approach of Bruhn compared to the effective widths calculated by the finite element based analysis by employing nonlinear material property. However, to obtain results from linear material model, nonlinear material model has to be constructed to get the collapse load. Analyses results of linear material models do not give the collapse load.
- Effective widths of skin stringer assemblies which have double row fastener arrangement, such as I and J section stringers, are close to each other irrespective of the analysis methodology employed. However, effective width of skin stringer assembly with Z_2 section stringer is far away from effective width results of other assemblies with double row fastener arrangement.
- For skin stringer assemblies with double row fasteners, effective widths calculated by substituting the stringer stresses at the collapse point calculated by the finite element analysis in the classical empirical effective width formula (Equation (3.10)) match well with the effective widths calculated by the classical empirical effective width formula alone.

- Results of the present analysis also showed that the classical effective width formula gives reasonable results which are comparable with the finite element based analysis results.
- According to results in above, nonlinear material model gives the more realistic result compare to empirical and linear material models.

CHAPTER 4

COMPOSITE PLATE BUCKLING

In this chapter, for certain geometries and laminate configurations composite buckling charts are obtained by using a script written in Python 2.7 to construct parametric finite element model in ABAQUS and perform automated buckling analysis. Variable parameters of composite plates are taken as material, number of plies, ply orientation which are selected according to common use in the aviation industry. To verify the results of the finite element model, analytical methods based on classical lamination theory and first order shear deformation theory are used to determine the critical buckling load of the composite plates.

In these methods, material of the composite plate is taken as orthotropic. In addition, the laminate is chosen as symmetric balance laminated and ply angles are decided as combination of 0, +45, -45 and 90 degrees.

Firstly, buckling analysis of composite plates is investigated by two different theories base on equivalent single layer theories, the classical laminated plate theory (CLPT) and first order shear deformation theory (FSDT) [41].

In the second part, analysis of composite plates is studied using defined mathematical methods.

In the third part, finite element model is constructed using the classical boundary conditions and loading condition is chosen as uniaxial compressive loading. Buckling coefficient graphs are obtained by processing the results of finite element analysis and these graphs are in section 4.3. Buckling coefficient charts for each type of lay-up configuration obtained by the analytical approaches and finite element method are compared with each other and discussions are made.

4.1. Classical and First-Order Laminate Theories of Composite Plate

4.1.1. Classical Laminated Plate Theory (CLPT)

Classical laminated plate theory is based on the Kirchhoff hypothesis. In this hypothesis, it is assumed that plane cross sections remain plane and normal to the middle-plane during deformations which means that the transverse shear strains are omitted.

4.1.1.1. KINEMATICS

The in-plane displacements are related to the normal displacements as follows [42]:

$$u(x, y, z) = u_0 - z \frac{\partial w}{\partial x}, \quad v(x, y, z) = v_0 - z \frac{\partial w}{\partial y}, \quad w(x, y, z) = w_0 \quad (4.1)$$

where u is the displacement in the x direction, v is the displacement in the y direction and w is the displacement in the z direction, while u_0 , v_0 and w_0 are displacements of the middle plane in x , y and z directions, respectively. Undeformed and deformed geometric descriptions of plate edge according to Kirchhoff assumptions are seen in the Figure 4.1. Based on the displacement field above, we can find the strains as follows:

$$\varepsilon = \begin{Bmatrix} \varepsilon_x \\ \varepsilon_y \\ \gamma_{xy} \end{Bmatrix} = \begin{bmatrix} \frac{\partial}{\partial x} & 0 \\ 0 & \frac{\partial}{\partial y} \\ \frac{\partial}{\partial y} & \frac{\partial}{\partial x} \end{bmatrix} \begin{Bmatrix} u \\ v \end{Bmatrix} = \begin{Bmatrix} \frac{\partial u_0}{\partial x} \\ \frac{\partial v_0}{\partial y} \\ \frac{\partial u_0}{\partial y} + \frac{\partial v_0}{\partial x} \end{Bmatrix} + z \begin{Bmatrix} -\frac{\partial^2 w_0}{\partial x^2} \\ -\frac{\partial^2 w_0}{\partial y^2} \\ -2\frac{\partial^2 w_0}{\partial x \partial y} \end{Bmatrix} = \begin{Bmatrix} \varepsilon_x^0 \\ \varepsilon_y^0 \\ \gamma_{xy}^0 \end{Bmatrix} + z \begin{Bmatrix} k_x \\ k_y \\ k_{xy} \end{Bmatrix} \quad (4.2)$$

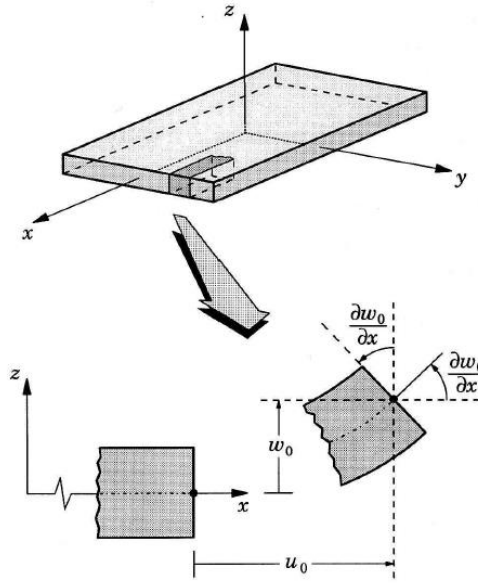


Figure 4.1: Undeformed and deformed geometries of an edge of a plate under the Kirchhoff assumptions [41]

4.1.1.2. MATERIAL LAW

Definition of tensor strains is given by Equation (4.3) [42]:

$$\begin{Bmatrix} \varepsilon_L \\ \varepsilon_T \\ \frac{1}{2}\gamma_{LT} \end{Bmatrix} = [T] \begin{Bmatrix} \varepsilon_x \\ \varepsilon_y \\ \frac{1}{2}\gamma_{xy} \end{Bmatrix} \quad (4.3)$$

Where $[T]$ is the transformation matrix. Using this definition, the stress strain relations are given by [42]:

$$\begin{aligned} \begin{Bmatrix} \sigma_x \\ \sigma_y \\ \tau_{xy} \end{Bmatrix} &= [T]^{-1} \begin{Bmatrix} \sigma_L \\ \sigma_T \\ \tau_{LT} \end{Bmatrix} = [T]^{-1} \begin{bmatrix} Q_{11} & Q_{12} & 0 \\ Q_{12} & Q_{22} & 0 \\ 0 & 0 & 2Q_{66} \end{bmatrix} \begin{Bmatrix} \varepsilon_L \\ \varepsilon_T \\ \frac{1}{2}\gamma_{LT} \end{Bmatrix} = [T]^{-1} [Q^*] [T] \begin{Bmatrix} \varepsilon_x \\ \varepsilon_y \\ \frac{1}{2}\gamma_{xy} \end{Bmatrix} \\ &= [\bar{Q}^*] \begin{Bmatrix} \varepsilon_x \\ \varepsilon_y \\ \frac{1}{2}\gamma_{xy} \end{Bmatrix} = [\bar{Q}] \begin{Bmatrix} \varepsilon_x \\ \varepsilon_y \\ \frac{1}{2}\gamma_{xy} \end{Bmatrix} = \begin{bmatrix} \bar{Q}_{11} & \bar{Q}_{12} & \bar{Q}_{16} \\ \bar{Q}_{12} & \bar{Q}_{22} & \bar{Q}_{26} \\ \bar{Q}_{16} & \bar{Q}_{26} & \bar{Q}_{66} \end{bmatrix} \begin{Bmatrix} \varepsilon_x \\ \varepsilon_y \\ \gamma_{xy} \end{Bmatrix} \end{aligned} \quad (4.4)$$

Equation (4.4) gives the stress-strain relation for orthotropic lamina referred to arbitrary axes. For the purpose of uniformity, a $[\bar{Q}]$ matrix is defined that relates engineering strains to the stresses referred to arbitrary axes.

Inserting of equation (4.2) into the equation (4.4) gives:

$$\begin{Bmatrix} \sigma_x \\ \sigma_y \\ \tau_{xy} \end{Bmatrix} = \begin{bmatrix} \bar{Q}_{11} & \bar{Q}_{12} & \bar{Q}_{16} \\ \bar{Q}_{12} & \bar{Q}_{22} & \bar{Q}_{26} \\ \bar{Q}_{16} & \bar{Q}_{26} & \bar{Q}_{66} \end{bmatrix} \begin{Bmatrix} \varepsilon_x^0 \\ \varepsilon_y^0 \\ \gamma_{xy}^0 \end{Bmatrix} + z \begin{bmatrix} \bar{Q}_{11} & \bar{Q}_{12} & \bar{Q}_{16} \\ \bar{Q}_{12} & \bar{Q}_{22} & \bar{Q}_{26} \\ \bar{Q}_{16} & \bar{Q}_{26} & \bar{Q}_{66} \end{bmatrix} \begin{Bmatrix} k_x \\ k_y \\ k_{xy} \end{Bmatrix} \quad (4.5)$$

4.1.1.3. RESULTS FORCES AND MOMENTS

The stresses change from layer to layer in a laminate. Hence it is convenient to deal with a simpler but equivalent system of forces and moments acting on a laminate cross section. Resultant force is obtained by integrating the corresponding stress through the laminate thickness h [42]:

$$\begin{Bmatrix} N_x \\ N_y \\ N_{xy} \end{Bmatrix} = \int_{-\frac{h}{2}}^{\frac{h}{2}} \begin{Bmatrix} \sigma_x \\ \sigma_x \\ \tau_{xy} \end{Bmatrix} dz = \sum_{i=1}^n \int_{h_{i-1}}^{h_i} \begin{Bmatrix} \sigma_x \\ \sigma_x \\ \tau_{xy} \end{Bmatrix}_i dz \quad (4.6)$$

Similarly, the resultant moment is obtained by integration through the thickness of the corresponding stress times the moment arm with respect to the middle plane [42]:

$$\begin{Bmatrix} M_x \\ M_y \\ M \end{Bmatrix} = \int_{-\frac{h}{2}}^{\frac{h}{2}} \begin{Bmatrix} \sigma_x \\ \sigma_x \\ \tau_{xy} \end{Bmatrix} z dz = \sum_{i=1}^n \int_{h_{i-1}}^{h_i} \begin{Bmatrix} \sigma_x \\ \sigma_x \\ \tau_{xy} \end{Bmatrix}_i z dz \quad (4.7)$$

Substitution of Equation (4.5) into equations (4.6) and (4.7) gives:

$$\begin{aligned}
\begin{Bmatrix} N_x \\ N_y \\ N_{xy} \end{Bmatrix} &= \sum_{i=1}^n \int_{h_{i-1}}^{h_i} \begin{bmatrix} \bar{Q}_{11} & \bar{Q}_{12} & \bar{Q}_{16} \\ \bar{Q}_{12} & \bar{Q}_{22} & \bar{Q}_{26} \\ \bar{Q}_{16} & \bar{Q}_{26} & \bar{Q}_{66} \end{bmatrix}_i dz \begin{Bmatrix} \varepsilon_x^0 \\ \varepsilon_y^0 \\ \gamma_{xy}^0 \end{Bmatrix} \\
&+ \sum_{i=1}^n \int_{h_{i-1}}^{h_i} z \begin{bmatrix} \bar{Q}_{11} & \bar{Q}_{12} & \bar{Q}_{16} \\ \bar{Q}_{12} & \bar{Q}_{22} & \bar{Q}_{26} \\ \bar{Q}_{16} & \bar{Q}_{26} & \bar{Q}_{66} \end{bmatrix}_i dz \begin{Bmatrix} k_x \\ k_y \\ k_{xy} \end{Bmatrix} \\
&= \begin{bmatrix} A_{11} & A_{12} & A_{16} \\ A_{12} & A_{22} & A_{26} \\ A_{16} & A_{26} & A_{66} \end{bmatrix} \begin{Bmatrix} \frac{\partial u_0}{\partial x} \\ \frac{\partial v_0}{\partial y} \\ \frac{\partial u_0}{\partial y} + \frac{\partial v_0}{\partial x} \end{Bmatrix} + \begin{bmatrix} B_{11} & B_{12} & B_{16} \\ B_{12} & B_{22} & B_{26} \\ B_{16} & B_{26} & B_{66} \end{bmatrix} \begin{Bmatrix} -\frac{\partial^2 w_0}{\partial x^2} \\ -\frac{\partial^2 w_0}{\partial y^2} \\ -2\frac{\partial^2 w_0}{\partial x \partial y} \end{Bmatrix}
\end{aligned} \tag{4.8}$$

$$\begin{aligned}
\begin{Bmatrix} M_x \\ M_y \\ M \end{Bmatrix} &= \sum_{i=1}^n \int_{h_{i-1}}^{h_i} z \begin{bmatrix} \bar{Q}_{11} & \bar{Q}_{12} & \bar{Q}_{16} \\ \bar{Q}_{12} & \bar{Q}_{22} & \bar{Q}_{26} \\ \bar{Q}_{16} & \bar{Q}_{26} & \bar{Q}_{66} \end{bmatrix}_i dz \begin{Bmatrix} \varepsilon_x^0 \\ \varepsilon_y^0 \\ \gamma_{xy}^0 \end{Bmatrix} \\
&+ \sum_{i=1}^n \int_{h_{i-1}}^{h_i} z^2 \begin{bmatrix} \bar{Q}_{11} & \bar{Q}_{12} & \bar{Q}_{16} \\ \bar{Q}_{12} & \bar{Q}_{22} & \bar{Q}_{26} \\ \bar{Q}_{16} & \bar{Q}_{26} & \bar{Q}_{66} \end{bmatrix}_i dz \begin{Bmatrix} k_x \\ k_y \\ k_{xy} \end{Bmatrix} \\
&= \begin{bmatrix} B_{11} & B_{12} & B_{16} \\ B_{12} & B_{22} & B_{26} \\ B_{16} & B_{26} & B_{66} \end{bmatrix} \begin{Bmatrix} \frac{\partial u_0}{\partial x} \\ \frac{\partial v_0}{\partial y} \\ \frac{\partial u_0}{\partial y} + \frac{\partial v_0}{\partial x} \end{Bmatrix} + \begin{bmatrix} D_{11} & D_{12} & D_{16} \\ D_{12} & D_{22} & D_{26} \\ D_{16} & D_{26} & D_{66} \end{bmatrix} \begin{Bmatrix} -\frac{\partial^2 w_0}{\partial x^2} \\ -\frac{\partial^2 w_0}{\partial y^2} \\ -2\frac{\partial^2 w_0}{\partial x \partial y} \end{Bmatrix}
\end{aligned} \tag{4.9}$$

4.1.1.4. EQUILIBRIUM EQUATIONS IN TERMS OF DISPLACEMENT

Equilibrium of forces in x, y direction for laminated thin plates are given in Equations (4.10) and (4.11), respectively. In addition, governing equation for buckling analysis for laminated thin plates is given in Equation (4.12). In the Appendix D.2, calculations of these equations are given in Equations (D.12), (D.13) and (D.25).

$$\frac{\partial N_x}{\partial x} + \frac{\partial N_{xy}}{\partial y} = 0 \tag{4.10}$$

$$\frac{\partial N_y}{\partial y} + \frac{\partial N_{xy}}{\partial x} = 0 \tag{4.11}$$

$$\frac{\partial^2 M_x}{\partial x^2} + \frac{\partial^2 M_{xy}}{\partial x \partial y} + \frac{\partial^2 M_y}{\partial y^2} + p^* = 0 \tag{4.12}$$

Where: $p^* = p + N_x \frac{\partial^2 w}{\partial x^2} + N_y \frac{\partial^2 w}{\partial y^2} + 2N_{xy} \frac{\partial^2 w}{\partial x \partial y} - \rho^* \frac{\partial^2 w}{\partial t^2}$

Equation (4.12) is used for the solution of the buckling load. Inserting Equation (4.9) into the Equation (4.12), we obtain:

$$\begin{aligned}
& -D_{11} \frac{\partial^4 w}{\partial x^4} - 4D_{16} \frac{\partial^4 w}{\partial x^3 \partial y} - (2D_{12} + 4D_{66}) \frac{\partial^4 w}{\partial x^2 \partial y^2} - 4D_{26} \frac{\partial^4 w}{\partial y^3 \partial x} - D_{22} \frac{\partial^4 w}{\partial y^4} + \\
& B_{11} \frac{\partial^3 u_0}{\partial x^3} + 3B_{16} \frac{\partial^3 u_0}{\partial x^2 \partial y} + (B_{12} + 2B_{66}) \frac{\partial^3 u_0}{\partial y^2 \partial x} + B_{26} \frac{\partial^3 u_0}{\partial y^3} + \\
& B_{16} \frac{\partial^3 v_0}{\partial x^3} + (B_{12} + 2B_{66}) \frac{\partial^3 v_0}{\partial x^2 \partial y} + 3B_{26} \frac{\partial^3 v_0}{\partial y^2 \partial x} + B_{22} \frac{\partial^3 v_0}{\partial y^3} \\
& + p^* = 0
\end{aligned} \tag{4.13}$$

For specially orthotropic laminates, their constitutive equations satisfy the following conditions [42]:

$$\begin{aligned}
A_{16} &= A_{26} = 0 \\
B_{ij} &= 0 \\
D_{16} &= D_{26} = 0
\end{aligned} \tag{4.14}$$

Incorporation of conditions above into Equation (4.13) simplifies the equilibrium equation for specially orthotropic laminates as given by Equation (4.15).

$$D_{11} \frac{\partial^4 w}{\partial x^4} + (2D_{12} + 4D_{66}) \frac{\partial^4 w}{\partial x^2 \partial y^2} + D_{22} \frac{\partial^4 w}{\partial y^4} = p^* \tag{4.15}$$

4.1.2. First Order Shear Deformation Theory (FSDT)

First order shear deformation theory is a bit more complicated compared to CPTL and it based on the Reissner-Mindlin hypothesis. In this theory, plane cross sections remain plane after deformation, however it does not have to remain normal to the reference plane. In this method, out-of-plane shear deformation is also included.

4.1.2.1. KINEMATICS

The displacement field for the FSDT based on the assumption is given in Equation (4.16) [43]. As well, undeformed and deformed geometric descriptions of plate edge according to first-order plate theory assumptions are seen in the Figure 4.2.

$$u(x, y, z) = u_0 + z\phi_x, \quad v(x, y, z) = v_0 + z\phi_y, \quad w(x, y, z) = w_0(x, y) \quad (4.16)$$

Where: $\phi_x = \frac{\partial u}{\partial z}$, $\phi_y = \frac{\partial v}{\partial z}$

which indicate that ϕ_x and ϕ_y are the rotations of the transverse normal about the y and the x axes, respectively.

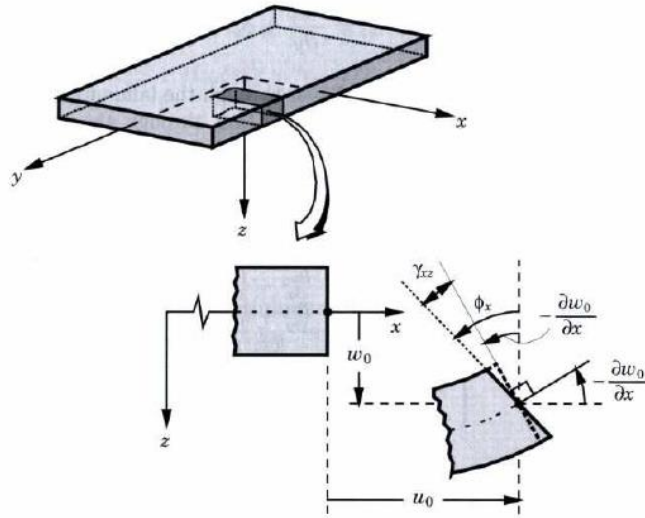


Figure 4.2: Undeformed and deformed geometries of an edge of a plate under the assumptions of the first-order plate theory [43].

It is convenient to split the strain vector into two parts, where ϵ_b is the axial-bending part and ϵ_s is the transverse shear part [44]. Axial and bending strain part of plate is given in the Equation (4.17), and equation for transverse shear strain of plate is given in Equation (4.18).

$$\varepsilon_b = \begin{Bmatrix} \varepsilon_x \\ \varepsilon_y \\ \gamma_{xy} \end{Bmatrix} = \begin{Bmatrix} \frac{\partial u_0}{\partial x} \\ \frac{\partial v_0}{\partial y} \\ \frac{\partial u_0}{\partial y} + \frac{\partial v_0}{\partial x} \end{Bmatrix} + z \begin{Bmatrix} \frac{\partial \phi_x}{\partial x} \\ \frac{\partial \phi_y}{\partial y} \\ \frac{\partial \phi_x}{\partial y} + \frac{\partial \phi_y}{\partial x} \end{Bmatrix} \quad (4.17)$$

$$\varepsilon_s = \begin{Bmatrix} \gamma_{yz} \\ \gamma_{xz} \end{Bmatrix} = \begin{Bmatrix} \frac{\partial v}{\partial z} + \frac{\partial w_0}{\partial y} \\ \frac{\partial u}{\partial z} + \frac{\partial w_0}{\partial x} \end{Bmatrix} = \begin{Bmatrix} \phi_y + \frac{\partial w_0}{\partial y} \\ \phi_x + \frac{\partial w_0}{\partial x} \end{Bmatrix} \quad (4.18)$$

4.1.2.2. MATERIAL LAW

Definition of tensor strains is given by Equation (4.19) [42]:

$$\begin{Bmatrix} \varepsilon_L \\ \varepsilon_T \\ \frac{1}{2}\gamma_{LT} \end{Bmatrix} = [T] \begin{Bmatrix} \varepsilon_x \\ \varepsilon_y \\ \frac{1}{2}\gamma_{xy} \end{Bmatrix} \quad (4.19)$$

The relations between stresses and strains are obtained utilizing linear elasticity. For the FSDT, it is useful to split stress-strain relation into two parts, involving axial-bending and transverse shear. Hence, by using the tensor strains, the axial and bending part can be expressed as:

$$\begin{Bmatrix} \sigma_x \\ \sigma_y \\ \tau_{xy} \end{Bmatrix} = \begin{bmatrix} \bar{Q}_{11} & \bar{Q}_{12} & \bar{Q}_{16} \\ \bar{Q}_{12} & \bar{Q}_{22} & \bar{Q}_{26} \\ \bar{Q}_{16} & \bar{Q}_{26} & \bar{Q}_{66} \end{bmatrix} \begin{Bmatrix} \frac{\partial u_0}{\partial x} \\ \frac{\partial v_0}{\partial y} \\ \frac{\partial u_0}{\partial y} + \frac{\partial v_0}{\partial x} \end{Bmatrix} + z \begin{bmatrix} \bar{Q}_{11} & \bar{Q}_{12} & \bar{Q}_{16} \\ \bar{Q}_{12} & \bar{Q}_{22} & \bar{Q}_{26} \\ \bar{Q}_{16} & \bar{Q}_{26} & \bar{Q}_{66} \end{bmatrix} \begin{Bmatrix} \frac{\partial \phi_x}{\partial x} \\ \frac{\partial \phi_y}{\partial y} \\ \frac{\partial \phi_x}{\partial y} + \frac{\partial \phi_y}{\partial x} \end{Bmatrix} \quad (4.20)$$

Then the transverse-shear part is given as [42]:

$$\begin{Bmatrix} \tau_{yz} \\ \tau_{xz} \end{Bmatrix} = k_{sc} \begin{bmatrix} \bar{Q}_{44} & \bar{Q}_{45} \\ \bar{Q}_{45} & \bar{Q}_{55} \end{bmatrix} \begin{Bmatrix} \gamma_{yz} \\ \gamma_{xz} \end{Bmatrix} = k \begin{bmatrix} \bar{Q}_{44} & \bar{Q}_{45} \\ \bar{Q}_{45} & \bar{Q}_{55} \end{bmatrix} \begin{Bmatrix} \phi_y + \frac{\partial w_0}{\partial y} \\ \phi_x + \frac{\partial w_0}{\partial x} \end{Bmatrix} \quad (4.21)$$

where k_{sc} is the shear correction coefficient.

4.1.2.3. RESULTS FORCES AND MOMENTS

The resultant force and resultant moment are obtained in the same way as the CLPT:

$$\begin{Bmatrix} N_x \\ N_y \\ N_{xy} \end{Bmatrix} = \begin{bmatrix} A_{11} & A_{12} & A_{16} \\ A_{12} & A_{22} & A_{26} \\ A_{16} & A_{26} & A_{66} \end{bmatrix} \begin{Bmatrix} \frac{\partial u_0}{\partial x} \\ \frac{\partial v_0}{\partial y} \\ \frac{\partial u_0}{\partial y} + \frac{\partial v_0}{\partial x} \end{Bmatrix} + \begin{bmatrix} B_{11} & B_{12} & B_{16} \\ B_{12} & B_{22} & B_{26} \\ B_{16} & B_{26} & B_{66} \end{bmatrix} \begin{Bmatrix} \frac{\partial \phi_x}{\partial x} \\ \frac{\partial \phi_y}{\partial y} \\ \frac{\partial \phi_x}{\partial y} + \frac{\partial \phi_y}{\partial x} \end{Bmatrix} \quad (4.22)$$

$$\begin{Bmatrix} M_x \\ M_y \\ M \end{Bmatrix} = \begin{bmatrix} B_{11} & B_{12} & B_{16} \\ B_{12} & B_{22} & B_{26} \\ B_{16} & B_{26} & B_{66} \end{bmatrix} \begin{Bmatrix} \frac{\partial u_0}{\partial x} \\ \frac{\partial v_0}{\partial y} \\ \frac{\partial u_0}{\partial y} + \frac{\partial v_0}{\partial x} \end{Bmatrix} + \begin{bmatrix} D_{11} & D_{12} & D_{16} \\ D_{12} & D_{22} & D_{26} \\ D_{16} & D_{26} & D_{66} \end{bmatrix} \begin{Bmatrix} \frac{\partial \phi_x}{\partial x} \\ \frac{\partial \phi_y}{\partial y} \\ \frac{\partial \phi_x}{\partial y} + \frac{\partial \phi_y}{\partial x} \end{Bmatrix} \quad (4.23)$$

Equations relating the shear-force resultants R_{yz} and R_{xz} to the shear strains γ_{yz} and γ_{xz} can be written as [42]:

$$\begin{Bmatrix} R_{yz} \\ R_{xz} \end{Bmatrix} = k \sum_{i=1}^n \int_{h_{i-1}}^{h_i} \begin{bmatrix} \bar{Q}_{44} & \bar{Q}_{45} \\ \bar{Q}_{45} & \bar{Q}_{55} \end{bmatrix} dz \begin{Bmatrix} \gamma_{yz}^0 \\ \gamma_{xz}^0 \end{Bmatrix} = k \begin{bmatrix} A_{44} & A_{45} \\ A_{45} & A_{55} \end{bmatrix} \begin{Bmatrix} \phi_y + \frac{\partial w_0}{\partial y} \\ \phi_x + \frac{\partial w_0}{\partial x} \end{Bmatrix} \quad (4.24)$$

4.1.2.4. EQUILIBRIUM EQUATIONS IN TERMS OF DISPLACEMENT

Equilibrium of moments in x, y direction for laminated thin plates are given in Equations (4.25) and (4.26), respectively. In addition, Equilibrium of forces in z direction for laminated thin plates is given in Equation (4.27). In the Appendix D.2, calculations of these equations are given in Equations (D.20), (D.22) and (D.24).

$$\frac{\partial M_x}{\partial x} + \frac{\partial M_{xy}}{\partial y} - R_{xz} = 0 \quad (4.25)$$

$$\frac{\partial M_y}{\partial y} + \frac{\partial M_{xy}}{\partial x} - R_{yz} = 0 \quad (4.26)$$

$$\frac{\partial R_{xz}}{\partial x} + \frac{\partial R_{yz}}{\partial y} + p^* = 0 \quad (4.27)$$

Where: $p^* = p + N_x \frac{\partial^2 w}{\partial x^2} + N_y \frac{\partial^2 w}{\partial y^2} + 2N_{xy} \frac{\partial^2 w}{\partial x \partial y} - \rho^* \frac{\partial^2 w}{\partial t^2}$

Constitutive equations for a specially orthotropic plate with the new displacement field still satisfy the conditions stated earlier:

$$\begin{aligned} A_{16} &= A_{26} = 0 \\ B_{ij} &= 0 \\ D_{16} &= D_{26} = 0 \\ A_{45} &= A_{54} = 0 \end{aligned} \quad (4.28)$$

In view of these conditions, equilibrium equations above can be written in terms of the displacement field as follows:

$$D_{11} \frac{\partial^2 \phi_x}{\partial x^2} + (D_{12} + D_{66}) \frac{\partial^2 \phi_y}{\partial x \partial y} + D_{66} \frac{\partial^2 \phi_x}{\partial y^2} - A_{55} k \left(\phi_x + \frac{\partial w}{\partial x} \right) = 0 \quad (4.29)$$

$$D_{22} \frac{\partial^2 \phi_y}{\partial x^2} + (D_{12} + D_{66}) \frac{\partial^2 \phi_x}{\partial x \partial y} + D_{66} \frac{\partial^2 \phi_y}{\partial y^2} - A_{44} k \left(\phi_y + \frac{\partial w}{\partial y} \right) = 0 \quad (4.30)$$

$$A_{55} k \left(\frac{\partial \phi_x}{\partial x} + \frac{\partial^2 w}{\partial x^2} \right) + A_{44} k \left(\frac{\partial \phi_y}{\partial y} + \frac{\partial^2 w}{\partial y^2} \right) + p^* = 0 \quad (4.31)$$

Equations (4.29)-(4.31) are three coupled second-order differential equations with w , ϕ_x and ϕ_y as the three unknowns.

4.2. Analysis of Specially Orthotropic Plates under Uniaxial Compressive Load using CLPT and FSDT

Calculation methods for critical buckling load of specially orthotropic composite plates under uniaxial compressive load is studied in this chapter. These calculations are done using CLPT and FSDT as described early. In addition, boundary condition of plates are chosen as classical boundary conditions, simply supported and clamped edge conditions. Composite plate geometric descriptions are given in the Figure 4.3.

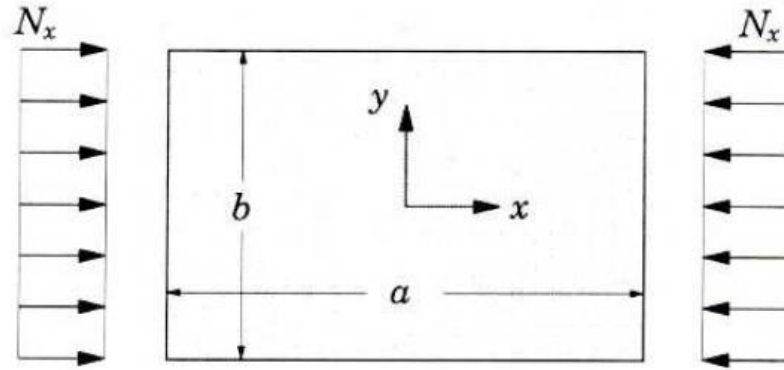


Figure 4.3: Plate with uniaxial compression load [41].

4.2.1. CLPT

4.2.1.1. BUCKLING OF PLATES WITH SIMPLY SUPPORTED BOUNDARY CONDITION UNDER UNIAXIAL COMPRESSIVE LOAD

For the buckling analysis, we assume that the only applied load is the in-plane compressive force in the x direction and all other loads are zero. From equation (4.15) we put $p^* = N_x \frac{\partial^2 w}{\partial x^2} = -N \frac{\partial^2 w}{\partial x^2}$. In this case, the equation governing the buckling problem is given by:

$$D_{11} \frac{\partial^4 w}{\partial x^4} + (2D_{12} + 4D_{66}) \frac{\partial^4 w}{\partial x^2 \partial y^2} + D_{22} \frac{\partial^4 w}{\partial y^4} + N \frac{\partial^2 w}{\partial x^2} = 0 \quad (4.32)$$

The plate edges are simply supported so that the transverse displacements at the edges and resultant moments about each edge are zero. These edge conditions are the boundary conditions, and mathematically expressed as follows [42]:

$$\begin{aligned} x = 0: \quad & w(0, y) = 0 & M_x(0, y) = 0 \\ x = a: \quad & w(a, y) = 0 & M_x(a, y) = 0 \\ y = 0: \quad & w(x, 0) = 0 & M_y(x, 0) = 0 \\ y = b: \quad & w(x, b) = 0 & M_y(x, b) = 0 \end{aligned} \quad (4.33)$$

A Navier solution of equation (4.32) that also satisfies the preceding boundary conditions is given by [42]:

$$w(x, y) = \sum_{n=1}^{\infty} \sum_{m=1}^{\infty} w_{mn} \sin\left(\frac{m\pi x}{a}\right) \sin\left(\frac{n\pi y}{b}\right) \quad (4.34)$$

where w_{mn} are the displacement coefficients, m and n are positive integers.

Substituting Equation (4.34) into the Equation (4.32) gives the buckling load as seen in Equation (4.35).

$$N = D_{11} \left(\frac{m\pi}{a}\right)^2 + (2D_{12} + 4D_{66}) \left(\frac{n\pi}{b}\right)^2 + D_{22} \left(\frac{a\pi}{m}\right)^2 \left(\frac{n}{b}\right)^4 \quad (4.35)$$

Thus, for each choice of m and n , there corresponds a unique value of the axial load N . The critical buckling load is the smallest of N , which can be obtained for $n = 1$ but m can be any integer number depending on the plate's geometric configuration.

4.2.1.2. BUCKLING OF PLATES WITH CLAMPED SUPPORTED BOUNDARY CONDITION UNDER UNIAXIAL COMPRESSIVE LOAD

Again, we assume that the only applied load is the in-plane compressive force in the x direction. For plates with all edges clamped, Rayleigh-Ritz method is used to solve the buckling problem. The method is based on the plate's potential energy. We now split the total potential energy in two parts, bending strain energy and the strain energy due to external forces [45]:

$$\Pi = U_b + U_p \quad (4.36)$$

where:

$$\begin{aligned}
U_b &= \frac{1}{2} \int_V \varepsilon^T \sigma \, dV = \frac{1}{2} \int_A \int_{-h/2}^{h/2} \varepsilon^T \bar{Q} \varepsilon \, dz \, dA = \frac{1}{2} \int_A \kappa^T D \kappa \, dA \\
&= \frac{1}{2} \int_0^b \int_0^a D_{11} \left(\frac{\partial^2 w}{\partial x^2} \right)^2 + 2D_{12} \left(\frac{\partial^2 w}{\partial x^2} \right) \left(\frac{\partial^2 w}{\partial y^2} \right) + D_{22} \left(\frac{\partial^2 w}{\partial y^2} \right)^2 \\
&\quad + 4D_{66} \left(\frac{\partial^2 w}{\partial x \partial y} \right)^2 \, dx \, dy
\end{aligned} \tag{4.37}$$

and

$$U_p = \frac{1}{2} \int_0^b \int_0^a -N \left(\frac{\partial w}{\partial x} \right)^2 \, dx \, dy \tag{4.38}$$

The boundary conditions associated with the clamped edges are given by [41]:

$$\begin{aligned}
x = 0: \quad w(0, y) = 0 \quad \frac{\partial w(0, y)}{\partial x} = 0 \\
x = a: \quad w(a, y) = 0 \quad \frac{\partial w(a, y)}{\partial x} = 0 \\
y = 0: \quad w(x, 0) = 0 \quad \frac{\partial w(x, 0)}{\partial y} = 0 \\
y = b: \quad w(x, b) = 0 \quad \frac{\partial w(x, b)}{\partial y} = 0
\end{aligned} \tag{4.39}$$

A solution that satisfies the preceding boundary conditions is given by [46]:

$$w(x, y) = \sum_{n=1}^{\infty} \sum_{m=1}^{\infty} w_{mn} \sin\left(\frac{m\pi x}{a}\right) \sin\left(\frac{n\pi x}{a}\right) \sin^2\left(\frac{\pi y}{b}\right) \tag{4.40}$$

where w_{mn} are the displacement coefficients, m and n are positive integers.

The equation above with only one term is usually enough to solve the buckling problem. So we assume that:

$$w(x, y) = w_{mn} \sin\left(\frac{m\pi x}{a}\right) \sin\left(\frac{n\pi y}{b}\right) \sin^2\left(\frac{\pi y}{b}\right) \quad (4.41)$$

Substitution of equation (4.41) into the equation (4.36) gives:

$$\Pi = \begin{cases} \frac{1}{2}\pi^4 w_{mn}^2 [D_{11} \frac{3}{4} \frac{b}{a^3} m^4 + D_{22} \frac{3}{4} \frac{a}{b^3} \\ + \left(\frac{1}{2}D_{12} + D_{66}\right) \frac{m^2}{ab}] - \frac{3}{32} \frac{w_{mn}^2 \pi^2 b m^2}{a} N, & m = n \\ \frac{1}{4}\pi^4 w_{mn}^2 [D_{11} \frac{3}{16} \frac{b}{a^3} (n^4 + 6m^2 n^2 + m^4) + D_{22} \frac{a}{b^3} \\ + \left(\frac{1}{2}D_{12} + D_{66}\right) \frac{n^2 + m^2}{ab}] - \frac{3}{64} \frac{w_{mn}^2 \pi^2 b (n^2 + m^2)}{a} N, & m \neq n \end{cases} \quad (4.42)$$

Equilibrium requires that $\delta\Pi = 0$, thus:

$$\frac{\partial\Pi}{\partial w_{mn}} \delta w_{mn} = 0 \quad \leftrightarrow \quad \frac{\partial\Pi}{\partial w_{mn}} = 0 \quad (4.43)$$

$$\frac{\partial\Pi}{\partial w_{mn}} = \begin{cases} \pi^2 w_{mn} [D_{11} \pi^2 \frac{3}{4} \frac{b}{a^3} m^4 + D_{22} \pi^2 \frac{3}{4} \frac{a}{b^3} \\ + \left(\frac{1}{2}D_{12} + D_{66}\right) \pi^2 \frac{m^2}{ab} - \frac{3}{16} \frac{b m^2}{a} N] = 0 & m = n \\ \frac{1}{2} \pi^2 w_{mn} [D_{11} \frac{3}{16} \frac{b}{a^3} \pi^2 (n^4 + 6m^2 n^2 + m^4) + D_{22} \frac{a}{b^3} \pi^2 \\ + \left(\frac{1}{2}D_{12} + D_{66}\right) \frac{\pi^2}{ab} (n^2 + m^2) - \frac{3}{16} \frac{b}{a} (n^2 + m^2) N] = 0 & m \neq n \end{cases} \quad (4.44)$$

Solving equation (4.44) for N, we obtain:

$$N = \begin{cases} \frac{4\pi^2 D_{11} m^2}{a^3} + \frac{4\pi^2 D_{22} a^2}{b^4 m^2} + \frac{16\pi^2}{3b^2} \left(\frac{1}{2}D_{12} + D_{66}\right), & m = \\ \frac{D_{11} \frac{\pi^2}{a^2} (n^4 + 6m^2 n^2 + m^4) + D_{22} \pi^2 \frac{16}{3} \frac{a^2}{b^4} + \left(\frac{1}{2}D_{12} + D_{66}\right) \frac{16}{3} \frac{\pi^2}{b^2} (m^2 + n^2)}{m^2 + n^2}, & m \neq \end{cases} \quad (4.45)$$

Thus, combination of m and n that gives the smallest value of N is the critical buckling load for a clamped plate.

4.2.2. FSDT

4.2.2.1. BUCKLING OF PLATES WITH SIMPLY SUPPORTED BOUNDARY CONDITION UNDER UNIAXIAL COMPRESSIVE LOAD

Since the only applied load is the force in x direction, from equation (4.31), $p^* = N_x \frac{\partial^2 w}{\partial x^2} = -N_x \frac{\partial^2 w}{\partial x^2}$. Based on equations (4.29)-(4.31), the equation set that is needed for the solution the buckling problem is given by:

$$D_{11} \frac{\partial^2 \phi_x}{\partial x^2} + (D_{12} + D_{66}) \frac{\partial^2 \phi_y}{\partial x \partial y} + D_{66} \frac{\partial^2 \phi_x}{\partial y^2} - A_{55} k \left(\phi_x + \frac{\partial w}{\partial x} \right) = 0 \quad (4.46)$$

$$D_{22} \frac{\partial^2 \phi_y}{\partial x^2} + (D_{12} + D_{66}) \frac{\partial^2 \phi_x}{\partial x \partial y} + D_{66} \frac{\partial^2 \phi_y}{\partial y^2} - A_{44} k \left(\phi_y + \frac{\partial w}{\partial y} \right) = 0 \quad (4.47)$$

$$A_{55} k \left(\frac{\partial \phi_x}{\partial x} + \frac{\partial^2 w}{\partial x^2} \right) + A_{44} k \left(\frac{\partial \phi_y}{\partial y} + \frac{\partial^2 w}{\partial y^2} \right) - N \frac{\partial^2 w}{\partial x^2} = 0 \quad (4.48)$$

Boundary conditions for the simply supported plate are the same as those for the CLPT given by Equation (4.33). The following double Fourier series are assumed to represent w , ϕ_x and ϕ_y [42]:

$$w(x, y) = \sum_{n=1}^{\infty} \sum_{m=1}^{\infty} w_{mn} \sin\left(\frac{m\pi x}{a}\right) \sin\left(\frac{n\pi y}{b}\right) \quad (4.49)$$

$$\phi_x(x, y) = \sum_{n=1}^{\infty} \sum_{m=1}^{\infty} x_{mn} \cos\left(\frac{m\pi x}{a}\right) \sin\left(\frac{n\pi y}{b}\right) \quad (4.50)$$

$$\phi_y(x, y) = \sum_{n=1}^{\infty} \sum_{m=1}^{\infty} y_{mn} \sin\left(\frac{m\pi x}{a}\right) \cos\left(\frac{n\pi y}{b}\right) \quad (4.51)$$

where w_{mn} , x_{mn} and y_{mn} are the series coefficients, and m and n are positive integers.

Using double Fourier series defined in Equations (4.49) to (4.51), simply supported boundary conditions defined in Equation (4.33) are satisfied. According to simply

supported boundary conditions, M_x equals to zero when the x is equal to zero. To verify these series written in above, moment x equilibrium equation written in matrix equation (4.23) is used and following expression is obtained:

$$M_x = D_{11} * \frac{\partial \phi_x}{\partial x} + D_{12} * \frac{\partial \phi_y}{\partial y} \quad (4.52)$$

$$M_x = -D_{11} * x_{mn} * \frac{m\pi}{a} \sin\left(\frac{m\pi x}{a}\right) \sin\left(\frac{n\pi y}{b}\right) - D_{12} * y_{mn} * \frac{n\pi}{b} \sin\left(\frac{m\pi x}{a}\right) \sin\left(\frac{n\pi y}{b}\right) \quad (4.53)$$

When the x value is substituted as zero, M_x equals to zero as seen in Equation (4.54).

$$M_x(0, y) = -D_{11} * x_{mn} * \frac{m\pi}{a} \sin(0) \sin\left(\frac{n\pi y}{b}\right) - D_{12} * y_{mn} * \frac{n\pi}{b} \sin(0) \sin\left(\frac{n\pi y}{b}\right) = 0 \quad (4.54)$$

For simply supported plates, it is enough to consider one term with m and n varying from each equation. Substitution of equations (4.49)-(4.51) into equations (4.46)-(4.48) gives the following matrix equation:

$$\begin{bmatrix} -D_{11}\alpha^2 - D_{66}\beta^2 - A_{55}k & -D_{12}\alpha\beta - D_{66}\alpha\beta & -A_{55}k\alpha \\ -D_{12}\alpha\beta - D_{66}\alpha\beta & -D_{22}\beta^2 - D_{66}\alpha^2 - A_{44}k & -A_{44}k\beta \\ -A_{55}k\alpha & -A_{44}k\beta & N\alpha^2 - A_{55}k\alpha^2 - A_{44}k\beta^2 \end{bmatrix} \begin{Bmatrix} x_{mn} \\ y_{mn} \\ w_{mn} \end{Bmatrix} = \begin{Bmatrix} 0 \\ 0 \\ 0 \end{Bmatrix} \quad (4.55)$$

where $\alpha = \frac{m\pi}{a}$, $\beta = \frac{n\pi}{b}$.

By defining:

$$\begin{aligned} C_1 &= -D_{11}\alpha^2 - D_{66}\beta^2 - A_{55}k \\ C_2 &= -D_{12}\alpha\beta - D_{66}\alpha\beta \\ C_3 &= -A_{55}k\alpha \\ C_4 &= -D_{22}\beta^2 - D_{66}\alpha^2 - A_{44}k \\ C_5 &= -A_{44}k\beta \end{aligned} \quad (4.56)$$

Equation (4.55) is simplified to:

$$\begin{bmatrix} C_1 & C_2 & C_3 \\ C_2 & C_4 & C_5 \\ C_3 & C_5 & N\alpha^2 + \alpha C_3 + \beta C_5 \end{bmatrix} * \begin{Bmatrix} x_{mn} \\ y_{mn} \\ w_{mn} \end{Bmatrix} = \begin{Bmatrix} 0 \\ 0 \\ 0 \end{Bmatrix} \quad (4.57)$$

We are seeking non-trivial solutions, thus,

$$\begin{vmatrix} C_1 & C_2 & C_3 \\ C_2 & C_4 & C_5 \\ C_3 & C_5 & N\alpha^2 + \alpha C_3 + \beta C_5 \end{vmatrix} = 0 \quad (4.58)$$

Solving equation (4.58) for N , we obtain:

$$N = \frac{C_1 C_5^2 + \alpha C_3 C_2^2 + \beta C_5 C_2^2 + C_4 C_3^2 - \alpha C_1 C_3 C_4 - \beta C_1 C_4 C_5 - 2C_2 C_3 C_5}{\alpha^2 (C_1 C_4 - C_2^2)} \quad (4.59)$$

The critical buckling load occurs at $n = 1$, while m can vary.

4.2.2.2. BUCKLING OF PLATES WITH CLAMPED SUPPORTED BOUNDARY CONDITION UNDER UNIAXIAL COMPRESSIVE LOAD

As the CLPT, the Rayleigh-Ritz method has been used to solve the buckling problem for the clamped plate. It is convenient to split the total potential energy in three parts, bending, transverse shear and external forces:

$$\Pi = U_b + U_s + U_p \quad (4.60)$$

where:

$$\begin{aligned} U_b &= \frac{1}{2} \int_V \varepsilon_b^T \sigma_b dV = \frac{1}{2} \int_A \int_{-h/2}^{h/2} \varepsilon_b^T \bar{Q} \varepsilon_b dz dA = \frac{1}{2} \int_A \kappa^T D \kappa dA \\ &= \frac{1}{2} \int_0^b \int_0^a D_{11} \left(\frac{\partial^2 w_b}{\partial x^2} \right)^2 + 2D_{12} \left(\frac{\partial^2 w_b}{\partial x^2} \right) \left(\frac{\partial^2 w_b}{\partial y^2} \right) + D_{22} \left(\frac{\partial^2 w_b}{\partial y^2} \right)^2 \\ &\quad + 4D_{66} \left(\frac{\partial^2 w_b}{\partial x \partial y} \right)^2 dx dy \end{aligned} \quad (4.61)$$

$$U_s = \frac{1}{2} \int_V \varepsilon_s^T \sigma_s dV = \frac{1}{2} \int_A \int_{-h/2}^{h/2} \varepsilon_s^T \bar{Q}_{skj} \varepsilon_s dz dA = \frac{1}{2} \int_A \varepsilon_s^T A_{skj} \varepsilon_s dA \quad (4.62)$$

$$= \frac{1}{2} k \int_0^b \int_0^a A_{44} \left(\frac{\partial w_s}{\partial y} \right)^2 + A_{55} \left(\frac{\partial w_s}{\partial x} \right)^2 dx dy$$

$$U_p = \frac{1}{2} \int_0^b \int_0^a -N \left(\frac{\partial w}{\partial x} \right)^2 dx dy \quad (4.63)$$

The boundary conditions associated with the clamped edges are again given by Equation (4.39). A solution that satisfies the preceding boundary conditions is given by [46]:

$$\begin{aligned} w(x, y) &= w_b + w_s \\ &= \sum_{n=1}^{\infty} \sum_{m=1}^{\infty} \left(\bar{w}_b \sin\left(\frac{m\pi x}{a}\right) \sin\left(\frac{n\pi x}{a}\right) \sin^2\left(\frac{\pi y}{b}\right) \right. \\ &\quad \left. + \bar{w}_s \sin\left(\frac{n\pi x}{a}\right) \sin\left(\frac{\pi y}{b}\right) \right) \end{aligned} \quad (4.64)$$

where \bar{w}_b and \bar{w}_s are the displacement coefficients for bending and transverse shear, and m and n are positive integers.

For a single term series,

$$w(x, y) = \bar{w}_b \sin\left(\frac{m\pi x}{a}\right) \sin\left(\frac{n\pi x}{a}\right) \sin^2\left(\frac{\pi y}{b}\right) + \bar{w}_s \sin\left(\frac{n\pi x}{a}\right) \sin\left(\frac{\pi y}{b}\right) \quad (4.65)$$

Equilibrium requires that $\delta\Pi = 0$, thus:

$$\frac{\partial\Pi}{\partial\bar{w}_b} \delta\bar{w}_b + \frac{\partial\Pi}{\partial\bar{w}_s} \delta\bar{w}_s = 0 \quad (4.66)$$

This implies,

$$\begin{Bmatrix} \frac{\partial\Pi}{\partial\bar{w}_b} \\ \frac{\partial\Pi}{\partial\bar{w}_s} \end{Bmatrix} = \begin{Bmatrix} 0 \\ 0 \end{Bmatrix} \quad (4.67)$$

Firstly, Equation (4.65) is substituted into the Equation (4.60). After that, derivation of Equations (4.60) gives two solutions as Equation (4.67). Finally, this expression is divided into two conditions, one for $m \neq 1$ and another $m = 1$.

For $m \neq 1$, Equation (4.67) gives following matrix equation:

$$\begin{bmatrix} H_1 + NH_2 & NH_3 \\ NH_3 & H_4 + NH_5 \end{bmatrix} \begin{Bmatrix} \bar{W}_b \\ \bar{W}_s \end{Bmatrix} = \begin{Bmatrix} 0 \\ 0 \end{Bmatrix} \quad (4.68)$$

where,

$$\begin{aligned} H_1 &= \frac{\pi^4}{32a^3b^3} (D_{11}b^4(18m^2 + 3 + 3m^4) + D_{12}a^2b^2(8 + 8m^2) + 16D_{22}a^4 \\ &\quad + D_{66}a^2b^2(16 + 16m^2)) \\ H_2 &= -\frac{\pi^2b(3m^6 + 3 + 3n^4 - 3m^4 - 3m^2 + 3m^2n^4 - 12m^2n^2 - 6n^2 - 6m^4n^2)}{32a(1 - 2n^2 + m^4 - 2m^2n^2 - 2m^2 + n^4)} \\ H_3 &= -\frac{8b(-mn^3 + (-1)^{m+n+1}mn^3)}{3a(1 - 2n^2 + m^4 - 2m^2n^2 - 2m^2 + n^4)} \\ H_4 &= \frac{k\pi^2}{4ab} (A_{44}a^2 + A_{55}n^2b^2) \\ H_5 &= -\frac{\pi^2b(n^2 + \pi^6 - 2m^2n^4 + m^4n^2 - 2n^4 - 2m^2n^2)}{4a(1 - 2n^2 + m^4 - 2m^2n^2 - 2m^2 + n^4)} \end{aligned} \quad (4.69)$$

Matrix equation (4.68) gives non-trivial solutions when the determinant of this matrix expressed is zero. This leads us to a second-order equation:

$$(H_2H_5 - H_3^2)N^2 + (H_1H_5 + H_2H_4)N + H_1H_4 = 0 \quad (4.70)$$

The smallest value of N is given by:

$$N = \frac{-(H_1H_5 + H_2H_4) - \sqrt{(H_1H_5 + H_2H_4)^2 - 4(H_2H_5 - H_3^2)H_1H_4}}{2(H_2H_5 - H_3^2)} \quad (4.71)$$

Combination of positive integers m and n gives the critical buckling load.

For $m = 1$, Equation (4.67) gives following matrix equation:

$$\begin{bmatrix} G_1 + NG_2 & NG_3 \\ NG_3 & G_4 + NG_5 \end{bmatrix} \begin{Bmatrix} \bar{W}_b \\ \bar{W}_s \end{Bmatrix} = \begin{Bmatrix} 0 \\ 0 \end{Bmatrix} \quad (4.72)$$

where,

$$\begin{aligned} G_1 &= \frac{\pi^4}{4a^3b^3} (3D_{11}b^4 + 2D_{12}a^2b^2 + 3D_{22}a^4 + 4D_{66}a^2b^2) \\ G_2 &= -\frac{3\pi^2b}{16a} \\ G_3 &= -\frac{8b(-n^3 + (-1)^{n+2}n^3)}{3a(n^4 - 4n^2)} \\ G_4 &= \frac{k\pi^2}{4ab} (A_{44}a^2 + A_{55}n^2b^2) \\ G_5 &= -\frac{\pi^2bn^2}{4a} \end{aligned} \quad (4.73)$$

Matrix equation (4.72) gives non-trivial solutions when the determinant of this matrix expressed is zero. A result of this, a second-order equation is obtained as:

$$(G_2G_5 - G_3^2)N^2 + (G_1G_5 + G_2G_4)N + G_1G_4 = 0 \quad (4.74)$$

Solving this, we obtain the smallest value of N :

$$N = \frac{-(G_1G_5 + G_2G_4) - \sqrt{(G_1G_5 + G_2G_4)^2 - 4(G_2G_5 - G_3^2)G_1G_4}}{2(G_2G_5 - G_3^2)} \quad (4.75)$$

The critical buckling load depends on the positive integer n .

4.3. Finite Element Model of Composite Plates

In this sub-chapter, finite element model description of the composite plate is explained. Most of the parts of modelling the composite plate are same as the metal model.

In the finite element model, boundary conditions of the plate are assumed as classical boundary conditions of the single panel which is defined in Chapter 2.1.

The geometry and the coordinate system of the composite plate are presented in Figure 4.4. Ply orientation angles are given with respect to x axis according to Figure 4.4.

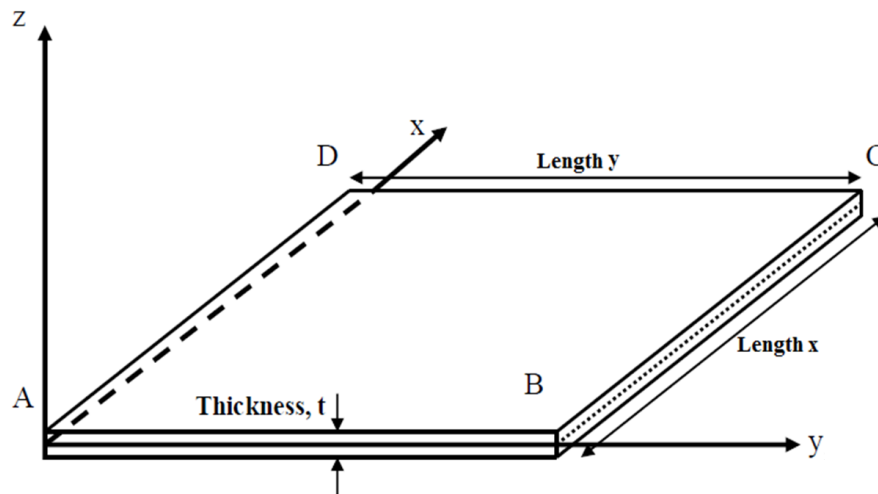


Figure 4.4: Definition of different geometrical parameters of the composite panels and the coordinate system

In the finite element model of composite plate, plate is modelled as 2D shell elements. Element type is chosen as quadrilateral element S4R. Element size is decided as 5 mm based on the mesh size study performed in Chapter 2.1. Moreover, the plate material is chosen as HexPly 8552 AS4 and at dry and room temperature condition properties of the composite material are given in Table 4.1. Detailed material properties can be seen in Appendix E, Figure E.1.

Table 4.1: Material properties of HexPly 8552 AS4 composite plate

$E_1(GPa)$	$128 * 10^3$	$G_{12}(MPa)$	114
$E_2(GPa)$	$1 * 10^3$	$G_{13}(MPa)$	114
ν_{12}	0.355	$G_{23}(MPa)$	114

Load is applied on the DC edge along the y-axis of the single panel as 1 N/mm shell edge load in the “-x” direction (compression) and the reaction edge of the panel is chosen as AB edge. In addition, the unloaded edges of the panel are AD and BC.

Finite element model is solved by using the “Buckle” step of ABAQUS [35] in linear buckling analysis for the lowest buckling eigenvalue and corresponding critical buckling load.

The critical buckling unit length load is obtained by finite element model using the lowest eigenvalue as shown in Equation (4.76),

$$N_{cr} = N_{app} * \lambda_{FE} \quad (4.76)$$

where N_{app} is the compressive shell edge load which is given as 1 N/mm in the “-x” direction. In addition, λ_{FE} is the first eigenvalue obtained from finite element analysis.

Then, using the critical buckling load, the affine plate buckling coefficient k_0 is calculated [47]:

$$k_0 = \frac{N_{cr} * b^2}{\pi^2 * \sqrt{D_{11}D_{22}}} \quad (4.77)$$

The modified buckling coefficient is calculated as [47]:

$$k_c = k_0 - 2D^* \quad (4.78)$$

where the generalized rigidity ratio D^* is given by,

$$D^* = \frac{D_{12} + 2D_{66}}{\sqrt{D_{11}D_{22}}} \quad (4.79)$$

In addition, plate affine ratio is calculated using equation [47]

$$\frac{a_o}{b_o} = \frac{a}{(D_{11})^{1/4}} \frac{(D_{22})^{1/4}}{b} \quad (4.80)$$

Using the plate affine ratio and the modified buckling coefficient values of plate, generic buckling curves for balanced orthotropic rectangular plates can be obtained. To do that, a Python script is written. Same as in the metallic part in the Chapter 2, various aspect ratio plates are solved using ABAQUS to obtain the buckling coefficient curves.

According to the model description made, a script is written Python 2.7 in order to create an ABAQUS finite element model, run the model and collect the lowest eigenvalue from the analysis results. The scripts are written for each composite plate and the following parameters are specified by the user;

- Plate length y
- Plate length x
- Plate material
- Ply thickness
- Ply orientation
- Ply repeat number
- Lay-up symmetry
- Boundary conditions

To minimize the time and sources, some of parameters of composite plates are fixed to certain values as,

- Plate length $x = 100$ mm
- Plate material = HexPly 8552 UD AS4
- Ply thickness = 0.13 mm
- Lay-up symmetry = True

In this study, one material is demonstrated however material number and type can be changed by modifying the script given in Appendix F.5.

Discrete values of the design parameters of composite plates are specified in a range. Upper and lower limits of the design parameters are decided based on the common used values in the aviation industry.

The following design parameters are specified between the upper and lower limits, and in total 81 finite element analyses are performed to draw curves for the buckling coefficients for each configuration. Step size of plate length y is chosen as 5 mm.

- Plate length $y = [100:5:500]$ mm
- Plate boundary conditions = [Simply supported, Clamped]
- Ply repeat number = [2,4]
- Ply configuration

Three different ply configurations are considered in this study.

- $(0^\circ/0^\circ)_S$
- $(0^\circ/90^\circ)_S$
- $(45^\circ/0^\circ/-45^\circ/90^\circ)_S$

To minimize the number of finite element analysis, for each parameter minimum of discrete values are selected within the upper-lower limits of each parameter. Panel length y has a remarkable effect on the buckling phenomena. Therefore, for the plate length y , more number of discrete analysis points is used in the finite element analyses. In addition, ply configuration has also significant effect however it is limited to three configurations due to lack of source and time.

Generic compressive coefficient buckling curves for balanced, orthotropic and symmetric composite plates are given in Figure 4.5 to Figure 4.7 for simply supported boundary conditions. In these figures, there are two curves for each plate thickness which depends on the ply repeat number and the ply orientation. As seen in Figure 4.5 to Figure 4.7, total thickness of plate is increased however modified buckling coefficient of plate is decreased. In contrast, this does not mean the buckling load of plate is decreased when the plate thickness is increased. To see that clearly, a comparison example is done with plate configuration seen in Table 4.2. The first plate total thickness is 1.04 mm and the second plate total thickness is 2.08 mm. Plates are assumed as simply supported at 4 edges.

Table 4.2: Input parameters of the example composite plates used in comparison

Plate material	HexPly 8552 UD AS4
Ply thickness (mm)	0.13
Ply configuration	$(0^\circ/90^\circ)_s$
Plate length x (mm)	100
Plate length y (mm)	200

Plates bending stiffness properties are calculated using Equation (D.7). Results are given in Table 4.3.

Table 4.3: Thin and thick composite plates thickness and stiffness properties

	Thin Plate	Thick Plate
Total Thickness (mm)	1.04	2.08
D_{11} ($N * mm$)	8617.49	60570.67
D_{22} ($N * mm$)	4432.87	43832.17
D_{12} ($N * mm$)	316.80	2534.42
D_{66} ($N * mm$)	10.69	85.49

Firstly, generalized rigidity ratio of plates are calculated using Equation (4.79). Affine ratio of plates are calculated with Equation (4.80) using stiffness and geometric properties given in Table 4.2 and Table 4.3, respectively. After the calculation of affine ratio, modified buckling coefficient of plates are obtained from Figure 4.6. Then, affine plate buckling coefficients are calculated for both plates using Equation (4.78). Finally, buckling load of plates are calculated using Equation (4.77). These results are given in Table 4.4. As seen in Table 4.4, modified buckling coefficient of thicker plate is less than thin one. However, buckling load of thicker plate is greater than thin one.

Table 4.4: Buckling load parameters of composite plates used in comparison

	Thin Plate	Thick Plate
D^*	0.05	0.05
a_0/b_0	1.69	1.84
$k_0 - 2D^*$	6.41	5.14
k_0	6.52	5.25
N (N/mm)	12.66	84.97

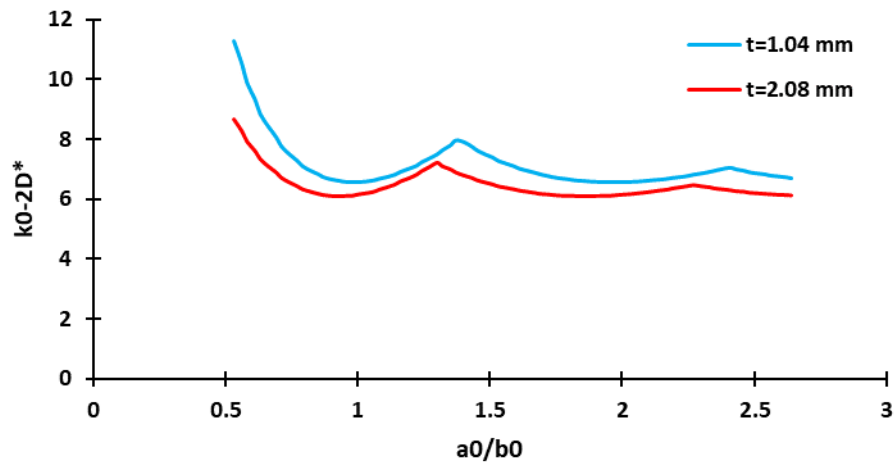


Figure 4.5: Compressive buckling coefficients for composite plates with simply supported loaded and unloaded edges (Ply orientation: $(0^\circ/0^\circ)_S$)

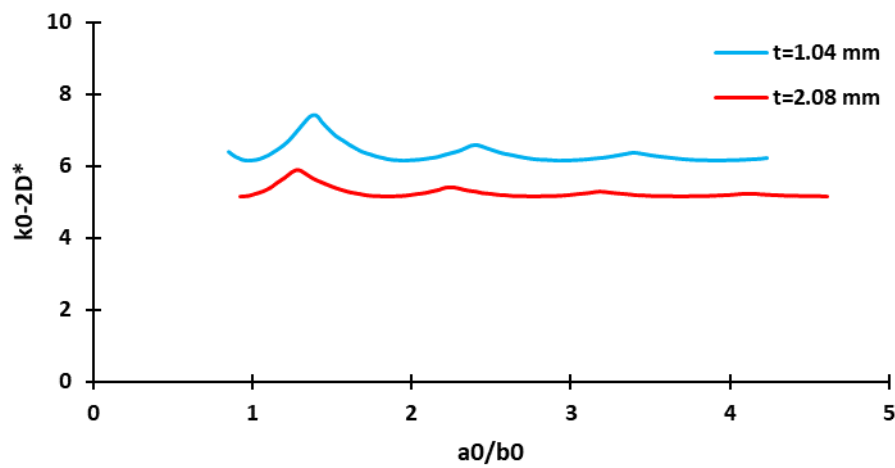


Figure 4.6: Compressive buckling coefficients for composite plates with simply supported loaded and unloaded edges (Ply orientation: $(0^\circ/90^\circ)_S$)

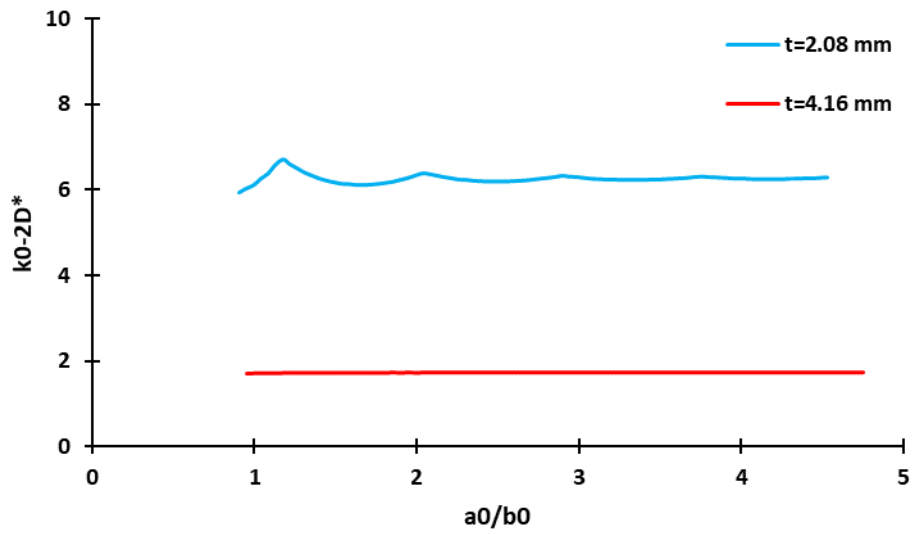


Figure 4.7: Compressive buckling coefficients for composite plates with simply supported loaded and unloaded edges (Ply orientation: $(45^\circ/0^\circ/-45^\circ/90^\circ)_S$)

Generic compressive buckling coefficient curves for balanced, orthotropic and symmetric composite plate are given in Figure 4.8 to Figure 4.10 for clamped boundary conditions.

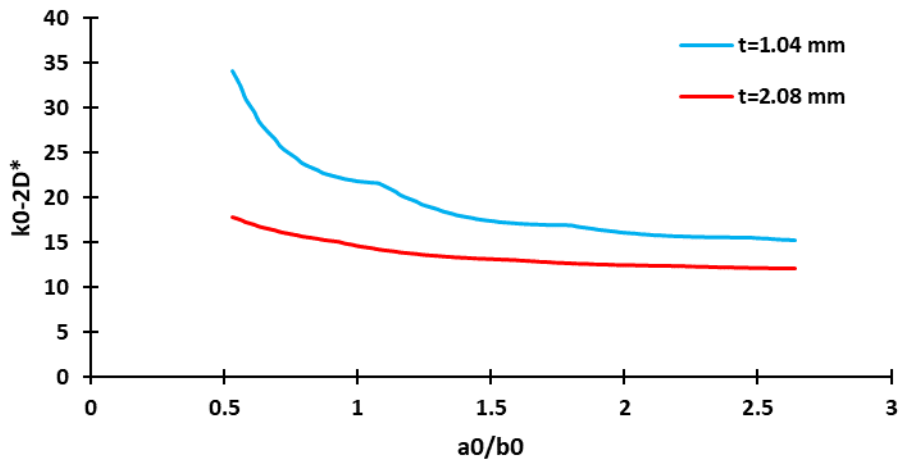


Figure 4.8: Compressive buckling coefficients for composite plates with clamped loaded and unloaded edges (Ply orientation: $(0^\circ/0^\circ)_S$)

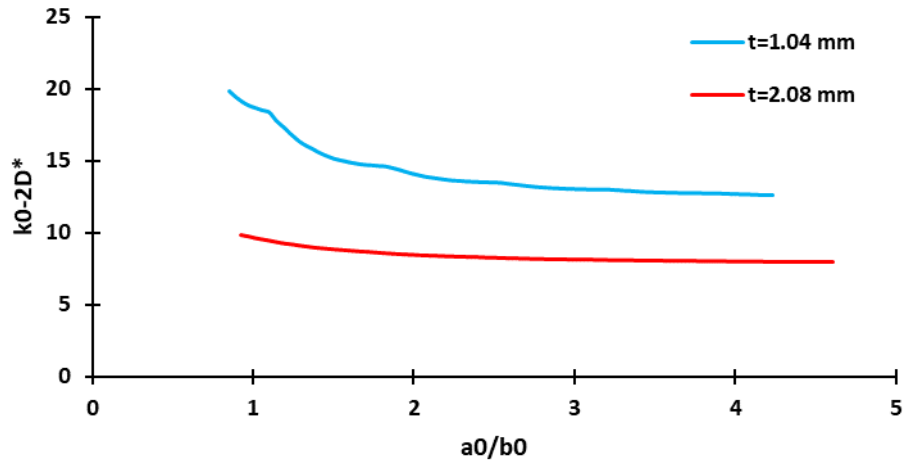


Figure 4.9: Compressive buckling coefficients for composite plates with clamped loaded and unloaded edges (Ply orientation: $(0^\circ/90^\circ)_S$)

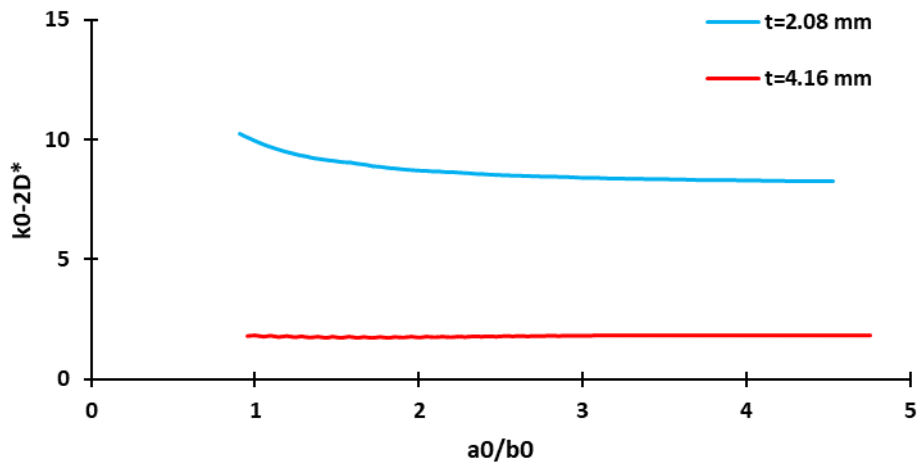


Figure 4.10: Compressive buckling coefficients for composite plates with clamped loaded and unloaded edges (Ply orientation: $(45^\circ/0^\circ/-45^\circ/90^\circ)_S$)

Buckling behaviour is affected by the total thickness of plate. As seen in the Figure 4.7 and Figure 4.10, thick plates' buckling coefficient is not affected by the plate aspect ratio. Moreover, as expected, buckling coefficient of plates with clamped edge condition is greater than one with the simply supported edge condition in the all ply configurations.

4.4. Comparison of Buckling Coefficient Curves obtained by CLPT, FSDT and FEA

In this section, buckling coefficient results obtained by the CLPT, FSDT and FEA methods are compared with each other. In Figure 4.11 and Figure 4.12, buckling coefficient curves obtained by each method are given for the simply supported boundary condition and $(0^\circ/0^\circ)_S$ ply orientation.

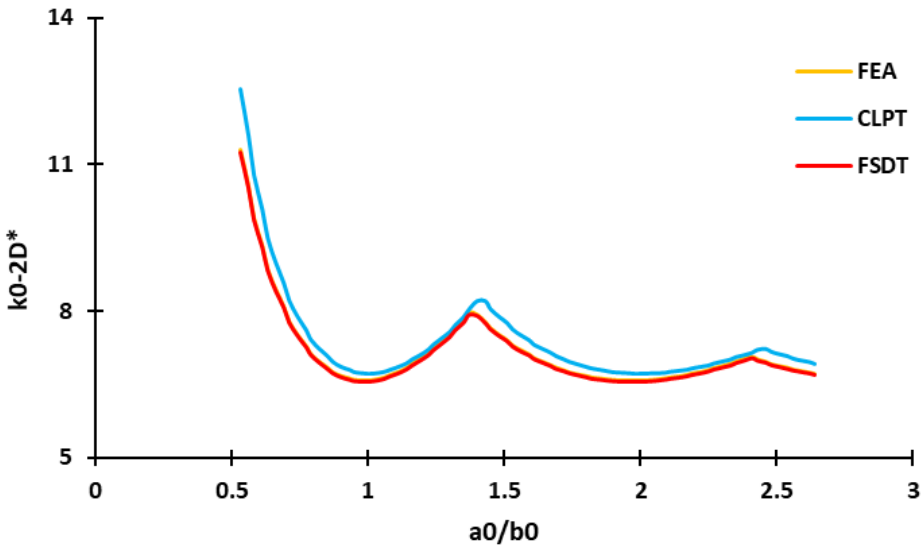


Figure 4.11: Compare of compressive buckling coefficients with all edges simply supported (Ply orientation: $(0^\circ/0^\circ)_S$, thickness of plate=1.04 mm)

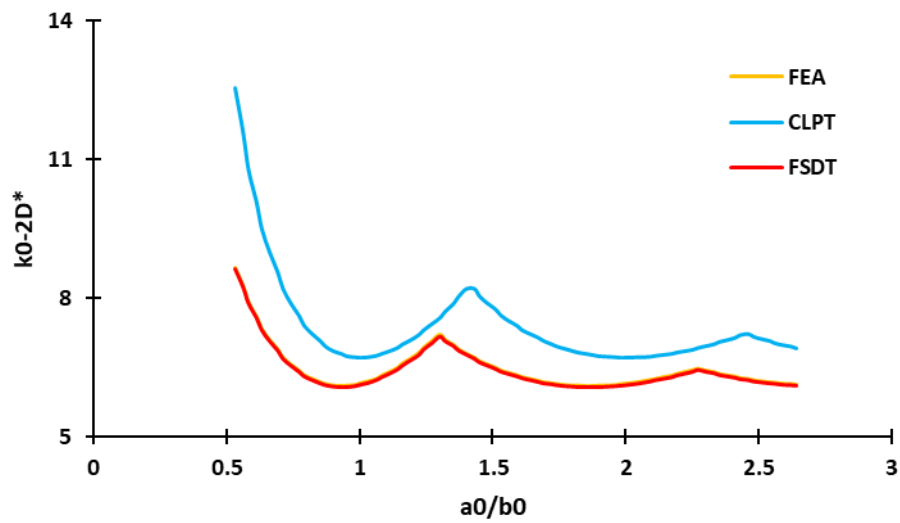


Figure 4.12: Compare of compressive buckling coefficients with all edges simply supported (Ply orientation: $(0^\circ/0^\circ)_S$, thickness of plate=2.08 mm)

In Figure 4.13 and Figure 4.14, buckling coefficient curves obtained by each method are given for the simply supported boundary condition and $(0^\circ/90^\circ)_S$ ply orientation.

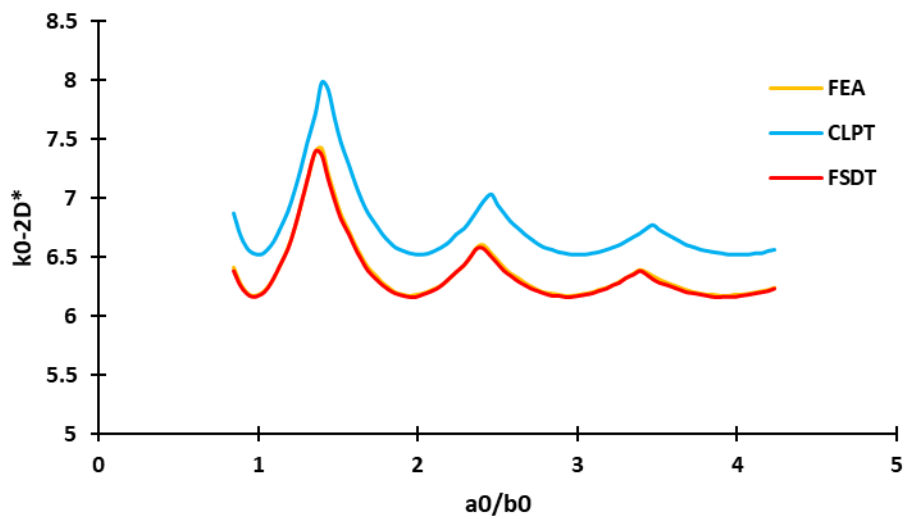


Figure 4.13: Compare of compressive buckling coefficients with all edges simply supported (Ply orientation: $(0^\circ/90^\circ)_S$, thickness of plate=1.04 mm)

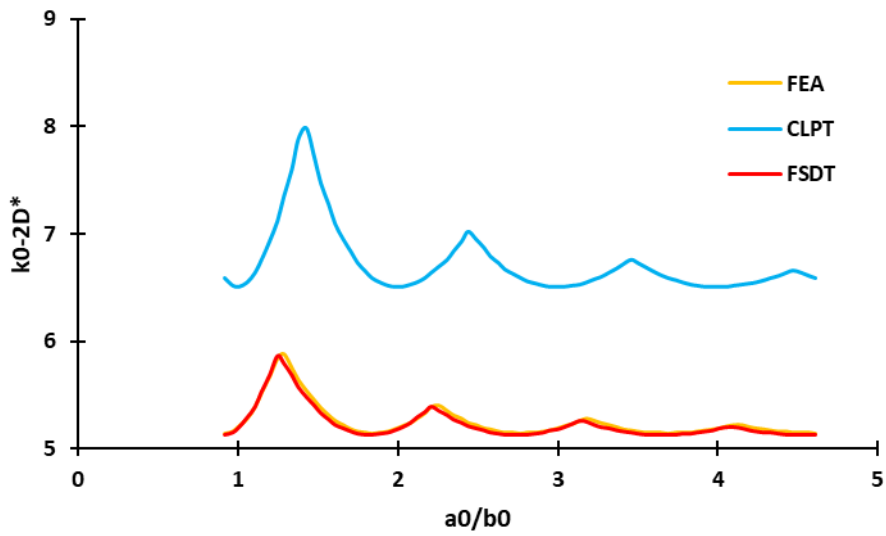


Figure 4.14: Compare of compressive buckling coefficients with all edges simply supported (Ply orientation: $(0^\circ/90^\circ)_s$, thickness of plate=2.08 mm)

In Figure 4.15 and Figure 4.16, buckling coefficient curves obtained by each method are given for the simply supported boundary condition and $(45^\circ/0^\circ/-45^\circ/90^\circ)_s$ ply orientation.

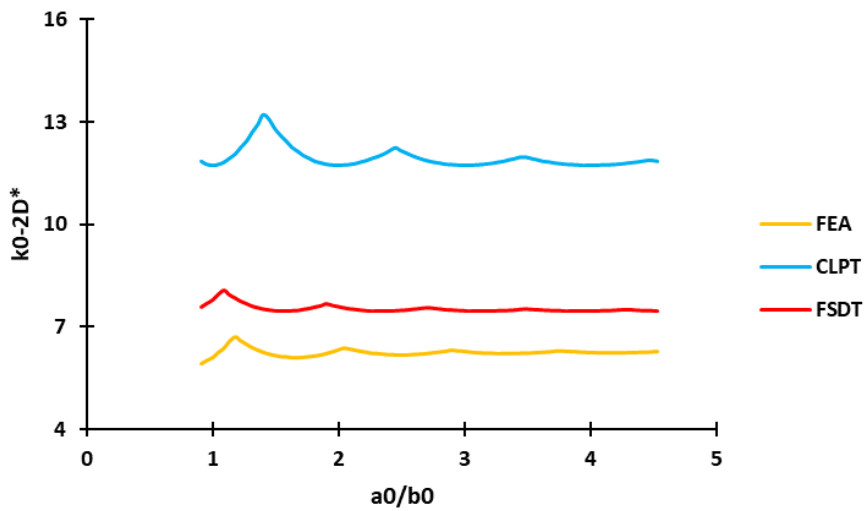


Figure 4.15: Compare of compressive buckling coefficients with all edges simply supported (Ply orientation: $(45^\circ/0^\circ/-45^\circ/90^\circ)_s$, thickness of plate=2.08 mm)

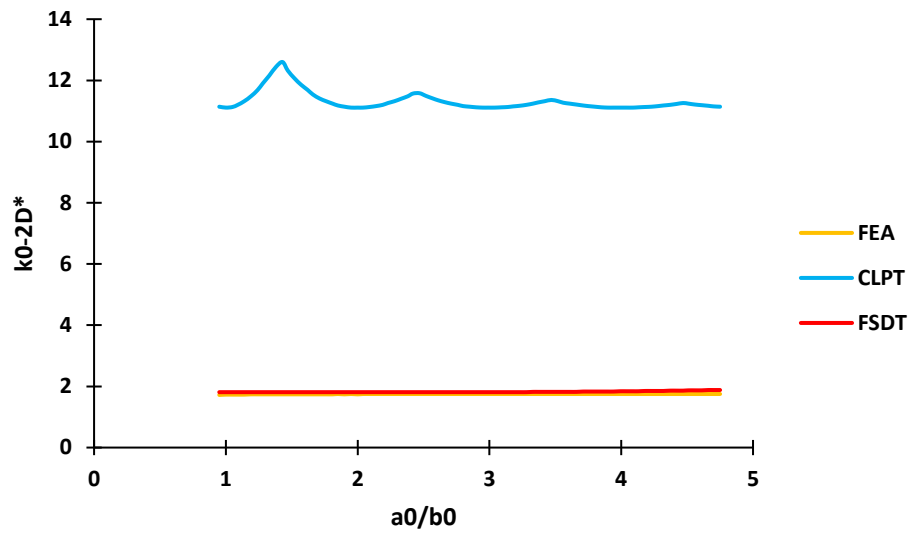


Figure 4.16: Compare of compressive buckling coefficients with all edges simply supported (Ply orientation: $(45^\circ/0^\circ/-45^\circ/90^\circ)_S$, thickness of plate=4.16 mm)

In Figure 4.17 and Figure 4.18, buckling coefficient curves obtained by each method are given for the clamped boundary condition and $(0^\circ/0^\circ)_S$ ply orientation.

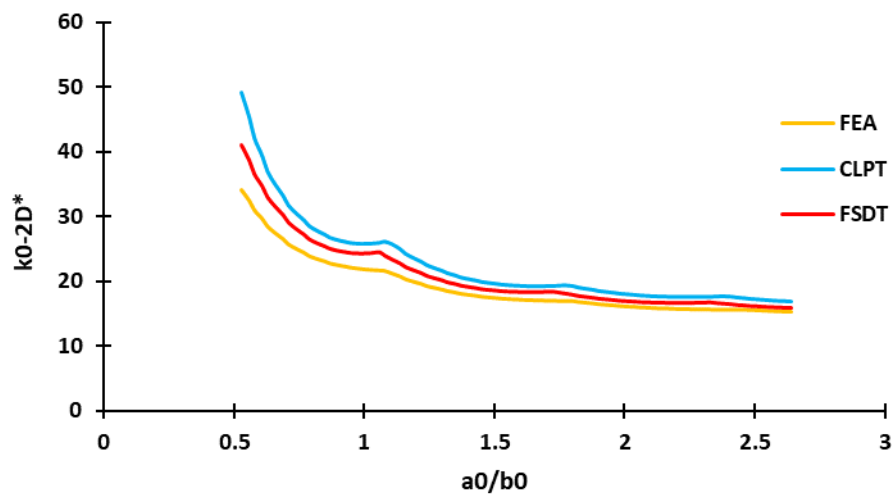


Figure 4.17: Compare of compressive buckling coefficients with all edges clamped (Ply orientation: $(0^\circ/0^\circ)_S$, thickness of plate=1.04 mm)

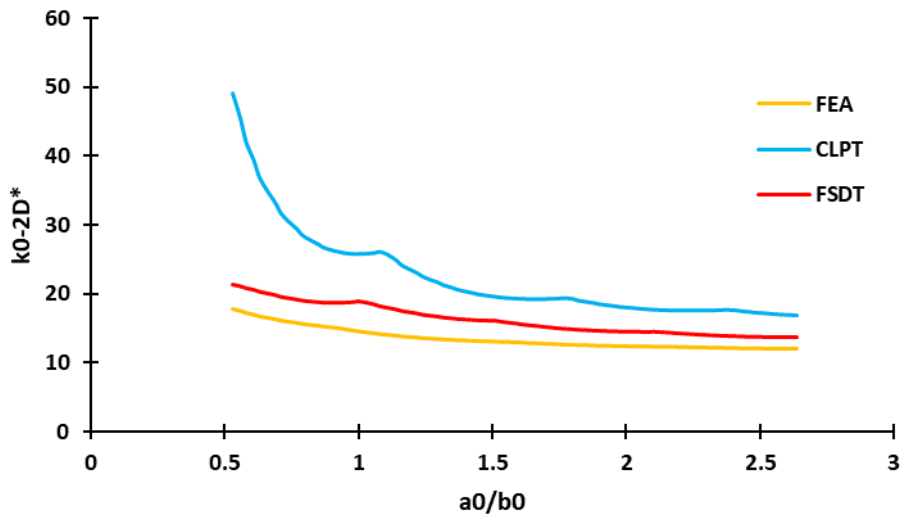


Figure 4.18: Compare of compressive buckling coefficients with all edges clamped (Ply orientation: $(0^\circ/0^\circ)_S$, thickness of plate=2.08 mm)

In Figure 4.19 and Figure 4.20, buckling coefficient curves obtained by each method are given for the clamped boundary condition and $(0^\circ/90^\circ)_S$ ply orientation.

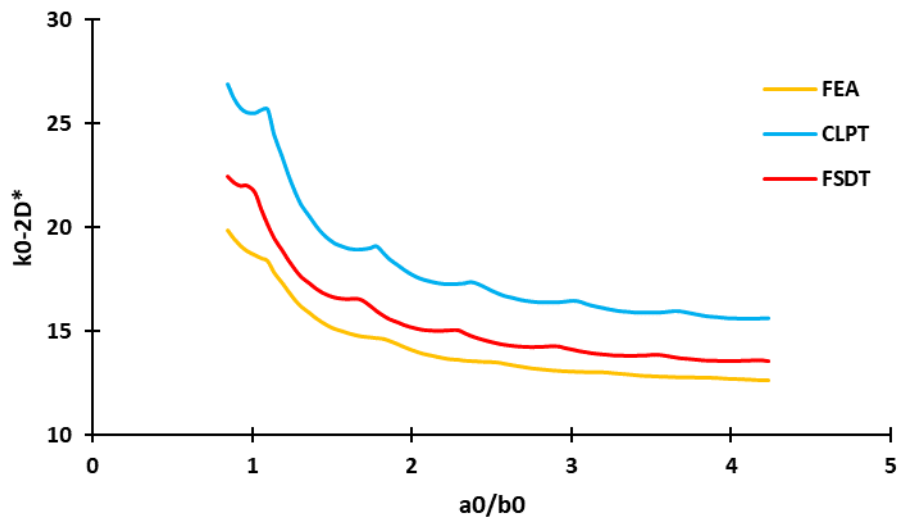


Figure 4.19: Compare of compressive buckling coefficients with all edges clamped (Ply orientation: $(0^\circ/90^\circ)_S$, thickness of plate=1.04 mm)

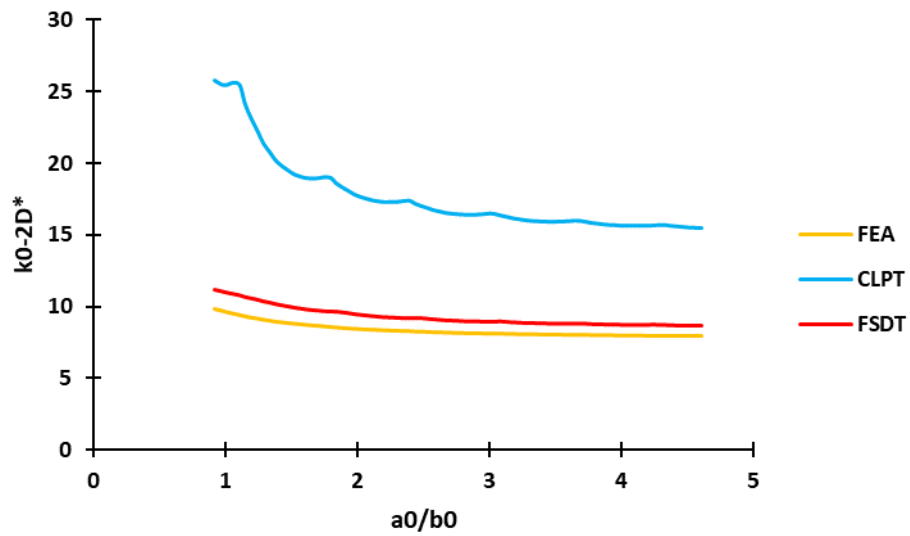


Figure 4.20: Compare of compressive buckling coefficients with all edges clamped (Ply orientation: $(0^\circ/90^\circ)_S$, thickness of plate=2.08 mm)

In Figure 4.21 and Figure 4.22 buckling coefficient curves obtained by each method are given for the clamped boundary condition and $(45^\circ/0^\circ/-45^\circ/90^\circ)_S$ ply orientation.

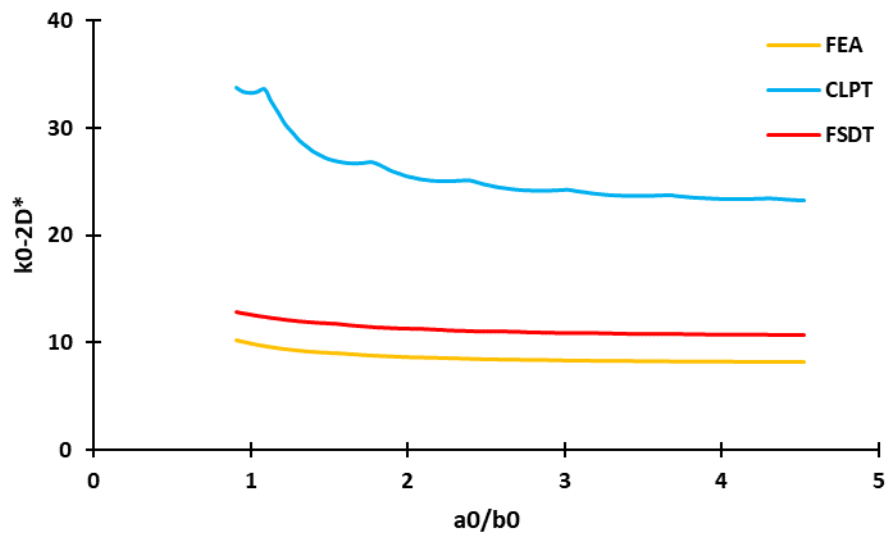


Figure 4.21: Compare of compressive buckling coefficients with all edges clamped (Ply orientation: $(45^\circ/0^\circ/-45^\circ/90^\circ)_S$, thickness of plate=2.08 mm)

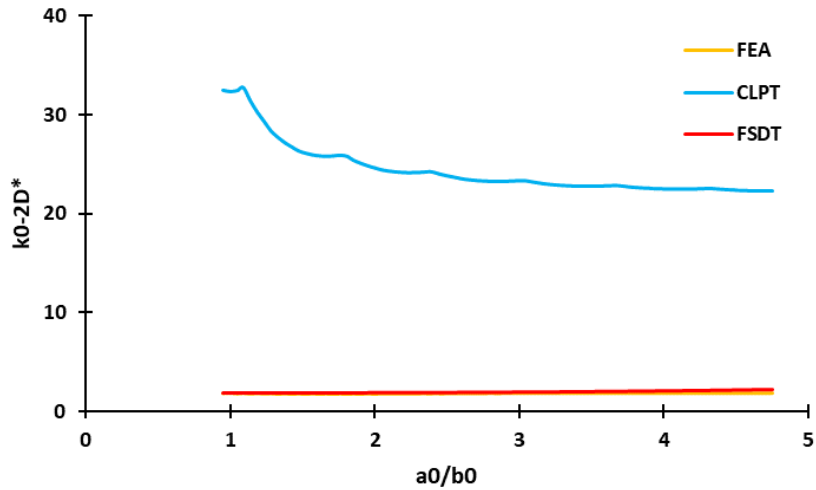


Figure 4.22: Compare of compressive buckling coefficients with all edges clamped (Ply orientation: $(45^\circ/0^\circ/-45^\circ/90^\circ)_S$, thickness of plate=4.16 mm)

In the Figure 4.23 and Figure 4.24, buckling coefficient curves obtained by finite element analysis for each ply orientation are given at the 2.08 mm plate thickness with all edges simply supported and clamped, respectively. To achieve the same plate thickness of 2.08 mm, for the $(0^\circ/0^\circ)_S$ and the $(0^\circ/90^\circ)_S$ ply orientations, 4 ply repeat is used whereas for the $(45^\circ/0^\circ/-45^\circ/90^\circ)_S$ ply orientation, 2 ply repeat is used.

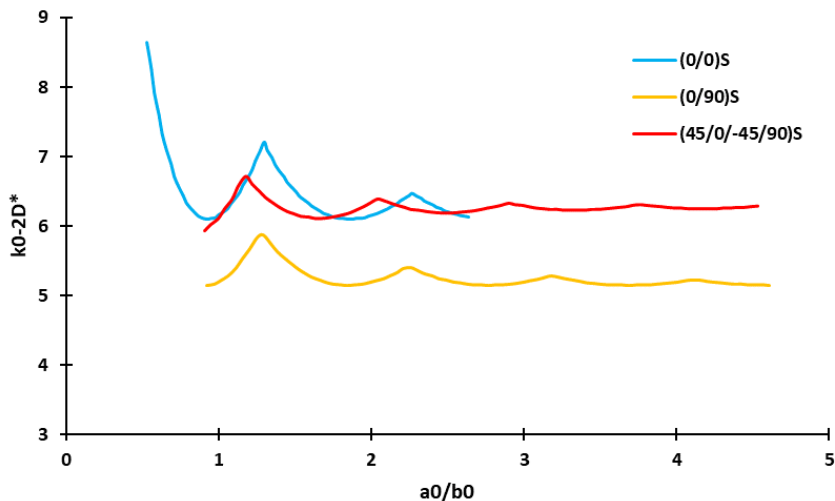


Figure 4.23: Compare of compressive buckling coefficients with all edges simply supported at the same plate thickness (2.08 mm)

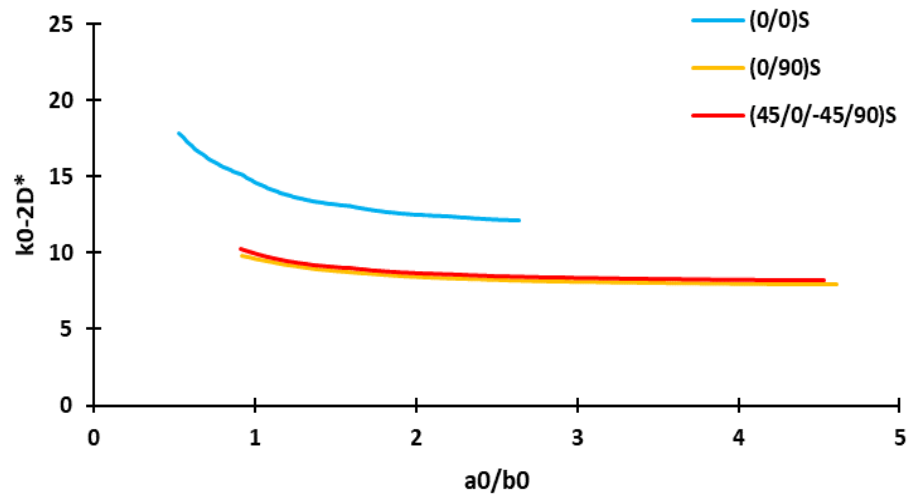


Figure 4.24: Compare of compressive buckling coefficients with all edges clamped at the same plate thickness (2.08 mm)

From the buckling coefficient curves presented, the following conclusions are inferred:

- Buckling coefficient curves obtained by the FSDT and FEA agree with each other considerably well for all laminate configurations and boundary conditions. For the clamped edge condition, results deviate slightly more compared to the simply supported edge condition. However, maximum difference between the FSDT and the FEA results is 3%.
- For composite plates with 0° ply angle, buckling coefficients obtained by the CLPT, FSDT and FEA agree with each other very well, especially for laminates with small thickness. As the thickness of the laminate increases, buckling coefficients obtained by the CLPT deviates from the FSDT and FEA results.
- For quasi-isotropic laminates having 0° , 90° and $\pm 45^\circ$ plies, the differences between the buckling coefficients determined by the finite element analysis and by the CLPT and FSDT increase. This could be due to the fact that the displacement forms assumed in the solutions performed by the CLPT and the FSDT may not represent the actual wave forms of the buckled state. Whereas, in finite element model, the actual buckled wave form can be predicted more

accurately since many elements are used in the finite element model as seen in Figure 4.25-Figure 4.27.

- For composite plates with 0° ply angle, pattern of buckling coefficient curve obtained by FEA is similar to pattern of metallic buckling curve.
- At the same plate thickness, for composite plates with all edges simply supported and 0° and 90° ply angles, buckling coefficient curve obtained by FEA is slightly different than the composite plate with 0° , $90^\circ \pm 45^\circ$ ply angles. However, patterns of these curves are similar to each other. Moreover, at the 2.08 mm plate thickness, for composite plates with all edges clamped and 0° and 90° plies, buckling coefficient results obtained by FEA is almost same as the results of composite plate with 0° , $90^\circ \pm 45^\circ$ plies.
- For thicker plates affine ratio of the plate is not effective on the buckling coefficient.

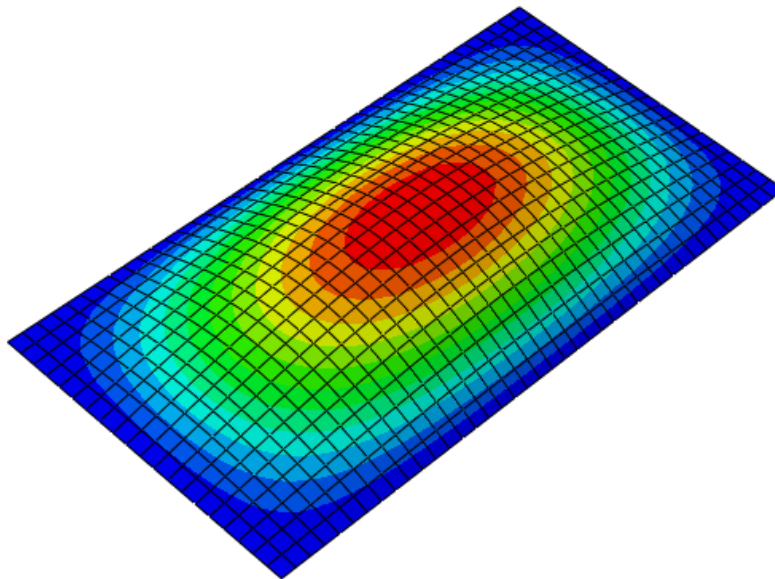


Figure 4.25: Example view of first buckled mode shape of plate with all edges simply supported (Ply orientation: $(0^\circ/0^\circ)_5$, thickness of plate=2.08 mm)

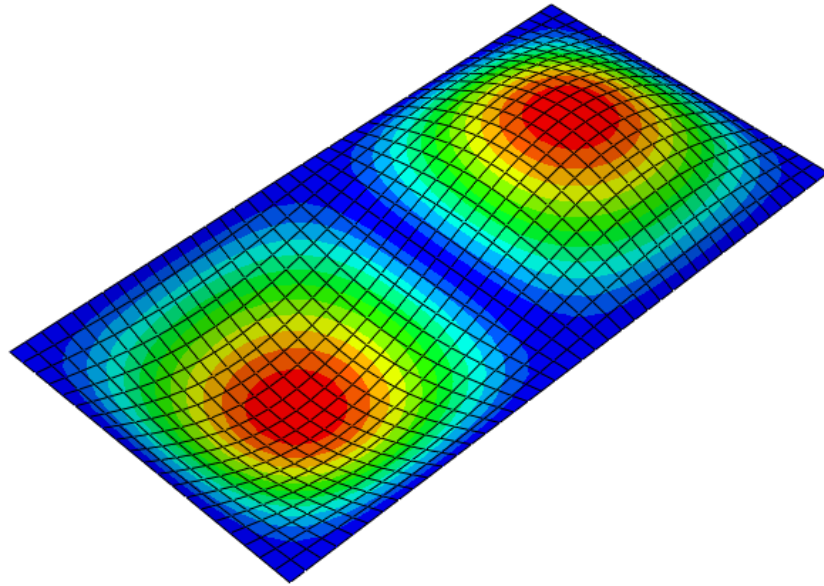


Figure 4.26: Example view of first buckled mode shape of plate with all edges simply supported (Ply orientation: $(0^\circ/90^\circ)_S$, thickness of plate=2.08 mm)

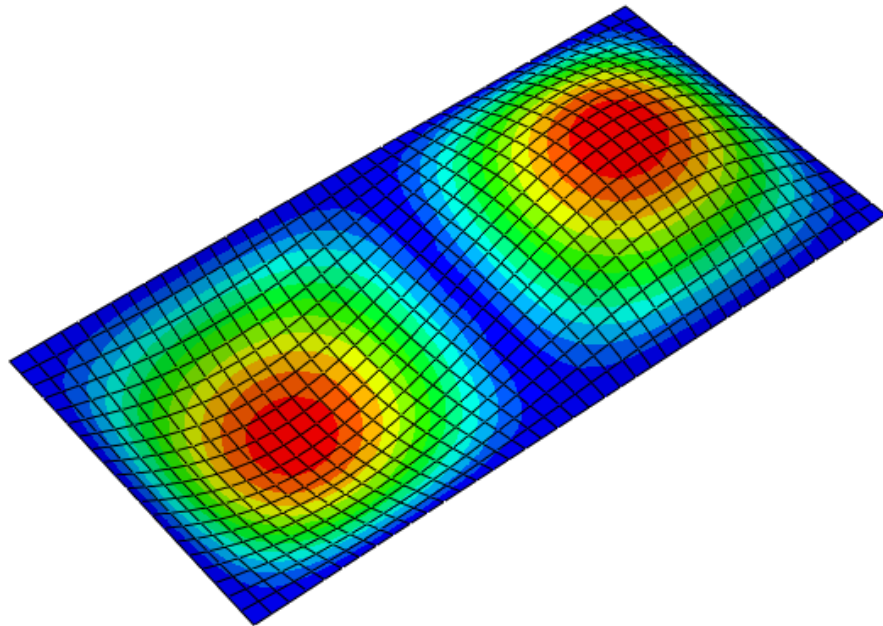


Figure 4.27: Example view of first buckled mode shape of plate with all edges simply supported (Ply orientation: $(45^\circ/0^\circ/-45^\circ/90^\circ)_S$, thickness of plate=2.08 mm)

CHAPTER 5

CONCLUSION AND FUTURE WORK

In Chapter 2, the effect of the boundary conditions on the buckling coefficients of stiffened flat panels is investigated by the finite element analysis. It is noted that depending on the restraint that the stringer along the unloaded edge of a skin-stringer panel provides, buckling coefficients obtained from finite element analysis may or may not agree with the buckling coefficients obtained by the analytical approach using the classical boundary conditions. For the skin-stringer assemblies with J, Z and T type stringers, buckling coefficients are determined by the finite element analyses for various combinations of the geometric properties of skin-stringer assemblies. Loaded edges of these assemblies are considered as clamped edge conditions. Finite element database for the buckling coefficients of skin-stringer assemblies for each stringer type is then processed to generate response surface (RS) and artificial neural network (ANN) approximations. Response surface and neural network approximations allow very fast determination of the buckling coefficients of skin-stringer assemblies for the selected stringer types provided that the geometric properties of the skin-stringer assembly are within the lower and upper limits of the geometric properties of the skin-stringer assemblies for which finite element analyses are conducted to generate the RS and train the ANN. To test the performance of the RS and the ANN generated, 10 additional random data sets are tested for each skin-stringer assembly with J, Z and T type stringer. It is seen that both the RS and the ANN methods give accurate buckling

coefficient results compared to the FEA results. For the skin-stringer assemblies with three stringer types, it is concluded that the ANN gives more accurate results compared to the RS. However, it is noted that ANN also has accuracy problems if the parameters of the ANN are not selected appropriately. To select the proper parameter set for the ANN, trial and error methodology is used. For instance, if the neuron number is lower than required neuron number, ANN gives inaccurate results. In addition, if the neuron number is higher than required neuron number, overfitting occurs in the ANN results. Therefore, required neuron number is decided with trial and error for each problem separately. Additionally, number of data sets is also very important in obtaining accurate ANN and RS. For the randomly selected 10 additional design sets, RMS values of the ANN are obtained as 0.0494, 0.0544, 0.0458 for the skin-stringer assemblies with J, Z and T type stringers, respectively. It is to be noted that buckling coefficients are in the range of 6-8 for the skin-stringer assemblies with J, Z and T type stringers. It is seen that for the 10 additional analyses for each stringer type, root mean square errors are very small compared to the magnitude of the buckling coefficients. This shows that ANN approximation produces very accurate buckling coefficients and it is deemed that such a fast and accurate approximate solver for the buckling coefficients based on ANN can be effectively used within the framework of optimization of skin-stringer assemblies.

In chapter 3, a comparative study on the post-buckling load redistribution in stiffened aircraft panels modeled with and without material nonlinearity is presented. For this purpose, a baseline stiffened panel is generated for the investigation of the material nonlinearity on the post-buckling behavior and on the effective width of the stiffened panel. To make a direct comparison with the classical empirical approach for the determination of the effective width of the skin panel, a stiffener section which provides classical clamped edge condition is designed by matching the compression buckling coefficient determined by the finite element analysis to the buckling coefficient of the panel with the classical clamped edge boundary condition. Post-buckling analysis of the skin-stringer assembly is performed utilizing linear and nonlinear material models in the finite element analysis to study the effect of material plasticity on the post-buckling behavior of the skin-stringer assembly.

Results are presented on the post-buckling behavior of skin-stringer assemblies with linear and nonlinear material properties in the finite element model for I, J and Z stringer shapes for the same panel dimensions. Load distributions obtained by the finite element analysis performed by the linear and nonlinear material models in the post-buckled stage revealed that for the skin-stringer assembly with the nonlinear material model, the peak load is significantly lower than the peak load for the linear material model case. Effective widths calculated by the finite element based analysis by employing nonlinear material property are higher than the effective widths calculated by employing linear material property. Since the peak loads drop when nonlinear material property is used in the finite element analysis, the increase in the effective width is considered to be reasonable. If the effective widths calculated by the finite element analysis employing finite element analysis with nonlinear material properties are taken as reference, for the skin stringer assemblies studied, classical effective width formula underestimates the effective widths between 20%-30% except assembly with Z_2 stringer section.

Effective widths calculated by the finite element based analysis by employing linear material property agree better with the effective widths calculated by the classical empirical approach of Bruhn compared to the effective widths calculated by the finite element based analysis by employing nonlinear material property. As an alternative method, effective widths are also calculated utilizing the stringer stresses determined by the finite element analysis at the point of collapse in the classical effective width formula. It is concluded that for skin stringer assemblies with double row fasteners, effective widths calculated by substituting the stringer stresses at the collapse point calculated by the finite element analysis in the classical empirical effective width formula match well with the effective widths calculated by the classical empirical effective width formula alone. Results of the present analysis also showed that the classical effective width formula gives reasonable results which are comparable with the finite element based analysis results.

In the chapter 4, generic compressive buckling curves of composite plates with different ply orientations are obtained using three different methods. These methods

are chosen as the CLPT, FSDT and FEM. To use the CLPT and FSDT methods, mathematical formulations are shown step by step in sections 4.1 and 4.2. Both simply supported and clamped edge conditions are investigated using the three methods. CLPT is chosen because it is the simplest method to determine the critical buckling load. However, the accuracy of the method is not good when the complexity of the ply orientations is increased. As the second mathematical method, FSDT is decided because this method gives the more accurate results compared to CLPT. In the FSDT, out-of-plane shear deformation is also included. Thus, results of FSDT are more accurate than the CLPT when compared to the finite element method. As the third and most realistic method, finite element modelling is chosen to calculate buckling load.

In this study, specific parameters are used to obtain the generic buckling coefficient curves. These parameters are the modified buckling coefficient and the plate's affine ratio. Using these parameters, generic buckling curves for balanced orthotropic rectangular plates are obtained for three different ply orientation configurations. These orientations are decided according to use in the aviation industry. These three methods are applied and buckling coefficient results are obtained for various plates thicknesses, affine ratios and boundary conditions using a Python script.

Generic buckling coefficient curves are obtained for both simply supported and clamped edge conditions. As expected, clamped edge results are higher than the simply supported cases. Moreover, for each ply orientation configuration, buckling curves are obtained. For the quasi-isotropic plates the effect of the skin thickness is higher on the buckling coefficients compared to the other configurations. In addition, the effect of the plate's affine ratio is not significant in thicker plates. Based on the results obtained for the composite buckling analysis, it is seen that the buckling coefficient curves obtained by the FSDT and the FEA agree with each other considerably well for all laminate configurations and boundary conditions. For the clamped edge condition, results deviate slightly more compared to the simply supported edge condition. However, maximum difference between the FSDT and the FEA results is 3%.

As for the future work, the experimental investigation of the post-buckling phenomenon is deemed to be the most important item. Determination of the post-

buckling load distribution experimentally is considered to be a worthwhile study to conduct as the future study.

REFERENCES

- [1] Bruhn, E. F. (1973). *Analysis and design of flight vehicle structures*. Indianapolis: Jacobs Pub.
- [2] Paul, A., & George, S. P. (2014, October). Buckling analysis of wing upper skin panels of a transport aircraft. *International Journal of Science, Engineering and Technology Research*, 3(10), 2868-2872.
- [3] Gerard, G., & Becker, H. (1957). *Handbook of structural stability. Pt. 3. Buckling of curved plates and shells*. Washington: NACA.
- [4] Timoshenko, S. P., & Gere, J. M. (1961). *Theory of elastic stability*. New York: McGraw-Hill Book.
- [5] Bulson, P. (1970). *The stability of flat plates*. London: Chatto & Windus.
- [6] Niu, M. C. (2011). *Airframe structural design: practical design information and data on aircraft structures*. Hong Kong: Conmilit Press.
- [7] Yu, C. (2003). *Buckling of rectangular plates under intermediate and end loads*. MS Thesis, National university of singapore, Department of civil engineering, Singapore.
- [8] Muameleci, M. (2014). *Linear and nonlinear buckling analyses of plates using finite element method*. MS Thesis, Linköping university, Department of management and engineering, Linköping,.

- [9] Riks, E. (2000). Buckling and post-buckling analysis of stiffened panels in wing box structures. *International Journal of Solids and Structures*, 37(46-47), 6795-6824. doi:10.1016/s0020-7683(99)00315-7
- [10] Tripp, L. L., Tamekuni, M., & Viswanathan, A. V. (1973). *A computer program for stresses and buckling of heated composite stiffened panels and other structures*. Washington: NASA.
- [11] Wittrick, W. H., & Williams, F. W. (1974, April). Buckling and vibration of anisotropic or isotropic plate assemblies under combined loadings. *International Journal of Mechanical Sciences*, 16(4), 209-239. doi:10.1016/0020-7403(74)90069-1
- [12] Murphy, A., Price, M., Gibson, A., & Armstrong, C. (2004). Efficient non-linear idealisations of aircraft fuselage panels in compression. *Finite Elements in Analysis and Design*, 40(13-14), 1977-1993. doi:10.1016/j.finel.2003.11.009
- [13] Lynch, C. J., & Sterling, S. (1998). A finite element study of the postbuckling behaviour of a flat stiffened panel. *21st Congress of International Council of the Aeronautical Sciences*, 1-10.
- [14] Weimin, S., Mingbo, T., Liang, G., & Dengke, D. (2008). Post-buckling simulation of an integral aluminum fuselage panel subjected to axial compression load. *2008 Asia Simulation Conference - 7th International Conference on System Simulation and Scientific Computing*, 893-897. doi:10.1109/asc-icsc.2008.4675489
- [15] Rhodes, J. (2002). Buckling of thin plates and members and early work on rectangular tubes. *Thin-Walled Structures*, 40(2), 87-108. doi:10.1016/s0263-8231(01)00054-4
- [16] Byklum, E., Steen, E., & Amdahl, J. (2004). A semi analytical model for global buckling and postbuckling analysis of stiffened panels. *Thin-Walled Structures*, 42(5), 701-171. doi:10.1016/j.tws.2003.12.006

- [17] Kopecki, T., & Świąch, Ł. (2014). Experimental and numerical analysis of post-buckling deformation states of integrally stiffened thin-walled components of load-bearing aircraft structures. *Journal of Theoretical and Applied Mechanics*, 52(4), 905-915. doi:10.15632/jtam-pl.52.4.905
- [18] Graciano, C., Casanova, E., & Martínez, J. (2011). Imperfection sensitivity of plate girder webs subjected to patch loading. *Journal of Constructional Steel Research*, 67(7), 1128-1133. doi:10.1016/j.jcsr.2011.02.006
- [19] Mert, M., & Kayran, A. (2016). Post buckling load redistribution of stiffened panels in aircraft wingbox structures. *57th AIAA/ASCE/AHS/ASC Structures, Structural Dynamics, and Materials Conference*, 1-12. doi:10.2514/6.2016-1974
- [20] Bedair, O. (2009). Analytical effective width equations for limit state design of thin plates under non-homogeneous in-plane loading. *Archive of Applied Mechanics*, 79(12), 1173-1189. doi:10.1007/s00419-009-0296-z
- [21] Dannemann, R. W. (1990). Effective width in elastic postbuckling of thin flanges. *International Specialty Conference on Cold-Formed Steel Structures*, 281-297.
- [22] Winter, G. (1947). *Strength of thin steel compression flanges*. Ithaca, NY: Cornell University.
- [23] Sheidaii, M. R., & Bahraminejad, R. (2012). Evaluation of compression member buckling and post-buckling behavior using artificial neural network. *Journal of Constructional Steel Research*, 70, 71-77. doi:10.1016/j.jcsr.2011.10.020
- [24] Yildirim, A., Akay, A. A., Gulasik, H., Coker, D., Gurses, E., & Kayran, A. (2015). Development of bolted flange design tool based on finite element analysis and artificial neural network. *Volume 9: Mechanics of Solids, Structures and Fluids*. doi:10.1115/imece2015-51021
- [25] Gomes, H. M., Awruch, A. M., & Lopes, P. A. (2011). Reliability based optimization of laminated composite structures using genetic algorithms and

- artificial neural networks. *Structural Safety*, 33(3), 186-195.
doi:10.1016/j.strusafe.2011.03.001
- [26] Gajewski, J., Golewski, P., & Sadowski, T. (2017). Geometry optimization of a thin-walled element for an air structure using hybrid system integrating artificial neural network and finite element method. *Composite Structures*, 159, 589-599. doi:10.1016/j.compstruct.2016.10.007
- [27] Sadovský, Z., & Soares, C. G. (2011). Artificial neural network model of the strength of thin rectangular plates with weld induced initial imperfections. *Reliability Engineering & System Safety*, 96(3), 713-717. doi:10.1016/j.ress.2011.02.010
- [28] Lanzi, L., & Giavotto, V. (2006). Post-buckling optimization of composite stiffened panels: Computations and experiments. *Composite Structures*, 73(2), 208-220. doi:10.1016/j.compstruct.2005.11.047
- [29] Mallela, U. K., & Upadhyay, A. (2016). Buckling load prediction of laminated composite stiffened panels subjected to in-plane shear using artificial neural networks. *Thin-Walled Structures*, 102, 158-164. doi:10.1016/j.tws.2016.01.025
- [30] Cankur, A. (2017). *Development of an artificial neural network based analysis method for skin-stringer structures*. Aerospace Engineering. Ankara: Middle East Technical University.
- [31] Yang, Q. J. (2009). *Simplified approaches to buckling of composite plates*. Faculty of Mathematics and Natural Science. Oslo: University of Oslo.
- [32] Masood, S. N., Viswamurthy, S. R., Gaddikeri, K. M., & Singh, A. K. (2014). Buckling and postbuckling of cocured composite stiffened panel under axial compression load. *Conference: National Seminar on Aerospace Structures (NASAS-18)*, 1-8.

- [33] Abramovich, H., & Weller, T. (2009). Buckling and postbuckling behavior of laminated composite stringer stiffened curved panels under axial compression: Experiments and design guidelines. *Journal of Mechanics of Materials and Structures*, 4(7-8), 1187-1207. doi:10.2140/jomms.2009.4.1187
- [34] Möcker, T., Linde, P., Kraschin, S., Goetz, F., Marsolek, J., & Wohlers, W. (2009). *Abaqus Fem analysis of the postbuckling behaviour of composite shell structures*. Hamburg: Institute of Composite Structures and Adaptive Systems.
- [35] Dassault Systèmes. (2014). *Abaqus Analysis User's Manuel*. Retrieved from Dassault Systèmes: Abaqus Version 6.14
- [36] Federal Aviation Administration. (2013). MMPDS-08: Metallic Materials Properties Development and Standardization. Washington, D.C.
- [37] MathWorks. (2016). *MATLAB 2016 Help*. Retrieved from MathWorks: MATLAB 2016 Help
- [38] Beale, M., Hagan, M., & Demuth, H. (1992). *Neural Network Toolbox: For Use with MATLAB;[User's Guide]*. MathWorks.
- [39] Rasmussen, K., Tim, B., & Bezkorovainy, P. (2002). *Strength Curves for Metal Plates in Compression, Research Report No R821*. The University of Sydney Department of Civil Engineering.
- [40] Spaink, A. (1999). *HSB 53211-01 Compressive strength of short metallic sections(crippling)*. Hamburg: Industrie Ausschuss Struktur Berechnungsunterlagen.
- [41] Reddy, J. (1997). *Mechanics of Laminated Composite Plates - Theory and Analysis* (1 ed.). USA: CRC Press.
- [42] Agarwal, B. D., Broutman, L. J., & Chandrashekhara, K. (2006). *Analysis and Performance of Fiber Composites* (3 ed.). USA: Wiley.

- [43] Reddy, J. (2004). *Mechanics of Laminated Composite Plates and Shells* (2 ed.). Texas, USA: CRC Press.
- [44] Geir, S. (2007). *Forelesningsnotat i MEK4560 Elementmetoden i Faststoffmekanikk*. Oslo: UiO.
- [45] Hayman, B. (2008). *Forelesningsnotat i MEK4540 Komposittmaterialer og -konstruksjoner*. Oslo: UiO.
- [46] Zenkert, D. (2005). *An Introduction to Sandwich Structures* (Student ed.). Stockholm.
- [47] Brunelle, E., & Oyibo, G. (1983). Generic Buckling Curves for Specially Orthotropic Rectangular Plates The Institute of Aeronautics and Astronautics. *AIAA*, 21(8), 1150-1156.
- [48] Hayman, B., Berggreen, C., Lundsgaard-Larsen, C., Delarche, A., Toftegaard, H., Dow, R., . . . Douka, C. (2009). *Studies of The Buckling of Composite Plates in Compression*. Norway-Denmark-UK-Greece: MARSTUCT.
- [49] Jensen, C. (2006). *Defects in FRP Panels and their Influence on Compressive Strength*. MS Thesis, Denmark.
- [50] Zenkert, D., & Battley, M. (2009). *Laminate and Sandwich Structures: Foundations of Fibre Composites* (2 ed.). Lyngby, Denmark: Polyteknisk Forlag.
- [51] Hexcel. (2016). *Resources/Data Sheets/Prepreg/8552/EU Version*. Retrieved from Hexcel Corporation: http://www.hexcel.com/user_area/content_media/raw/HexPly_8552_eu_Data_Sheet.pdf

APPENDIX A

PROCEDURE OF LINEAR BUCKLING ANALYSIS

In ABAQUS, the procedure of linear buckling analysis is explained in this Appendix [35]. To obtain the critical buckling load in FEA, singular stiffness matrix has to be solved. In an eigenvalue buckling problem, loads are sought for which the model stiffness matrix becomes singular, so that the problem has nontrivial solutions, as shown in Equation (A.1),

$$K^{MN} * v^M = 0 \quad (\text{A.1})$$

where K^{MN} is the tangent stiffness matrix when the loads are applied, and the v^M is the nontrivial displacement solution vector. The applied loads can consist of distributed loads, pressures, concentrated forces, nonzero prescribed displacements.

The buckling loads are calculated relative to the base state of the structure. If the eigenvalue buckling procedure is the first step in an analysis, the initial conditions form the base state; otherwise, the base state is the current state of the model at the end of the last general analysis step. Thus, the base state can include preloads (“dead” loads), P^N . The preloads are often zero in classical eigenvalue buckling problems. If geometric nonlinearity is omitted, the base state geometry is the original configuration of the body. An incremental loading pattern, Q^N is defined in the eigenvalue buckling

prediction step. The magnitude of this loading is not important; it will be scaled by the load multipliers, λ_i found in the eigenvalue problem:

$$(K_0^{NM} + \lambda_i * K_{\Delta}^{NM}) * v_i^M = 0 \quad (\text{A.2})$$

where

K_0^{NM} is the stiffness matrix corresponding to the base state, which includes the effects of the preloads, P^N (if any);

K_{Δ}^{NM} is the differential initial stress and load stiffness matrix due to the incremental loading pattern, Q^N ;

λ_i are the eigenvalues;

v_i^M are the buckling mode shapes (eigenvectors);

M and N refer to degrees of freedom M and N of the whole model; and

“i” refers to the i’th buckling mode.

The critical buckling loads are then given by $P^N + \lambda_i Q^N$. Normally, the lowest value of λ_i is of interest.

The buckling mode shapes, v_i^M , are normalized vectors and do not represent actual magnitudes of deformation at the critical load. They are normalized so that the maximum displacement component is 1.0.

ABAQUS can extract eigenvalues and eigenvectors for symmetric matrices only; therefore, K_0^{NM} and K_{Δ}^{NM} are symmetrized. If the matrices have significant unsymmetrical parts, the eigenvalue problem may not be exactly what you expected to solve.

APPENDIX B

MATERIAL PROPERTIES ALUMINUM 2024 T3 CLAD SHEET

Specification	AMS 4037 and AMS-QQ-A-250/4*				
Form	Sheet				
Temper	T3				
Thickness, in.	0.008-0.009	0.010-0.128		0.129 - 0.249	
Basis	S	A	B	A	B
Mechanical Properties:					
F_u , ksi:					
L	64	64	65	64	66
LT	63	63	64	63	65
ST
F_y , ksi:					
L	47	47	48	47	48
LT	42	42	43	42	43
ST
$F_{0.2}$, ksi:					
L	39	39	40	39	40
LT	45	45	46	45	46
ST
$F_{0.01}$, ksi:					
L	39	39	40	40	41
$F_{0.005}$, ksi:					
(e/D = 1.5)	104	104	106	106	107
(e/D = 2.0)	129	129	131	131	133
$F_{0.002}$, ksi:					
(e/D = 1.5)	73	73	75	73	75
(e/D = 2.0)	88	88	90	88	90
e , percent:					
LT	10	<i>d</i>	...	<i>d</i>	...
E , 10^3 ksi					
	10.5				
E_c , 10^3 ksi					
	10.7				
G , 10^3 ksi					
	4.0				
μ					
	0.33				
Physical Properties:					
ω , lb/in. ³	0.100				
C , K , and α					

Figure B.1: Material properties of aluminum 2024 T3 clad sheet [36]

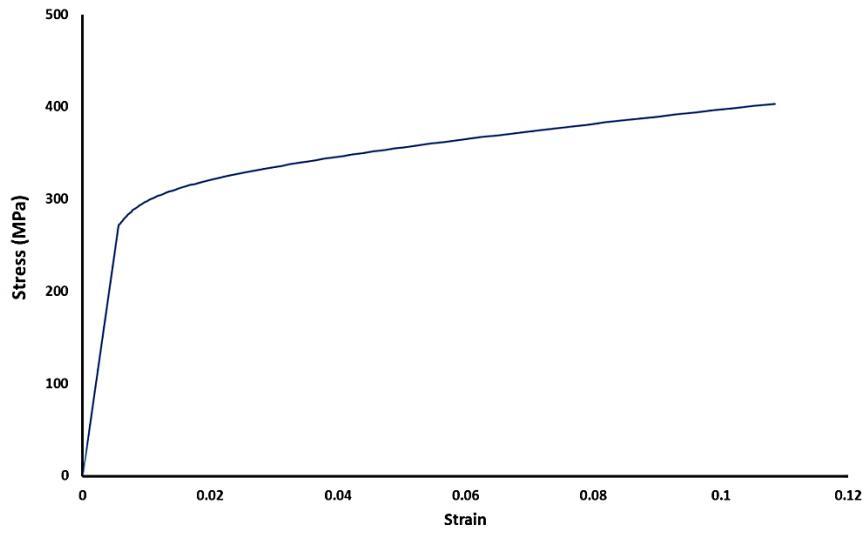


Figure B.2: True stress-strain graph of Aluminum 2024 T3 clad sheet [36] [39]

Table B.1: True stress-strain data of Aluminum 2024 T3 clad sheet [36] [39]

Stress (MPa)	Strain	Stress (MPa)	Strain	Stress (MPa)	Strain
250.45	0	300.89	0.017364	384.92	0.121213
251.49	0.000119	302.22	0.018369	387.59	0.125193
252.52	0.000239	303.56	0.019417	390.31	0.129257
253.56	0.000361	304.92	0.020511	393.09	0.133405
254.60	0.000484	306.30	0.021651	395.91	0.137636
255.64	0.000609	307.69	0.022839	398.78	0.141951
256.68	0.000737	309.10	0.024075	401.70	0.146351
257.72	0.000869	310.53	0.025361	404.68	0.150835
258.76	0.001005	311.98	0.026698	407.70	0.155404
259.80	0.001146	313.45	0.028087	410.79	0.160059
260.85	0.001293	314.94	0.029529	413.92	0.164798
261.89	0.001447	316.44	0.031026	417.12	0.169623
262.94	0.001608	317.98	0.032578	420.37	0.174533
264.00	0.001777	319.53	0.034186	423.68	0.179528
265.05	0.001956	321.10	0.035851	427.04	0.184609
266.11	0.002144	322.70	0.037575	430.47	0.189775

Table B.2 Continued

Stress (MPa)	Strain	Stress (MPa)	Strain	Stress (MPa)	Strain
267.17	0.002343	324.32	0.039359	433.96	0.195027
268.23	0.002554	325.97	0.041204	437.51	0.200364
269.30	0.002778	327.64	0.04311	441.13	0.205786
270.38	0.003015	329.34	0.045079	444.81	0.211293
271.45	0.003267	331.07	0.047111	448.55	0.216885
272.54	0.003535	332.82	0.049209	452.36	0.222562
273.62	0.003819	334.60	0.051372	456.24	0.228323
274.71	0.004121	336.40	0.053602	460.18	0.234168
275.81	0.004441	338.24	0.055899	464.20	0.240097
276.92	0.004781	340.11	0.058265	468.28	0.24611
278.03	0.005141	342.01	0.0607	472.44	0.252206
279.15	0.005524	343.94	0.063205	476.67	0.258385
280.27	0.005929	345.90	0.065782	480.98	0.264646
281.40	0.006358	347.89	0.068431	485.36	0.27099
282.54	0.006812	349.92	0.071153	489.81	0.277415
283.69	0.007292	351.98	0.073948	494.35	0.283921
284.85	0.007798	354.08	0.076818	498.96	0.290508
286.02	0.008334	356.21	0.079763	503.65	0.297175
287.19	0.008898	358.39	0.082784	508.42	0.303922
288.38	0.009493	360.59	0.085881	513.28	0.310747
289.58	0.010119	362.84	0.089056	518.21	0.317651
290.78	0.010779	365.12	0.092309	523.24	0.324633
292.00	0.011471	367.45	0.095641	528.34	0.331691
293.23	0.012199	369.82	0.099052	533.54	0.338827
294.48	0.012963	372.22	0.102543	538.82	0.346038
295.73	0.013764	374.67	0.106114	544.19	0.353324
297.00	0.014604	377.17	0.109766	549.66	0.360684
298.28	0.015483	379.70	0.113499	555.21	0.368118
299.58	0.016403	382.29	0.117315	560.86	0.375625

APPENDIX C

LOCAL BUCKLING STRINGERS IN SKIN-STIFFENER ASSEMBLIES

Local buckling of stiffeners is checked according to the method presented in Bruhn [1]. Cross-section of the stiffener is divided into rectangular elements and critical stress for each of these elements is calculated as follows:

$$k_c^* = \frac{k_c * \pi^2}{12 * (1 - \nu^2)} \quad (C.1)$$

$$F_{lb_i} = k_c^* * E * \left(\frac{t_i}{b_i}\right)^2 \quad (C.2)$$

where the index i represents the section element, and k_c^* is the modified buckling coefficient and for elements supported at one side and simply supported loaded edges k_c^* values are obtained by averaging case 5 ($k_c = 0.406, k_c^* = 0.367$) and case 4 ($k_c = 1.25, k_c^* = 1.12$) in Figure C.1. Similarly, for elements supported at both sides, k_c^* is defined as average k_c^* values of case 3 ($k_c = 4.0, k_c^* = 3.61$) and case 1 ($k_c = 6.97, k_c^* = 6.3$) in Figure C.1.

After calculating the buckling allowable of each section element, the minimum value is determined as the local buckling allowable of the whole section.

$$F_{lb} = \min(F_{lb_i}) \quad (C.3)$$

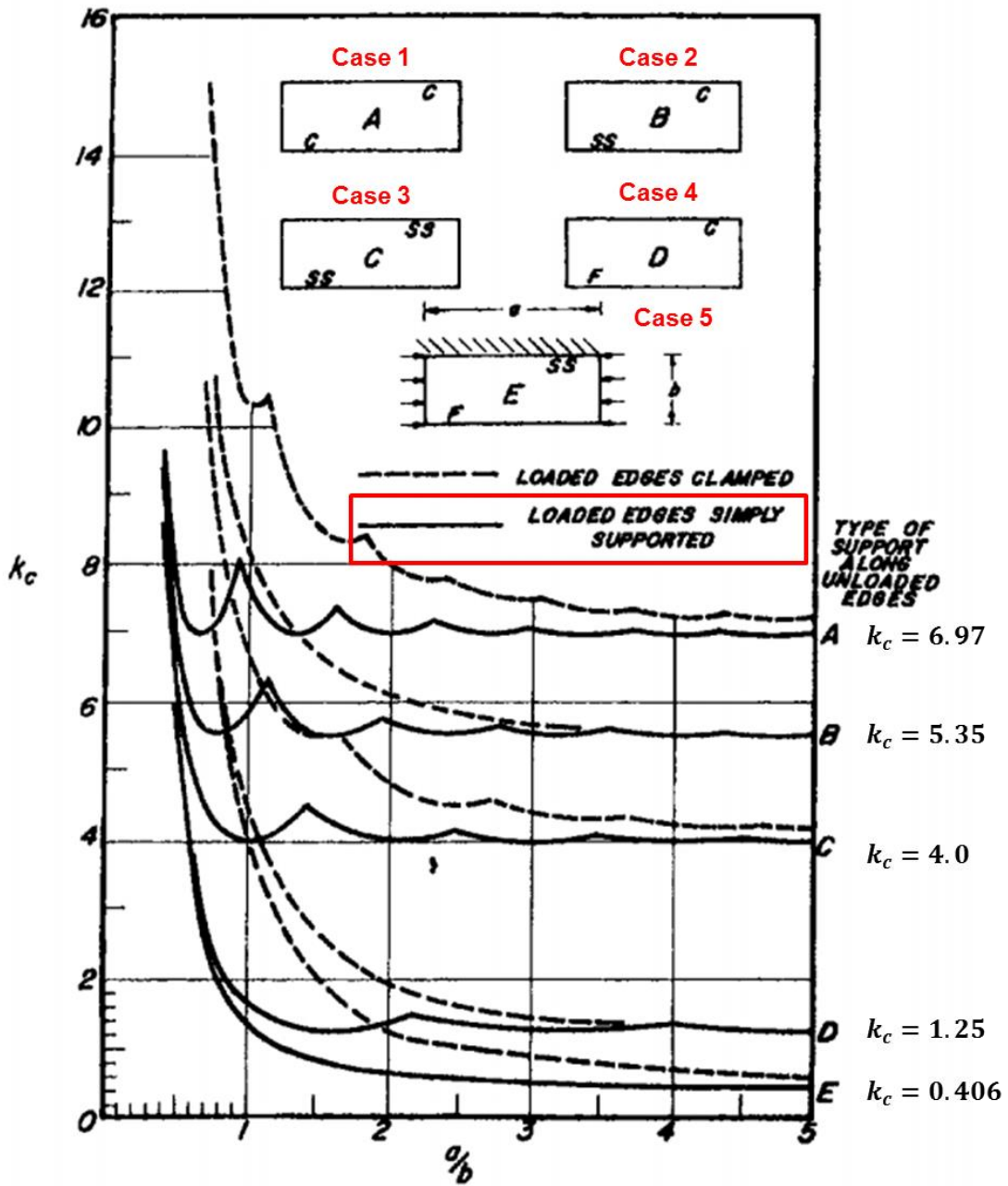


Figure C.1: Buckling factors for several edge conditions [1]

APPENDIX D

ELASTIC COEFFICIENT AND COMPLIANCE MATRICES AND GOVERNING EQUILIBRIUM EQUATIONS OF COMPOSITE PLATES

D.1 Elastic Coefficient and Compliance Matrices of Composite Plates

For the first method, CLPT, stiffness matrices are obtained as seen in Equations (D.5), (D.6) and (D.7). To do that, firstly, compliance matrix is obtained as Equation (D.1). [S] is known as the compliance tensor. It should be evident that the compliance tensor has the same symmetric properties as the elastic tensor [E] and same type of transformation law. The number of independent components of compliance tensor can be reduced in manner similar to elasticity tensor. At the end, compliance matrix for an orthotropic material for the two dimensional case is obtained as [42]:

$$[S] = \begin{bmatrix} \frac{1}{E_1} & -\frac{\nu_{21}}{E_2} & 0 \\ -\frac{\nu_{12}}{E_1} & \frac{1}{E_2} & 0 \\ 0 & 0 & \frac{1}{G_{12}} \end{bmatrix} \quad (D.1)$$

Transformation matrix is found following equation [42]:

$$[T] = \begin{bmatrix} \cos^2 \theta & \sin^2 \theta & 2 \sin \theta \cos \theta \\ \sin^2 \theta & \cos^2 \theta & -2 \sin \theta \cos \theta \\ -\sin \theta \cos \theta & \sin \theta \cos \theta & \cos^2 \theta - \sin^2 \theta \end{bmatrix} \quad (D.2)$$

Where θ is the fiber orientation angle.

Stiffness matrix of composite plate is calculated as [42]:

$$[Q] = [S]^{-1} \quad (D.3)$$

$$[\bar{Q}] = [T]^{-1}[Q][T] \quad (D.4)$$

Elements of the Extensional stiffness matrix which is defined as “A” is calculated the following way [42]:

$$A_{ij} = \sum_{k=1}^n (\bar{Q}_{ij})_k (h_k - h_{k-1}) \quad (D.5)$$

In addition, elements of the coupling stiffness matrix, “B”, is obtained as [42]:

$$B_{ij} = \frac{1}{2} \sum_{k=1}^n (\bar{Q}_{ij})_k (h_k^2 - h_{k-1}^2) \quad (D.6)$$

Moreover, elements of the bending stiffness matrix, “D”, are given as [42]:

$$D_{ij} = \frac{1}{3} \sum_{k=1}^n (\bar{Q}_{ij})_k (h_k^3 - h_{k-1}^3) \quad (D.7)$$

Where $i = 1,2,3$ and $j = 1,2,3$. “ h_k ” is the vertical distance from mid-plane of the plate ($z=0$) to the upper surface of the k^{th} lamina (layer) as seen in Figure D.1 .

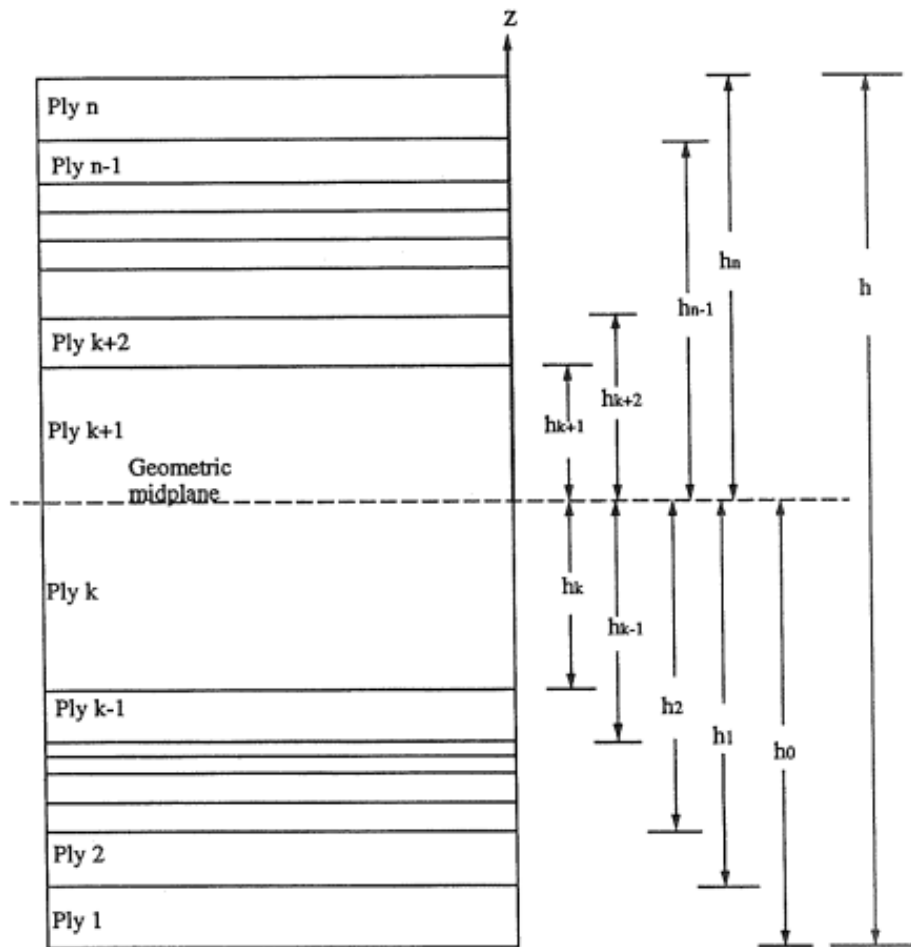


Figure D.1: Cross section view of a laminate

For the second method, FSDT, plane shear term has to be added into the formulation. Shear correction factor is used in the determination of the transverse shear stiffness matrix. Shear correction factor is obtained from Table D.1.

Table D.1: Typical shear correction coefficient [49]

Material Type	Homogeneous	Composite	Sandwich
Shear Correction Factor	5/6	5/6	1

Transverse shear stiffness matrix of a ply is given by [43]:

$$[Q]_{shr} = \begin{bmatrix} G_{23} & 0 \\ 0 & G_{13} \end{bmatrix} \quad (D.8)$$

Transformation matrix for shear part is obtained as [43]:

$$[T]_{shr} = \begin{bmatrix} \cos \theta & -\sin \theta \\ \sin \theta & \cos \theta \end{bmatrix} \quad (D.9)$$

Transformed transverse shear stiffness matrix for a ply is calculated as [42]:

$$[\bar{Q}]_{shr} = [T]_{shr}^{-1} [Q]_{shr} [T]_{shr} \quad (D.10)$$

Finally, transverse shear stiffness matrix for the laminate is obtained as [43]:

$$(A_{ij})_{shr} = k_{shr} \sum_{k=1}^n ((\bar{Q}_{ij})_k)_{shr} (h_k - h_{k-1}) \quad (D.11)$$

Where $i = 4,5$ and $j = 4,5$.

D.2 Governing Equations of Composite Plates

Figure D.2 and Figure D.3 show the infinitesimally small elements with the resultant forces and moments to obtain the force and moment equivalence equations in the composite plate buckling. For equilibrium, resultant forces and moments are zero.

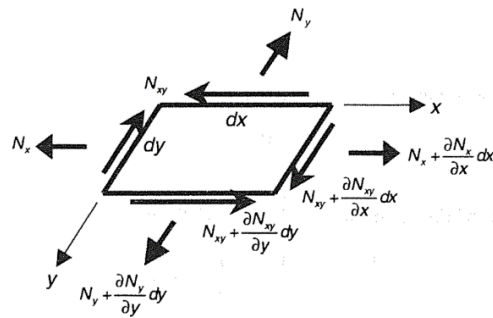


Figure D.2: A differential element with in-plane force resultants [42]

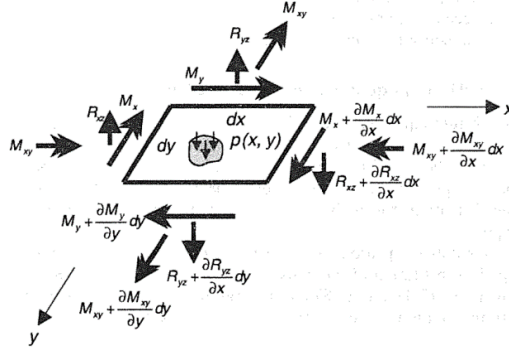


Figure D.3: A differential element with moment resultants, shear force resultants and applied transverse forces [42]

Equilibrium of forces in the x direction according to Figure D.2 is obtained as:

$$\begin{aligned}
 -N_x dy + \left(N_x + \frac{\partial N_x}{\partial x} dx \right) dy - N_{xy} dx + \left(N_{xy} + \frac{\partial N_{xy}}{\partial y} dy \right) dx &= 0 \\
 \Rightarrow \frac{\partial N_x}{\partial x} + \frac{\partial N_{xy}}{\partial y} &= 0
 \end{aligned} \tag{D.12}$$

Equilibrium of forces in the y direction according to Figure D.2 is obtained as:

$$\begin{aligned}
 -N_y dx + \left(N_y + \frac{\partial N_y}{\partial y} dy \right) dx - N_{xy} dy + \left(N_{xy} + \frac{\partial N_{xy}}{\partial x} dx \right) dy &= 0 \\
 \Rightarrow \frac{\partial N_y}{\partial y} + \frac{\partial N_{xy}}{\partial x} &= 0
 \end{aligned} \tag{D.13}$$

Equilibrium of forces in the z direction according to Figure D.2 is obtained with the projection of transverse normal forces as:

$$\begin{aligned}
 -R_{xz} dy + \left(R_{xz} + \frac{\partial R_{xz}}{\partial x} dx \right) dy - R_{yz} dx + \left(R_{yz} + \frac{\partial R_{yz}}{\partial y} dy \right) dx + p dx dy &= 0 \\
 \Rightarrow \frac{\partial R_{xz}}{\partial x} + \frac{\partial R_{yz}}{\partial y} + p &= 0
 \end{aligned} \tag{D.14}$$

According to Figure D-3, contributions of the in-plane normal and shear forces in the z direction are given by:

$$-N_x \frac{\partial \omega}{\partial x} dy + \left(N_x + \frac{\partial N_x}{\partial x} dx \right) dy \left(\frac{\partial \omega}{\partial x} + \frac{\partial^2 \omega}{\partial x^2} dx \right) = N_x \frac{\partial^2 \omega}{\partial x^2} dx dy + \frac{\partial N_x}{\partial x} \frac{\partial \omega}{\partial x} dx dy \quad (D.15)$$

$$\begin{aligned} -N_{yx} \frac{\partial \omega}{\partial x} dy + \left(N_{xy} + \frac{\partial N_{yx}}{\partial y} dy \right) dx \left(\frac{\partial \omega}{\partial x} + \frac{\partial^2 \omega}{\partial x \partial y} dy \right) \\ = N_{yx} \frac{\partial^2 \omega}{\partial x \partial y} dx dy + \frac{\partial N_{yx}}{\partial y} \frac{\partial \omega}{\partial x} dx dy \end{aligned} \quad (D.16)$$

$$-N_y \frac{\partial \omega}{\partial y} dx + \left(N_y + \frac{\partial N_y}{\partial y} dy \right) dx \left(\frac{\partial \omega}{\partial y} + \frac{\partial^2 \omega}{\partial y^2} dy \right) = N_y \frac{\partial^2 \omega}{\partial y^2} dx dy + \frac{\partial N_y}{\partial y} \frac{\partial \omega}{\partial y} dx dy \quad (D.17)$$

$$\begin{aligned} -N_{xy} \frac{\partial \omega}{\partial y} dy + \left(N_{xy} + \frac{\partial N_{xy}}{\partial x} dx \right) dy \left(\frac{\partial \omega}{\partial y} + \frac{\partial^2 \omega}{\partial x \partial y} dx \right) \\ = N_{xy} \frac{\partial^2 \omega}{\partial x \partial y} dx dy + \frac{\partial N_{xy}}{\partial x} \frac{\partial \omega}{\partial y} dx dy \end{aligned} \quad (D.18)$$

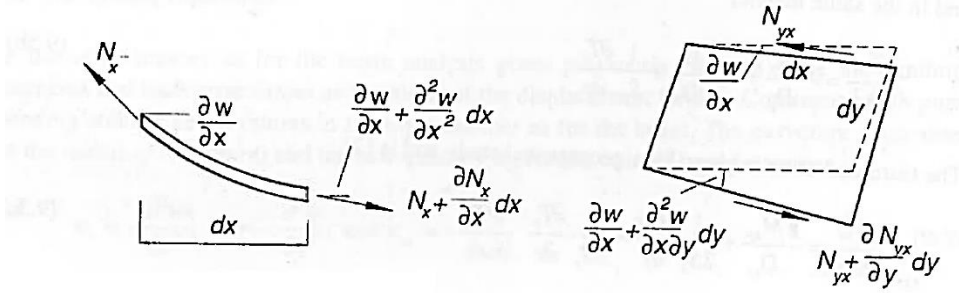


Figure D.4: Force projection of in-plane normal and shear forces in the z direction [50]

At the end of the equilibrium in the z direction including force projection, Equation (D.19) is obtained after summing all contributions of the in-plane forces using the equations (D.15), (D.16), (D.17) and (D.18) and omitting higher order terms in dx and dy .

$$\begin{aligned} N_x \frac{\partial^2 \omega}{\partial x^2} dx dy + N_{yx} \frac{\partial^2 \omega}{\partial x \partial y} dx dy + N_y \frac{\partial^2 \omega}{\partial y^2} dx dy + N_{xy} \frac{\partial^2 \omega}{\partial x \partial y} dx dy \\ + \frac{\partial \omega}{\partial y} dx dy \left(\frac{\partial N_y}{\partial y} + \frac{\partial N_{xy}}{\partial x} \right) + \frac{\partial \omega}{\partial x} dx dy \left(\frac{\partial N_x}{\partial x} + \frac{\partial N_{xy}}{\partial y} \right) \\ = N_x \frac{\partial^2 \omega}{\partial x^2} + N_y \frac{\partial^2 \omega}{\partial y^2} + 2N_{yx} \frac{\partial^2 \omega}{\partial x \partial y} \end{aligned} \quad (D.19)$$

Then, the final expression for the equilibrium in the z direction is obtained by summing the transverse forces given in Equation (D.14) and in-plane normal and shear forces given in Equation (D.19) as:

$$\frac{\partial R_{xz}}{\partial x} + \frac{\partial R_{yz}}{\partial y} + p + N_x \frac{\partial^2 \omega}{\partial x^2} + N_y \frac{\partial^2 \omega}{\partial y^2} + 2N_{yx} \frac{\partial^2 \omega}{\partial x \partial y} - \rho^* \frac{\partial^2 \omega}{\partial t^2} = 0 \quad (\text{D.20})$$

where ρ^* is the surface weight or mass of the plate.

After obtaining the equations for the force equilibrium, moment equilibrium equations are obtained in all directions using Figure D.3. In all moment equations, high order terms are neglected for the simplicity.

Equilibrium of moments in x direction according to Figure D.3 is obtained as:

$$\begin{aligned} M_y dx + \left(M_y + \frac{\partial M_y}{\partial y} dy \right) dx + M_{xy} dy - \left(M_{xy} + \frac{\partial M_{xy}}{\partial x} dx \right) dy \\ + \left(R_{yz} + \frac{\partial R_{yz}}{\partial y} dy \right) dx dy + \left(R_{xz} + \frac{\partial R_{xz}}{\partial x} dx \right) dy \frac{dy}{2} - R_{xz} dy \frac{dy}{2} \\ + p dx dy \frac{dy}{2} = 0 \end{aligned} \quad (\text{D.21})$$

Equation (D.21) is divided into “ $dx dy$ ” terms after that high order derivative terms are neglected. The moment equation in the x direction simplifies to:

$$\frac{\partial M_y}{\partial y} + \frac{\partial M_{xy}}{\partial x} - R_{yz} = 0 \quad (\text{D.22})$$

Equilibrium of moments in the y direction according to Figure D.3 is obtained as:

$$\begin{aligned} M_x dy + \left(M_x + \frac{\partial M_x}{\partial x} dx \right) dy + M_{xy} dx - \left(M_{xy} + \frac{\partial M_{xy}}{\partial y} dy \right) dx \\ + \left(R_{xz} + \frac{\partial R_{xz}}{\partial x} dx \right) dx dy + \left(R_{yz} + \frac{\partial R_{yz}}{\partial y} dy \right) dx \frac{dx}{2} - R_{yz} dx \frac{dx}{2} \\ + p dx dy \frac{dx}{2} = 0 \end{aligned} \quad (\text{D.23})$$

Same as the x direction, simple version of moment equation in the y direction is determined as:

$$\frac{\partial M_x}{\partial x} + \frac{\partial M_{xy}}{\partial y} - R_{xz} = 0 \quad (\text{D.24})$$

Finally, Equation (D.25) is obtained by substituting Equations (D.22) and (D.24) into the Equation (D.20) as the governing equation for buckling analysis.

$$\frac{\partial^2 M_x}{\partial x^2} + 2 \frac{\partial^2 M_{xy}}{\partial x \partial y} + \frac{\partial^2 M_y}{\partial y^2} + p + N_x \frac{\partial^2 \omega}{\partial x^2} + N_y \frac{\partial^2 \omega}{\partial y^2} + 2N_{yx} \frac{\partial^2 \omega}{\partial x \partial y} - \rho^* \frac{\partial^2 \omega}{\partial t^2} = 0 \quad (\text{D.25})$$

APPENDIX E

MATERIAL PROPERTIES HEXPLY 8552 AS4

Physical Properties

	Units	AS4	IM7
Fibre Density	g/cm ³ (lb/in ³)	1.79 (0.065)	1.77 (0.064)
Filament count/tow		12K	12K
Resin density	g/cm ³ (lb/in ³)	1.30 (0.047)	1.30 (0.047)
Nominal Cured Ply Thickness 8552 /35%/134	mm (inch)	0.130 (0.0051)	0.131 (0.0052)
Nominal Fibre Volume	%	57.42	57.70
Nominal Laminate Density	g/cm ³ (lb/in ³)	1.58 (0.057)	1.57 (0.057)

Mechanical Properties

Test	Units	Temp °C (°F)	Condition	AS4	IM7
0°Tensile Strength	MPa (ksi)	-55 (-67)	Dry	1903 (267)	2572 (373)
		25 (77)	Dry	2207 (320)	2724 (395)
		91 (195)	Dry	–	2538 (368)*
90°Tensile Strength	MPa (ksi)	-55 (-67)	Dry	–	174 (25.3)
		25 (77)	Dry	81 (11.7)	64 (9.3)
		93 (200)	Dry	75 (10.9)	92 (13.3)*
0°Tensile Modulus	GPa (msi)	-55 (-67)	Dry	134 (19.4)	163 (23.7)
		25 (77)	Dry	141 (20.5)	164 (23.8)
		91 (195)	Dry	–	163 (23.7)*
90°Tensile Modulus	GPa (msi)	–	–	–	–
		25 (77)	Dry	10 (1.39)	12 (1.7)
		93 (200)	Dry	8 (1.22)	10 (1.5)*
0°Compression Strength	MPa (ksi)	-55 (-67)	Dry	1586 (230)	–
		25 (77)	Dry	1531 (222)	1690 (245)
		91 (195)	Dry	1296 (184)	1483 (215)
0°Compression Modulus	GPa (msi)	-55 (-67)	Dry	124 (18)	–
		25 (77)	Dry	128 (18.6)	150 (21.7)
		91 (195)	Dry	122 (17.7)	162 (23.5)
0° ILSS (Shortbeam shear)	MPa (ksi)	-55 (-67)	Dry	164 (23.8)	–
		25 (77)	Dry	128 (18.5)	137(19.9)
		91 (195)	Dry	122 (14.7)	94 (13.6)*
		25 (77)	Wet	117 (16.9)	115 (16.7)
		71 (160)	Wet	84 (12.2)	80 (11.6)**
In-plane Shear Strength	MPa (ksi)	25 (77)	Dry	114 (16.6)	120 (17.4)
		93 (200)	Dry	105 (15.2)	106 (15.4)*

Bold 93°C (200°F) *Bold** 104°C (220°F) *Bold*** 82°C (180°F)

Figure E.1: Material properties of HexPly 8552 AS4 at dry and room temperature [51]

APPENDIX F

SCRIPTS

F.1 Linear Metal Single Panel Buckling Python Scripts

```
# Importing necessary modules
from part import *
from material import *
from section import *
from assembly import *
from step import *
from interaction import *
from load import *
from mesh import *
from optimization import *
from job import *
from sketch import *
from visualization import *
from connectorBehavior import *
import math

# Skin geometric properties
sk_x = 100.0
sk_z = 0.0
sk_t = 2.0

# Material properties
Ec = 73774.0
E = 72395.0
density = 2768.0
poisson = 0.33
Fcy = 269.0
nc = 15.0

# Applied shell edge load
flow = 1.0
```

```

#Paths
save_path = r'C:\Users\.....\Single Panel\Model\sp_comp'
# Loop for boundary conditions
for bc_type in ['ss','cl']:

    # Loop for applied load type
    for load_type in ['comp','shear']:

        #Paths
        model_path = r'C:\Users\.....\Single Panel\Model\sp_'+bc_type+'_'+load_type
        result_path = r'C:\Users\.....\Single Panel\Result\sp_'+bc_type+'_'+load_type

        # Initialize output file
        results = open(result_path+'.csv',"w+")
        results.write("Ratio FEM Bruhn\n")

        # Creating panels with different edge length ratio
        for sk_y in range(100, 505, 5):
            # Defining model name
            modelname = 'sp_'+ bc_type +'_'+ load_type +'_'+ str(sk_y)
            mdb.Model(modelType=STANDARD_EXPLICIT, name=modelname)
            mn = mdb.models[modelname]

            # Creating sketch of panel
            mn.ConstrainedSketch(name='__profile__', sheetSize=200.0)
            mn.sketches['__profile__'].rectangle(point1=(0.0, 0.0),point2=(sk_x, sk_y))

            # Creating part of panel
            mn.Part(dimensionality=THREE_D, name='panel', type=DEFORMABLE_BODY)
            mn.parts['panel'].BaseShell(sketch=mn.sketches['__profile__'])
            del mn.sketches['__profile__']

            # Creating material
            mn.Material(name='AL2024')
            mn.materials['AL2024'].Elastic(table=((Ec, poisson), ))
            mn.materials['AL2024'].Density(table=((density, ), ))

            # Assigning section of panel
            mn.HomogeneousShellSection(idealization=NO_IDEALIZATION,
            integrationRule=SIMPSON, material='AL2024', name='Section-1', numIntPts=5,
            poissonDefinition=DEFAULT, preIntegrate=OFF, temperature=GRADIENT,
            thickness=sk_t, thicknessField="", thicknessModulus=None, thicknessType=
            UNIFORM, useDensity=OFF)
            mn.parts['panel'].Set(faces=
            mn.parts['panel'].faces.getSequenceFromMask(['[#1 ]', ], ),
            name='Set-1')
            mn.parts['panel'].SectionAssignment(offset=0.0, offsetField=
            "", offsetType=MIDDLE_SURFACE, region=
            mn.parts['panel'].sets['Set-1'], sectionName='Section-1',
            thicknessAssignment=FROM_SECTION)

            # Mesh control
            mn.parts['panel'].setMeshControls(elemShape=QUAD, regions=
            mn.parts['panel'].faces.getSequenceFromMask(['[#1 ]', ], ),
            technique=SWEEP)

            # Creating mesh seeds of panel
            mn.parts['panel'].seedPart(deviationFactor=0.1,
            minSizeFactor=0.1, size=5.0)

            # Generating mesh

```



```

mn.parts['panel'].generateMesh()
mn.rootAssembly.DatumCsysByDefault(CARTESIAN)
mn.rootAssembly.Instance(dependent=ON, name='panel-1', part=
    mn.parts['panel'])

# Creating the set from panel upper edge nodes
upedge = mn.parts['panel'].edges.findAt(((sk_x/2.0,sk_y,sk_z,))
upgeoset = mn.parts['panel'].Set(name = 'geoset', edges = upedge)
nodenums = []
for node in upgeoset.nodes:
    nodenums.append(node.label)
fnodenum = [nodenums[0]]
mn.parts['panel'].SetFromNodeLabels(name = 'up corner', nodeLabels = tuple(fnodenum))
mn.parts['panel'].SetFromNodeLabels(name = 'up nodes', nodeLabels = tuple(nodenums))

# Creating set from panel righth edge nodes
riedge = mn.parts['panel'].edges.findAt(((sk_x,sk_y/2.0,sk_z,))
rigeoset = mn.parts['panel'].Set(name = 'geoset', edges = riedge)
nodenums = []
for node in rigeoset.nodes:
    nodenums.append(node.label)
mn.parts['panel'].SetFromNodeLabels(name = 'righth nodes', nodeLabels = tuple(nodenums))

# Creating set from panel left edge nodes
leedge = mn.parts['panel'].edges.findAt(((0.0,sk_y/2.0,sk_z,))
legeoset = mn.parts['panel'].Set(name = 'geoset', edges = leedge)
nodenums = []
for node in legeoset.nodes:
    nodenums.append(node.label)
mn.parts['panel'].SetFromNodeLabels(name = 'left nodes', nodeLabels = tuple(nodenums))

# Creating set from panel down edge nodes
doedge = mn.parts['panel'].edges.findAt(((sk_x/2.0,0.0,sk_z,))
dorgeoset = mn.parts['panel'].Set(name = 'geoset', edges = doedge)
nodenums = []
for node in dogeoset.nodes:
    nodenums.append(node.label)
fnodenum = [nodenums[(len(nodenums)-1)]]
mn.parts['panel'].SetFromNodeLabels(name = 'down corner', nodeLabels = tuple(fnodenum))
mn.parts['panel'].SetFromNodeLabels(name = 'down nodes', nodeLabels = tuple(nodenums))

# Creating buckling step with subspace solver
mn.BuckleStep(description='buckling', maxIterations=3000, vectors=10,
    name='Step-1', numEigen=3, previous='Initial', eigensolver=SUBSPACE )

# Defining boundary conditions of panel
if bc_type=='ss':
    mn.DisplacementBC(amplitude=UNSET, buckleCase=
        PERTURBATION_AND_BUCKLING, createStepName='Step-1', distributionType=
        UNIFORM, fieldName="", fixed=OFF, localCsys=None, name='up_cor', region=
        mn.rootAssembly.instances['panel-1'].sets['up corner'], u1=0.0, u2=0.0,
        u3=0.0, ur1=UNSET, ur2=UNSET, ur3=UNSET)
    mn.DisplacementBC(amplitude=UNSET, buckleCase=
        PERTURBATION_AND_BUCKLING, createStepName='Step-1', distributionType=
        UNIFORM, fieldName="", fixed=OFF, localCsys=None, name='down_cor', region=
        mn.rootAssembly.instances['panel-1'].sets['down corner'], u1=UNSET, u2=0.0,
        u3=0.0, ur1=UNSET, ur2=UNSET, ur3=UNSET)
    mn.DisplacementBC(amplitude=UNSET, buckleCase=
        PERTURBATION_AND_BUCKLING, createStepName='Step-1', distributionType=
        UNIFORM, fieldName="", fixed=OFF, localCsys=None, name='down', region=
        mn.rootAssembly.instances['panel-1'].sets['down nodes'], u1=UNSET, u2=UNSET,

```

```

    u3=0.0, ur1=UNSET, ur2=UNSET, ur3=UNSET)
mn.DisplacementBC(amplitude=UNSET, buckleCase=
PERTURBATION_AND_BUCKLING, createStepName='Step-1', distributionType=
UNIFORM, fieldName="", fixed=OFF, localCsys=None, name='up', region=
mn.rootAssembly.instances['panel-1'].sets['up nodes'], u1=UNSET, u2=UNSET,
u3=0.0, ur1=UNSET, ur2=UNSET, ur3=UNSET)
mn.DisplacementBC(amplitude=UNSET, buckleCase=
PERTURBATION_AND_BUCKLING, createStepName='Step-1', distributionType=
UNIFORM, fieldName="", fixed=OFF, localCsys=None, name='left', region=
mn.rootAssembly.instances['panel-1'].sets['left nodes'], u1=UNSET, u2=UNSET,
u3=0.0, ur1=UNSET, ur2=UNSET, ur3=UNSET)
mn.DisplacementBC(amplitude=UNSET, buckleCase=
PERTURBATION_AND_BUCKLING, createStepName='Step-1', distributionType=
UNIFORM, fieldName="", fixed=OFF, localCsys=None, name='righth', region=
mn.rootAssembly.instances['panel-1'].sets['righth nodes'], u1=UNSET, u2=UNSET,
u3=0.0, ur1=UNSET, ur2=UNSET, ur3=UNSET)
elif bc_type=='cl':
mn.DisplacementBC(amplitude=UNSET, buckleCase=
PERTURBATION_AND_BUCKLING, createStepName='Step-1', distributionType=
UNIFORM, fieldName="", fixed=OFF, localCsys=None, name='up_cor', region=
mn.rootAssembly.instances['panel-1'].sets['up corner'], u1=0.0, u2=0.0,
u3=0.0, ur1=UNSET, ur2=UNSET, ur3=UNSET)
mn.DisplacementBC(amplitude=UNSET, buckleCase=
PERTURBATION_AND_BUCKLING, createStepName='Step-1', distributionType=
UNIFORM, fieldName="", fixed=OFF, localCsys=None, name='down_cor', region=
mn.rootAssembly.instances['panel-1'].sets['down corner'], u1=UNSET, u2=0.0,
u3=0.0, ur1=UNSET, ur2=UNSET, ur3=UNSET)
mn.DisplacementBC(amplitude=UNSET, buckleCase=
PERTURBATION_AND_BUCKLING, createStepName='Step-1', distributionType=
UNIFORM, fieldName="", fixed=OFF, localCsys=None, name='down', region=
mn.rootAssembly.instances['panel-1'].sets['down nodes'], u1=UNSET, u2=UNSET,
u3=0.0, ur1=0.0, ur2=UNSET, ur3=UNSET)
mn.DisplacementBC(amplitude=UNSET, buckleCase=
PERTURBATION_AND_BUCKLING, createStepName='Step-1', distributionType=
UNIFORM, fieldName="", fixed=OFF, localCsys=None, name='up', region=
mn.rootAssembly.instances['panel-1'].sets['up nodes'], u1=UNSET, u2=UNSET,
u3=0.0, ur1=0.0, ur2=UNSET, ur3=UNSET)
mn.DisplacementBC(amplitude=UNSET, buckleCase=
PERTURBATION_AND_BUCKLING, createStepName='Step-1', distributionType=
UNIFORM, fieldName="", fixed=OFF, localCsys=None, name='left', region=
mn.rootAssembly.instances['panel-1'].sets['left nodes'], u1=UNSET, u2=UNSET,
u3=0.0, ur1=UNSET, ur2=0.0, ur3=UNSET)
mn.DisplacementBC(amplitude=UNSET, buckleCase=
PERTURBATION_AND_BUCKLING, createStepName='Step-1', distributionType=
UNIFORM, fieldName="", fixed=OFF, localCsys=None, name='righth', region=
mn.rootAssembly.instances['panel-1'].sets['righth nodes'], u1=UNSET, u2=UNSET,
u3=0.0, ur1=UNSET, ur2=0.0, ur3=UNSET)

# Creating loads
if load_type=='comp':
mn.rootAssembly.Surface(name='Surf-1', side1Edges=
mn.rootAssembly.instances['panel-1'].edges.getSequenceFromMask(
(['#4'], ), ))
mn.ShellEdgeLoad(createStepName='Step-1', distributionType=
UNIFORM, field="", localCsys=None, magnitude=flow, name='Load-1', region=
mn.rootAssembly.surfaces['Surf-1'])
mn.rootAssembly.Surface(name='Surf-2', side1Edges=
mn.rootAssembly.instances['panel-1'].edges.getSequenceFromMask(
(['#1'], ), ))
mn.ShellEdgeLoad(createStepName='Step-1', distributionType=
UNIFORM, field="", localCsys=None, magnitude=flow, name='Load-2', region=

```

```

        mn.rootAssembly-surfaces['Surf-2'])
elif load_type=='shear':
    mn.rootAssembly.Surface(name='Surf-1', side1Edges=
        mn.rootAssembly.instances['panel-1'].edges.getSequenceFromMask(
            ('[#4 ]', ), ))
    mn.ShellEdgeLoad(createStepName='Step-1', distributionType=
        UNIFORM, field="", localCsys=None, magnitude=-flow, name='Load-1', traction=SHEAR, region=
        mn.rootAssembly-surfaces['Surf-1'])
    mn.rootAssembly.Surface(name='Surf-2', side1Edges=
        mn.rootAssembly.instances['panel-1'].edges.getSequenceFromMask(
            ('[#1 ]', ), ))
    mn.ShellEdgeLoad(createStepName='Step-1', distributionType=
        UNIFORM, field="", localCsys=None, magnitude=-flow, name='Load-2', traction=SHEAR, region=
        mn.rootAssembly-surfaces['Surf-2'])
    mn.rootAssembly.Surface(name='Surf-3', side1Edges=
        mn.rootAssembly.instances['panel-1'].edges.getSequenceFromMask(
            ('[#2 ]', ), ))
    mn.ShellEdgeLoad(createStepName='Step-1', distributionType=
        UNIFORM, field="", localCsys=None, magnitude=flow, name='Load-3', traction=SHEAR, region=
        mn.rootAssembly-surfaces['Surf-3'])
    mn.rootAssembly.Surface(name='Surf-4', side1Edges=
        mn.rootAssembly.instances['panel-1'].edges.getSequenceFromMask(
            ('[#8 ]', ), ))
    mn.ShellEdgeLoad(createStepName='Step-1', distributionType=
        UNIFORM, field="", localCsys=None, magnitude=flow, name='Load-4', traction=SHEAR, region=
        mn.rootAssembly-surfaces['Surf-4'])

# Creating job
mdb.Job(atTime=None, contactPrint=OFF, description="", echoPrint=OFF,
    explicitPrecision=SINGLE, getMemoryFromAnalysis=True, historyPrint=OFF,
    memory=90, memoryUnits=PERCENTAGE, model=modelname, modelPrint=OFF,
    multiprocessingMode=DEFAULT, name=modelname, nodalOutputPrecision=SINGLE,
    numCpus=1, numGPUs=0, queue=None, scratch="", type=ANALYSIS,
    userSubroutine="", waitHours=0, waitMinutes=0)

# Submitting the job
mdb.jobs[modelname].submit(consistencyChecking=OFF)
mdb.jobs[modelname].waitForCompletion()

# Reading first eigenvalue from .dat file
filename = model_path + '_' + str(sk_y) + '.dat'
wordlist = []
starttorecord = False
f = open(filename)
for line in f:
    if " MODE NO   EIGENVALUE" in line:
        starttorecord = True
    for word in line.split():
        if word is 'THE':
            starttorecord = False
        if starttorecord == True:
            wordlist.append(word)
f.close()
if float(wordlist[4])>0.0:
    eigenvalue = float(wordlist[4])
elif float(wordlist[6])>0.0:
    eigenvalue = float(wordlist[6])
elif float(wordlist[8])>0.0:
    eigenvalue = float(wordlist[8])
else:
    eigenvalue = 0.0

```

```

# Calculating buckling coefficient
k = (flow/sk_t * eigenvalue) * pow((sk_x/sk_t),2.0) * 12.0 * (1.0-
pow(poisson,2.0))/(pow(math.pi,2.0)*Ec)

# Reading buckling coefficient from plots of Bruhn
shorteredge = min(sk_x, sk_y)
largeredge = max(sk_x, sk_y)
x = largeredge / shorteredge
if bc_type=='ss':
    if load_type=='comp':
        if x < 0.45:
            K = 8.55
        elif (x >= 0.45) and (x < 1.437):
            K = -
69.66 * pow(x, 5) + 363.28 * pow(x, 4) - 745.99 * pow(x, 3) + 757.82 * pow(x, 2) - 383.38 * x + 81.978
        elif (1.437 <= x) and (x < 2.474):
            K = 1.1819 * pow(x, 2) - 4.974 * x + 9.2349
        elif (2.474 <= x) and (x < 3.48):
            K = 0.5638 * pow(x, 2) - 3.4225 * x + 9.1792
        else:
            K = 0.0142 * pow(x, 2) - 0.184 * x + 4.5554
    elif load_type=='shear':
        if (x < 2.212):
            K = -3.5363 * pow(x, 3) + 20.082 * pow(x, 2) - 38.676 * x + 31.81
        elif (2.212 <= x) and (x < 3.154):
            K = -0.2234 * pow(x, 3) + 2.3507 * pow(x, 2) - 8.2362 * x + 15.425
        else:
            K = -0.2437 * x + 6.7141
    elif bc_type=='cl':
        if load_type=='comp':
            if (x >= 0.65652) and (x < 0.89837):
                K = - 4905.2 * pow(x, 4) + 15581 * pow(x, 3) - 18433 * pow(x, 2) + 9606.6 * x - 1844.7
            elif (x >= 0.89837) and (x < 1.10526):
                K = - 148.29 * pow(x, 3) + 466.91 * pow(x, 2) - 488.75 * x + 180.49
            elif (x >= 1.10526) and (x < 1.4584):
                K = 2.7242 * pow(x, 3) + 1.1611 * pow(x, 2) - 22.033 * x + 29.777
            elif (x >= 1.4584) and (x < 1.78906):
                K = 4.7166 * pow(x, 2) - 15.58 * x + 21.24
            elif (x >= 1.78906) and (x < 2.36817):
                K = - 20.508 * pow(x, 4) + 170.29 * pow(x, 3) - 525.33 * pow(x, 2) + 712.31 * x - 349.51
            elif (x >= 2.36817) and (x < 2.98828):
                K = 1.3593 * pow(x, 3) - 9.7797 * pow(x, 2) + 22.557 * x - 8.7549
            elif (x >= 2.98828) and (x < 3.70121):
                K = 1.0002 * pow(x, 2) - 6.8909 * x + 19.265
            elif (x >= 3.70121) and (x < 4.36245):
                K = 0.941 * pow(x, 2) - 7.7078 * x + 23.11
            elif (x >= 4.36245) and (x <= 5.0):
                K = 0.8153 * pow(x, 2) - 7.7061 * x + 25.493
        elif load_type=='shear':
            if (1.0 <= x) and (x < 2.18893):
                K = 40.615 * pow(x, 6) - 412.18 * pow(x, 5) + 1725.8 * pow(x, 4) - 3814.8 * pow(x, 3) + 4695.7
* pow(x, 2) - 3056.3 * x + 836
            elif (2.18893 <= x) and (x < 2.99848):
                K = 1.2656 * pow(x, 3) - 8.9195 * pow(x, 2) + 20.19 * x - 4.668
            elif (2.99848 <= x) and (x <= 5.0):
                K = -0.0274 * pow(x, 6) + 0.8406 * pow(x, 5) -
10.101 * pow(x, 4) + 61.822 * pow(x, 3) - 204.98 * pow(x, 2) + 350.57 * x - 232.37

# Writing results to output file
results.write("%f %f %f" %(sk_y/sk_x,k,K)+"\n")

```

```

    results.close()
try:
    del mdb.models['Model-1']
except:
    None
# Saving the model
mdb.saveAs(
    pathName=save_path+'.cae')

```

F.2 Linear Metal Stiffened Panel Buckling Python Scripts

- Example code to construct the skin-stringer model with J stringer section

```

# Importing necessary modules
from part import *
from material import *
from section import *
from assembly import *
from step import *
from interaction import *
from load import *
from mesh import *
from optimization import *
from job import *
from sketch import *
from visualization import *
from connectorBehavior import *
import math
import time

# Counter for script time
start_t_time = time.time()

# Paths
save_path='C:/Users/...../Model/Model_J/model_j'

# Initialize result file
results = open(r"C:\Users\.....\Results\output_J_min_inertia.txt","w+")

# Given Edge Load (N/mm)
Edge_load = 1.0

# Material properties (Al 2024 T3 Sheet thk: 0.23-3.25 mm)
Ec = 73774.0
E = 72395.0
density = 2768.0
poisson = 0.33
Fcy = 269.0
nc = 15.0

# Skin geometry
sk_x = 450.0
sk_ys = [150.0*3.0,225.0*3.0,300.0*3.0,375.0*3.0,450.0*3.0]
sk_ts = [0.813,1.016,1.27]

# Stringer "J" geometry
str_l = 450.0
str_ts = [0.813,1.016,1.27]
str_hs = [10.0,17.0,24.0,30.0]

```

```

str_cs = [10.0,14.0,18.0,22.0]
str_bs = [10.0,14.0,18.0]

# Fasteners' diameter
fast_d = 3.2

# Total number of models which will be created in this script
total_count = len(str_hs)*len(str_cs)*len(str_bs)*len(str_ts)*len(sk_ts)*len(sk_ys)
print "Total model number: ", total_count

# Function of flat metal panel compressive buckling coefficient
def graph_Kc_flat(x,bc):
    """
    Ref: Analysis and Design of Flight Vehicle Structures - E.F.Bruhn
    * Kc is obtained from Figure C5.2 for flat panels
    Loaded edges are clamped.
    Conditions are only exceptable for unloaded edges
    """
    if bc=='cl':
        if x < 0.76493:
            y = -56.0565*x + 57.1876
        elif (0.76493 <= x) and (x < 1.14273):
            y = -551.9651*pow(x, 4) + 2079.3509*pow(x, 3) - 2870.2033*pow(x, 2) + 1706.6187*x - 353.426
        elif (1.14273 <= x) and (x < 1.85911):
            y = -6.1616*pow(x, 3) + 34.8139*pow(x, 2) - 65.0106*x + 48.5687
        elif (1.85911 <= x) and (x < 2.3433):
            y = -15.9873*pow(x, 4) + 127.1208*pow(x, 3) - 373.7913*pow(x, 2) + 479.4634*x - 216.8528
        elif (2.3433 <= x) and (x < 3.3987):
            y = 13.6994*pow(x, 5) - 198.9195*pow(x, 4) + 1149.7887*pow(x, 3) - 3306.5735*pow(x, 2) + 4730.1783*x - 2684.554
        elif (3.3987 <= x) and (x < 4.15706):
            y = 10.807*pow(x, 4) - 163.8182*pow(x, 3) + 929.1075*pow(x, 2) - 2336.7822*x + 2206.491
        elif (4.15706 <= x) and (x <= 5.0142):
            y = 1.9679*pow(x, 3) - 27.1906*pow(x, 2) + 124.8755*x - 183.3227
        else:
            y = 7.2802
        return y
    elif bc=='ss':
        if x < 1.33459:
            y = 116.1071*pow(x, 4) - 512.1754*pow(x, 3) + 847.8765*pow(x, 2) - 628.8651*x + 183.9239
        elif (1.33459 <= x) and (x < 1.68636):
            y = 2.5557*pow(x, 2) - 8.0374*x + 11.8528
        elif (1.68636 <= x) and (x < 2.76429):
            y = 12.4466*pow(x, 6) - 166.4906*pow(x, 5) + 921.7798*pow(x, 4) - 2704.0495*pow(x, 3) + 4434.9741*pow(x, 2) - 3860.3466*x + 1400.7332
        elif (2.76429 <= x) and (x <= 4.95153):
            y = -
            0.2663*pow(x, 5) + 5.2351*pow(x, 4) - 40.8202*pow(x, 3) + 157.8018*pow(x, 2) - 302.6058*x + 234.8432
        else:
            y = 4.2274
        return y

# Function of flat metal panel shear buckling coefficient
def graph_Ks_flat(x,bc):
    """
    Ref: Analysis and Design of Flight Vehicle Structures - E.F.Bruhn
    Ks is obtained from Figure C5.11 for flat panels
    Loaded edges are clamped.
    Conditions are only exceptable for unloaded edges
    """
    if bc=='cl':

```

```

    if x < 1.39646:
        y = 617.3722*pow(x, 4) - 3049.2054*pow(x, 3) + 5640.7618*pow(x, 2) - 4637.94*x + 1444.5082
    elif (1.39646 <= x) and (x < 2.79647):
        y = -0.2876*pow(x, 3) + 3.08*pow(x, 2) - 10.558*x + 21.4866
    elif (2.79647 <= x) and (x < 5.0):
        y = 0.2326*pow(x, 5) - 4.577*pow(x, 4) + 35.6865*pow(x, 3) - 137.6532*pow(x, 2) + 262.3421*x - 18
7.6865
    else:
        y = 9.6226
    return y
elif bc=='ss':
    if x < 1.79125:
        y = -
23.165*pow(x, 6) + 154.3269*pow(x, 5) - 380.7138*pow(x, 4) + 376.5476*pow(x, 3) - 1.3356*pow(x, 2) - 2
51.0012*x + 135.069
    elif (x <= 1.79125) and (x < 2.57994):
        y = 0.1192*pow(x, 3) - 0.7131*pow(x, 2) + 0.5982*x + 7.1608
    elif (x <= 2.57994) and (x < 3.70882):
        y = 0.075*pow(x, 3) - 0.3925*pow(x, 2) + 0.0756*x + 7.135
    elif (x <= 3.70882) and (x < 5.0):
        y = -0.2125*x + 6.6311
    else:
        y = 5.5684
    return y

# Function of plasticity correction
def get_plastic_stress(nc,Fscr_el,Ec,Fcy):
    """
    See HSB 52100-01 plasticity correction
    """
    return Fcr

for sk_y_key,sk_y in enumerate(sk_ys):
    for sk_t_key,sk_t in enumerate(sk_ts):
        sk_ratio = sk_x / (sk_y/3.0)
        Ireqs = []
        K_values = []

        # Unloaded edge boundary conditions (clamped or simply supported)
        for bc in ["cl","ss"]:
            Ks = graph_Ks_flat(sk_ratio,bc)
            Kc = graph_Kc_flat(sk_ratio,bc)
            K_value = [Ks,Kc]
            K_values.append(K_value)
            Fscr_el = Ks*math.pi**2.0*Ec/(12.0*(1.0-poisson**2.0))*(sk_t/(sk_y/3.0))**2.0
            Fscr = get_plastic_stress(nc,Fscr_el,Ec,Fcy)
            Ireq = (2.29*sk_x/sk_t)*(Fscr*sk_t**2.0)/(33.0*E)**(4.0/3.0)
            Ireqs.append(Ireq)
            Ireq_moi=min(Ireqs)

        # Results of panels with classical boundary conditions and minimum required inertia are written into t
he result file
        results.write("%-15s %6.2f %-
15s %6.2f" %("Skin length y: ",(sk_y/3.0)," Skin thickness: ",sk_t)+"\n")
        results.write("%-30s %-15s %6.2f %-
30s %6.2f" %("Min. stiffener inertia", "For clamped: ",Ireqs[0]," For simply supported",Ireqs[1])+"\n")
        results.write("%-30s %-15s %6.2f %-
30s %6.2f" %("Shear buckling coefficient", "For clamped: ",K_values[0][0]," For simply supported",K_values[
1][0])+"\n")

```

```

results.write("%-30s %-15s %6.2f %-
30s %6.2f" %("Compressive buckling coefficient", "For clamped: ",K_values[0][1], " For simply supported",K
values[1][1])+"\n"+"")

for str_h_key,str_h in enumerate(str_hs):
    for str_c_key,str_c in enumerate(str_cs):
        for str_b_key,str_b in enumerate(str_bs):
            for str_t_key,str_t in enumerate(str_ts):
                # Inertia and area of stringer is calculated
                r1_dx = str_b
                r1_dy = str_t
                r2_dx = str_t
                r2_dy = str_h-2.0*str_t
                r3_dx = str_c
                r3_dy = str_t
                r1_A = r1_dx * r1_dy
                r2_A = r2_dx * r2_dy
                r3_A = r3_dx * r3_dy
                r1_Ix = (1.0 / 12.0) * r1_dx * r1_dy**3.0
                r2_Ix = (1.0 / 12.0) * r2_dx * r2_dy**3.0
                r3_Ix = (1.0 / 12.0) * r3_dx * r3_dy**3.0
                parts = [
                    {dx_cg': max(r1_dx-
r2_dx/2.0,r3_dx/2.0) + r2_dx/2.0 - r1_dx/2.0, 'dy_cg': r1_dy / 2.0, 'A':r1_A, 'Ix':r1_Ix},
                    {dx_cg': max(r1_dx-
r2_dx/2.0,r3_dx/2.0), 'dy_cg': r1_dy + r2_dy / 2.0, 'A':r2_A, 'Ix':r2_Ix},
                    {dx_cg': max(r1_dx-
r2_dx/2.0,r3_dx/2.0), 'dy_cg': r1_dy + r2_dy + r3_dy / 2.0, 'A':r3_A, 'Ix':r3_Ix},
                ]
                Ad_t = 0.0
                A_t = 0.0
                for part in parts:
                    Ad_t += part['A'] * part['dy_cg']
                    A_t += part['A']
                cg_y = Ad_t / A_t
                Istr = 0.0
                for part in parts:
                    Istr += (part['Ix'] + part['A'] * part['dy_cg']**2.0 - cg_y * part['A'] * part['dy_cg'])

                # Geometric properties of stringer are written into the result file
                results.write("%-25s %6.2f %-20s %6.2f %-20s %6.2f %-
20s %6.2f" %(" Stringer height: ",str_h, " Stringer c width: ",str_c, " Stringer b width: ",str_b," Stringer thic
kness: ",str_t)+"\n")
                results.write("%-25s %6.2f" %(" Stiffener inertia: ",Istr)+"\n"+"")

                # To satisfy the stiffened panel condition, stringer inertia is checked.
                if Ireq_moi<Istr:
                    # Creating model of stiffened panel buckling (spb)
                    model_name = "spb_J_"+str(str_h_key)+str(str_c_key)+str(str_b_key)+str(str_t_key)+str(sk_t
_key)+str(sk_y_key)
                    mdb.Model(modelType=STANDARD_EXPLICIT, name=model_name)
                    mn=mdb.models[model_name]

                    # Creating material
                    mn.Material(name='Al_2024_T3_Sheet')
                    mn.materials['Al_2024_T3_Sheet'].Elastic(table=((Ec, poisson),))
                    mn.materials['Al_2024_T3_Sheet'].Density(table=((density),))

                    # Creating sketch of skin
                    mn.ConstrainedSketch(name='__profile__', sheetSize=200.0)
                    mn.sketches['__profile__'].rectangle(point1=(0.0, 0.0), point2=(sk_x, sk_y))

```



```

# Creating part of skin
mn.Part(dimensionality=THREE_D, name='Skin', type=DEFORMABLE_BODY)
mn.parts['Skin'].BaseShell(sketch=mn.sketches['_profile_'])
del mn.sketches['_profile_']

# Creating partition
p_sk = mn.parts['Skin']
f_sk, e_sk, d_sk = p_sk.faces, p_sk.edges, p_sk.datums
t = p_sk.MakeSketchTransform(sketchPlane=f_sk[0], sketchUpEdge=e_sk[2],
    sketchPlaneSide=SIDE1, origin=(sk_x*0.5, sk_y*0.5, 0.0))
s = mn.ConstrainedSketch(name='_profile_',
    sheetSize=1272.79, gridSpacing=31.81, transform=t)
g, v, d1, c = s.geometry, s.vertices, s.dimensions, s.constraints
s.setPrimaryObject(option=SUPERIMPOSE)
p_sk.projectReferencesOntoSketch(sketch=s, filter=COPLANAR_EDGES)
s.Line(point1=(-sk_y/6.0, sk_x*0.5), point2=(-sk_y/6.0, -sk_x*0.5))
s.VerticalConstraint(entity=g[6], addUndoState=False)
s.PerpendicularConstraint(entity1=g[5], entity2=g[6], addUndoState=False)
s.CoincidentConstraint(entity1=v[4], entity2=g[5], addUndoState=False)
s.CoincidentConstraint(entity1=v[5], entity2=g[3], addUndoState=False)
s.Line(point1=(0, sk_x*0.5), point2=(0, -sk_x*0.5))
s.VerticalConstraint(entity=g[7], addUndoState=False)
s.PerpendicularConstraint(entity1=g[5], entity2=g[7], addUndoState=False)
s.CoincidentConstraint(entity1=v[6], entity2=g[5], addUndoState=False)
s.CoincidentConstraint(entity1=v[7], entity2=g[3], addUndoState=False)
s.Line(point1=(sk_y/6.0, sk_x*0.5), point2=(sk_y/6.0, -sk_x*0.5))
s.VerticalConstraint(entity=g[8], addUndoState=False)
s.PerpendicularConstraint(entity1=g[5], entity2=g[8], addUndoState=False)
s.CoincidentConstraint(entity1=v[8], entity2=g[5], addUndoState=False)
s.CoincidentConstraint(entity1=v[9], entity2=g[3], addUndoState=False)
pickedFaces = f_sk.getSequenceFromMask(mask=('[#1 ]', ), )
p_sk.PartitionFaceBySketch(sketchUpEdge=e_sk[2], faces=pickedFaces, sketch=s)
s.unsetPrimaryObject()
del mn.sketches['_profile_']

# Creating skin section
mn.HomogeneousShellSection(name='Skin_Sec',
    preIntegrate=OFF, material='Al_2024_T3_Sheet', thicknessType=UNIFORM,
    thickness=sk_t, thicknessField="", idealization=NO_IDEALIZATION,
    poissonDefinition=DEFAULT, thicknessModulus=None, temperature=GRADIENT,
    useDensity=OFF, integrationRule=SIMPSON, numIntPts=5)

# Assigning skin section
faces = f_sk.getSequenceFromMask(mask=('[#f ]', ), )
region = p_sk.Set(faces=faces, name='Skin_faces_set')
p_sk.SectionAssignment(region=region, sectionName='Skin_Sec', offset=0.0,
    offsetType=MIDDLE_SURFACE, offsetField="",
    thicknessAssignment=FROM_SECTION)

# Mesh control of skin
pickedRegions = f_sk.getSequenceFromMask(mask=('[#f ]', ), )
p_sk.setMeshControls(regions=pickedRegions, elemShape=QUAD, technique=SWEEP)

# Mesh seed of skin
p_sk.seedPart(deviationFactor=0.1, minSizeFactor=0.1, size=5.0)

# Generate mesh of skin
p_sk.generateMesh()

# Creating sketch of stringer

```

```

s = mn.ConstrainedSketch(name='_profile_', sheetSize=200.0)
g, v, d, c = s.geometry, s.vertices, s.dimensions, s.constraints
s.setPrimaryObject(option=STANDALONE)
s.Line(point1=(-str_c*0.5, 0.0), point2=(str_c*0.5, 0.0))
s.HorizontalConstraint(entity=g[2], addUndoState=False)
s.Line(point1=(0.0, 0.0), point2=(0.0, str_h))
s.VerticalConstraint(entity=g[3], addUndoState=False)
s.PerpendicularConstraint(entity1=g[2], entity2=g[3], addUndoState=False)
s.CoincidentConstraint(entity1=v[2], entity2=g[2], addUndoState=False)
s.EqualDistanceConstraint(entity1=v[0], entity2=v[1], midpoint=v[2], addUndoState=False)

s.Line(point1=(0.0, str_h), point2=(str_b, str_h))
s.HorizontalConstraint(entity=g[4], addUndoState=False)
s.PerpendicularConstraint(entity1=g[3], entity2=g[4], addUndoState=False)

# Creating part of stringer
mn.Part(name='Stringer', dimensionality=THREE_D,type=DEFORMABLE_BODY)
mn.parts['Stringer'].BaseShellExtrude(sketch=s, depth=str_l)
del mn.sketches['_profile_']

# Creating stringer section
mn.HomogeneousShellSection(name='Stringer_Sec',
preIntegrate=OFF, material='Al_2024_T3_Sheet', thicknessType=UNIFORM,
thickness=str_t, thicknessField="", idealization=NO_IDEALIZATION,
poissonDefinition=DEFAULT, thicknessModulus=None, temperature=GRADIENT,
useDensity=OFF, integrationRule=SIMPSON, numIntPts=5)

# Assigning stringer section
p_str = mn.parts['Stringer']
f_str = p_str.faces
faces = f_str.getSequenceFromMask(mask=('[#f]', ), )
region = p_str.Set(faces=faces, name='Stringer_faces_set')
p_str.SectionAssignment(region=region, sectionName='Stringer_Sec', offset=0.0,
offsetType=MIDDLE_SURFACE, offsetField="",
thicknessAssignment=FROM_SECTION)

# Mesh control of stringer
pickedRegions = f_str.getSequenceFromMask(mask=('[#f]', ), )
p_str.setMeshControls(regions=pickedRegions, elemShape=QUAD, technique=SWEEP)

# Mesh seed of stringer
p_str.seedPart(deviationFactor=0.1, minSizeFactor=0.1, size=2.0)

# Generate mesh of stringer
p_str.generateMesh()

# Creating buckling step
mn.BuckleStep(name='Buckle-
Step', previous='Initial', numEigen=3, vectors=28, maxIterations=3000)

# Creating assembly instances
a_ss = mn.rootAssembly
a_ss.DatumCsysByDefault(CARTESIAN)
a_ss.Instance(dependent=ON, name='Skin-1', part=p_sk)

# Creating Stringer 1
mn.rootAssembly.DatumCsysByDefault(CARTESIAN)
mn.rootAssembly.Instance(dependent=ON, name='Stringer-1', part=p_str)

# Stringer 1 place is decided

```

```

        a_ss.rotate(instanceList=('Stringer-
1', ), axisPoint=(0.0, 0.0, 0.0), axisDirection=(0.0, 1.0, 0.0), angle=90.0)
        a_ss.rotate(instanceList=('Stringer-
1', ), axisPoint=(0.0, 0.0, 0.0), axisDirection=(1.0, 0.0, 0.0), angle=90.0)
        a_ss.translate(instanceList=('Stringer-1', ), vector=(0.0, sk_y/3.0, (sk_t+str_t)*0.5))

# Creating Stringer 2
a_ss.LinearInstancePattern(instanceList=('Stringer-
1', ), direction1=(1.0, 0.0, 0.0), direction2=(0.0, 1.0, 0.0), number1=1, number2=2, spacing1=str_l, spacing2
=sk_y/3.0)
a_ss.features.changeKey(fromName='Stringer-1-lin-1-2', toName='Stringer-2')

# Creating Connector section as beam
mn.ConnectorSection(name='Fastener_Con_Sec', assembledType=BEAM)

# Creating Fasteners
const_attach = [['#20'],4,1,'1'],[['#4'],2,0,'2']]
for key in range(2):
    e_str = a_ss.instances['Stringer-'+str(key+1)].edges
    v_str = a_ss.instances['Stringer-'+str(key+1)].vertices
    f_str = a_ss.instances['Stringer-'+str(key+1)].faces
    for const in const_attach:
        # Creating attachment points
        edges1 = e_str.getSequenceFromMask(mask=(const[0], ), )
        geomEdges=edges1
        a_ss.AttachmentPointsOffsetFromEdges(edges=geomEdges, startPoint=v_str[const[1]],
        referenceFace=f_str[const[2]], name='Str'+str(key+1)+'-Attachment Points-
'+const[3],
        pointCreationMethod=BY_NUMBER, offsetFromStartPoint=2.0*fast_d+1.0, numberOfP
oints=27,
        offsetFromEndPoint=2.0*fast_d+1.0, numberOfRows=1, offsetFromEdges= str_c*0.25,
        patterningMethod=PATTERN_ORTHOGONALLY, setName='Str'+str(key+1)+'-
Attachment Points-Set '+const[3])

# Assigning a section to fastener
region=a_ss.sets['Str'+str(key+1)+'-Attachment Points-Set '+const[3]]
a_ss.engineeringFeatures.PointFastener( name='Str'+str(key+1)+'-Fasteners-
'+const[3], region=region,
        sectionName='Fastener_Con_Sec', directionVector=(v_str[7], a_ss.instances['Stringer-
'+str(key+1)].
        InterestingPoint(edge=e_str[8], rule=MIDDLE)), physicalRadius=fast_d*0.5, additional
Mass=0.0001)

# Creating boundary conditions at initial step
v_sk = a_ss.instances['Skin-1'].vertices
e_sk = a_ss.instances['Skin-1'].edges

#Creating boundary conditions sets
verts1 = v_sk.getSequenceFromMask(mask=('#200'], ), )
a_ss.Set(vertices=verts1, name='Set_mid_point')
dict_bc = {'#44']:'side_edges', '#c28']:'load_edge', '#1282']:'reaction_edge',}
for key_bc, str_bc in dict_bc.items():
    edges1 = e_sk.getSequenceFromMask(mask=(key_bc, ), )
    a_ss.Set(edges=edges1, name='Set_'+str_bc)

# Assigning boundary conditions on sets
region = a_ss.sets['Set_mid_point']
mn.DisplacementBC(name='BC_mid_point',
        createStepName='Initial', region=region, u1=UNSET, u2=SET, u3=UNSET,
        ur1=UNSET, ur2=UNSET, ur3=UNSET, amplitude=UNSET, distributionType=UNIFORM,

```

```

        fieldName="", localCsys=None)
    region = a_ss.sets['Set_side_edges']
    mn.DisplacementBC(name='BC_side_edges',
        createStepName='Initial', region=region, u1=UNSET, u2=UNSET, u3=SET,
        ur1=SET, ur2=UNSET, ur3=UNSET, amplitude=UNSET, distributionType=UNIFORM,
        fieldName="", localCsys=None)
    region = a_ss.sets['Set_load_edge']
    mn.DisplacementBC(name='BC_load_edge',
        createStepName='Initial', region=region, u1=UNSET, u2=UNSET, u3=SET,
        ur1=UNSET, ur2=SET, ur3=UNSET, amplitude=UNSET, distributionType=UNIFORM,
        fieldName="", localCsys=None)
    region = a_ss.sets['Set_reaction_edge']
    mn.DisplacementBC(name='BC_reaction_edge',
        createStepName='Initial', region=region, u1=SET, u2=UNSET, u3=SET,
        ur1=UNSET, ur2=SET, ur3=UNSET, amplitude=UNSET, distributionType=UNIFORM,
        fieldName="", localCsys=None)

    # Creating shell edge load
    loaded_edges = e_sk.getSequenceFromMask(mask=('[#c28 ]', ), )
    region = a_ss.Surface(side1Edges=loaded_edges, name='Loaded Edge Surface')
    mn.ShellEdgeLoad(name='Shell Load',
        createStepName='Buckle-Step', region=region, magnitude=Edge_load,
        distributionType=UNIFORM, field="", localCsys=None)

    # Creating job
    job_name = 'job_' + model_name
    mdb.Job(name=job_name, model=model_name, description="", type=ANALYSIS,
        atTime=None, waitMinutes=0, waitHours=0, queue=None, memory=99,
        memoryUnits=PERCENTAGE, getMemoryFromAnalysis=True,
        explicitPrecision=SINGLE, nodalOutputPrecision=SINGLE, echoPrint=OFF,
        modelPrint=OFF, contactPrint=OFF, historyPrint=OFF, userSubroutine="",
        scratch="", resultsFormat=ODB, multiprocessingMode=DEFAULT, numCpus=1,
        numGPUs=0)
results.close()
del mdb.models['Model-1']

# Saving the model
mdb.saveAs(pathName=save_path+'.cae')

# Stopping the time calculator
end_t_time = time.time()
m=divmod(end_t_time-start_t_time,60)
n=divmod(m[0],60)
print "Total time: ",n[0],n[1],m[1]

```

- Example code to process finite element results for skin-stringer model with J stringer section

```

# Importing necessary modules
from part import *
from material import *
from section import *
from assembly import *
from step import *
from interaction import *
from load import *
from mesh import *
from optimization import *
from job import *

```

```

from sketch import *
from visualization import *
from connectorBehavior import *
import math
import time

# Counter for script time
start_t_time = time.time()

# Defining maximum number of submissions can be given at the same time
max_sub = 5
ini_sub = 0

# Paths
save_path = 'C:/Users/...../Model/Model_J/model_j'
model_path = r'C:/Users/Enes/Desktop/AIAC/Versions/V7/Model/Model_J/'

# Initialize result files
results = open(r"C:\Users\.....\Results\output_J.txt","w+")
results_excel = open(r"C:\Users\.....\Results\excel_output_J.txt","w+")

# Given Edge Load (N/mm)
Edge_load = 1.0

# Material properties (Al 2024 T3 Sheet thk: 0.23-3.25 mm)
Ec = 73774.0
E = 72395.0
density = 2768.0
poisson = 0.33
Fcy = 269.0
nc = 15.0

# Skin geometry
sk_x = 450.0
sk_ys = [150.0*3.0,225.0*3.0,300.0*3.0,375.0*3.0,450.0*3.0]
sk_ts = [0.813,1.016,1.27]

# Stringer "J" geometry
str_l = 450.0
str_ts = [0.813,1.016,1.27]
str_hs = [10.0,17.0,24.0,30.0]
str_cs = [10.0,14.0,18.0,22.0]
str_bs = [10.0,14.0,18.0]

# Fasteners' diameter
fast_d = 3.2

# Initialize output file
results.write("%-20s %6.0f %-20s %6.2f %-20s %6.2f" %("Material Ec: ",Ec," Material poisson: ",poisson," Material density: ",density)+"\n")
results.write("%-20s %6.2f %-20s %6.2f %-20s %6.2f" %("Skin length x: ",sk_x," Stringer length: ",str_l," Fastener diameter: ",fast_d)+"\n"+"")

# Total number of models which will be created in this script
total_count = len(str_hs)*len(str_cs)*len(str_bs)*len(str_ts)*len(sk_ts)*len(sk_ys)
print "Total model number: ", total_count
count=1

# Initialize dictionary for excel output file
excel_dic = {"Skin_length_y":[],"Skin_thickness":[],"Stringer_heigh":[],"Stringer_c_width":[],"Stringer_b_wid
th":[],"Stringer_thickness":[],"kc":[]}

```

```

# Function of flat metal panel compressive buckling coefficient
def graph_Kc_flat(x,bc):
    """
    Ref: Analysis and Design of Flight Vehicle Structures - E.F.Bruhn
    Kc is obtained from Figure C5.2 for flat panels
    Loaded edges are clamped.
    Conditions are only acceptable for unloaded edges
    """
    if bc=='cl':
        if x < 0.76493:
            y = -56.0565*x + 57.1876
        elif (0.76493 <= x) and (x < 1.14273):
            y = -551.9651*pow(x, 4) + 2079.3509*pow(x, 3) - 2870.2033*pow(x, 2) + 1706.6187*x - 353.426
        elif (1.14273 <= x) and (x < 1.85911):
            y = -6.1616*pow(x, 3) + 34.8139*pow(x, 2) - 65.0106*x + 48.5687
        elif (1.85911 <= x) and (x < 2.3433):
            y = -15.9873*pow(x, 4) + 127.1208*pow(x, 3) - 373.7913*pow(x, 2) + 479.4634*x - 216.8528
        elif (2.3433 <= x) and (x < 3.3987):
            y = 13.6994*pow(x, 5) - 198.9195*pow(x, 4) + 1149.7887*pow(x, 3) - 3306.5735*pow(x, 2) + 4730.1
783*x - 2684.554
        elif (3.3987 <= x) and (x < 4.15706):
            y = 10.807*pow(x, 4) - 163.8182*pow(x, 3) + 929.1075*pow(x, 2) - 2336.7822*x + 2206.491
        elif (4.15706 <= x) and (x <= 5.0142):
            y = 1.9679*pow(x, 3) - 27.1906*pow(x, 2) + 124.8755*x - 183.3227
        else:
            y = 7.2802
        return y
    elif bc=='ss':
        if x < 1.33459:
            y = 116.1071*pow(x, 4) - 512.1754*pow(x, 3) + 847.8765*pow(x, 2) - 628.8651*x + 183.9239
        elif (1.33459 <= x) and (x < 1.68636):
            y = 2.5557*pow(x, 2) - 8.0374*x + 11.8528
        elif (1.68636 <= x) and (x < 2.76429):
            y = 12.4466*pow(x, 6) - 166.4906*pow(x, 5) + 921.7798*pow(x, 4) - 2704.0495*pow(x, 3) + 4434.97
41*pow(x, 2) - 3860.3466*x + 1400.7332
        elif (2.76429 <= x) and (x <= 4.95153):
            y = -
0.2663*pow(x, 5) + 5.2351*pow(x, 4) - 40.8202*pow(x, 3) + 157.8018*pow(x, 2) - 302.6058*x + 234.8432
        else:
            y = 4.2274
        return y

for sk_y_key,sk_y in enumerate(sk_ys):
    for sk_t_key,sk_t in enumerate(sk_ts):
        for str_h_key,str_h in enumerate(str_hs):
            for str_c_key,str_c in enumerate(str_cs):
                for str_b_key,str_b in enumerate(str_bs):
                    for str_t_key,str_t in enumerate(str_ts):
                        # Job name is described
                        job_name = "job_spb_J_"+str(str_h_key)+str(str_c_key)+str(str_b_key)+str(str_t_key)+str(sk_t
key)+str(sk_y_key)

                        # Checked whether there is such a job name
                        try:
                            start_time = time.time()
                            print "Model number: ",count
                            job_model = mdb.jobs[job_name]

                        # Checked to see if the job has already been submitted
                        try:

```

```

dir_logfile = model_path + job_name+".log"
logfile = open(dir_logfile)
comp = False

# Checked to see that the job is completed
for line in logfile:
    if "Abaqus JOB "+job_name+" COMPLETED" in line:
        print " completed"
        comp = True
logfile.close()

# Submission check
if comp==False:
    # Submit the job
    job_model.submit(consistencyChecking=OFF)
    ini_sub +=1

    # Multi-submission is permitted for this code
    # Maximum number of submission is checked
    if ini_sub >= max_sub:
        job_model.waitForCompletion()
        ini_sub = 0
        end_time = time.time()
    else:
        end_time = time.time()
except:
    # Submit the job
    job_model.submit(consistencyChecking=OFF)
    ini_sub +=1

    # Multi-submission is permitted for this code
    # Maximum number of submission is checked
    if ini_sub >= max_sub:
        job_model.waitForCompletion()
        ini_sub = 0
        end_time = time.time()

# Estimated time is calculated
if count%(max_sub*2) == 0:
    em=divmod([(total_count-count)*(end_time-start_time)/max_sub,60])
    en=divmod(em[0],60)
    print "Estimated remaning time: ",en[0],en[1],em[1]
    count+=1
except:
    None

for sk_y_key,sk_y in enumerate(sk_ys):
    sk_ratio = sk_x / (sk_y/3.0)
    kc_bruhn =[]
    # Literature graphs are used to get comp. buckling coeffients with classical boundary condition assumpti
    on
    # Unloaded edge boundary conditions (clamped or simply supported)
    for bc in ["cl","ss"]:
        kc_bruhn.append(graph_Kc_flat(sk_ratio,bc))
    for sk_t_key,sk_t in enumerate(sk_ts):
        for str_h_key,str_h in enumerate(str_hs):
            for str_c_key,str_c in enumerate(str_cs):
                for str_b_key,str_b in enumerate(str_bs):
                    for str_t_key,str_t in enumerate(str_ts):
                        # Defining the job name

```

```
job_name = "job_spb_L_" + str(str_h_key) + str(str_c_key) + str(str_b_key) + str(str_t_key) + str(sk_t_key) + str(sk_y_key)
```

```
# Obtain the eigenvalue
```

```
try:
```

```
    dir_datfile = model_path + job_name + '.dat'
```

```
    wordlist = []
```

```
    starttorecord = False
```

```
    datfile = open(dir_datfile)
```

```
    for line in datfile:
```

```
        if "MODE NO EIGENVALUE" in line:
```

```
            starttorecord = True
```

```
            for word in line.split():
```

```
                if word == 'THE':
```

```
                    starttorecord = False
```

```
                if starttorecord:
```

```
                    wordlist.append(word)
```

```
            if float(wordlist[4]) > 0.0:
```

```
                eigenvalue = float(wordlist[4])
```

```
            elif float(wordlist[6]) > 0.0:
```

```
                eigenvalue = float(wordlist[6])
```

```
            elif float(wordlist[8]) > 0.0:
```

```
                eigenvalue = float(wordlist[8])
```

```
            else:
```

```
                eigenvalue = 0.0
```

```
    datfile.close()
```

```
    Fccr = eigenvalue * Edge_load / sk_t
```

```
# Compressive buckling coefficient is calculated using eigenvalue obtained from FEA
```

```
kc = Fccr * (sk_y / 3.0) ** 2.0 * 12.0 * (1.0 - poisson ** 2.0) / (Ec * (math.pi * sk_t) ** 2.0)
```

```
kc_star = kc * math.pi ** 2.0 / (12.0 * (1.0 - poisson ** 2.0))
```

```
# Write the excel data
```

```
excel_dic["Skin_length_y"].append(sk_y / 3.0)
```

```
excel_dic["Skin_thickness"].append(sk_t)
```

```
excel_dic["Stringer_height"].append(str_h)
```

```
excel_dic["Stringer_c_width"].append(str_c)
```

```
excel_dic["Stringer_b_width"].append(str_b)
```

```
excel_dic["Stringer_thickness"].append(str_t)
```

```
excel_dic["kc"].append(kc)
```

```
# Write the input data
```

```
results.write("%-25s %6.2f %-20s %6.2f %-20s %6.2f %-20s %6.2f %-20s %6.2f %-20s %6.2f %-"
              "20s %6.2f" % (" Skin length y: ", (sk_y / 3.0), " Skin thickness: ", sk_t, " Stringer height: ", str_h, " Stringer c width: ", str_c, " Stringer b width: ", str_b, " Stringer thickness: ", str_t) + "\n")
```

```
# Write the output data
```

```
results.write("%-25s %6.2f %-20s %6.2f %-20s %6.2f %-20s %6.2f" % (" Eigenvalue: ", eigenvalue, " Fccr: ", Fccr, " kc_star: ", kc_star) + "\n")
```

```
results.write("%-25s %6.3f %-20s %6.3f %-20s %6.3f %-20s %6.3f" % (" kc: ", kc, " Bruhn kc(clamped): ", kc_bruhn[0], " Bruhn kc(ss): ", kc_bruhn[1]) + "\n" + "\n")
```

```
except:
```

```
    None
```

```
# Excel output results are written into the output file
```

```
for excel_key, excel_data in excel_dic.items():
```

```
    results_excel.write("%-20s" % (excel_key))
```

```
    for excel_var in excel_data:
```

```
        results_excel.write("%8.2f" % (excel_var))
```

```
    results_excel.write("\n")
```

```
if excel_key == "kc":
```

```
    results_excel.write("\n")
```



```

results.close()
results_excel.close()

# Saving the model
mdb.saveAs(pathName=save_path+'.cae')

# Stopping the time calculator
end_t_time = time.time()
m=divmod(end_t_time-start_t_time,60)
n=divmod(m[0],60)
print "Total time: " ,n[0],n[1],m[1]

```

F.3 ANN Matlab Script

```

% Clearing the workspace and command window
clc; clear all; close all;
warning('off','MATLAB:xlswrite:AddSheet');
% Interval of ANN parameters which is tried to get max. performance in ANN.
% Order T,Z,J
% neurons = {[6],[6],[8]};
% ratios = {[70,20,10],[90,5,5],[70,15,15]};
types = ['T','Z','J'];
neurons = {[10],[10],[10]};
ratios = {[70,20,10],[70,15,15],[75,15,10]}, ...
{[70,20,10],[70,15,15],[75,15,10]},...
{[70,20,10],[70,15,15],[75,15,10]};
trials = 10;
t_n= length(neurons{1})*length(types)*length(ratios{1})*trials;
t_n_disp = sprintf('Total number of iteration : %d',t_n);
disp(t_n_disp)
i_n=1;
for ii=1:length(types);
type=types(ii);
str_type_disp = sprintf('Stringer type : %s',type);
disp(str_type_disp)
% Opening excel file to read ANN database inputs, additional ten sample
% cases input and output values
data = xlsread('ANN_abaqus.xlsx',strcat('Data_',type));
sample = xlsread('ANN_abaqus.xlsx',strcat('Sample_',type));
fem_output = xlsread('ANN_abaqus.xlsx',...
strcat('Sample_Results_',type),'B1:K1');
% Input matrix is rearranged.
num_data = size(data,1);
for kk=3:1:num_data;
input(kk-2,:)=data(kk,:);
end
target = data(1,:);
for nn=1:length(neurons{ii});
neuron = neurons{ii}(nn);
pre_rse = 1.0;
for rr=1:length(ratios{ii});
ratio = ratios{ii}{rr};
for ss=1:trials;
network = fitnet(neuron);

```

```

network.inputs{1}.processFcns = {'removeconstantrows',...
'mapminmax'};
network.outputs{2}.processFcns = {'removeconstantrows',...
'mapminmax'};
network.divideFcn = 'dividerand';
network.divideMode = 'sample';
% Configuring the ANN parameters to use in training itself
network.divideParam.trainRatio = ratio(1)/100;
network.divideParam.valRatio = ratio(2)/100;
network.divideParam.testRatio = ratio(3)/100;
network.trainFcn = 'trainlm';
network.performFcn = 'mse';
% Parameters can be changed after the training method
% described ('trainlm')
network.trainParam.max_fail = 500;
network.trainParam.epochs = 1500;
network.plotFcns = {'plotperform','plottrainstate',...
'ploterrhist','plotregression','plotfit'};
[network,tr] = train(network,input,target);
% ANN results, errors and performance values are stored.
output = network(input);
error = gsubtract(target,output);
performance = perform(network,target,output);
% Target input values are stored to calculate performances
% of ANN.
trainTargets = target .* tr.trainMask{1};
valTargets = target .* tr.valMask{1};
testTargets = target .* tr.testMask{1};
% ANN performances are calculated.
trainPerformance = perform(network,trainTargets,output);
valPerformance = perform(network,valTargets,output);
testPerformance = perform(network,testTargets,output);
% Root square error is calculated according to results of
% additional ten FE analyses.
sample_output = network(sample) ;
square_error = 0;
for ff=1:1:length(fem_output);
square_error=square_error+(fem_output(ff)- ...
sample_output(ff))^2;
end
rse = (square_error/length(fem_output))^0.5;
% If the previous root square error is greater than current
% calculated value, current ANN paramters are saved to
% workspace.
if pre_rse>rse;
% Creating the performance plot and
% then saving the plot
plotperform(tr);
saveas(gcf,strcat('perf_',type,'.png'));
% Creating the training state values plot and
% then saving the plot
plottrainstate(tr)
saveas(gcf,strcat('trn_',type,'.png'));

```

```

% Creating the regression plot and then saving the plot
trOut = output(tr.trainInd);
vOut = output(tr.valInd);
tsOut = output(tr.testInd);
trTarg = target(tr.trainInd);
vTarg = target(tr.valInd);
tsTarg = target(tr.testInd);
plotregression(trTarg, trOut, 'Train', vTarg, vOut, ...
'Validation', tsTarg, tsOut, 'Testing',...
target, output, 'All')
saveas(gcf, strcat('regr_', type, '.png'));
% Closing all figures
close all;
% Saving results into the workspace
eval([strcat('data_', type) '=data;']);
eval([strcat('sample_', type) '=sample;']);
eval([strcat('input_', type) '=input;']);
eval([strcat('target_', type) '=target;']);
eval([strcat('neuron_', type) '=neuron;']);
eval([strcat('ratio_', type) '=ratio;']);
eval([strcat('network_', type) '=network;']);
eval([strcat('tr_', type) '=tr;']);
eval([strcat('output_', type) '=output;']);
eval([strcat('error_', type) '=error;']);
eval([strcat('performance_', type) '=performance;']);
eval([strcat('trainTargets_', type) '=trainTargets;']);
eval([strcat('valTargets_', type) '=valTargets;']);
eval([strcat('testTargets_', type) '=testTargets;']);
eval([strcat('trainPerformance_', type)...
'=trainPerformance;']);
eval([strcat('valPerformance_', type)...
'=valPerformance;']);
eval([strcat('testPerformance_', type)...
'=testPerformance;']);
eval([strcat('sample_output_', type)...
'=sample_output;'])
eval([strcat('fem_output_', type)...
'=fem_output;'])
pre_rse=rse;
end
clear network tr output error performance trainTargets ...
valTargets testTargets rse trainPerformance...
valPerformance testPerformance sample_output...
square_error ff
r_n = t_n-i_n;
r_n_disp = sprintf('Remaining number of iteration : %d', r_n);
disp(r_n_disp)
i_n = i_n+1;
end
end
clear ratio neuron pre_rse pre_count ss rr
end
clear data sample input target num_data fem_output nn kk

```

```

% Final reslts of additional ten analyses are written into the excel
% file.
sample_output_tmp = eval(strcat('sample_output_',type));
for ee=1:1:length(sample_output_tmp);
range=sprintf('%c','A'+ee,'3');
xlswrite('ANN_abaqus.xlsx',sample_output_tmp(ee),...
strcat('Sample_Results_',type), range);
end
clear range sample_output_tmp ee type
end
clear ii i_n r_n t_n
% Saving the ANN workspace.
save ANN_workspace.mat;
% Opening the excel file.
winopen('ANN_abaqus.xlsx');
disp('Calculation is over!');

```

F.4 Metal Stiffened Panel Post-Buckling Python Scripts

- Example code to construct the skin-stringer model with I stringer section

```

# Importing necessary modules
from part import *
from material import *
from section import *
from assembly import *
from step import *
from interaction import *
from load import *
from mesh import *
from optimization import *
from job import *
from sketch import *
from visualization import *
from connectorBehavior import *
import math
import time

# Counter for script time
start_t_time = time.time()

# Paths
save_path='C:/Users/...../Model/Model_I/v6_i'

# Initialize result file
results = open(r"C:\Users\.....\Results\Model_I\output_I_min_inertia.txt","w+")

# Given displacement load (mm)
Disp_load = -2.0

# Element size of parts (mm)
ele_size_sk = 5.0
ele_size_str = 2.0

# Material properties (Al 2024 T3 Sheet thk: 0.23-3.25 mm)
Ec = 73774.0

```

```

E = 72395.0
density = 2768.0
poisson = 0.33
Fcy = 269.0
nc = 15.0

# Skin geometry
sk_x = 450.0
sk_ys = [150.0*3.0]
sk_ts = [0.813]

# Stringer "I" geometry
str_l = 450.0
str_ts = [1.016]
str_hs = [25.0]
str_cs = [20.0]
str_bs = [15.0]

# Fasteners' diameter
fast_d = 3.2

# Total number of models which will be created in this script
total_count = 4*len(str_hs)*len(str_cs)*len(str_bs)*len(str_ts)*len(sk_ts)*len(sk_ys)
print "Total model number: ", total_count

# Function of flat metal panel compressive buckling coefficient
def graph_Kc_flat(x,bc):
    """
    Ref: Analysis and Design of Flight Vehicle Structures - E.F.Bruhn
    Kc is obtained from Figure C5.2 for flat panels
    Loaded edges are clamped.
    Conditions are only exceptable for unloaded edges
    """
    if bc=='cl':
        if x < 0.76493:
            y = -56.0565*x + 57.1876
        elif (0.76493 <= x) and (x < 1.14273):
            y = -551.9651*pow(x, 4) + 2079.3509*pow(x, 3) - 2870.2033*pow(x, 2) + 1706.6187*x - 353.426
        elif (1.14273 <= x) and (x < 1.85911):
            y = -6.1616*pow(x, 3) + 34.8139*pow(x, 2) - 65.0106*x + 48.5687
        elif (1.85911 <= x) and (x < 2.3433):
            y = -15.9873*pow(x, 4) + 127.1208*pow(x, 3) - 373.7913*pow(x, 2) + 479.4634*x - 216.8528
        elif (2.3433 <= x) and (x < 3.3987):
            y = 13.6994*pow(x, 5) - 198.9195*pow(x, 4) + 1149.7887*pow(x, 3) - 3306.5735*pow(x, 2) + 4730.1783*x - 2684.554
        elif (3.3987 <= x) and (x < 4.15706):
            y = 10.807*pow(x, 4) - 163.8182*pow(x, 3) + 929.1075*pow(x, 2) - 2336.7822*x + 2206.491
        elif (4.15706 <= x) and (x <= 5.0142):
            y = 1.9679*pow(x, 3) - 27.1906*pow(x, 2) + 124.8755*x - 183.3227
        else:
            y = 7.2802
        return y
    elif bc=='ss':
        if x < 1.33459:
            y = 116.1071*pow(x, 4) - 512.1754*pow(x, 3) + 847.8765*pow(x, 2) - 628.8651*x + 183.9239
        elif (1.33459 <= x) and (x < 1.68636):
            y = 2.5557*pow(x, 2) - 8.0374*x + 11.8528
        elif (1.68636 <= x) and (x < 2.76429):
            y = 12.4466*pow(x, 6) - 166.4906*pow(x, 5) + 921.7798*pow(x, 4) - 2704.0495*pow(x, 3) + 4434.9741*pow(x, 2) - 3860.3466*x + 1400.7332
        elif (2.76429 <= x) and (x <= 4.95153):

```

```

    y = -
0.2663*pow(x, 5) + 5.2351*pow(x, 4) - 40.8202*pow(x, 3) + 157.8018*pow(x, 2) - 302.6058*x + 234.8432
    else:
        y = 4.2274
    return y

# Function of flat metal panel shear buckling coefficient
def graph_Ks_flat(x,bc):
    """
    Ref: Analysis and Design of Flight Vehicle Structures - E.F.Bruhn
    Ks is obtained from Figure C5.11 for flat panels
    Loaded edges are clamped.
    Conditions are only exceptable for unloaded edges
    """
    if bc=='cl':
        if x < 1.39646:
            y = 617.3722*pow(x, 4) - 3049.2054*pow(x, 3) + 5640.7618*pow(x, 2) - 4637.94*x + 1444.5082
        elif (1.39646 <= x) and (x < 2.79647):
            y = -0.2876*pow(x, 3) + 3.08*pow(x, 2) - 10.558*x + 21.4866
        elif (2.79647 <= x) and (x < 5.0):
            y = 0.2326*pow(x, 5) - 4.577*pow(x, 4) + 35.6865*pow(x, 3) - 137.6532*pow(x, 2) + 262.3421*x - 18
7.6865
        else:
            y = 9.6226
        return y
    elif bc=='ss':
        if x < 1.79125:
            y = -
23.165*pow(x, 6) + 154.3269*pow(x, 5) - 380.7138*pow(x, 4) + 376.5476*pow(x, 3) - 1.3356*pow(x, 2) - 2
51.0012*x + 135.069
        elif (x <= 1.79125) and (x < 2.57994):
            y = 0.1192*pow(x, 3) - 0.7131*pow(x, 2) + 0.5982*x + 7.1608
        elif (x <= 2.57994) and (x < 3.70882):
            y = 0.075*pow(x, 3) - 0.3925*pow(x, 2) + 0.0756*x + 7.135
        elif (x <= 3.70882) and (x < 5.0):
            y = -0.2125*x + 6.6311
        else:
            y = 5.5684
        return y

# Function of plasticity correction
def get_plastic_stress(nc,Fscr_el,Ec,Fcy):
    """
    See HSB 52100-01 plasticity correction
    """
    return Fcr

for sk_y_key,sk_y in enumerate(sk_ys):
    for sk_t_key,sk_t in enumerate(sk_ts):
        sk_ratio = sk_x / (sk_y/3.0)
        Ireqs = []
        K_values = []

        # Unloaded edge boundary conditions (clamped or simply supported)
        for bc in ["cl","ss"]:
            Ks = graph_Ks_flat(sk_ratio,bc)
            Kc = graph_Kc_flat(sk_ratio,bc)
            K_value = [Ks,Kc]
            K_values.append(K_value)
            Fscr_el = Ks*math.pi**2.0*Ec/(12.0*(1.0-poisson**2.0))*(sk_t/(sk_y/3.0))**2.0
            Fscr = get_plastic_stress(nc,Fscr_el,Ec,Fcy)

```

```

Ireq = (2.29*sk_x/sk_t)*(Fscr*sk_t*((sk_y/3.0)**2.0)/(33.0*E))**(4.0/3.0)
Ireqs.append(Ireq)
Ireq_moi=max(Ireqs)

# Results of panels with classical boundary conditions and minimum required inertia are written into the result file
results.write("%-15s %6.2f %-
15s %6.2f" %("Skin length y: ",(sk_y/3.0)," Skin thickness: ",sk_t)+"\n")
results.write("%-30s %-15s %6.2f %-
30s %6.2f" %("Min. stiffener inertia", "For clamped: ",Ireqs[0]," For simply supported",Ireqs[1])+"\n")
results.write("%-30s %-15s %6.2f %-
30s %6.2f" %("Shear buckling coefficient", "For clamped: ",K_values[0][0]," For simply supported",K_values[1][0])+"\n")
results.write("%-30s %-15s %6.2f %-
30s %6.2f" %("Compressive buckling coefficient", "For clamped: ",K_values[0][1]," For simply supported",K_values[1][1])+"\n"+"")

for str_h_key,str_h in enumerate(str_hs):
    for str_c_key,str_c in enumerate(str_cs):
        for str_b_key,str_b in enumerate(str_bs):
            for str_t_key,str_t in enumerate(str_ts):
                # Second moment of inertia and area of stringer are calculated
                r1_dx = str_b
                r1_dy = str_t
                r2_dx = str_t
                r2_dy = str_h-2.0*str_t
                r3_dx = str_c
                r3_dy = str_t
                r1_A = r1_dx * r1_dy
                r2_A = r2_dx * r2_dy
                r3_A = r3_dx * r3_dy
                r1_Ix = (1.0 / 12.0) * r1_dx * r1_dy**3.0
                r2_Ix = (1.0 / 12.0) * r2_dx * r2_dy**3.0
                r3_Ix = (1.0 / 12.0) * r3_dx * r3_dy**3.0
                parts = [
                    {'dx_cg': max(r1_dx,r3_dx) / 2.0, 'dy_cg': r1_dy / 2.0, 'A':r1_A, 'Ix':r1_Ix},
                    {'dx_cg': max(r1_dx,r3_dx) / 2.0, 'dy_cg': r1_dy + r2_dy / 2.0, 'A':r2_A, 'Ix':r2_Ix},
                    {'dx_cg': max(r1_dx,r3_dx) / 2.0, 'dy_cg': r1_dy + r2_dy + r3_dy / 2.0, 'A':r3_A, 'Ix':r3_Ix},
                ]
                Ad_t = 0.0
                A_t = 0.0
                for part in parts:
                    Ad_t += part['A'] * part['dy_cg']
                    A_t += part['A']
                cg_y = Ad_t / A_t
                Istr = 0.0
                for part in parts:
                    Istr += (part['Ix'] + part['A'] * part['dy_cg']** 2.0 - cg_y * part['A'] * part['dy_cg'])

                # Geometric properties of stringer are written into the result file
                results.write("%-25s %6.2f %-20s %6.2f %-20s %6.2f %-
20s %6.2f" %(" Stringer heigth: ",str_h, " Stringer c width: ",str_c, " Stringer b width: ",str_b," Stringer thickness: ",str_t)+"\n")
                results.write("%-25s %6.2f %-
25s %6.2f" %(" Stiffener inertia: ",Istr, " Stiffener area:",A_t)+"\n"+"")

                # To satisfy the stiffened panel condition, stringer inertia is checked.
                if Ireq_moi<Istr:
                    # Model 0
                    # Creating model of panel buckling (pb)

```

```

model_name = "0_pb_I_"+str(str_h_key)+str(str_c_key)+str(str_b_key)+str(str_t_key)+str(sk_
t_key)+str(sk_y_key)
mdb.Model(modelType=STANDARD_EXPLICIT, name=model_name)
mn=mdb.models[model_name]

# Creating material
mn.Material(name='Al_2024_T3_Sheet')
mn.materials['Al_2024_T3_Sheet'].Elastic(table=((Ec, poisson), ))
mn.materials['Al_2024_T3_Sheet'].Density(table=((density, ), ))

# Creating sketch of skin
mn.ConstrainedSketch(name='__profile__', sheetSize=200.0)
mn.sketches['__profile__'].rectangle(point1=(0.0, 0.0), point2=(sk_x, sk_y/3.0))

# Creating part of skin
mn.Part(dimensionality=THREE_D, name='Skin', type=DEFORMABLE_BODY)
mn.parts['Skin'].BaseShell(sketch=mn.sketches['__profile__'])
del mn.sketches['__profile__']

# Creating skin section
mn.HomogeneousShellSection(name='Skin_Sec',
preIntegrate=OFF, material='Al_2024_T3_Sheet', thicknessType=UNIFORM,
thickness=sk_t, thicknessField="", idealization=NO_IDEALIZATION,
poissonDefinition=DEFAULT, thicknessModulus=None, temperature=GRADIENT,
useDensity=OFF, integrationRule=SIMPSON, numIntPts=5)

# Assigning skin section
p_sk = mn.parts['Skin']
f_sk, e_sk, d_sk = p_sk.faces, p_sk.edges, p_sk.datums
faces = f_sk.getSequenceFromMask(mask=('[#1 ]', ), )
region = p_sk.Set(faces=faces, name='Skin_faces_set')
p_sk.SectionAssignment(region=region, sectionName='Skin_Sec', offset=0.0,
offsetType=MIDDLE_SURFACE, offsetField="",
thicknessAssignment=FROM_SECTION)

# Mesh control of skin
pickedRegions = f_sk.getSequenceFromMask(mask=('[#1 ]', ), )
p_sk.setMeshControls(regions=pickedRegions, elemShape=QUAD, technique=SWEEP)

# Mesh seed of skin
p_sk.seedPart(deviationFactor=0.1, minSizeFactor=0.1, size=ele_size_sk)

# Generate mesh of skin
p_sk.generateMesh()

# Creating Buckling step
mn.BuckleStep(name='Buckle-
Step', previous='Initial', numEigen=3, vectors=28, maxIterations=3000)

# Creating assembly instances
a_ss = mn.rootAssembly
a_ss.DatumCsysByDefault(CARTESIAN)
a_ss.Instance(dependent=ON, name='Skin-1', part=p_sk)

# Creating boundary conditions at initial step
v_sk = a_ss.instances['Skin-1'].vertices
e_sk = a_ss.instances['Skin-1'].edges
n_sk = a_ss.instances['Skin-1'].nodes

# Creating boundary conditions sets
verts1 = v_sk.getSequenceFromMask(mask=('[#8 ]', ), )

```



```

verts2 = v_sk.getSequenceFromMask(mask=['[#2 ]', ],)
a_ss.Set(vertices=verts1, name='Set_reaction_cor_point')
a_ss.Set(vertices=verts2, name='Set_loaded_cor_point')
dict_bc = {'[#5 ]': 'side_edges', '#2 ]': 'load_edge', '#8 ]': 'reaction_edge'}
for key_bc, str_bc in dict_bc.items():
    if str_bc=='reaction_edge':
        mask_node_ids=(
            '[#1 #0 #8000000 #0:2 #400000 #0:2 #20000',
            '#0:2 #1000 #0:2 #80 #0:2 #4 #0',
            '#20000000 #0:2 #1000000 #0:2 #80000 #0:2 #4000',
            '#0:2 #200 #0:2 #10 #0 #80000000 #0:2',
            '#4000000 #0:2 #200000 #0:2 #10000 #0:2 #800',
            '#0:2 #40 #0:2 #2 #0 #10000000 #0:2',
            '#800000 #0:2 #40000 #0:2 #2000 #0:2 #100',
            '#0:2 #8 #0 #40000000 #0:2 #2000000 #0:2',
            '#100000 #0:2 #8000 #0:2 #400 ]',)
        nodes1 = n_sk.getSequenceFromMask(mask=mask_node_ids, )
        a_ss.Set(nodes=nodes1, name='Set_'+str_bc)
    else:
        edges1 = e_sk.getSequenceFromMask(mask=(key_bc, ),)
        a_ss.Set(edges=edges1, name='Set_'+str_bc)

# Assigning boundary conditions on sets
region = a_ss.sets['Set_reaction_cor_point']
mn.DisplacementBC(name='BC_reac_cor_point',
    createStepName='Initial', region=region, u1=UNSET, u2=SET, u3=UNSET,
    ur1=UNSET, ur2=UNSET, ur3=UNSET, amplitude=UNSET, distributionType=UNIFORM,
    fieldName="", localCsys=None)
region = a_ss.sets['Set_side_edges']
mn.DisplacementBC(name='BC_side_edges',
    createStepName='Initial', region=region, u1=UNSET, u2=UNSET, u3=SET,
    ur1=SET, ur2=UNSET, ur3=UNSET, amplitude=UNSET, distributionType=UNIFORM,
    fieldName="", localCsys=None)
region = a_ss.sets['Set_load_edge']
mn.DisplacementBC(name='BC_load_edge',
    createStepName='Initial', region=region, u1=UNSET, u2=UNSET, u3=SET,
    ur1=UNSET, ur2=SET, ur3=UNSET, amplitude=UNSET, distributionType=UNIFORM,
    fieldName="", localCsys=None)
region = a_ss.sets['Set_reaction_edge']
mn.DisplacementBC(name='BC_reaction_edge',
    createStepName='Initial', region=region, u1=SET, u2=UNSET, u3=SET,
    ur1=UNSET, ur2=SET, ur3=UNSET, amplitude=UNSET, distributionType=UNIFORM,
    fieldName="", localCsys=None)

# Modifying boundary conditions at buckle step
mn.boundaryConditions['BC_load_edge'].setValuesInStep(
    stepName='Buckle-Step', u1=Disp_load, buckleCase=PERTURBATION_AND_BUCKLING)

# Creating job
job_name = 'job_'+ model_name
mdb.Job(name=job_name, model=model_name, description="", type=ANALYSIS,
    atTime=None, waitMinutes=0, waitHours=0, queue=None, memory=90,
    memoryUnits=PERCENTAGE, getMemoryFromAnalysis=True,
    explicitPrecision=SINGLE, nodalOutputPrecision=SINGLE, echoPrint=OFF,
    modelPrint=OFF, contactPrint=OFF, historyPrint=OFF, userSubroutine="",
    scratch="", resultsFormat=ODB, multiprocessingMode=DEFAULT, numCpus=1,
    numGPUs=0)

"""
!!!!!!!!!!!!!!!!!!!!!!!!!!!!
!!!!!!!!!!!!!!!!!!!!!!!!!!!!

```



```

s.CoincidentConstraint(entity1=v[9], entity2=g[3], addUndoState=False)
pickedFaces = f_sk.getSequenceFromMask(mask=('[#1 ]', ), )
p_sk.PartitionFaceBySketch(sketchUpEdge=e_sk[2], faces=pickedFaces, sketch=s)
s.unsetPrimaryObject()
del mn.sketches['_profile_']

# Creating skin section
mn.HomogeneousShellSection(name='Skin_Sec',
    preIntegrate=OFF, material='Al_2024_T3_Sheet', thicknessType=UNIFORM,
    thickness=sk_t, thicknessField="", idealization=NO_IDEALIZATION,
    poissonDefinition=DEFAULT, thicknessModulus=None, temperature=GRADIENT,
    useDensity=OFF, integrationRule=SIMPSON, numIntPts=5)

# Assigning skin section
faces = f_sk.getSequenceFromMask(mask=('[#f ]', ), )
region = p_sk.Set(faces=faces, name='Skin_faces_set')
p_sk.SectionAssignment(region=region, sectionName='Skin_Sec', offset=0.0,
    offsetType=MIDDLE_SURFACE, offsetField="",
    thicknessAssignment=FROM_SECTION)

# Mesh control of skin
pickedRegions = f_sk.getSequenceFromMask(mask=('[#f ]', ), )
p_sk.setMeshControls(regions=pickedRegions, elemShape=QUAD, technique=SWEEP)

# Mesh seed of skin
p_sk.seedPart(deviationFactor=0.1, minSizeFactor=0.1, size=ele_size_sk)

# Generate mesh of skin
p_sk.generateMesh()

# Creating sketch of stringer
s = mn.ConstrainedSketch(name='_profile_', sheetSize=200.0)
g, v, d, c = s.geometry, s.vertices, s.dimensions, s.constraints
s.setPrimaryObject(option=STANDALONE)
s.Line(point1=(-str_c*0.5, 0.0), point2=(str_c*0.5, 0.0))
s.HorizontalConstraint(entity=g[2], addUndoState=False)
s.Line(point1=(-str_b*0.5, str_h), point2=(str_b*0.5, str_h))
s.HorizontalConstraint(entity=g[3], addUndoState=False)
s.Line(point1=(0.0, 0.0), point2=(0.0, str_h))
s.VerticalConstraint(entity=g[4], addUndoState=False)
s.PerpendicularConstraint(entity1=g[2], entity2=g[4], addUndoState=False)
s.CoincidentConstraint(entity1=v[4], entity2=g[2], addUndoState=False)
s.EqualDistanceConstraint(entity1=v[0], entity2=v[1], midpoint=v[4], addUndoState=False)

s.EqualDistanceConstraint(entity1=v[2], entity2=v[3], midpoint=v[5], addUndoState=False)

# Creating part of stringer
mn.Part(name='Stringer', dimensionality=THREE_D, type=DEFORMABLE_BODY)
mn.parts['Stringer'].BaseShellExtrude(sketch=s, depth=str_l)
del mn.sketches['_profile_']

# Creating stringer section
mn.HomogeneousShellSection(name='Stringer_Sec',
    preIntegrate=OFF, material='Al_2024_T3_Sheet', thicknessType=UNIFORM,
    thickness=str_t, thicknessField="", idealization=NO_IDEALIZATION,
    poissonDefinition=DEFAULT, thicknessModulus=None, temperature=GRADIENT,
    useDensity=OFF, integrationRule=SIMPSON, numIntPts=5)

# Assigning stringer section
p_str = mn.parts['Stringer']

```

```

f_str = p_str.faces
faces = f_str.getSequenceFromMask(mask=['[#1f]', ],)
region = p_str.Set(faces=faces, name='Stringer_faces_set')
p_str.SectionAssignment(region=region, sectionName='Stringer_Sec', offset=0.0,
    offsetType=MIDDLE_SURFACE, offsetField="",
    thicknessAssignment=FROM_SECTION)

# Mesh control of stringer
pickedRegions = f_str.getSequenceFromMask(mask=['[#1f]', ],)
p_str.setMeshControls(regions=pickedRegions, elemShape=QUAD, technique=SWEEP)

# Mesh seed of stringer
p_str.seedPart(deviationFactor=0.1, minSizeFactor=0.1, size=2.0)

# Generate mesh of stringer
p_str.generateMesh()

# Creating buckling step
mn.BuckleStep(name='Buckle-
Step', previous='Initial', numEigen=3, vectors=28, maxIterations=3000)

# Creating assembly instances
a_ss = mn.rootAssembly
a_ss.DatumCsysByDefault(CARTESIAN)
a_ss.Instance(dependent=ON, name='Skin-1', part=p_sk)

# Creating Stringer 1
mn.rootAssembly.DatumCsysByDefault(CARTESIAN)
mn.rootAssembly.Instance(dependent=ON, name='Stringer-1', part=p_str)

# Stringer 1 place is decided
a_ss.rotate(instanceList=('Stringer-
1', ), axisPoint=(0.0, 0.0, 0.0), axisDirection=(0.0, 1.0, 0.0), angle=90.0)
a_ss.rotate(instanceList=('Stringer-
1', ), axisPoint=(0.0, 0.0, 0.0), axisDirection=(1.0, 0.0, 0.0), angle=90.0)
a_ss.translate(instanceList=('Stringer-1', ), vector=(0.0, sk_y/3.0, (sk_t+str_t)*0.5))

# Creating Stringer 2
a_ss.LinearInstancePattern(instanceList=('Stringer-
1', ), direction1=(1.0, 0.0, 0.0), direction2=(0.0, 1.0, 0.0), number1=1, number2=2, spacing1=str_l, spacing2
=sk_y/3.0)
a_ss.features.changeKey(fromName='Stringer-1-lin-1-2', toName='Stringer-2')

# Creating connector section as beam
mn.ConnectorSection(name='Fastener_Con_Sec', assembledType=BEAM)

# Creating fasteners
const_attach = [['[#20 ]',4,1,'1'],['[#4 ]',2,0,'2']]
for key in range(2):
    e_str = a_ss.instances['Stringer-'+str(key+1)].edges
    v_str = a_ss.instances['Stringer-'+str(key+1)].vertices
    f_str = a_ss.instances['Stringer-'+str(key+1)].faces
    for const in const_attach:
        # Creating attachment points
        edges1 = e_str.getSequenceFromMask(mask=(const[0], ),)
        geomEdges=edges1
        a_ss.AttachmentPointsOffsetFromEdges(edges=geomEdges, startPoint=v_str[const[1]],
            referenceFace=f_str[const[2]], name='Str'+str(key+1)+'-Attachment Points-
'+const[3],
            pointCreationMethod=BY_NUMBER, offsetFromStartPoint=2.0*fast_d+1.0, numberOfP
oints=27,

```

```

        offsetFromEndPoint=2.0*fast_d+1.0, numberOfRows=1, offsetFromEdges= str_c*0.25,

        patterningMethod=PATTERN_ORTHOGONALLY, setName='Str'+str(key+1)+'-
Attachment Points-Set '+const[3])

        # Assigning a section to fastener
        region=a_ss.sets['Str'+str(key+1)+'-Attachment Points-Set '+const[3]]
        a_ss.engineeringFeatures.PointFastener( name='Str'+str(key+1)+'-Fasteners-
'+const[3], region=region,
        sectionName='Fastener_Con_Sec', directionVector=(v_str[7], a_ss.instances['Stringer-
'+str(key+1)].
        InterestingPoint(edge=e_str[8], rule=MIDDLE)), physicalRadius=fast_d*0.5, additional
Mass=0.0001)

        # Creating boundary conditions at initial step
        v_sk = a_ss.instances['Skin-1'].vertices
        e_sk = a_ss.instances['Skin-1'].edges
        n_sk = a_ss.instances['Skin-1'].nodes

        # Creating boundary conditions sets
        verts1 = v_sk.getSequenceFromMask(mask=('[#200 ]', ), )
        verts2 = v_sk.getSequenceFromMask(mask=('[#100 ]', ), )
        a_ss.Set(vertices=verts1, name='Set_reaction_mid_point')
        a_ss.Set(vertices=verts2, name='Set_loaded_mid_point')
        dict_bc = {'[#44 ]':'side_edges', '#c28 ]':'load_edge', '#1282 ]':'reaction_edge'}
        for key_bc, str_bc in dict_bc.items():
            if str_bc=='reaction_edge':
                nodes1 = n_sk.getSequenceFromMask(mask=('[#296 #0:2 #ffffff8 #0:10 #ffffffe0 #3 #0
', '#f8000000 #1ff #7ffe0 ]', ), )
                a_ss.Set(nodes=nodes1, name='Set_'+str_bc)
            else:
                edges1 = e_sk.getSequenceFromMask(mask=(key_bc, ), )
                a_ss.Set(edges=edges1, name='Set_'+str_bc)

        # Assigning boundary conditions on sets
        region = a_ss.sets['Set_reaction_mid_point']
        mn.DisplacementBC(name='BC_reac_mid_point',
        createStepName='Initial', region=region, u1=UNSET, u2=SET, u3=UNSET,
        ur1=UNSET, ur2=UNSET, ur3=UNSET, amplitude=UNSET, distributionType=UNIFORM,
        fieldName="", localCsys=None)
        region = a_ss.sets['Set_side_edges']
        mn.DisplacementBC(name='BC_side_edges',
        createStepName='Initial', region=region, u1=UNSET, u2=UNSET, u3=SET,
        ur1=SET, ur2=UNSET, ur3=UNSET, amplitude=UNSET, distributionType=UNIFORM,
        fieldName="", localCsys=None)
        region = a_ss.sets['Set_load_edge']
        mn.DisplacementBC(name='BC_load_edge',
        createStepName='Initial', region=region, u1=UNSET, u2=UNSET, u3=SET,
        ur1=UNSET, ur2=SET, ur3=UNSET, amplitude=UNSET, distributionType=UNIFORM,
        fieldName="", localCsys=None)
        region = a_ss.sets['Set_reaction_edge']
        mn.DisplacementBC(name='BC_reaction_edge',
        createStepName='Initial', region=region, u1=SET, u2=UNSET, u3=SET,
        ur1=UNSET, ur2=SET, ur3=UNSET, amplitude=UNSET, distributionType=UNIFORM,
        fieldName="", localCsys=None)

        # Modifying boundary conditions at buckle step
        mn.boundaryConditions['BC_load_edge'].setValuesInStep(
        stepName='Buckle-Step', u1=Disp_load, buckleCase=PERTURBATION_AND_BUCKLING)

        # Creating job

```



```

s.PerpendicularConstraint(entity1=g[5], entity2=g[6], addUndoState=False)
s.CoincidentConstraint(entity1=v[4], entity2=g[5], addUndoState=False)
s.CoincidentConstraint(entity1=v[5], entity2=g[3], addUndoState=False)
s.Line(point1=(0, sk_x*0.5), point2=(0, -sk_x*0.5))
s.VerticalConstraint(entity=g[7], addUndoState=False)
s.PerpendicularConstraint(entity1=g[5], entity2=g[7], addUndoState=False)
s.CoincidentConstraint(entity1=v[6], entity2=g[5], addUndoState=False)
s.CoincidentConstraint(entity1=v[7], entity2=g[3], addUndoState=False)
s.Line(point1=(sk_y/6.0, sk_x*0.5), point2=(sk_y/6.0, -sk_x*0.5))
s.VerticalConstraint(entity=g[8], addUndoState=False)
s.PerpendicularConstraint(entity1=g[5], entity2=g[8], addUndoState=False)
s.CoincidentConstraint(entity1=v[8], entity2=g[5], addUndoState=False)
s.CoincidentConstraint(entity1=v[9], entity2=g[3], addUndoState=False)
pickedFaces = f_sk.getSequenceFromMask(mask=['[#1]', ], )
p_sk.PartitionFaceBySketch(sketchUpEdge=e_sk[2], faces=pickedFaces, sketch=s)
s.unsetPrimaryObject()
del mn.sketches['_profile_']

# Creating skin section
mn.HomogeneousShellSection(name='Skin_Sec',
    preIntegrate=OFF, material='Al_2024_T3_Sheet', thicknessType=UNIFORM,
    thickness=sk_t, thicknessField='', idealization=NO_IDEALIZATION,
    poissonDefinition=DEFAULT, thicknessModulus=None, temperature=GRADIENT,
    useDensity=OFF, integrationRule=SIMPSON, numIntPts=5)

# Assigning skin section
faces = f_sk.getSequenceFromMask(mask=['[#f]', ], )
region = p_sk.Set(faces=faces, name='Skin_faces_set')
p_sk.SectionAssignment(region=region, sectionName='Skin_Sec', offset=0.0,
    offsetType=MIDDLE_SURFACE, offsetField='',
    thicknessAssignment=FROM_SECTION)

# Mesh control of skin
pickedRegions = f_sk.getSequenceFromMask(mask=['[#f]', ], )
p_sk.setMeshControls(regions=pickedRegions, elemShape=QUAD, technique=SWEEP)

# Mesh seed of skin
p_sk.seedPart(deviationFactor=0.1, minSizeFactor=0.1, size=ele_size_sk)

# Generate mesh of skin
p_sk.generateMesh()

# Creating sketch of stringer
s = mn.ConstrainedSketch(name='_profile_', sheetSize=200.0)
g, v, d, c = s.geometry, s.vertices, s.dimensions, s.constraints
s.setPrimaryObject(option=STANDALONE)
s.Line(point1=(-str_c*0.5, 0.0), point2=(str_c*0.5, 0.0))
s.HorizontalConstraint(entity=g[2], addUndoState=False)
s.Line(point1=(-str_b*0.5, str_h), point2=(str_b*0.5, str_h))
s.HorizontalConstraint(entity=g[3], addUndoState=False)
s.Line(point1=(0.0, 0.0), point2=(0.0, str_h))
s.VerticalConstraint(entity=g[4], addUndoState=False)
s.PerpendicularConstraint(entity1=g[2], entity2=g[4], addUndoState=False)
s.CoincidentConstraint(entity1=v[4], entity2=g[2], addUndoState=False)
s.EqualDistanceConstraint(entity1=v[0], entity2=v[1], midpoint=v[4], addUndoState=False)

s.EqualDistanceConstraint(entity1=v[2], entity2=v[3], midpoint=v[5], addUndoState=False)

# Creating part of stringer
mn.Part(name='Stringer', dimensionality=THREE_D, type=DEFORMABLE_BODY)

```

```

mn.parts['Stringer'].BaseShellExtrude(sketch=s, depth=str_l)
del mn.sketches['__profile__']

# Creating stringer section
mn.HomogeneousShellSection(name='Stringer_Sec',
preIntegrate=OFF, material='Al_2024_T3_Sheet', thicknessType=UNIFORM,
thickness=str_t, thicknessField="", idealization=NO_IDEALIZATION,
poissonDefinition=DEFAULT, thicknessModulus=None, temperature=GRADIENT,
useDensity=OFF, integrationRule=SIMPSON, numIntPts=5)

# Assigning stringer section
p_str = mn.parts['Stringer']
f_str = p_str.faces
faces = f_str.getSequenceFromMask(mask=['[#1f]', ],)
region = p_str.Set(faces=faces, name='Stringer_faces_set')
p_str.SectionAssignment(region=region, sectionName='Stringer_Sec', offset=0.0,
offsetType=MIDDLE_SURFACE, offsetField="",
thicknessAssignment=FROM_SECTION)

# Mesh control of stringer
pickedRegions = f_str.getSequenceFromMask(mask=['[#1f]', ],)
p_str.setMeshControls(regions=pickedRegions, elemShape=QUAD, technique=SWEEP)

# Mesh seed of stringer
p_str.seedPart(deviationFactor=0.1, minSizeFactor=0.1, size=ele_size_str)

# Generate mesh of stringer
p_str.generateMesh()

# Creating Post-Buckling step
mn.StaticStep(name='Post-Buckle-Step', previous='Initial',
maxNumInc=150, stabilizationMagnitude=0.0002,
stabilizationMethod=DISSIPATED_ENERGY_FRACTION,
continueDampingFactors=False, adaptiveDampingRatio=0.05, initialInc=0.005,
minInc=1e-05, maxInc=0.2, nlgeom=ON)

# Creating assembly instances
a_ss = mn.rootAssembly
a_ss.DatumCsysByDefault(CARTESIAN)
a_ss.Instance(dependent=ON, name='Skin-1', part=p_sk)

# Creating Stringer 1
mn.rootAssembly.DatumCsysByDefault(CARTESIAN)
mn.rootAssembly.Instance(dependent=ON, name='Stringer-1', part=p_str)

# Stringer 1 place is decided
a_ss.rotate(instanceList=('Stringer-
1', ), axisPoint=(0.0, 0.0, 0.0), axisDirection=(0.0, 1.0, 0.0), angle=90.0)
a_ss.rotate(instanceList=('Stringer-
1', ), axisPoint=(0.0, 0.0, 0.0), axisDirection=(1.0, 0.0, 0.0), angle=90.0)
a_ss.translate(instanceList=('Stringer-1', ), vector=(0.0, sk_y/3.0, (sk_t+str_t)*0.5))

# Creating Stringer 2
a_ss.LinearInstancePattern(instanceList=('Stringer-
1', ), direction1=(1.0, 0.0, 0.0), direction2=(0.0, 1.0, 0.0), number1=1, number2=2, spacing1=str_l, spacing2
=sk_y/3.0)
a_ss.features.changeKey(fromName='Stringer-1-lin-1-2', toName='Stringer-2')

# Creating connector section as beam
mn.ConnectorSection(name='Fastener_Con_Sec', assembledType=BEAM)

```



```

# Creating fasteners
const_attach = [['#20'],4,1,'1'],[['#4'],2,0,'2']]
for key in range(2):
    e_str = a_ss.instances['Stringer-'+str(key+1)].edges
    v_str = a_ss.instances['Stringer-'+str(key+1)].vertices
    f_str = a_ss.instances['Stringer-'+str(key+1)].faces
    for const in const_attach:
        # Creating attachment points
        edges1 = e_str.getSequenceFromMask(mask=(const[0],),)
        geomEdges=edges1
        a_ss.AttachmentPointsOffsetFromEdges(edges=geomEdges, startPoint=v_str[const[1]],
        referenceFace=f_str[const[2]], name='Str'+str(key+1)+'-Attachment Points-
'+const[3],
        pointCreationMethod=BY_NUMBER, offsetFromStartPoint=2.0*fast_d+1.0, numberOfP
oints=27,
        offsetFromEndPoint=2.0*fast_d+1.0, numberOfRows=1, offsetFromEdges= str_c*0.25,
        patterningMethod=PATTERN_ORTHOGONALLY, setName='Str'+str(key+1)+'-
Attachment Points-Set '+const[3])

        # Assigning a section to fastener
        region=a_ss.sets['Str'+str(key+1)+'-Attachment Points-Set '+const[3]]
        a_ss.engineeringFeatures.PointFastener( name='Str'+str(key+1)+'-Fasteners-
'+const[3], region=region,
        sectionName='Fastener_Con_Sec', directionVector=(v_str[7], a_ss.instances['Stringer-
'+str(key+1)].
        InterestingPoint(edge=e_str[8], rule=MIDDLE)), physicalRadius=fast_d*0.5, additional
Mass=0.0001)

# Creating boundary conditions at initial step
v_sk = a_ss.instances['Skin-1'].vertices
e_sk = a_ss.instances['Skin-1'].edges
n_sk = a_ss.instances['Skin-1'].nodes

# Creating boundary conditions sets
verts1 = v_sk.getSequenceFromMask(mask=('[#200]',),)
verts2 = v_sk.getSequenceFromMask(mask=('[#100]',),)
a_ss.Set(vertices=verts1, name='Set_reaction_mid_point')
a_ss.Set(vertices=verts2, name='Set_loaded_mid_point')
dict_bc = {'[#44]':'side_edges', '#c28]':'load_edge', '#1282]':'reaction_edge',}
for key_bc, str_bc in dict_bc.items():
    if str_bc=='reaction_edge':
        nodes1 = n_sk.getSequenceFromMask(mask=('[#296 #0:2 #ffffff8 #0:10 #ffffffe0 #3 #0
', '#f8000000 #1ff #7ffe0]',),)
        a_ss.Set(nodes=nodes1, name='Set_'+str_bc)
    else:
        edges1 = e_sk.getSequenceFromMask(mask=(key_bc,),)
        a_ss.Set(edges=edges1, name='Set_'+str_bc)

# Assigning boundary conditions on sets
region = a_ss.sets['Set_reaction_mid_point']
mn.DisplacementBC(name='BC_reac_mid_point',
    createStepName='Initial', region=region, u1=UNSET, u2=SET, u3=UNSET,
    ur1=UNSET, ur2=UNSET, ur3=UNSET, amplitude=UNSET, distributionType=UNIFORM,
    fieldName="", localCsys=None)
region = a_ss.sets['Set_side_edges']
mn.DisplacementBC(name='BC_side_edges',
    createStepName='Initial', region=region, u1=UNSET, u2=UNSET, u3=SET,
    ur1=SET, ur2=UNSET, ur3=UNSET, amplitude=UNSET, distributionType=UNIFORM,
    fieldName="", localCsys=None)
region = a_ss.sets['Set_load_edge']

```



```

!!!!!!!!!!!!!!!!!!!!!!!!!!!!!!
!!!!!!!!!!!!!!!!!!!!!!!!!!!!!!
""

# Model 3
# Creating model of stiffened panel post-buckling-nonlinear (sppbn)
model_name = "3_sppbn_I"+str(str_h_key)+str(str_c_key)+str(str_b_key)+str(str_t_key)+str
(sk_t_key)+str(sk_y_key)
mdb.Model(modelType=STANDARD_EXPLICIT, name=model_name)
mn=mdb.models[model_name]

# Creating material
mn.Material(name='Al_2024_T3_Sheet')
mn.materials['Al_2024_T3_Sheet'].Elastic(table=((Ec, poisson), ))
mn.materials['Al_2024_T3_Sheet'].Density(table=((density, ), ))
mn.materials['Al_2024_T3_Sheet'].Plastic(table=((
271.5582718, 0.0), (272.5980053, 0.000124595), (273.6381335, 0.0002497), (
274.6787599, 0.000375688), (275.7200026, 0.000502975), (276.7619911,
0.000632015), (277.8048658, 0.000763293), (278.8487766, 0.000897323), (
279.8938829, 0.001034642), (280.9403524, 0.00117581), (281.9883612,
0.001321408), (283.0380933, 0.001472038), (284.0897405, 0.001628319), (
285.1435019, 0.001790885), (286.1995841, 0.00196039), (287.2582009,
0.0021375), (288.3195731, 0.002322897), (289.3839284, 0.002517276), (
290.4515014, 0.002721347), (291.5225334, 0.00293583), (292.5972725,
0.003161458), (293.6759734, 0.003398975), (294.7588975, 0.003649137), (
295.8463124, 0.003912709), (296.9384926, 0.004190468), (298.0357187,
0.004483198), (299.138278, 0.004791694), (300.246464, 0.005116759), (
301.3605767, 0.005459204), (302.4809224, 0.00581985), (303.6078137,
0.006199521), (304.7415696, 0.006599053), (305.8825151, 0.007019287), (
307.0309819, 0.007461069), (308.1873078, 0.007925253), (309.3518367,
0.008412696), (310.5249189, 0.008924264), (311.7069111, 0.009460825), (
312.8981759, 0.010023252), (314.0990824, 0.010612422), (315.3100059,
0.011229217), (316.5313278, 0.01187452), (317.7634359, 0.01254922), (
319.0067241, 0.013254204), (320.2615927, 0.013990367), (321.528448,
0.0147586), (322.8077029, 0.015559799), (324.099776, 0.016394859), (
325.4050928, 0.017264676), (326.7240844, 0.018170147), (328.0571887,
0.019112167), (329.4048495, 0.02009163), (330.767517, 0.021109431), (
332.1456478, 0.022166461), (333.5397044, 0.02326361), (334.950156,
0.024401764), (336.3774778, 0.025581808), (337.8221515, 0.026804621), (
339.2846649, 0.02807108), (340.7655123, 0.029382057), (342.2651942,
0.030738418), (343.7842174, 0.032141024), (345.3230952, 0.033590732), (
346.8823471, 0.035088389), (348.462499, 0.036634838), (350.0640831,
0.038230914), (351.687638, 0.039877443), (353.3337087, 0.041575244), (
355.0028467, 0.043325127), (356.6956097, 0.045127891), (358.4125619,
0.046984327), (360.1542739, 0.048895215), (361.9213227, 0.050861324), (
363.7142918, 0.052883413), (365.5337711, 0.054962228), (367.380357,
0.057098503), (369.2546522, 0.059292959), (371.1572662, 0.061546305), (
373.0888147, 0.063859234), (375.0499199, 0.066232428), (377.0412107,
0.068666553), (379.0633224, 0.071162259), (381.1168968, 0.073720182), (
383.2025823, 0.076340942), (385.3210339, 0.079025142), (387.4729129,
0.081773368), (389.6588875, 0.084586192), (391.8796323, 0.087464164), (
394.1358284, 0.090407819), (396.4281639, 0.093417674), (398.7573329,
0.096494226), (401.1240367, 0.099637953), (403.5289829, 0.102849316), (
405.9728859, 0.106128753), (408.4564666, 0.109476686), (410.9804527,
0.112893513), (413.5455785, 0.116379615), (416.1525851, 0.11993535), (
418.8022202, 0.123561056), (421.4952381, 0.12725705), (424.2324001,
0.131023627), (427.0144741, 0.134861061), (429.8422346, 0.138769605), (
432.7164631, 0.142749488), (435.6379476, 0.146800919), (438.6074831,
0.150924085), (441.6258714, 0.155119149), (444.6939208, 0.159386253), (
447.8124467, 0.163725517), (450.9822713, 0.168137038), (454.2042234,
0.172620889), (457.479139, 0.177177124), (460.8078605, 0.181805773), (

```

```

464.1912376, 0.186506842), (467.6301266, 0.191280317), (471.1253907,
0.19612616), (474.6779002, 0.201044314), (478.2885321, 0.206034695), (
481.9581704, 0.211097201), (485.687706, 0.216231707), (489.4780367,
0.221438067), (493.3300673, 0.226716112), (497.2447097, 0.232065652), (
501.2228824, 0.237486479), (505.2655113, 0.24297836), (509.3735289,
0.248541045), (513.5478751, 0.25417426), (517.7894965, 0.259877715), (
522.0993469, 0.265651098), (526.4783869, 0.271494077), (530.9275846,
0.277406303), (535.4479147, 0.283387407), (540.0403591, 0.289437001), (
544.7059069, 0.29555468), (549.4455542, 0.301740022), (554.2603041,
0.307992586), (559.1511671, 0.314311915), (564.1191604, 0.320697535), (
569.1653088, 0.327148956), (574.2906438, 0.333665674), (579.4962044,
0.340247167), (584.7830365, 0.3468929), (590.1521934, 0.353602323), (
595.6047353, 0.360374872), (601.1417299, 0.36720997), (606.764252,
0.374107027)))

# Creating sketch of skin
mn.ConstrainedSketch(name='__profile__', sheetSize=200.0)
mn.sketches['__profile__'].rectangle(point1=(0.0, 0.0), point2=(sk_x, sk_y))

# Creating part of skin
mn.Part(dimensionality=THREE_D, name='Skin', type=DEFORMABLE_BODY)
mn.parts['Skin'].BaseShell(sketch=mn.sketches['__profile__'])
del mn.sketches['__profile__']

# Creating partition
p_sk = mn.parts['Skin']
f_sk, e_sk, d_sk = p_sk.faces, p_sk.edges, p_sk.datums
t = p_sk.MakeSketchTransform(sketchPlane=f_sk[0], sketchUpEdge=e_sk[2],
sketchPlaneSide=SIDE1, origin=(sk_x*0.5, sk_y*0.5, 0.0))
s = mn.ConstrainedSketch(name='__profile__',
sheetSize=1272.79, gridSpacing=31.81, transform=t)
g, v, d1, c = s.geometry, s.vertices, s.dimensions, s.constraints
s.setPrimaryObject(option=SUPERIMPOSE)
p_sk.projectReferencesOntoSketch(sketch=s, filter=COPLANAR_EDGES)
s.Line(point1=(-sk_y/6.0, sk_x*0.5), point2=(-sk_y/6.0, -sk_x*0.5))
s.VerticalConstraint(entity=g[6], addUndoState=False)
s.PerpendicularConstraint(entity1=g[5], entity2=g[6], addUndoState=False)
s.CoincidentConstraint(entity1=v[4], entity2=g[5], addUndoState=False)
s.CoincidentConstraint(entity1=v[5], entity2=g[3], addUndoState=False)
s.Line(point1=(0, sk_x*0.5), point2=(0, -sk_x*0.5))
s.VerticalConstraint(entity=g[7], addUndoState=False)
s.PerpendicularConstraint(entity1=g[5], entity2=g[7], addUndoState=False)
s.CoincidentConstraint(entity1=v[6], entity2=g[5], addUndoState=False)
s.CoincidentConstraint(entity1=v[7], entity2=g[3], addUndoState=False)
s.Line(point1=(sk_y/6.0, sk_x*0.5), point2=(sk_y/6.0, -sk_x*0.5))
s.VerticalConstraint(entity=g[8], addUndoState=False)
s.PerpendicularConstraint(entity1=g[5], entity2=g[8], addUndoState=False)
s.CoincidentConstraint(entity1=v[8], entity2=g[5], addUndoState=False)
s.CoincidentConstraint(entity1=v[9], entity2=g[3], addUndoState=False)
pickedFaces = f_sk.getSequenceFromMask(mask=('[#1 ]',),)
p_sk.PartitionFaceBySketch(sketchUpEdge=e_sk[2], faces=pickedFaces, sketch=s)
s.unsetPrimaryObject()
del mn.sketches['__profile__']

# Creating skin section
mn.HomogeneousShellSection(name='Skin_Sec',
preIntegrate=OFF, material='Al_2024_T3_Sheet', thicknessType=UNIFORM,
thickness=sk_t, thicknessField="", idealization=NO_IDEALIZATION,
poissonDefinition=DEFAULT, thicknessModulus=None, temperature=GRADIENT,
useDensity=OFF, integrationRule=SIMPSON, numIntPts=5)

```

```

# Assigning skin section
faces = f_sk.getSequenceFromMask(mask=('[#f]', ), )
region = p_sk.Set(faces=faces, name='Skin_faces_set')
p_sk.SectionAssignment(region=region, sectionName='Skin_Sec', offset=0.0,
    offsetType=MIDDLE_SURFACE, offsetField="",
    thicknessAssignment=FROM_SECTION)

# Mesh control of skin
pickedRegions = f_sk.getSequenceFromMask(mask=('[#f]', ), )
p_sk.setMeshControls(regions=pickedRegions, elemShape=QUAD, technique=SWEEP)

# Mesh seed of skin
p_sk.seedPart(deviationFactor=0.1, minSizeFactor=0.1, size=ele_size_sk)

# Generate mesh of skin
p_sk.generateMesh()

# Creating sketch of stringer
s = mn.ConstrainedSketch(name='__profile__', sheetSize=200.0)
g, v, d, c = s.geometry, s.vertices, s.dimensions, s.constraints
s.setPrimaryObject(option=STANDALONE)
s.Line(point1=(-str_c*0.5, 0.0), point2=(str_c*0.5, 0.0))
s.HorizontalConstraint(entity=g[2], addUndoState=False)
s.Line(point1=(-str_b*0.5, str_h), point2=(str_b*0.5, str_h))
s.HorizontalConstraint(entity=g[3], addUndoState=False)
s.Line(point1=(0.0, 0.0), point2=(0.0, str_h))
s.VerticalConstraint(entity=g[4], addUndoState=False)
s.PerpendicularConstraint(entity1=g[2], entity2=g[4], addUndoState=False)
s.CoincidentConstraint(entity1=v[4], entity2=g[2], addUndoState=False)
s.EqualDistanceConstraint(entity1=v[0], entity2=v[1], midpoint=v[4], addUndoState=False)

s.EqualDistanceConstraint(entity1=v[2], entity2=v[3], midpoint=v[5], addUndoState=False)

# Creating part of stringer
mn.Part(name='Stringer', dimensionality=THREE_D,type=DEFORMABLE_BODY)
mn.parts['Stringer'].BaseShellExtrude(sketch=s, depth=str_l)
del mn.sketches['__profile__']

# Creating stringer section
mn.HomogeneousShellSection(name='Stringer_Sec',
    preIntegrate=OFF, material='Al_2024_T3_Sheet', thicknessType=UNIFORM,
    thickness=str_t, thicknessField="", idealization=NO_IDEALIZATION,
    poissonDefinition=DEFAULT, thicknessModulus=None, temperature=GRADIENT,
    useDensity=OFF, integrationRule=SIMPSON, numIntPts=5)

# Assigning stringer section
p_str = mn.parts['Stringer']
f_str = p_str.faces
faces = f_str.getSequenceFromMask(mask=('[#1f]', ), )
region = p_str.Set(faces=faces, name='Stringer_faces_set')
p_str.SectionAssignment(region=region, sectionName='Stringer_Sec', offset=0.0,
    offsetType=MIDDLE_SURFACE, offsetField="",
    thicknessAssignment=FROM_SECTION)

# Mesh control of stringer
pickedRegions = f_str.getSequenceFromMask(mask=('[#1f]', ), )
p_str.setMeshControls(regions=pickedRegions, elemShape=QUAD, technique=SWEEP)

# Mesh seed of stringer
p_str.seedPart(deviationFactor=0.1, minSizeFactor=0.1, size=ele_size_str)

```

```

# Generate mesh of stringer
p_str.generateMesh()

# Creating Post-Buckling step
mn.StaticStep(name='Post-Buckle-Step', previous='Initial',
maxNumInc=150, stabilizationMagnitude=0.0002,
stabilizationMethod=DISSIPATED_ENERGY_FRACTION,
continueDampingFactors=False, adaptiveDampingRatio=0.05, initialInc=0.005,
minInc=1e-05, maxInc=0.2, nlgeom=ON)

# Creating assembly instances
a_ss = mn.rootAssembly
a_ss.DatumCsysByDefault(CARTESIAN)
a_ss.Instance(dependent=ON, name='Skin-1', part=p_sk)

# Creating Stringer 1
mn.rootAssembly.DatumCsysByDefault(CARTESIAN)
mn.rootAssembly.Instance(dependent=ON, name='Stringer-1', part=p_str)

# Stringer 1 place is decided
a_ss.rotate(instanceList=('Stringer-
1', ), axisPoint=(0.0, 0.0, 0.0), axisDirection=(0.0, 1.0, 0.0), angle=90.0)
a_ss.rotate(instanceList=('Stringer-
1', ), axisPoint=(0.0, 0.0, 0.0), axisDirection=(1.0, 0.0, 0.0), angle=90.0)
a_ss.translate(instanceList=('Stringer-1', ), vector=(0.0, sk_y/3.0, (sk_t+str_t)*0.5))

# Creating Stringer 2
a_ss.LinearInstancePattern(instanceList=('Stringer-
1', ), direction1=(1.0, 0.0, 0.0), direction2=(0.0, 1.0, 0.0), number1=1, number2=2, spacing1=str_l, spacing2
=sk_y/3.0)
a_ss.features.changeKey(fromName='Stringer-1-lin-1-2', toName='Stringer-2')

# Creating connector section as beam
mn.ConnectorSection(name='Fastener_Con_Sec', assembledType=BEAM)

# Creating fasteners
const_attach = [['#20'],4,1,'1'],[['#4'],2,0,'2']]
for key in range(2):
    e_str = a_ss.instances['Stringer-'+str(key+1)].edges
    v_str = a_ss.instances['Stringer-'+str(key+1)].vertices
    f_str = a_ss.instances['Stringer-'+str(key+1)].faces
    for const in const_attach:
        # Creating attachment points
        edges1 = e_str.getSequenceFromMask(mask=(const[0], ), )
        geomEdges=edges1
        a_ss.AttachmentPointsOffsetFromEdges(edges=geomEdges, startPoint=v_str[const[1]],
referenceFace=f_str[const[2]], name='Str'+str(key+1)+'-Attachment Points-
'+const[3],
pointCreationMethod=BY_NUMBER, offsetFromStartPoint=2.0*fast_d+1.0, numberOfP
oints=27,
offsetFromEndPoint=2.0*fast_d+1.0, numberOfRows=1, offsetFromEdges= str_c*0.25,
patterningMethod=PATTERN_ORTHOGONALLY, setName='Str'+str(key+1)+'-
Attachment Points-Set '+const[3])

# Assigning a section to fastener
region=a_ss.sets['Str'+str(key+1)+'-Attachment Points-Set '+const[3]]
a_ss.engineeringFeatures.PointFastener( name='Str'+str(key+1)+'-Fasteners-
'+const[3], region=region,

```

```

        sectionName='Fastener_Con_Sec', directionVector=(v_str[7], a_ss.instances['Stringer-
'+str(key+1)].
        InterestingPoint(edge=e_str[8], rule=MIDDLE)), physicalRadius=fast_d*0.5, additional
Mass=0.0001)

# Creating boundary conditions at initial step
v_sk = a_ss.instances['Skin-1'].vertices
e_sk = a_ss.instances['Skin-1'].edges
n_sk = a_ss.instances['Skin-1'].nodes

# Creating boundary conditions sets
verts1 = v_sk.getSequenceFromMask(mask=('[#200 ]', ), )
verts2 = v_sk.getSequenceFromMask(mask=('[#100 ]', ), )
a_ss.Set(vertices=verts1, name='Set_reaction_mid_point')
a_ss.Set(vertices=verts2, name='Set_loaded_mid_point')
dict_bc = {'[#44 ]': 'side_edges', '#c28 ]': 'load_edge', '#1282 ]': 'reaction_edge'}
for key_bc, str_bc in dict_bc.items():
    if str_bc=='reaction_edge':
        nodes1 = n_sk.getSequenceFromMask(mask=('[#296 #0:2 #ffffff8 #0:10 #ffffffe0 #3 #0
', '#f8000000 #1ff #7ffe0 ]', ), )
        a_ss.Set(nodes=nodes1, name='Set_'+str_bc)
    else:
        edges1 = e_sk.getSequenceFromMask(mask=(key_bc, ), )
        a_ss.Set(edges=edges1, name='Set_'+str_bc)

# Assigning boundary conditions on sets
region = a_ss.sets['Set_reaction_mid_point']
mn.DisplacementBC(name='BC_reac_mid_point',
    createStepName='Initial', region=region, u1=UNSET, u2=SET, u3=UNSET,
    ur1=UNSET, ur2=UNSET, ur3=UNSET, amplitude=UNSET, distributionType=UNIFORM,
    fieldName="", localCsys=None)
region = a_ss.sets['Set_side_edges']
mn.DisplacementBC(name='BC_side_edges',
    createStepName='Initial', region=region, u1=UNSET, u2=UNSET, u3=SET,
    ur1=SET, ur2=UNSET, ur3=UNSET, amplitude=UNSET, distributionType=UNIFORM,
    fieldName="", localCsys=None)
region = a_ss.sets['Set_load_edge']
mn.DisplacementBC(name='BC_load_edge',
    createStepName='Initial', region=region, u1=UNSET, u2=UNSET, u3=SET,
    ur1=UNSET, ur2=SET, ur3=UNSET, amplitude=UNSET, distributionType=UNIFORM,
    fieldName="", localCsys=None)
region = a_ss.sets['Set_reaction_edge']
mn.DisplacementBC(name='BC_reaction_edge',
    createStepName='Initial', region=region, u1=SET, u2=UNSET, u3=SET,
    ur1=UNSET, ur2=SET, ur3=UNSET, amplitude=UNSET, distributionType=UNIFORM,
    fieldName="", localCsys=None)

# Modifying boundary conditions at post-buckle step
mn.boundaryConditions['BC_load_edge'].setValuesInStep(
    stepName='Post-Buckle-Step', u1=Disp_load)

# Creating history outputs
mn.HistoryOutputRequest(name='H-Output-2',
    createStepName='Post-Buckle-
Step', variables=('U1', ), region=a_ss.sets['Set_loaded_mid_point'],
    sectionPoints=DEFAULT, rebar=EXCLUDE)
mn.HistoryOutputRequest(name='H-Output-3',
    createStepName='Post-Buckle-
Step', variables=('RF1', ), region=a_ss.sets['Set_reaction_edge'],
    sectionPoints=DEFAULT, rebar=EXCLUDE)
str_ids = ['1', '2']

```

```

        c_str = 6
        for str_id in str_ids:
            f_str = a_ss.instances['Stringer-'+str_id].faces
            face_str = f_str.getSequenceFromMask(mask=('[#1f]', ),)
            a_ss.Set(faces=face_str, name='Set_Str_'+str_id)
            mn.HistoryOutputRequest(name='H-Output-'+str(c_str),
                createStepName='Post-Buckle-Step', variables=('S11', ),
                region=a_ss.sets['Set_Str_'+str_id], sectionPoints=DEFAULT,
                rebar=EXCLUDE)
            c_str+=1

        # Creating job
        job_name = 'job_'+ model_name
        mdb.Job(name=job_name, model=model_name, description="", type=ANALYSIS,
            atTime=None, waitMinutes=0, waitHours=0, queue=None, memory=90,
            memoryUnits=PERCENTAGE, getMemoryFromAnalysis=True,
            explicitPrecision=SINGLE, nodalOutputPrecision=SINGLE, echoPrint=OFF,
            modelPrint=OFF, contactPrint=OFF, historyPrint=OFF, userSubroutine="",
            scratch="", resultsFormat=ODB, multiprocessingMode=DEFAULT, numCpus=8, numDomai
ns=8,
            numGPUs=0)
        results.close()
    try:
        del mdb.models['Model-1']
    except:
        None

    # Saving the model
    mdb.saveAs(
        pathName=save_path+'.cae')

    # Stopping the time calculator
    end_t_time = time.time()
    m=divmod(end_t_time-start_t_time,60)
    n=divmod(m[0],60)
    print "Total time: ",n[0],n[1],m[1]

```

- Example code to process finite element results for skin-stringer model with I stringer section

```

# Importing necessary modules
from part import *
from material import *
from section import *
from assembly import *
from step import *
from interaction import *
from load import *
from mesh import *
from optimization import *
from job import *
from sketch import *
from visualization import *
from connectorBehavior import *
import math
import time

```



```

# Counter for script time
start_t_time = time.time()

# Selecting the which models have to be analyzed using FE
need_to_solve=[0,1,2,3]

# Initialize result file
results = open(r"C:\Users\.....\Results\Model_I\output_I.txt","w+")

# Paths
model_path = r'C:/Users/...../Model/Model_I/'
save_path = 'C:/Users/...../Model/Model_I/v6_i'
result_path = 'C:/Users/...../Results/Model_I/'

# Given displacement load (mm)
Disp_load = -2.0

# Element size of parts (mm)
ele_size_sk = 5.0
ele_size_str = 2.0

# Material properties (Al 2024 T3 Sheet thk: 0.23-3.25 mm)
Ec = 73774.0
E = 72395.0
density = 2768.0
poisson = 0.33
Fcy = 269.0
nc = 15.0

# Skin geometry
sk_x = 450.0
sk_ys = [150.0*3.0]
sk_ts = [0.813]

# Stringer "I" geometry
str_l = 450.0
str_ts = [1.016]
str_hs = [25.0]
str_cs = [20.0]
str_bs = [15.0]

# Fasteners' diameter
fast_d = 3.2

# Constant terms are written in the result file
results.write("%-22s %9.0f %-22s %6.2f %-
22s %6.2f" %("Material Ec: ",Ec," Material poisson: ",poisson," Material density: ",density)+"\n")
results.write("%-22s %9.2f %-22s %6.2f %-
22s %6.2f" %("Skin length x: ",sk_x," Stringer length: ",str_l," Fastener diameter: ",fast_d)+"\n"+"")

# Total number of models which will be created in this script
total_count = len(str_hs)*len(str_cs)*len(str_bs)*len(str_ts)*len(sk_ts)*len(sk_ys)*len(need_to_solve)
print "Total model number: ", total_count
count=1

# Function of flat metal panel compressive buckling coefficient
def graph_Kc_flat(x,bc):
    """
    Ref: Analysis and Design of Flight Vehicle Structures - E.F.Bruhn
    Kc is obtained from Figure C5.2 for flat panels

```

```

Loaded edges are clamped.
Conditions are only exceptable for unloaded edges
"""
if bc=='cl':
    if x < 0.76493:
        y = -56.0565*x + 57.1876
    elif (0.76493 <= x) and (x < 1.14273):
        y = -551.9651*pow(x, 4) + 2079.3509*pow(x, 3) - 2870.2033*pow(x, 2) + 1706.6187*x - 353.426
    elif (1.14273 <= x) and (x < 1.85911):
        y = -6.1616*pow(x, 3) + 34.8139*pow(x, 2) - 65.0106*x + 48.5687
    elif (1.85911 <= x) and (x < 2.3433):
        y = -15.9873*pow(x, 4) + 127.1208*pow(x, 3) - 373.7913*pow(x, 2) + 479.4634*x - 216.8528
    elif (2.3433 <= x) and (x < 3.3987):
        y = 13.6994*pow(x, 5) - 198.9195*pow(x, 4) + 1149.7887*pow(x, 3) - 3306.5735*pow(x, 2) + 4730.1
783*x - 2684.554
    elif (3.3987 <= x) and (x < 4.15706):
        y = 10.807*pow(x, 4) - 163.8182*pow(x, 3) + 929.1075*pow(x, 2) - 2336.7822*x + 2206.491
    elif (4.15706 <= x) and (x <= 5.0142):
        y = 1.9679*pow(x, 3) - 27.1906*pow(x, 2) + 124.8755*x - 183.3227
    else:
        y = 7.2802
    return y
elif bc=='ss':
    if x < 1.33459:
        y = 116.1071*pow(x, 4) - 512.1754*pow(x, 3) + 847.8765*pow(x, 2) - 628.8651*x + 183.9239
    elif (1.33459 <= x) and (x < 1.68636):
        y = 2.5557*pow(x, 2) - 8.0374*x + 11.8528
    elif (1.68636 <= x) and (x < 2.76429):
        y = 12.4466*pow(x, 6) - 166.4906*pow(x, 5) + 921.7798*pow(x, 4) - 2704.0495*pow(x, 3) + 4434.97
41*pow(x, 2) - 3860.3466*x + 1400.7332
    elif (2.76429 <= x) and (x <= 4.95153):
        y = -
0.2663*pow(x, 5) + 5.2351*pow(x, 4) - 40.8202*pow(x, 3) + 157.8018*pow(x, 2) - 302.6058*x + 234.8432
    else:
        y = 4.2274
    return y

for sk_y_key,sk_y in enumerate(sk_ys):
    sk_ratio = sk_x / (sk_y/3.0)
    kc_bruhn = []
    # Literature graphs are used to get comp. buckling coefficients with classical boundary condition assumpti
on
    # Unloaded edge boundary conditions (clamped or simply supported)
    for bc in ["cl","ss"]:
        kc_bruhn.append(graph_Kc_flat(sk_ratio,bc))
    for sk_t_key,sk_t in enumerate(sk_ts):
        for str_h_key,str_h in enumerate(str_hs):
            for str_c_key,str_c in enumerate(str_cs):
                for str_b_key,str_b in enumerate(str_bs):
                    for str_t_key,str_t in enumerate(str_ts):
                        if 0 in need_to_solve:
                            # Model 0
                            # Creating model of panel buckling (pb)
                            # Job name is described
                            job_name = 'job_0_pb_1'+str(str_h_key)+str(str_c_key)+str(str_b_key)+str(str_t_key)+str(sk_
t_key)+str(sk_y_key)

                            # Checked whether there is such a job name
                            try:
                                # Starting the time of analysis
                                start_time = time.time()

```

```

# Submitting the job
print "Panel Buckling Model Number: ",count
mdb.jobs[job_name].submit(consistencyChecking=OFF)
mdb.jobs[job_name].waitForCompletion()

# Obtain the eigenvalue
dir_datfile = model_path + job_name+'.dat'
wordlist = []
starttorecord = False
datfile = open(dir_datfile)
for line in datfile:
    if "MODE NO EIGENVALUE" in line:
        starttorecord = True
    for word in line.split():
        if word=="THE":
            starttorecord = False
        if starttorecord:
            wordlist.append(word)
    if float(wordlist[4])>0.0:
        eigenvalue = float(wordlist[4])
    elif float(wordlist[6])>0.0:
        eigenvalue = float(wordlist[6])
    elif float(wordlist[8])>0.0:
        eigenvalue = float(wordlist[8])
    else:
        eigenvalue = 0.0
    datfile.close()
Fccr=eigenvalue*abs(Disp_load)/sk_x*Ec

# Compressive buckling coefficient is calculated using eigenvalue obtained from FEA
kc=Fccr*(sk_y/3.0)**2.0*12.0*(1.0-poisson**2.0)/(Ec*(math.pi*sk_t)**2.0)
kc_star=kc*math.pi**2.0/(12.0*(1.0-poisson**2.0))

# Percentage error between literature result and FE result
dif_kc = abs(kc-kc_bruhn[0])/kc*100.0

# Write the input data
results.write("%-22s" %("Single Panel")+"\n")
results.write("%-22s %9.2f %-
22s %6.2f" %("Skin length y: ",(sk_y/3.0)," Skin thickness: ",sk_t)+"\n")

# Write the output data
results.write("%-22s %9.7f %-22s %6.2f %-
22s %6.2f" %("Eigenvalue: ",eigenvalue," Fccr: ",Fccr," kc_star: ",kc_star)+"\n")
results.write("%-22s %9.3f %-22s %6.3f %-
22s %6.3f" %("kc: ",kc," Bruhn kc(clamped): ",kc_bruhn[0]," Difference %: ",dif_kc)+"\n"+"")

# Ending the time of analysis
end_time = time.time()

# Estimated time is calculated
if count%10 == 0:
    em=divmod((total_count-count)*(end_time-start_time),60)
    en=divmod(em[0],60)
    print "Estimated remaning time: ",en[0],en[1],em[1]
except:
    None

"""
!!!!!!!!!!!!!!!!!!!!!!!!!!!!!!

```



```

mdb.jobs[job_name].waitForCompletion()

# Opening odb file
session.openOdb(name=model_path+job_name+'.odb')
odb = session.odbs[model_path+job_name+'.odb']

# Creating XY-Datas of displacement node
Disp_name = 'Lin_Displ_Data_U1_9'
Disp_session = session.XYDataFromHistory(name=Disp_name, odb=odb,
outputVariableName='Spatial displacement: U1 PI: SKIN-
1 Node 9 in NSET SET_LOADED_MID_POINT',
steps=('Post-Buckle-Step',),)

# List of reaction nodes( by order of x)
Reac_node_list = [8]
for node_id in range(29):
    Reac_node_list.append(454+node_id)
Reac_node_list.append(5)
for node_id in range(14):
    Reac_node_list.append(614+node_id)
Reac_node_list.append(10)
for node_id in range(14):
    Reac_node_list.append(572+node_id)
Reac_node_list.append(2)
for node_id in range(29):
    Reac_node_list.append(100+node_id)
Reac_node_list.append(3)

# Creating XY-Datas of reaction nodes
Node_session_name_list = []
Node_session_list = []
for node_id in Reac_node_list:
    Node_session_name = 'Lin_Reac_Data_RF1_'+str(node_id)
    Node_session = session.XYDataFromHistory(name=Node_session_name, odb=odb,
outputVariableName='Reaction force: RF1 PI: SKIN-
1 Node '+str(node_id)+' in NSET SET_REACTION_EDGE',
steps=('Post-Buckle-Step',),)
    Node_session_name_list += (Node_session_name,)
    Node_session_list+=(Node_session,)

# Displacement vs total reaction force graph
Disp_force_graph=combine(-Disp_session, sum(Node_session_list))
Disp_force_graph.setValues(sourceDescription='combine (-
'+Disp_name+', sum('+str(Node_session_name_list)+')')
tmpName = Disp_force_graph.name
session.xyDataObjects.changeKey(tmpName, 'Lin_Displ_vs_Reac_Data')
Graph_disp_reac = session.xyDataObjects['Lin_Displ_vs_Reac_Data']

# Writing into the output file
session.writeXYReport(fileName = result_path + 'Data_graph_disp_vs_reac(Linear).rpt', ap
pendMode=OFF, xyData=(Graph_disp_reac,))
session.writeXYReport(fileName = result_path + 'Data_nodes_disp_vs_reac(Linear).rpt', ap
pendMode=OFF, xyData=Node_session_list)

# Stringer local stress calculation part
# This part is non-parametric
str_first_edge_ids = [1125,1126]
str_edge_incs = [[-225,225],[-1,1]]

# This part is parametic
str_eles_num = int(round(str_l/ele_size_str))

```



```

!!!!!!!!!!!!!!!!!!!!!!!!!!!!!!
!!!!!!!!!!!!!!!!!!!!!!!!!!!!!!
!!!!!!!!!!!!!!!!!!!!!!!!!!!!!!
!!!!!!!!!!!!!!!!!!!!!!!!!!!!!!
!!!!!!!!!!!!!!!!!!!!!!!!!!!!!!
!!!!!!!!!!!!!!!!!!!!!!!!!!!!!!
"""
if 3 in need_to_solve:
    # Model 3
    # Creating model of stiffened panel post-buckling-nonlinear (sppbn)
    # Job name is described
    job_name = 'job_3_sppbn_I_'+str(str_h_key)+str(str_c_key)+str(str_b_key)+str(str_t_key)+str
(sk_t_key)+str(sk_y_key)

    # Checked whether there is such a job name
    try:
        print "Nonlinear Post-buckling Model Number: ",count
        # Try to open odb file without submitting the job
        try:
            # Opening odb file
            session.openOdb(name=model_path+job_name+'.odb')
            odb = session.odbs[model_path+job_name+'.odb']
        except:
            # Submitting the job
            mdb.jobs[job_name].submit(consistencyChecking=OFF)
            mdb.jobs[job_name].waitForCompletion()

            # Opening odb file
            session.openOdb(name=model_path+job_name+'.odb')
            odb = session.odbs[model_path+job_name+'.odb']

        # Creating XY-Datas of displacement node
        Disp_name = 'Non_Disp_Data_U1_9'
        Disp_session = session.XYDataFromHistory(name='Non_Disp_Data_U1_9', odb=odb,
        outputVariableName='Spatial displacement: U1 PI: SKIN-
1 Node 9 in NSET SET_LOADED_MID_POINT',
        steps=('Post-Buckle-Step', ),)

    # List of reaction nodes( by order of x)
    Reac_node_list = [8]
    for node_id in range(29):
        Reac_node_list.append(454+node_id)
    Reac_node_list.append(5)
    for node_id in range(14):
        Reac_node_list.append(614+node_id)
    Reac_node_list.append(10)
    for node_id in range(14):
        Reac_node_list.append(572+node_id)
    Reac_node_list.append(2)
    for node_id in range(29):
        Reac_node_list.append(100+node_id)
    Reac_node_list.append(3)

    # Creating XY-Datas of reaction nodes
    Node_session_name_list = ()
    Node_session_list = ()
    for node_id in Reac_node_list:
        Node_session_name = 'Non_Reac_Data_RF1_'+str(node_id)
        Node_session = session.XYDataFromHistory(name=Node_session_name, odb=odb,

```



```

        outputVariableName='Reaction force: RF1 PI: SKIN-
1 Node '+str(node_id)+' in NSET SET_REACTION_EDGE',
        steps=('Post-Buckle-Step', ),)
        Node_session_name_list += (Node_session_name,)
        Node_session_list+=(Node_session,)

        # Displacement vs total reaction force graph
        Disp_force_graph=combine(-Disp_session, sum(Node_session_list))
        Disp_force_graph.setValues( sourceDescription='combine (-
'+Disp_name+', sum('+str(Node_session_name_list)+')')
        tmpName = Disp_force_graph.name
        session.xyDataObjects.changeKey(tmpName, 'Non_Disp_vs_Reac_Data')
        Graph_disp_reac = session.xyDataObjects['Non_Disp_vs_Reac_Data']

        # Writing into the output file
        session.writeXYReport(fileName = result_path + 'Data_graph_disp_vs_reac(Nonlinear).rpt',
appendMode=OFF, xyData=(Graph_disp_reac,))
        session.writeXYReport(fileName = result_path + 'Data_nodes_disp_vs_reac(Nonlinear).rpt',
appendMode=OFF, xyData=Node_session_list)

        # Stringer local stress calculation part
        # This part is non-parametric
        str_first_edge_ids = [1125,1126]
        str_edge_incs = [[-225,225],[-1,1]]

        # This part is parametic
        str_eles_num = int(round(str_l/ele_size_str))
        str_edges_eles_num = [int(round(str_c/(2.0*ele_size_str))),int(round(str_c/(2.0*ele_size_st
r)))]

        str_ids = [1,2]
        for str_id in str_ids:
            graph_str_eles = ()
            for str_ele_num in range(str_eles_num):
                str_eles_data=()
                str_eles_name=()
                for str_edge_eles_key,str_edge_eles_num in enumerate(str_edges_eles_num):
                    for str_edge_ele_num in range(str_edge_eles_num):
                        for sur in range(2):
                            if sur==0:
                                sur_key = 'SPOS'
                                sur_val = '(fraction = 1:0)'
                            else:
                                sur_key = 'SNEG'
                                sur_val = '(fraction = -1:0)'
                            str_ele_id = str_first_edge_ids[str_edge_eles_key] + str_edge_ele_num * str_edge_i
ncs[0][str_edge_eles_key]+ str_ele_num * str_edge_incs[1][str_edge_eles_key]
                            str_ele_name = 'Non_Sec_Data_STR'+str(str_id)+'_S11_'+str(str_ele_id)+'_'+sur_k
ey
                            str_ele_data = session.XYDataFromHistory(name=str_ele_name, odb=odb,
                                outputVariableName='Stress components: S11 PI: STRINGER-
'+str(str_id)+' Element '+str(str_ele_id)+' Int Point 1 Sec Pt '+sur_key+', '+sur_val+' in ELSET SET_STR_'+str
(str_id),
                                steps=('Post-Buckle-Step', ),)
                            str_eles_name +=(str_ele_name,)
                            str_eles_data +=(str_ele_data,)

        # Element stress on the stringer flange which is connected to skin is calculated by the
averaging the upper and lower sides of the element stresses
        str_ele_graph=sum(str_eles_data)/(len(str_eles_data))
        str_ele_graph.setValues(

```

```

        sourceDescription='sum('+str(str_eles_name)+')')
        tmpName = str_ele_graph.name
        session.xyDataObjects.changeKey(tmpName, 'Non_Str'+str(str_id)+'_Data_Part_'+str(s
tr_ele_num))
        graph_str_ele = session.xyDataObjects['Non_Str'+str(str_id)+'_Data_Part_'+str(str_ele_
num)]
        graph_str_eles +=(graph_str_ele,)
        for str_ele_name in str_eles_name:
            del session.xyDataObjects[str_ele_name]

# Writing into the output file
        session.writeXYReport(fileName = result_path + 'Str'+str(str_id)+'_Data(Nonlinear).rpt',
appendMode=OFF, xyData=graph_str_eles)
    except:
        None
        count+=1
results.close()

# Saving the model
mdb.saveAs(
    pathName=save_path+'.cae')

# Stopping the time calculator
end_t_time = time.time()
m=divmod(end_t_time-start_t_time,60)
n=divmod(m[0],60)
print "Total time: " ,n[0],n[1],m[1]

```

F.5 Composite Single Panel Buckling Python Scripts

- Example code to construct the composite panel model with simply supported boundary condition

```

# Importing necessary modules
from abaqus import *
from abaqusConstants import *
from caeModules import *
from driverUtils import executeOnCaeStartup
from part import *
from material import *
from section import *
from assembly import *
from step import *
from interaction import *
from load import *
from mesh import *
from optimization import *
from job import *
from sketch import *
from visualization import *
from connectorBehavior import *
import math
import time

# Counter for script time
start_t_time = time.time()

# Paths

```

```

save_path='C:/Users/.....'

# Given edge load (N/mm)
Edge_load = 1.0

# Material properties
# In this case, material is Carbon/epoxy,Hexply 8552S/37RC/AGP280/C
mats=[]
mats.append(
{"mat_des" : "Carbon_epoxy",
"E1":54000, "E2":54000, "Nu12":0.05,
"G12":4.5e3, "G13":4.5e3, "G23":4.5e3}
)

# Skin geometry
# sk_x is the unloaded edge
# sk_y is the loaded edge
sk_xs = []
sk_ys = []
ply_ts = [0.28]
for xdist in range(100, 505, 5):
    sk_xs.append(xdist)
for ydist in range(100, 105, 5):
    sk_ys.append(ydist)

#Ply sequences
ply_props = []
ply_props.append({"sym":True,"ply_sq":[0,0],"ply_repeat":[2,4]})
ply_props.append({"sym":True,"ply_sq":[0,90],"ply_repeat":[1,2]})
ply_props.append({"sym":True,"ply_sq":[45,0,-45,90],"ply_repeat":[1,2]})

# Total number of models which will be created in this script
total_count = 0
for ply_prop in ply_props:
    total_count += len(mats)*len(ply_ts)*len(ply_prop["ply_repeat"])*len(sk_xs)*len(sk_ys)
print "Total model number: ", total_count

for mat_key,mat in enumerate(mats):
    for ply_t_key,ply_t in enumerate(ply_ts):
        for ply_prop_key,ply_prop in enumerate(ply_props):
            ply_repeats = ply_prop["ply_repeat"]
            for ply_repeat_key, ply_repeat in enumerate(ply_repeats):
                for sk_x_key,sk_x in enumerate(sk_xs):
                    for sk_y_key,sk_y in enumerate(sk_ys):

                        # Creating model of composite panel buckling (cpb)
                        print "Creating model"
                        model_name = "cpb_" +str(mat_key)+str(ply_t_key)+str(ply_prop_key)+str(ply_repeat_key)+
str(sk_x_key)+str(sk_y_key)
                        mdb.Model(modelType=STANDARD_EXPLICIT, name=model_name)
                        mn=mdb.models[model_name]

                        # Creating material
                        print "Creating model"
                        mn.Material(name=mat["mat_des"])
                        mn.materials[mat["mat_des"]].Elastic(
                            type=LAMINA, table=((
                                mat["E1"], mat["E2"],mat["Nu12"],
                                mat["G12"], mat["G13"], mat["G23"]), ))

                        # Creating sketch of skin

```

```

print "Creating sketch of skin"
mn.ConstrainedSketch(name='_profile_', sheetSize=200.0)
mn.sketches['_profile_'].rectangle(point1=(0.0, 0.0), point2=(sk_x, sk_y))

# Creating part of skin
print "Creating part of skin"
mn.Part(dimensionality=THREE_D, name='Skin', type=DEFORMABLE_BODY)
mn.parts['Skin'].BaseShell(sketch=mn.sketches['_profile_'])
del mn.sketches['_profile_']

# Creating Layup orientation
print "Creating Layup orientation"
layupOrientation = None
p_sk = mn.parts['Skin']
f_sk, e_sk, d_sk = p_sk.faces, p_sk.edges, p_sk.datums
faces = f_sk.getSequenceFromMask(mask=('[#1 ]', ), )
region_sk=regionToolset.Region(faces=faces)
compositeLayup = p_sk.CompositeLayup(
    name='CompositeLayup-1', description="", elementType=SHELL,
    offsetType=MIDDLE_SURFACE, symmetric=ply_prop["sym"],
    thicknessAssignment=FROM_SECTION)
compositeLayup.Section(preIntegrate=OFF, integrationRule=SIMPSON,
    thicknessType=UNIFORM, poissonDefinition=DEFAULT, temperature=GRADIENT,
    useDensity=OFF)
compositeLayup.ReferenceOrientation(orientationType=GLOBAL, localCsys=None,
    fieldName="", additionalRotationType=ROTATION_NONE, angle=0.0, axis=AXIS_3)
ply_sq = []
for rep in range(ply_repeat):
    for ply_ang in ply_prop["ply_sq"]:
        ply_sq.append(ply_ang)
    for ply_n,ply_ang in enumerate(ply_sq):
        compositeLayup.CompositePly(suppressed=False, plyName='Ply-
'+str(ply_n+1), region=region_sk,material=mat["mat_des"], thicknessType=SPECIFY_THICKNESS, thickness
=ply_t,orientationType=SPECIFY_ORIENT, orientationValue=ply_ang,additionalRotationType=ROTATION_
NONE, additionalRotationField="", axis=AXIS_3, angle=0.0, numIntPoints=3)

# Mesh control of skin
print "Mesh control of skin"
pickedRegions = f_sk.getSequenceFromMask(mask=('[#1 ]', ), )
p_sk.setMeshControls(regions=pickedRegions, elemShape=QUAD, technique=SWEEP)

# Mesh seed of skin
print "Mesh seed of skin"
p_sk.seedPart(deviationFactor=0.1, minSizeFactor=0.1, size=5.0)

# Generate mesh of skin
print "Generate mesh of skin"
p_sk.generateMesh()

# Creating Buckling step
print "Creating Buckling step"
mn.BuckleStep(name='Buckle-
Step', previous='Initial', numEigen=8, vectors=28, maxIterations=3000)

# Creating assembly instances
print "Creating assembly instances"
a_sk = mn.rootAssembly
a_sk.DatumCsysByDefault(CARTESIAN)
a_sk.Instance(dependent=ON, name='Skin-1', part=p_sk)

# Creating boundary conditions at initial step

```

```

print "Creating boundary conditions at initial step"
edges_bc = {'[#2]': 'loaded_edge', '#8]': 'opp_loaded_edge', '#5]': 'unloaded_edges'}
e_sk = a_sk.instances['Skin-1'].edges
for edge_key, edge_des in edges_bc.items():
    edges1 = e_sk.getSequenceFromMask(mask=(edge_key, ), )
    a_sk.Set(edges=edges1, name='Set_'+edge_des)
v_sk = a_sk.instances['Skin-1'].vertices
verts_bc = {'[#8]': 'lb_cor', '#2]': 'rt_cor'}
for vert_key, vert_des in verts_bc.items():
    verts1 = v_sk.getSequenceFromMask(mask=(vert_key, ), )
    a_sk.Set(vertices=verts1, name='Set_'+vert_des)

# Assigning boundary conditions using sets
print "Assigning boundary conditions using sets"
region = a_sk.sets['Set_lb_cor']
mn.DisplacementBC(name='BC_lb_cor', createStepName='Initial',
    region=region, u1=SET, u2=SET, u3=SET, ur1=UNSET, ur2=UNSET, ur3=UNSET,
    amplitude=UNSET, distributionType=UNIFORM, fieldName="", localCsys=None)
region = a_sk.sets['Set_rt_cor']
mn.DisplacementBC(name='BC_rt_cor', createStepName='Initial',
    region=region, u1=UNSET, u2=SET, u3=UNSET, ur1=UNSET, ur2=UNSET, ur3=UNSET,
    amplitude=UNSET, distributionType=UNIFORM, fieldName="", localCsys=None)
region = a_sk.sets['Set_loaded_edge']
mn.DisplacementBC(name='BC_loaded_edge', createStepName='Initial',
    region=region, u1=UNSET, u2=UNSET, u3=SET, ur1=UNSET, ur2=UNSET, ur3=UNSET,
    amplitude=UNSET, distributionType=UNIFORM, fieldName="", localCsys=None)
region = a_sk.sets['Set_opp_loaded_edge']
mn.DisplacementBC(name='BC_opp_loaded_edge', createStepName='Initial',
    region=region, u1=SET, u2=UNSET, u3=SET, ur1=UNSET, ur2=UNSET, ur3=UNSET,
    amplitude=UNSET, distributionType=UNIFORM, fieldName="", localCsys=None)
region = a_sk.sets['Set_unloaded_edges']
mn.DisplacementBC(name='BC_unloaded_edges', createStepName='Initial',
    region=region, u1=UNSET, u2=UNSET, u3=SET, ur1=UNSET, ur2=UNSET, ur3=UNSET,
    amplitude=UNSET, distributionType=UNIFORM, fieldName="", localCsys=None)

# Applying shell edge load on the skin loaded edge
print "Applying shell edge load on the skin loaded edge"
load_edges = ['#2]']
for load_key, load_edge in enumerate(load_edges):
    s_edges = e_sk.getSequenceFromMask(mask=(load_edge, ), )
    region = a_sk.Surface(side1Edges=s_edges, name='Surf_loaded_edge'+str(load_key+1))
    mn.ShellEdgeLoad(name='Load_buckling'+str(load_key+1), createStepName='Buckle-
Step',
        region=region, magnitude=Edge_load, distributionType=UNIFORM, field="",
        localCsys=None)

# Creating job
print "Creating job"
job_name = 'job_'+ model_name
mdb.Job(name=job_name, model=model_name, description="", type=ANALYSIS,
    atTime=None, waitMinutes=0, waitHours=0, queue=None, memory=90,
    memoryUnits=PERCENTAGE, getMemoryFromAnalysis=True,
    explicitPrecision=SINGLE, nodalOutputPrecision=SINGLE, echoPrint=OFF,
    modelPrint=OFF, contactPrint=OFF, historyPrint=OFF, userSubroutine="",
    scratch="", resultsFormat=ODB, multiprocessingMode=DEFAULT, numCpus=1,
    numGPUs=0)
try:
    del mdb.models['Model-1']
except:
    None

```

```

# Saving the model
print "Saving model"
mdb.saveAs(pathName=save_path+'.cae')

# Stopping the time calculator
end_t_time = time.time()
m=divmod(end_t_time-start_t_time,60)
n=divmod(m[0],60)
print "Total time: " ,n[0],n[1],m[1]

```

- Example code to process finite element results for the composite panel model with simply supported boundary condition

```

# Importing necessary modules
from abaqus import *
from abaqusConstants import *
from caeModules import *
from driverUtils import executeOnCaeStartup
from part import *
from material import *
from section import *
from assembly import *
from step import *
from interaction import *
from load import *
from mesh import *
from optimization import *
from job import *
from sketch import *
from visualization import *
from connectorBehavior import *
import math
import time

# Counter for script time
start_t_time = time.time()

# Defining maximum number of submissions can be given at the same time
max_sub = 5
ini_sub = 0

# Paths
save_path='C:/Users/...../Model/ss/comp_ss_buckling'
model_path = r'C:/Users/...../Model/ss/'

# Initialize results' path
result_path = r"C:\Users\.....\Results\comp_ss_buckling_loads"
result_excel_path = r"C:\Users\.....\Results\excel\comp_ss_buckling_loads"

# Given edge load (N/mm)
Edge_load = 1.0

# Material properties
# In this case, material is Carbon/epoxy,Hexply 8552S/37RC/AGP280/C
mats=[]
mats.append(
{"mat_des": "Carbon_epoxy",
"E1":54000, "E2":54000, "Nu12":0.05,
"G12":4.5e3, "G13":4.5e3, "G23":4.5e3}

```

```

)

# Skin geometry
# sk_x is the unloaded edge
# sk_y is the loaded edge
sk_xs = []
sk_ys = []
ply_ts = [0.28]
for xdist in range(100, 505, 5):
    sk_xs.append(xdist)
for ydist in range(100, 105, 5):
    sk_ys.append(ydist)

#Ply Sequence
ply_props = []
ply_props.append({"sym":True,"ply_sq":[0],"ply_repeat":[2,4]})
ply_props.append({"sym":True,"ply_sq":[0,90],"ply_repeat":[1,2]})
ply_props.append({"sym":True,"ply_sq":[45,0,-45,90],"ply_repeat":[1,2]})

# Total number of models which will be created in this script
total_count = 0
for ply_prop in ply_props:
    total_count += len(mats)*len(ply_ts)*len(ply_prop["ply_repeat"])*len(sk_xs)*len(sk_ys)
print "Total model number: ", total_count
count = 1

for mat_key,mat in enumerate(mats):
    for ply_t_key,ply_t in enumerate(ply_ts):
        for ply_prop_key,ply_prop in enumerate(ply_props):
            ply_repeats = ply_prop["ply_repeat"]
            for ply_repeat_key, ply_repeat in enumerate(ply_repeats):
                for sk_x_key,sk_x in enumerate(sk_xs):
                    for sk_y_key,sk_y in enumerate(sk_ys):
                        # Job name is described
                        start_time = time.time()
                        job_name = 'job_cpb_'+str(mat_key)+str(ply_t_key)+str(ply_prop_key)+str(ply_repeat_key)+s
tr(sk_x_key)+str(sk_y_key)
                        print "Model number: ",count
                        job_model = mdb.jobs[job_name]

                        # Checked to see if the job has already been submitted
                        try:
                            dir_logfile = model_path + job_name+".log"
                            logfile = open(dir_logfile)
                            comp = False

                        # Checked to see that the job is completed
                        for line in logfile:
                            if "Abaqus JOB "+job_name+" COMPLETED" in line:
                                print " completed"
                                comp = True
                        logfile.close()

                        # Submission check
                        if comp==False:
                            job_model.submit(consistencyChecking=OFF)
                            ini_sub +=1

                        # Multi-submission is permitted for this code
                        # Maximum number of submission is checked
                        if ini_sub >= max_sub:

```

```

        job_model.waitForCompletion()
        ini_sub = 0
        end_time = time.time()
    else:
        end_time = time.time()

    except:
        # Submit the job
        job_model.submit(consistencyChecking=OFF)
        ini_sub +=1

        # Multi-submission is permitted for this code
        # Maximum number of submission is checked
        if ini_sub >= max_sub:
            job_model.waitForCompletion()
            ini_sub = 0
            end_time = time.time()

        # Estimated time is calculated
        if count%(max_sub*2) == 0:
            em=divmod((total_count-count)*(end_time-start_time)/max_sub,60)
            en=divmod(em[0],60)
            print "Estimated remaning time: ",en[0],en[1],em[1]
            count+=1
# Checked whether all analyses are completed
for mat_key,mat in enumerate(mats):
    for ply_t_key,ply_t in enumerate(ply_ts):
        for ply_prop_key,ply_prop in enumerate(ply_props):
            ply_repeats = ply_prop["ply_repeat"]
            for ply_repeat_key, ply_repeat in enumerate(ply_repeats):
                for sk_x_key,sk_x in enumerate(sk_xs):
                    for sk_y_key,sk_y in enumerate(sk_ys):
                        job_name ='job_cpb_'+str(mat_key)+str(ply_t_key)+str(ply_prop_key)+str(ply_repeat_key)+
tr(sk_x_key)+str(sk_y_key)
                        job_model.waitForCompletion()

for mat_key,mat in enumerate(mats):
    for ply_t_key,ply_t in enumerate(ply_ts):
        for ply_prop_key,ply_prop in enumerate(ply_props):
            ply_repeats = ply_prop["ply_repeat"]
            for ply_repeat_key, ply_repeat in enumerate(ply_repeats):
                # Writing the input data into the result file
                results = open(result_path+"_"+str(mat_key)+str(ply_t_key)+str(ply_prop_key)+str(ply_repeat_key)
)+".txt","w+")
                results_excel = open(result_excel_path+"_"+str(mat_key)+str(ply_t_key)+str(ply_prop_key)+str(ply
_repeat_key)+".txt","w+")

                # Writing the excel graphs' headings into the result file which is used to construct excel
                results_excel.write("%20s %20s %20s %20s %20s %20s" %("a0/b0","k0-2D*(E)","k0-
2D*(C)","k0-2D*(F)","error(E-C)","error(E-F)")+ "\n"+ "\n")

                # Writing the material properties into the result file
                results.write("%-25s %20s " %("Material description: ", mat["mat_des"]))+ "\n")
                results.write("%-25s %6.2f %-20s %6.2f %-
20s %6.2f" %("Material E1: ", mat["E1"], " Material E2: ", mat["E2"], " Material Nu12: ", mat["Nu12"]))+ "\n
)
                results.write("%-25s %6.2f %-20s %6.2f %-
20s %6.2f" %("Material G12: ", mat["G12"], " Material G13: ", mat["G13"], " Material G23: ", mat["G23"]))+ "\
n")

                # Writing the ply thickness and symmetric condition into the result file

```



```

results.write("%-25s %6.2f %-
20s %10s" %("Ply thickness: ", ply_t, " Ply symmetric: ", ply_prop["sym"]+"\n")

# Ply directions and angles are described to use in A,B,D matrices
ply_sq = []
for rep in range(ply_repeat):
    for ply_ang in ply_prop["ply_sq"]:
        ply_sq.append(ply_ang)
if ply_prop["sym"]:
    for ply_ang in reversed(ply_sq):
        ply_sq.append(ply_ang)

# Writing the ply directions and angles into the result file
results.write("%-25s" %("Ply Directions: "))
for ply_ang in ply_sq:
    results.write("%6d" %(ply_ang))
results.write("\n"+"")

for sk_x_key,sk_x in enumerate(sk_xs):
    for sk_y_key,sk_y in enumerate(sk_ys):
        # Defining the job name
        job_name = 'job_cpb_'+str(mat_key)+str(ply_t_key)+str(ply_prop_key)+str(ply_repeat_key)+s
tr(sk_x_key)+str(sk_y_key)

# Obtain the eigenvalue (Critical buckling load according to FEA)
dir_datfile = model_path + job_name+'.dat'
wordlist = []
starttorecord = False
datfile = open(dir_datfile)
for line in datfile:
    if " MODE NO  EIGENVALUE" in line:
        starttorecord = True
        for word in line.split():
            if word=="THE":
                starttorecord = False
            if starttorecord:
                wordlist.append(word)
        if float(wordlist[4])>0.0:
            eigenvalue = float(wordlist[4])
        elif float(wordlist[6])>0.0:
            eigenvalue = float(wordlist[6])
        elif float(wordlist[8])>0.0:
            eigenvalue = float(wordlist[8])
        else:
            eigenvalue = 0.0
    datfile.close()

# Total number of composite layers are calculated
ply_n_total = len(ply_sq)
h_tot = ply_n_total * ply_t

# Each layers of "h" matrix is the vertical distance from the mid-
plane of the plate (z=0) to the upper surface of the considered lamina(layer)
h = []
for ply_n in range(ply_n_total+1):
    h.append(-h_tot/2.0 + ply_n * ply_t)

# Initialize the A and D matrices
D11=0.0; D12=0.0; D22=0.0; D66=0.0; A44=0.0; A55=0.0

#"kk" is the shear correction coefficient

```

```
kk = 5.0/6.0
```

```
# A and D matrices are calculated in this part
```

```
for ply_n,ply_ang in enumerate(ply_sq):
```

```
# In-plane compliance coefficients for orthotropic materials in material axis
```

```
S11 = 1.0/mat["E1"]
```

```
S12 = -mat["Nu12"]/mat["E1"]
```

```
S22 = 1.0/mat["E2"]
```

```
S66 = 1.0/mat["G12"]
```

```
# In-plane elastic coefficients for orthotropic materials in material axis
```

```
Q11 = S22/(S11*S22-S12**2.0)
```

```
Q12 = -S12/(S11*S22-S12**2.0)
```

```
Q22 = S11/(S11*S22-S12**2.0)
```

```
Q66 = 1.0/S66
```

```
# Problem axis angle cosine and sine values
```

```
cs = math.cos(ply_ang*math.pi/180.0)
```

```
sn = math.sin(ply_ang*math.pi/180.0)
```

```
# Transformation of in-plane elastic coefficients for orthotropic materials in problem axis
```

```
bQ11 = Q11*cs**4+2.0*(Q12+2.0*Q66)*(cs**2.0)*(sn**2.0)+Q22*sn**4.0
```

```
bQ22 = Q11*sn**4+2.0*(Q12+2.0*Q66)*(cs**2.0)*(sn**2.0)+Q22*cs**4.0
```

```
bQ12 = Q12*cs**4+(Q11+Q22-4.0*Q66)*(cs**2.0)*(sn**2.0)+Q12*sn**4.0
```

```
bQ66 = (Q11+Q22-2.0*Q12)*(cs**2.0)*(sn**2.0)+Q66*((cs**2.0)-(sn**2.0))**2.0
```

```
#Q1=[G23 0 ; 0 G13]
```

```
#T1 = [cs -sn; sn cs]
```

```
#T1_inv = [cs sn; -sn cs]
```

```
#bbQ = T1_inv * Q1 *T1
```

```
#bbQ is the 2x2 matrix
```

```
bbQ44 = cs**2.0*mat["G23"]+sn**2.0*mat["G13"]
```

```
bbQ55 = sn**2.0*mat["G23"]+cs**2.0*mat["G13"]
```

```
# Necessary values of A and D matrices
```

```
D11 += bQ11 * (h[ply_n+1]**3.0-h[ply_n]**3.0)
```

```
D22 += bQ22 * (h[ply_n+1]**3.0-h[ply_n]**3.0)
```

```
D12 += bQ12 * (h[ply_n+1]**3.0-h[ply_n]**3.0)
```

```
D66 += bQ66 * (h[ply_n+1]**3.0-h[ply_n]**3.0)
```

```
A44 += bbQ44 * (h[ply_n+1]-h[ply_n])
```

```
A55 += bbQ55 * (h[ply_n+1]-h[ply_n])
```

```
# D matrix values
```

```
D11/=3.0
```

```
D22/=3.0
```

```
D12/=3.0
```

```
D66/=3.0
```

```
# Composite buckling parameters according to FEA
```

```
D_star = (D12+2.0*D66)/(D11*D22)**0.5
```

```
ratio_a0b0 = (sk_x*(D22)**0.25)/(sk_y*(D11)**0.25)
```

```
# Composite plate buckling coefficient according to FEA
```

```
k0_E = (eigenvalue * sk_y**2.0)/(pi*(D11*D22)**0.5)
```

```
k_E = k0_E-2.0*D_star
```

```
# The Classical Laminated Plate Theory
```

```
# Critical bucling load when n=1 and m varying
```

```
# "a" equals to "sk_x" (unloaded edge) and "b" equals to "sk_y" (loaded edge)
```

```
N_Cs = []
```

```
nn_Cs = []
```

```

mm_Cs = []
pi = math.pi

# Critical buckling load calculation for simply supported plate
for num1 in range(1):
    nn_C = num1 + 1
    for num2 in range(10):
        mm_C = num2 + 1
        N_C = D11*(mm_C*pi/sk_x)**2.0+(2.0*D12+4.0*D66)*(pi/sk_y)**2.0+D22*(sk_x*pi/mm
_C)**2.0*(1.0/sk_y)**4.0
        nn_Cs.append(nn_C)
        mm_Cs.append(mm_C)
        N_Cs.append(N_C)
    N_key_C = N_Cs.index(min(N_Cs))
    mm_cri_C = mm_Cs[N_key_C]
    nn_cri_C = nn_Cs[N_key_C]

# Critical buckling load according to CLPT
N_cri_C = N_Cs[N_key_C]

# Percentage error of critical buckling load between FEA result and CLPT result
N_err_C = abs(N_cri_C-eigenvalue)/eigenvalue*100.0

# Composite plate buckling coefficient according to CLPT
k0_C = (N_cri_C * sk_y**2.0)/(pi*(D11*D22)**0.5)
k_C = k0_C-2.0*D_star

#The First-Order Shear Deformation Theory
N_Fs = []
nn_Fs=[]
mm_Fs = []

# Critical buckling load calculation for simply supported plate
for num1 in range(10):
    nn_F = num1 + 1
    for num2 in range(10):
        mm_F = num2 + 1
        alpha = mm_F*pi/sk_x
        beta = nn_F*pi/sk_y
        C1 = -D11*alpha**2.0-D66*beta**2.0-A55*kk
        C2 = -D12*alpha*beta-D66*alpha*beta
        C3 = -A55*kk*alpha
        C4 = -D22*beta**2.0-D66*alpha**2.0-A44*kk
        C5 = -A44*kk*beta
        N_F = (C1*C5**2.0+alpha*C3*C2**2.0+beta*C2**2.0*C5+C3**2.0*C4-alpha*C1*C3*C4-
beta*C1*C4*C5-2.0*C2*C3*C5)/(alpha**2.0*(C1*C4-C2**2.0))
        mm_Fs.append(mm_F)
        nn_Fs.append(nn_F)
        N_Fs.append(N_F)
    N_key_F = N_Fs.index(min(N_Fs))
    mm_cri_F = mm_Fs[N_key_F]
    nn_cri_F = nn_Fs[N_key_F]

# Critical buckling load according to FSDT
N_cri_F = N_Fs[N_key_F]

# Percentage error of critical buckling load between FEA result and FSDT result
N_err_F = abs(N_cri_F-eigenvalue)/eigenvalue*100.0

# Composite plate buckling coefficient according to FSDT
k0_F = (N_cri_F * sk_y**2.0)/(pi*(D11*D22)**0.5)

```

```

k_F = k0_F-2.0*D_star

# Write the output data into the result file
results.write("%-25s %6.2f %-20s %6.2f %-
20s %6.2f" %(" Skin length y: ", sk_y, " Skin length x: ", sk_x, " Total thickness: ",h_tot )+"\n")
results.write("%-25s %6.2f %-20s %6.2f %-20s %6.2f %-20s %6.2f %-
20s %6.2f" %(" Eigenvalue: ",eigenvalue, " CLPT N (m="+str(mm_cri_C)+" and n="+str(nn_cri_C)+"): ", N_c
ri_C, " FSDT N (m="+str(mm_cri_F)+" and n="+str(nn_cri_F)+"): ",N_cri_F, " CLPT error %: ",N_err_C, " FSDT
error %: ",N_err_F)+"\n"+"")

# Write the output data into the result excel file
results_excel.write("%20.2f%20.2f%20.2f%20.2f%20.2f%20.2f" %(ratio_a0b0, k_E, k_C, k
_F, N_err_C, N_err_F)+"\n")
results.close()
results_excel.close()

# Saving the model
mdb.saveAs(pathName=save_path+'.cae')

# Stopping the time calculator
end_t_time = time.time()
m=divmod(end_t_time-start_t_time,60)
n=divmod(m[0],60)
print "Total time: ",n[0],n[1],m[1]

```

- Example code to construct the composite panel model with clamped boundary condition

```

# Importing necessary modules
from abaqus import *
from abaqusConstants import *
from caeModules import *
from driverUtils import executeOnCaeStartup
from part import *
from material import *
from section import *
from assembly import *
from step import *
from interaction import *
from load import *
from mesh import *
from optimization import *
from job import *
from sketch import *
from visualization import *
from connectorBehavior import *
import math
import time

# Counter for script time
start_t_time = time.time()

# Paths

```

```

save_path='C:/Users/...../Model/cl/comp_cl_buckling'

# Given edge load (N/mm)
Edge_load = 1.0

# Material properties
# In this case, material is Carbon/epoxy,Hexply 8552S/37RC/AGP280/C
mats=[]
mats.append(
{"mat_des" : "Carbon_epoxy",
"E1":54000, "E2":54000, "Nu12":0.05,
"G12":4.5e3, "G13":4.5e3, "G23":4.5e3}
)

# Skin geometry
# sk_x is the unloaded edge
# sk_y is the loaded edge
sk_xs = []
sk_ys = []
ply_ts = [0.28]
for xdist in range(100, 505, 5):
    sk_xs.append(xdist)
for ydist in range(100, 105, 5):
    sk_ys.append(ydist)
#Ply sequences
ply_props = []
ply_props.append({"sym":True, "ply_sq":[0], "ply_repeat":[2,4]})
ply_props.append({"sym":True, "ply_sq":[0,90], "ply_repeat":[1,2]})
ply_props.append({"sym":True, "ply_sq":[45,0,-45,90], "ply_repeat":[1,2]})

# Total number of models which will be created in this script
total_count = 0
for ply_prop in ply_props:
    total_count += len(mats)*len(ply_ts)*len(ply_prop["ply_repeat"])*len(sk_xs)*len(sk_ys)
print "Total model number: ", total_count

for mat_key,mat in enumerate(mats):
    for ply_t_key,ply_t in enumerate(ply_ts):
        for ply_prop_key,ply_prop in enumerate(ply_props):
            ply_repeats = ply_prop["ply_repeat"]
            for ply_repeat_key, ply_repeat in enumerate(ply_repeats):
                for sk_x_key,sk_x in enumerate(sk_xs):
                    for sk_y_key,sk_y in enumerate(sk_ys):

                        # Creating model of composite panel buckling (cpb)
                        print "Creating model"
                        model_name = "cpb_" +str(mat_key)+str(ply_t_key)+str(ply_prop_key)+str(ply_repeat_key)+
str(sk_x_key)+str(sk_y_key)
                        mdb.Model(modelType=STANDARD_EXPLICIT, name=model_name)
                        mn=mdb.models[model_name]

                        # Creating material
                        print "Creating model"
                        mn.Material(name=mat["mat_des"])
                        mn.materials[mat["mat_des"]].Elastic(
                            type=LAMINA, table=((
                                mat["E1"], mat["E2"],mat["Nu12"],
                                mat["G12"], mat["G13"], mat["G23"]),))

                        # Creating sketch of skin
                        print "Creating sketch of skin"

```

```

mn.ConstrainedSketch(name='__profile__', sheetSize=200.0)
mn.sketches['__profile__'].rectangle(point1=(0.0, 0.0), point2=(sk_x, sk_y))

# Creating part of skin
print "Creating part of skin"
mn.Part(dimensionality=THREE_D, name='Skin', type=DEFORMABLE_BODY)
mn.parts['Skin'].BaseShell(sketch=mn.sketches['__profile__'])
del mn.sketches['__profile__']

# Creating Layup orientation
print "Creating Layup orientation"
layupOrientation = None
p_sk = mn.parts['Skin']
f_sk, e_sk, d_sk = p_sk.faces, p_sk.edges, p_sk.datums
faces = f_sk.getSequenceFromMask(mask=('[#1 ]', ), )
region_sk=regionToolset.Region(faces=faces)
compositeLayup = p_sk.CompositeLayup(
    name='CompositeLayup-1', description="", elementType=SHELL,
    offsetType=MIDDLE_SURFACE, symmetric=ply_prop["sym"],
    thicknessAssignment=FROM_SECTION)
compositeLayup.Section(preIntegrate=OFF, integrationRule=SIMPSON,
    thicknessType=UNIFORM, poissonDefinition=DEFAULT, temperature=GRADIENT,
    useDensity=OFF)
compositeLayup.ReferenceOrientation(orientationType=GLOBAL, localCsys=None,
    fieldName="", additionalRotationType=ROTATION_NONE, angle=0.0, axis=AXIS_3)

ply_sq = []
for rep in range(ply_repeat):
    for ply_ang in ply_prop["ply_sq"]:
        ply_sq.append(ply_ang)
    for ply_n,ply_ang in enumerate(ply_sq):
        compositeLayup.CompositePly(suppressed=False, plyName='Ply-
'+str(ply_n+1), region=region_sk, material=mat["mat_des"], thicknessType=SPECIFY_THICKNESS, thicknes
s=ply_t, orientationType=SPECIFY_ORIENT, orientationValue=ply_ang, additionalRotationType=ROTATIO
N_NONE, additionalRotationField="", axis=AXIS_3, angle=0.0, numIntPoints=3)

# Mesh control of skin
print "Mesh control of skin"
pickedRegions = f_sk.getSequenceFromMask(mask=('[#1 ]', ), )
p_sk.setMeshControls(regions=pickedRegions, elemShape=QUAD, technique=SWEEP)

# Mesh seed of skin
print "Mesh seed of skin"
p_sk.seedPart(deviationFactor=0.1, minSizeFactor=0.1, size=5.0)

# Generate mesh of skin
print "Generate mesh of skin"
p_sk.generateMesh()

# Creating buckling step
print "Creating Buckling step"
mn.BuckleStep(name='Buckle-
Step', previous='Initial', numEigen=8, vectors=28, maxIterations=3000)

# Creating assembly instances
print "Creating assembly instances"
a_sk = mn.rootAssembly
a_sk.DatumCsysByDefault(CARTESIAN)
a_sk.Instance(dependent=ON, name='Skin-1', part=p_sk)

# Creating boundary conditions at initial step

```

```

print "Creating boundary conditions at initial step"
edges_bc = {'[#2]': 'loaded_edge', '#8]': 'opp_loaded_edge', '#5]': 'unloaded_edges'}
e_sk = a_sk.instances['Skin-1'].edges
for edge_key, edge_des in edges_bc.items():
    edges1 = e_sk.getSequenceFromMask(mask=(edge_key, ), )
    a_sk.Set(edges=edges1, name='Set_'+edge_des)
v_sk = a_sk.instances['Skin-1'].vertices
verts_bc = {'[#8]': 'lb_cor', '#2]': 'rt_cor'}
for vert_key, vert_des in verts_bc.items():
    verts1 = v_sk.getSequenceFromMask(mask=(vert_key, ), )
    a_sk.Set(vertices=verts1, name='Set_'+vert_des)

# Assigning boundary conditions using sets
print "Assigning boundary conditions using sets"
region = a_sk.sets['Set_lb_cor']
mn.DisplacementBC(name='BC_lb_cor', createStepName='Initial',
    region=region, u1=SET, u2=SET, u3=SET, ur1=UNSET, ur2=UNSET, ur3=UNSET,
    amplitude=UNSET, distributionType=UNIFORM, fieldName="", localCsys=None)
region = a_sk.sets['Set_rt_cor']
mn.DisplacementBC(name='BC_rt_cor', createStepName='Initial',
    region=region, u1=UNSET, u2=SET, u3=UNSET, ur1=UNSET, ur2=UNSET, ur3=UNSET,
    amplitude=UNSET, distributionType=UNIFORM, fieldName="", localCsys=None)
region = a_sk.sets['Set_loaded_edge']
mn.DisplacementBC(name='BC_loaded_edge', createStepName='Initial',
    region=region, u1=UNSET, u2=UNSET, u3=SET, ur1=UNSET, ur2=SET, ur3=UNSET,
    amplitude=UNSET, distributionType=UNIFORM, fieldName="", localCsys=None)
region = a_sk.sets['Set_opp_loaded_edge']
mn.DisplacementBC(name='BC_opp_loaded_edge', createStepName='Initial',
    region=region, u1=SET, u2=UNSET, u3=SET, ur1=UNSET, ur2=SET, ur3=UNSET,
    amplitude=UNSET, distributionType=UNIFORM, fieldName="", localCsys=None)
region = a_sk.sets['Set_unloaded_edges']
mn.DisplacementBC(name='BC_unloaded_edges', createStepName='Initial',
    region=region, u1=UNSET, u2=UNSET, u3=SET, ur1=SET, ur2=UNSET, ur3=UNSET,
    amplitude=UNSET, distributionType=UNIFORM, fieldName="", localCsys=None)

# Applying shell edge load on the skin loaded edge
print "Applying shell edge load on the skin loaded edge"
load_edges = ['#2]']
for load_key, load_edge in enumerate(load_edges):
    s_edges = e_sk.getSequenceFromMask(mask=(load_edge, ), )
    region = a_sk.Surface(side1Edges=s_edges, name='Surf_loaded_edge'+str(load_key+1))
    mn.ShellEdgeLoad(name='Load_buckling'+str(load_key+1), createStepName='Buckle-
Step',
        region=region, magnitude=Edge_load, distributionType=UNIFORM, field="",
        localCsys=None)

# Creating job
print "Creating job"
job_name = 'job_'+ model_name
mdb.Job(name=job_name, model=model_name, description="", type=ANALYSIS,
    atTime=None, waitMinutes=0, waitHours=0, queue=None, memory=90,
    memoryUnits=PERCENTAGE, getMemoryFromAnalysis=True,
    explicitPrecision=SINGLE, nodalOutputPrecision=SINGLE, echoPrint=OFF,
    modelPrint=OFF, contactPrint=OFF, historyPrint=OFF, userSubroutine="",
    scratch="", resultsFormat=ODB, multiprocessingMode=DEFAULT, numCpus=1,
    numGPUs=0)
try:
    del mdb.models['Model-1']
except:
    None

```

```

# Saving the model
print "Saving model"
mdb.saveAs(pathName=save_path+'.cae')

# Stopping the time calculator
end_t_time = time.time()
m=divmod(end_t_time-start_t_time,60)
n=divmod(m[0],60)
print "Total time: " ,n[0],n[1],m[1]

```

- Example code to process finite element results for the composite panel model with clamped boundary condition

```

# Importing necessary modules
from abaqus import *
from abaqusConstants import *
from caeModules import *
from driverUtils import executeOnCaeStartup
from part import *
from material import *
from section import *
from assembly import *
from step import *
from interaction import *
from load import *
from mesh import *
from optimization import *
from job import *
from sketch import *
from visualization import *
from connectorBehavior import *
import math
import time

# Counter for script time
start_t_time = time.time()

# Defining maximum number of submissions can be given at the same time
max_sub = 5
ini_sub = 0

# Paths
save_path='C:/Users/...../Model/cl/comp_cl_buckling'
model_path = r'C:/Users/...../Model/cl/'

# Initialize results' path
result_path = r"C:\Users\.....\Results\comp_cl_buckling_loads"
result_excel_path = r"C:\Users\.....\Results\excel\comp_cl_buckling_loads"

# Given edge load (N/mm)
Edge_load = 1.0

# Material properties
# In this case, material is Carbon/epoxy,Hexply 8552S/37RC/AGP280/C
mats=[]
mats.append(
{ "mat_des" : "Carbon_epoxy",
"E1":54000,"E2":54000,"Nu12":0.05,
"G12":4.5e3,"G13":4.5e3,"G23":4.5e3}

```



```

)

# Skin geometry
# sk_x is the unloaded edge
# sk_y is the loaded edge
sk_xs = []
sk_ys = []
ply_ts = [0.28]
for xdist in range(100, 505, 5):
    sk_xs.append(xdist)
for ydist in range(100, 105, 5):
    sk_ys.append(ydist)

#Ply Sequence
ply_props = []
ply_props.append({"sym":True,"ply_sq":[0],"ply_repeat":[2,4]})
ply_props.append({"sym":True,"ply_sq":[0,90],"ply_repeat":[1,2]})
ply_props.append({"sym":True,"ply_sq":[45,0,-45,90],"ply_repeat":[1,2]})

# Total number of models which will be created in this script
total_count = 0
for ply_prop in ply_props:
    total_count += len(mats)*len(ply_ts)*len(ply_prop["ply_repeat"])*len(sk_xs)*len(sk_ys)
print "Total model number: ", total_count
count = 1

for mat_key,mat in enumerate(mats):
    for ply_t_key,ply_t in enumerate(ply_ts):
        for ply_prop_key,ply_prop in enumerate(ply_props):
            ply_repeats = ply_prop["ply_repeat"]
            for ply_repeat_key,ply_repeat in enumerate(ply_repeats):
                for sk_x_key,sk_x in enumerate(sk_xs):
                    for sk_y_key,sk_y in enumerate(sk_ys):
                        # Job name is described
                        start_time = time.time()
                        job_name = 'job_cpb_'+str(mat_key)+str(ply_t_key)+str(ply_prop_key)+str(ply_repeat_key)+s
tr(sk_x_key)+str(sk_y_key)
                        print "Model number: ",count
                        job_model = mdb.jobs[job_name]

                        # Checked to see if the job has already been submitted
                        try:
                            dir_logfile = model_path + job_name+".log"
                            logfile = open(dir_logfile)
                            comp = False

                        # Checked to see that the job is completed
                        for line in logfile:
                            if "Abaqus JOB "+job_name+" COMPLETED" in line:
                                print " completed"
                                comp = True
                        logfile.close()

                        # Submission check
                        if comp==False:
                            job_model.submit(consistencyChecking=OFF)
                            ini_sub +=1

                        # Multi-submission is permitted for this code
                        # Maximum number of submission is checked
                        if ini_sub >= max_sub:

```

```

        job_model.waitForCompletion()
        ini_sub = 0
        end_time = time.time()
    else:
        end_time = time.time()

    except:
        # Submit the job
        job_model.submit(consistencyChecking=OFF)
        ini_sub +=1

        # Multi-submission is permitted for this code
        # Maximum number of submission is checked
        if ini_sub >= max_sub:
            job_model.waitForCompletion()
            ini_sub = 0
            end_time = time.time()

        # Estimated time is calculated
        if count%(max_sub*2) == 0:
            em=divmod((total_count-count)*(end_time-start_time)/max_sub,60)
            en=divmod(em[0],60)
            print "Estimated remaning time: ",en[0],en[1],em[1]
        count+=1

# Checked whether all analyses are completed
for mat_key,mat in enumerate(mats):
    for ply_t_key,ply_t in enumerate(ply_ts):
        for ply_prop_key,ply_prop in enumerate(ply_props):
            ply_repeats = ply_prop["ply_repeat"]
            for ply_repeat_key, ply_repeat in enumerate(ply_repeats):
                for sk_x_key,sk_x in enumerate(sk_xs):
                    for sk_y_key,sk_y in enumerate(sk_ys):
                        job_name ='job_cpb_'+str(mat_key)+str(ply_t_key)+str(ply_prop_key)+str(ply_repeat_key)+str(sk_x_key)+str(sk_y_key)
                        job_model.waitForCompletion()

for mat_key,mat in enumerate(mats):
    for ply_t_key,ply_t in enumerate(ply_ts):
        for ply_prop_key,ply_prop in enumerate(ply_props):
            ply_repeats = ply_prop["ply_repeat"]
            for ply_repeat_key, ply_repeat in enumerate(ply_repeats):
                # Writing the input data into the result file
                results = open(result_path+"_"+str(mat_key)+str(ply_t_key)+str(ply_prop_key)+str(ply_repeat_key)+".txt","w+")
                results_excel = open(result_excel_path+"_"+str(mat_key)+str(ply_t_key)+str(ply_prop_key)+str(ply_repeat_key)+".txt","w+")

                # Writing the excel graphs' headings into the result file which is used to construct excel
                results_excel.write("%20s %20s %20s %20s %20s %20s" %("a0/b0","k0-2D*(E)","k0-2D*(C)","k0-2D*(F)","error(E-C)","error(E-F)")+ "\n"+" \n")

                # Writing the material properties into the result file
                results.write("%-25s %20s" %("Material description: ", mat["mat_des"]))+"\n")
                results.write("%-25s %6.2f %-20s %6.2f %-20s %6.2f" %("Material E1: ", mat["E1"], " Material E2: ", mat["E2"], " Material Nu12: ", mat["Nu12"]))+"\n")
            )
            results.write("%-25s %6.2f %-20s %6.2f %-20s %6.2f" %("Material G12: ", mat["G12"], " Material G13: ", mat["G13"], " Material G23: ", mat["G23"]))+"\n")

```

```

# Writing the ply thickness and symmetric condition into the result file
results.write("%-25s %6.2f %-
20s %10s" %("Ply thickness: ", ply_t, " Ply symmetric: ", ply_prop["sym"]+"\n")

# Ply directions and angles are described to use in A,B,D matrices
ply_sq = []
for rep in range(ply_repeat):
    for ply_ang in ply_prop["ply_sq"]:
        ply_sq.append(ply_ang)
if ply_prop["sym"]:
    for ply_ang in reversed(ply_sq):
        ply_sq.append(ply_ang)

# Writing the ply directions and angles into the result file
results.write("%-25s" %("Ply Directions: "))
for ply_ang in ply_sq:
    results.write("%6d" %(ply_ang))
results.write("\n"+"")

for sk_x_key,sk_x in enumerate(sk_xs):
    for sk_y_key,sk_y in enumerate(sk_ys):
        # Defining the job name
        job_name = 'job_cpb_' +str(mat_key)+str(ply_t_key)+str(ply_prop_key)+str(ply_repeat_key)+s
tr(sk_x_key)+str(sk_y_key)

# Obtain the eigenvalue (Critical buckling load according to FEA)
dir_datfile = model_path + job_name+'.dat'
wordlist = []
starttorecord = False
datfile = open(dir_datfile)
for line in datfile:
    if " MODE NO  EIGENVALUE" in line:
        starttorecord = True
        for word in line.split():
            if word=="THE":
                starttorecord = False
            if starttorecord:
                wordlist.append(word)
if float(wordlist[4])>0.0:
    eigenvalue = float(wordlist[4])
elif float(wordlist[6])>0.0:
    eigenvalue = float(wordlist[6])
elif float(wordlist[8])>0.0:
    eigenvalue = float(wordlist[8])
else:
    eigenvalue = 0.0
datfile.close()

# Total number of composite layers are calculated
ply_n_total = len(ply_sq)
h_tot = ply_n_total * ply_t

# Each layers of "h" matrix is the vertical distance from the mid-
plane of the plate (z=0) to the upper surface of the considered lamina(layer)
h = []
for ply_n in range(ply_n_total+1):
    h.append(-h_tot/2.0 + ply_n * ply_t)

# Initialize the A and D matrices
D11=0.0; D12=0.0; D22=0.0; D66=0.0; A44=0.0; A55=0.0

```

```

# "kk" is the shear correction coefficient
kk = 5.0/6.0

# A and D matrices are calculated in this part
for ply_n,ply_ang in enumerate(ply_sq):
# In-plane compliance coefficients for orthotropic materials in material axis
S11 = 1.0/mat["E1"]
S12 = -mat["Nu12"]/mat["E1"]
S22 = 1.0/mat["E2"]
S66 = 1.0/mat["G12"]

# In-plane elastic coefficients for orthotropic materials in material axis
Q11 = S22/(S11*S22-S12**2.0)
Q12 = -S12/(S11*S22-S12**2.0)
Q22 = S11/(S11*S22-S12**2.0)
Q66 = 1.0/S66

# Problem axis angle cosine and sine values
cs = math.cos(ply_ang*math.pi/180.0)
sn = math.sin(ply_ang*math.pi/180.0)

# Transformation of in-
plane elastic coefficients for orthotropic materials in problem axis
bQ11 = Q11*cs**4+2.0*(Q12+2.0*Q66)*(cs**2.0)*(sn**2.0)+Q22*sn**4.0
bQ22 = Q11*sn**4+2.0*(Q12+2.0*Q66)*(cs**2.0)*(sn**2.0)+Q22*cs**4.0
bQ12 = Q12*cs**4+(Q11+Q22-4.0*Q66)*(cs**2.0)*(sn**2.0)+Q12*sn**4.0
bQ66 = (Q11+Q22-2.0*Q12)*(cs**2.0)*(sn**2.0)+Q66*((cs**2.0)-(sn**2.0))**2.0

# Q1=[G23 0 ; 0 G13]
# T1 = [cs -sn; sn cs]
# T1_inv = [cs sn; -sn cs]
# bbQ = T1_inv * Q1 *T1
# bbQ is the 2x2 matrix
bbQ44 = cs**2.0*mat["G23"]+sn**2.0*mat["G13"]
bbQ55 = sn**2.0*mat["G23"]+cs**2.0*mat["G13"]

# Necessary values of A and D matrices
D11 += bQ11 * (h[ply_n+1]**3.0-h[ply_n]**3.0)
D22 += bQ22 * (h[ply_n+1]**3.0-h[ply_n]**3.0)
D12 += bQ12 * (h[ply_n+1]**3.0-h[ply_n]**3.0)
D66 += bQ66 * (h[ply_n+1]**3.0-h[ply_n]**3.0)
A44 += bbQ44 * (h[ply_n+1]-h[ply_n])
A55 += bbQ55 * (h[ply_n+1]-h[ply_n])

# D matrix values
D11/=3.0
D22/=3.0
D12/=3.0
D66/=3.0

# Composite buckling parameters according to FEA
D_star = (D12+2.0*D66)/(D11*D22)**0.5
ratio_a0b0 = (sk_x*(D22)**0.25)/(sk_y*(D11)**0.25)

# Composite plate buckling coefficient according to FEA
k0_E = (eigenvalue * sk_y**2.0)/(pi*(D11*D22)**0.5)
k_E = k0_E-2.0*D_star

# The Classical Laminated Plate Theory
# Critical buclng load when n=1 and m varying
# "a" equals to "sk_x" (unloaded edge) and "b" equals to "sk_y" (loaded edge)

```

```

N_Cs = []
nn_Cs = []
mm_Cs = []
pi = math.pi

# Critical buckling load calculation for clamped plate
for num1 in range(10):
    nn_C = num1 + 1
    for num2 in range(10):
        mm_C = num2 + 1
        if nn_C==mm_C:
            N_C = (4.0*pi**2.0*D11*mm_C**2.0)/sk_x**2.0+(4.0*pi**2.0*D22*sk_x**2.0)/(sk_y**4
.0*mm_C**2.0)+16.0*pi**2.0/(3.0*sk_y**2.0)*(0.5*D12+D66)
        else:
            N_C = (D11*pi**2.0/sk_x**2.0*(nn_C**4.0+6.0*nn_C**2.0*mm_C**2.0+mm_C**4.0)+D2
2*pi**2.0*16.0*sk_x**2.0/(3.0*sk_y**4.0)+(0.5*D12+D66)*16.0*pi**2.0/(3.0*sk_y**2.0)*(nn_C**2.0+mm_
C**2.0))/(nn_C**2.0+mm_C**2.0)
            nn_Cs.append(nn_C)
            mm_Cs.append(mm_C)
            N_Cs.append(N_C)
    N_key_C = N_Cs.index(min(N_Cs))
    mm_cri_C = mm_Cs[N_key_C]
    nn_cri_C = nn_Cs[N_key_C]

# Critical buckling load according to CLPT
N_cri_C = N_Cs[N_key_C]

# Percentage error of critical buckling load between FEA result and CLPT result
N_err_C = abs(N_cri_C-eigenvalue)/eigenvalue*100.0

# Composite plate buckling coefficient according to CLPT
k0_C = (N_cri_C * sk_y**2.0)/(pi*(D11*D22)**0.5)
k_C = k0_C-2.0*D_star

#The First-Order Shear Deformation Theory
N_Fs = []
nn_Fs = []
mm_Fs = []

# Critical buckling load calculation for clamped plate
for num1 in range(10):
    nn_F = num1 + 1
    for num2 in range(10):
        mm_F = num2 + 1
        if (1.0-2.0*nn_F**2.0+mm_F**4.0-2.0*mm_F**2.0*nn_F**2.0-
2.0*mm_F**2.0+nn_F**4.0)!=0.0 :
            if mm_F==1:
                G1 = pi**4.0*(3.0*D11*sk_y**4.0+2.0*D12*sk_x**2.0*sk_y**2.0+3.0*D22*sk_x**4.0+
4.0*D66*sk_x**2.0*sk_y**2.0)/(4.0*sk_x**3.0*sk_y**3.0)
                G2 = -(pi**2.0*sk_y*(3.0*nn_F**4.0-12.0*nn_F**2.0))/(16.0*sk_x*(nn_F**4.0-
4.0*nn_F**2.0))
                G3 = -(8.0*sk_y*(-nn_F**3.0+(-1.0)**(nn_F+2.0)*nn_F**3.0))/(3.0*sk_x*(nn_F**4.0-
4.0*nn_F**2.0))
                G4 = kk*pi**2.0*(A44*sk_x**2.0+A55*nn_F**2.0*sk_y**2.0)/(4.0*sk_x*sk_y)
                G5 = -(pi**2.0*sk_y*(nn_F**6.0-4.0*nn_F**4.0))/(4.0*sk_x*(nn_F**4.0-
4.0*nn_F**2.0))
                N_F = (-(G1*G5+G2*G4)-((G1*G5+G2*G4)**2.0-4.0*(G2*G5-
G3**2.0)*G1*G4)**0.5)/(2.0*(G2*G5-G3**2.0))
            else:

```

```

H1 = pi**4.0*(D11*sk_y**4.0*(18.0*mm_F**2.0+3.0+3.0*mm_F**4.0)+D12*sk_x**2.
0*sk_y**2.0*(8.0+8.0*mm_F**2.0)+16.0*D22*sk_x**4.0+D66*sk_x**2.0*sk_y**2.0*(16.0+16.0*mm_F**2.0
)/(32.0*sk_x**3.0*sk_y**3.0)
H2 = -(pi**2.0*sk_y*(3.0*mm_F**6.0+3.0+3.0*nn_F**4.0-3.0*mm_F**4.0-
3.0*mm_F**2.0+3.0*mm_F**2.0*nn_F**4.0-12.0*mm_F**2.0*nn_F**2.0-6.0*nn_F**2.0-
6.0*mm_F**4.0*nn_F**2.0))/(32.0*sk_x*(1.0-2.0*nn_F**2.0+mm_F**4.0-2.0*mm_F**2.0*nn_F**2.0-
2.0*mm_F**2.0+nn_F**4.0))
H3 = -(8.0*sk_y*(-mm_F*nn_F**3.0+(-
1.0)**(mm_F+nn_F+1.0)*mm_F*nn_F**3.0))/(3.0*sk_x*(1.0-2.0*nn_F**2.0+mm_F**4.0-
2.0*mm_F**2.0*nn_F**2.0-2.0*mm_F**2.0+nn_F**4.0))
H4 = kk*pi**2.0*(A44*sk_x**2.0+A55*nn_F**2.0*sk_y**2.0)/(4.0*sk_x*sk_y)
H5 = -(pi**2.0*sk_y*(nn_F**2.0+nn_F**6.0-
2.0*mm_F**2.0*nn_F**4.0+mm_F**4.0*nn_F**2.0-2.0*nn_F**4.0-
2.0*mm_F**2.0*nn_F**2.0))/(4.0*sk_x*(1.0-2.0*nn_F**2.0+mm_F**4.0-2.0*mm_F**2.0*nn_F**2.0-
2.0*mm_F**2.0+nn_F**4.0))
N_F = (-(H1*H5+H2*H4)-((H1*H5+H2*H4)**2.0-4.0*(H2*H5-
H3**2.0)*H1*H4)**0.5)/(2.0*(H2*H5-H3**2.0))
mm_Fs.append(mm_F)
nn_Fs.append(nn_F)
N_Fs.append(N_F)
N_key_F = N_Fs.index(min(N_Fs))
mm_cri_F = mm_Fs[N_key_F]
nn_cri_F = nn_Fs[N_key_F]

# Critical buckling load according to FSDT
N_cri_F = N_Fs[N_key_F]

# Percentage error of critical buckling load between FEA result and FSDT result
N_err_F = abs(N_cri_F-eigenvalue)/eigenvalue*100.0

# Composite plate buckling coefficient according to FSDT
k0_F = (N_cri_F * sk_y**2.0)/(pi*(D11*D22)**0.5)
k_F = k0_F-2.0*D_star

# Write the output data into the result file
results.write("%-25s %6.2f %-20s %6.2f %-
20s %6.2f" %(" Skin length y: ", sk_y, " Skin length x: ", sk_x, " Total thickness: ",h_tot)+"\n")
results.write("%-25s %6.2f %-20s %6.2f %-20s %6.2f %-
20s %6.2f" %(" Eigenvalue: ",eigenvalue, " CLPT N (m="+str(mm_cri_C)+" and n="+str(nn_cri_C)+"): ", N_c
ri_C, " FSDT N (m="+str(mm_cri_F)+" and n="+str(nn_cri_F)+"): ", N_cri_F, " CLPT error %: ",N_err_C, " FSDT
error %: ",N_err_F)+"\n"+"")

# Write the output data into the result excel file
results_excel.write("%20.2f %20.2f %20.2f %20.2f %20.2f %20.2f" %(ratio_a0b0, k_E, k_C, k
_F, N_err_C, N_err_F)+"\n")
results.close()
results_excel.close()

# Saving the model
mdb.saveAs(pathName=save_path+'.cae')

# Stopping the time calculator
end_t_time = time.time()
m=divmod(end_t_time-start_t_time,60)
n=divmod(m[0],60)
print "Total time: " ,n[0],n[1],m[1]

```